

MASTER THESIS

Molecular weight distribution impact on morphology, crystallinity and mechanical properties

A study on different types of homo-polypropylene



LUNDS
UNIVERSITET

Master Thesis by Malin Petersén – Engineering Nanoscience

Malin.petersen10@gmail.com

Supervisors:

Claes Oveby Tetra Pak

Christine Billstein Tetra Pak

Patric Jannasch LTH

Examiner:

Reine Wallenberg

Abstract

This master thesis is the result of cooperation between Lund University and Tetra Pak, performed by a student at Engineering Nanoscience, LTH. The aim is to explain how different molecular weights and molecular weight distribution of isotactic homo-polypropylene affect resulting properties. Examined properties are mechanical properties by tensile testing and tensile impact, shear viscosity by capillary rheometry and crystallinity by Differential Scanning Calorimetry.

Aim was also to find good rheological measures for polydispersity, by comparing these measures of molecular weight distribution by Size Exclusion Chromatography. These rheological examinations were executed by use of oscillating rheometry sweeps at different temperatures and calculations build upon equations found in literature.

The different types of polypropylene examined for mechanical properties were injection moulded. In injection moulding shear forces create an anisotropic resulting material, with higher orientation in the direction of shear. This was examined by testing the mechanical properties in different directions of injection moulded plates. The plates were stored after processing to examine if the properties vary during storage, up to 6 weeks. Scanning Electron Microscopy was utilised to analyse the different zones created by injection moulding in the cross section of the plates.

Findings were among other that molecular weight distribution strongly influence the mechanical properties, and that the mechanical properties vary widely with storage time after injection moulding. This variations over time is assumed to arise from post crystallisation and physical ageing.

Keywords: Molecular weight; Molecular weight distribution; isotactic Polypropylene

Sammanfattning

Denna masteruppsats är ett samarbete mellan Lunds Tekniska Högskola och Tetra Pak, utförd av en student vid programmet Teknisk Nanovetenskap. Målet med examensarbetet är att förklara hur molekylvikt och molekylviktsfördelning av isotaktiskt homo-polypropylene påverkar vissa materialegenskaper. Egenskaper undersökta är mekaniska egenskaper genom dragprovning och slagprovning, skjuvviskositet mätt med kapillär rheometer och kristallinitet med hjälp av Differential Scanning Calorimetry.

Målet var också att hitta en bra mätmetod för att beräkna bredd på molekylvikt med hjälp av reologi på ett rättvisande sätt. Detta gjordes genom att jämföra olika mått på molekylviktsfördelning framräknad från reologiska data med molekylviktdata från storlekskromatografi. Reologi mätningar gjordes med oscillerande parallella plattor rheometer, med frekvenssvep.

De olika typerna av polypropylene som undersöktes mekaniskt var formsprutade till plattor, där sedan hundben stansades ut. I formsprutning är den flytande polymeren under skjuvning, resulterande i ett anisotropiskt material med högre orientering av polymerkedjor i skjuvriktningen. Mekaniska egenskaper testades i olika riktningar på plattorna. Plattorna var lagrade efter formsprutning för att undersöka om egenskaperna varierade över tid, i 6 veckor. Svepelektronmikroskop användes för att undersöka olika zoner av orientering som uppstår vid formsprutning genom att undersöka tvärsnittsarean av plattorna i maskinriktning.

Upptäckter var bland annat att molekylviktsfördelning starkt influerar de mekaniska egenskaperna, och att de mekaniska egenskaperna varierar mycket över tid efter formsprutning, i upp till 4-6 veckor i vissa undersökta grades. Variationer tros bero på efterkristallisation och fysisk åldring.

Sökord: Molekylvikt; Molekylviktsfördelning, Isotaktisk Polypropylene

Acknowledgement

To make this thesis possible, I want to thank Tetra Pak for use of machines and expertise. The Material Analysis Lab at Tetra Pak has performed tensile impact tests and provided with all rheology measurements, essential for the thesis. INEOS have provided with grades and SEC measurements and calculations, also essential for this thesis. LTH have been very helpful by letting me use the SEM and provided me with skilled competence regarding sample preparation and know-how in operating the microscope.

A big thank you:

Christine Billstein - mentor Tetra Pak

Claes Oveby - mentor Tetra Pak

Patric Jannasch - Professor at Centre for Analysis and Synthesis - mentor LTH

Lena Dahlberg - Material Analysis – lab

Pascale Godon - Technical support INEOS and material supplier

Reine Wallenberg - Professor, Director of nCHREM – SEM

Likewise, acknowledge to: Parastoo Salavati (Material Analyses – lab), Eskil Andreasson (expertise), Elin Persson Jutemar (expertise), Andreas Hein (compounding), Andreas Danielsson (IMM) that have been very helpful with different parts during my work.

Contents

ABBREVIATIONS	9
1 Introduction.....	10
2 Background	11
2.1 Introduction – Interest from industry	11
2.2 Polymer Theory.....	12
2.2.1 <i>Molecular Weight (M_w) and Molecular Weight Distribution (MWD)</i>	12
2.2.1.1 <i>Characterisation method - SEC</i>	14
2.2.2 <i>Chain configuration - tacticity</i>	14
2.2.3 <i>Crystallinity - Morphology</i>	15
2.2.4 <i>Post crystallisation</i>	17
2.2.5 <i>Physical ageing</i>	18
2.2.5.1 <i>DSC – Differential Scanning Calorimetry</i>	18
2.2.5.2 <i>WAXS and SAXS</i>	19
2.2.6 <i>Mechanical response</i>	19
2.2.6.1 <i>Tensile test</i>	20
2.2.6.2 <i>Tensile Impact</i>	21
2.2.7 <i>Microscopy techniques</i>	21
2.2.7.1 <i>SEM</i>	21
2.2.8 <i>Rheology of polymers</i>	22
2.2.8.1 <i>Oscillatory Rheometry – Parallel plates</i>	26
2.2.8.2 <i>Capillary Rheometer</i>	26
2.3 Processing/Injection moulding– polymer application.....	27
2.3.1 <i>Injection moulding</i>	27
2.3.2 <i>Compounding - twin screw extruder</i>	29
3 Objectives.....	31
4 Scope.....	32
5 Experimental Set-Up/Method	33
5.1 Polypropylene grades	33
5.2 Test planning	34
5.3 Test set up and procedure.....	34
5.3.1 <i>Twin-screw extrusion – Mixing polymer</i>	34

5.3.2	<i>Injection moulding</i>	36
5.3.3	<i>Tensile test</i>	37
5.3.3.1	<i>Punching dogbones</i>	37
5.3.3.2	<i>Tensile testing</i>	38
5.3.4	<i>Tensile impact</i>	39
5.3.5	<i>SEM</i>	40
5.3.6	<i>DSC</i>	42
5.3.6.1	<i>Enthalpy and heat flow</i>	42
5.3.6.2	<i>DSC Onset</i>	44
5.3.7	<i>Capillary rheometer</i>	44
5.3.8	<i>Oscillatory rheometry</i>	45
5.4	<i>Analysis of test methods</i>	46
5.4.1	<i>Tensile tests</i>	46
5.4.1.1	<i>Change of direction of punching (CD)</i>	46
5.4.1.2	<i>Change of speed of tensile test (CD)</i>	47
5.4.1.3	<i>Change of direction of dogbone in machine</i>	48
5.4.1.4	<i>Change of distance from edge when punching plates (MD)</i>	49
5.4.1.5	<i>Observed difference in tension between CD, MD and DD</i>	51
5.4.1.6	<i>Conclusion</i>	52
5.4.2	<i>DSC</i>	53
5.4.2.1	<i>Conclusion</i>	54
6	Results	55
6.1	<i>Oscillatory rheometry</i>	55
6.2	<i>Tensile tests</i>	56
6.2.1	<i>Machine direction (MD)</i>	58
6.2.1.1	<i>Yield point</i>	59
6.2.1.2	<i>Youngs modulus</i>	60
6.2.1.3	<i>Elongation at break</i>	62
6.2.2	<i>Cross direction (CD)</i>	64
6.2.2.1	<i>General shape of measured force/displacement curve, key values</i>	64
6.2.2.2	<i>Yield point</i>	65
6.2.2.3	<i>Youngs modulus</i>	67

6.2.2.4	<i>Elongation at break</i>	68
6.2.3	<i>Diagonal direction (DD)</i>	70
6.2.3.1	<i>General shape of measured force/displacement curve</i>	70
6.2.3.2	<i>Yield point</i>	71
6.2.3.3	<i>Youngs modulus</i>	72
6.2.3.4	<i>Elongation at break</i>	74
6.2.4	<i>Summary of stability</i>	75
6.2.5	<i>Pictures of fractured dogbones</i>	76
6.3	<i>Tensile Impact</i>	79
6.4	<i>SEM</i>	81
6.5	<i>DSC</i>	83
6.5.1	<i>Enthalpy and heat flow diagrams</i>	83
6.5.2	<i>Onset</i>	83
6.6	<i>Capillary rheometry</i>	84
7	Discussion	86
7.1	<i>Oscillatory rheometry</i>	86
7.2	<i>Tensile tests</i>	87
7.2.1	<i>General discussion</i>	87
7.2.2	<i>Young's modulus, yield point and elongation at break</i>	89
7.2.2.1	<i>Youngs modulus</i>	89
7.2.2.2	<i>Yield point</i>	90
7.2.2.3	<i>Elongation at break</i>	91
7.2.2.4	<i>Performance measured from compounded grades</i>	92
7.2.3	<i>Change of properties during storage</i>	93
7.2.4	<i>General conclusions</i>	94
7.2.5	<i>Discussion regarding validity</i>	95
7.3	<i>Tensile impact</i>	96
7.4	<i>SEM</i>	97
7.5	<i>DSC</i>	98
7.6	<i>Capillary Rheometer</i>	99
8	Conclusions and major findings	99
8.1	<i>Rheology</i>	99

8.2	MWD and Mw influence on mechanical properties	100
8.3	Crystallinity and microstructure	100
9	Proposals for future work	101
10	References	102
11	Appendix.....	105
11.1	Test analysis	105
11.1.1	<i>Punching of dogbones</i>	105
11.2	Oscillatory rheometer	106
11.3	Tensile tests	118
11.3.1	<i>MD – all grades.....</i>	118
11.3.2	<i>CD – all grades</i>	119
11.3.3	<i>DD – all grades.....</i>	120
11.3.4	<i>Youngs modulus.....</i>	122
11.3.5	<i>Yield point</i>	125
11.4	Tensile Impact	128
11.5	DSC	129
11.5.1	<i>Enthalpy and peak melt temperature – first melting</i>	129
11.5.2	<i>Enthalpy and peak melt temperature – second melting</i>	130
11.5.3	<i>Grade 1.....</i>	131
11.5.4	<i>Grade 2.....</i>	132
11.5.5	<i>Grade 3.....</i>	133
11.5.6	<i>Grade 4.....</i>	134
11.5.7	<i>Grade 5.....</i>	135
11.5.8	<i>Grade 6.....</i>	136
11.6	Capillary rheometry.....	138
11.7	SEC result plot and raw data	139
11.8	Categorising of grades.....	148

ABBREVIATIONS

CD = Cross Direction

CI = Confidence Interval (by 95%)

DD = Diagonal direction

DSC = Differential Scanning Calorimetry

Homo-PP = homo polypropylene

SEC = Size Exclusion Chromatography

IMM = Injection Moulding Machine

MD = Machine direction

MFR = Melt Flow Rate

MFI = Melt Flow Index

M_n = Number-average molecular weight

M_w = Weight-average molecular weight

M_z = Z-average molecular weight

MWD = Molecular Weight Distribution

PDI = Polydispersity Index

PP = Polypropylene, Polypropene

T_g = Glass transition temperature

T_m = Melting temperature

SAXS = Small Angle X-ray Scattering

SEM = Scanning Electron Microscopy

WAXS = Wide Angle X-ray Scattering

1 Introduction

In the processing and applications of polymers the crystallinity, rheology, resulting morphology and mechanical properties are of great importance. Among factors that influence these properties, the molecular weight of the polymer and the molecular weight distribution are of great importance. Different types of synthesized homo-polypropylene (of 92-96% isotacticity) are in this work examined to analyse regarding how the M_w (Molecular weight) and MWD (molecular weight distribution) impact those properties. The analysis methods used are Differential Scanning Calorimetry (DSC) to study the degree of crystallinity and change of this during storage, tensile tests and tensile impact to analyse mechanical properties and capillary and oscillatory rheometry to analyse melt rheology determine the MWD of the polymers. These properties are not only influenced by the M_w and MWD, among other factors, the temperature is strongly influencing the properties. Therefore, the tests that are temperature sensitive were performed at ambient temperature (23 °C) and 50% humidity if nothing else is specified. Also, storage of samples were in climatized rooms.

The motive behind the thesis is to get a better understanding of different grades of polypropylene to better understand which type of polymer that should be used in certain applications. Today there is not a complete view regarding which M_w and MWD that should be requested from suppliers to get the best grade for a certain application. Data and conclusions based on the outcome of this Master thesis will be utilized by specialists at Tetra Pak that have deeper insight in what properties that are best for certain applications. The benefit is that the learnings can be used to optimise the choice of polymers, serve as input in problem solving and reduce time and cost during validations.

2 Background

In order to fully understand the measurements and tests performed in this work, there is a need of knowing the fundamental properties of polymers. This section comprehends the theory of polymers that are necessary to analyse and interpret performed analyses of polypropylene. It does also include descriptions of the test methods from a theoretical point of view. Information regarding why this is of relevance for companies such as Tetra Pak will also be explained.

2.1 Introduction – Interest from industry

Tetra Pak is a leading global food packing and processing company, and to stay leading innovation and research must be central. When gathering deeper insight and knowledge about the properties of the materials and processes, optimisation can be done, in terms of e. g. material sufficiency and time when injection moulding. In products such as caps and closures made from polymers, certain properties are of importance in different parts of the product. Examples of different caps and closures can be seen in Figure 1.



Figure 1. (left) Examples of Tetra Pak closures and caps, and (right) the layers/structures of a three-component cap.

When opening a three-component cap, the bridges in between the tamper evidence ring and the top part of the lid must break at an appropriate rotational force, not to be too elastic or brittle. Another important thing to regard is the cutter in the cap, that must be sharp enough to cut through the packaging material. For the cutter to work, the yield point must be high enough so that the cutter does not start to deform. Those properties are measured and compared to defined requirements. Two test methods assumed to be appropriate to use regarding mechanical properties are tensile test and tensile impact strength, where the first examine properties as *yield point*, *elongation* and *Young's modulus*. Tensile impact tests examine the polymer properties when deformed by a higher impact, similar to a drop test and measure resilience of the material, how much energy the material absorb before fracture.

Structural parameters of different polymers affect its processability. When shaping a cap from raw material, the polymer is injection moulded. To injection mould, plastic in the form of pellets are melted and sheared at high shear rates through an extruder. It is then cooled down in the mould that is a cavity, shaped as the product, to crystallise and finally being ejected.

These steps imply that the melt properties of the polymer are of high importance to ensure that a good processability is possible together with a good time scale. During production the desire is a high output (short cycle time) and a good quality, but often do properties as a low melt flow viscosity result in a weaker material. To examine the processability the polymers rheology is of interest and can be measured by a capillary rheometer to achieve high shear rates similar to those in the extruder, but also lower shear rates similar to those that can be seen in thicker parts in the mould. In the cold mould the polymer freeze. This is when the majority of the crystallisation of the polymer takes place, although for polypropylene this crystallisation can continue over a larger time scale. The degree of crystallinity affects the properties, hence, it is of interest to find out when this crystallisation is finalised. The assumption is that post crystallisation can be examined by DSC, since the melting point and enthalpy is affected by the overall present crystallinity.

When relating polymers to each other the M_w and the MWD are central. If it is understood how these key parameters affect the properties in the product and during production a company can tailor-make and purchase polymers that fit certain special applications. Gaining more knowledge regarding the properties of polypropylene and the previous described properties are the aims of this thesis.

2.2 Polymer Theory

A polymer is built from monomers, comparable to small building blocks. These building blocks are connected to each other, repeating themselves, creating a long chain. The molecular weight (M_w) is a measure of the chain length, the number of the repeated units reflected in total weight of the chain. This chain can behave very differently depending on which atoms and building blocks that are present, how the monomers are connected to each other and the length of the chain. Polymers are either amorphous or semi-crystalline. Amorphous polymers have a disordered entangled state of chains. Semi-crystalline polymers have partly a crystalline ordered crystal lattice and partly an amorphous ordering of chains (Fried, 2014). The properties of a polymer vary with chain configuration (building blocks and order) and chain conformation. The conformation which is the shape of the polymer chain, is dynamic and can change since there is a possible rotational freedom for the atoms around the bonding. In this section, different properties and attributes of polymers will be discussed.

2.2.1 Molecular Weight (M_w) and Molecular Weight Distribution (MWD)

The M_w of a polymer influence the mechanical properties of the material and the rheological behaviour. Longer molecular chains give more entanglements in the amorphous phase and for semi-crystalline areas better tie in the crystalline regions. (Spoormaker, 2002) Lower M_w allows the chains to rearrange more rapidly generating a slightly higher crystallinity, but do as well invite more chain ends into the structure, hence creating a weaker structure in tensile loading. It is an industrial challenge to keep a high M_w and a high output, since with increasing M_w the melt flow rate (MFR) is decreasing. Melt Flow Index, MFI, or Melt Flow

Rate, are measurements to characterize the ease of flow of melted polymer. M_w and MFI are proportional to each other in a monomodal polymer, when the M_w is increasing the MFI is decreasing, it is harder to flow the melt. The reason behind this is that with increasing molecular weight, the entanglement between polymer chains will increase, this affects the flow in a reducing manner. A lower M_w results in loss of impact, tensile strength or punctual resistance. (Edward P. Moore, 1996)

A typical polymer sample does seldom contain just one length of chains. It comprises a wider distribution of chains due to synthesis method and reactivity. To describe a polymer a classification widely uses is the average molecular weight. There are different ways of describing this, where the two most common are by *number weighted molecular weight*, \bar{M}_n or the *mass weighted molecular weight*, \bar{M}_w . The number average molecular weight is calculated by summarising all molecular weights divided by their total number. The weight average molecular weight is when summarising the molecular weights multiplied by their weight fractions. The \bar{M}_n is a good measurement of the chain length of the polymer, while \bar{M}_w is a good measurement of the statistical size. These two measurements can give different measures of the average molecular weight, and can be used to calculate the *polydispersity index*, *PDI*.

$$PDI = \frac{\bar{M}_w}{\bar{M}_n}$$

The polydispersity index is used to describe the MWD. There are other measurements to describe polydispersity as well, but this is the one most widely used. Another measure of polydispersity is M_z/M_w , where M_z is an average molecular weight that is more sensitive of high molecular weight chains.

The MWD describes the broadness of molecular weights present in the resin. The larger PDI, the broader MWD (Polymerdatabase, 2015). The MWD influences the crystallinity and stiffness of the polymer. With a wider distribution the crystallinity increases, and gives higher orientation rate when injection moulded. This since longer molecules orient more in the shear direction and with a broader MWD longer polymers are present. Higher grade of orientation gives higher modulus in the flow direction.

Broadening of M_w can be achieved by polymerizing widely different M_w 's in separate reactor stages and mix, but that is a method with limitations of homogenization in later processing steps in the injection mould or extrusion due to different viscosities within the polymer. (Edward P. Moore, 1996). When synthesizing a bimodal MWD commonly two different catalysts are used, that possess a relative productivity to the other, hence synthesizing molecular chains of different length. The active site is normally different types of transition metals of the catalyst which activity will be tuned by other factors, as water content in the reactor, temperature or carbon dioxide present (Mink, et al., 1996).

It is unknown what method that is used to synthesize the polymer used in this test, since it is a company secret of the supplier.

2.2.1.1 Characterisation method - SEC

To determine the MWD the method SEC (Size Exclusion Chromatography), also called GPC (Gel Permeation Chromatography), can be used. The polymer in form of a dilute solution is pumped across a column with a defined distribution in porosity. The molecular chains will be separated into different pores due to how large hydrodynamic volume the polymer coils have. This takes shorter time for larger molecules since they do not get trapped in the pores. Hence, different sized molecules elute at different times. If the instrument is properly calibrated the curve of eluted material versus time becomes the MWD after calculations. From this method it is possible to determine the weight average M_w , number average M_n , Z-weight average M_z . (Edward P. Moore, 1996). In this thesis, the result from SEC will be compared by rheological calculations to analyse the MWD of the grades.

2.2.2 Chain configuration - tacticity

Polypropylene is a polymer synthesized by a chain growth polymerization with an initiator required. The monomer is propylene and the catalyst varies between different types of polymerization. The polymerization is finished after termination. Depending on how the monomers are coupled to the growing chain, different tacticity is the result.

Tacticity is a way to describe the configuration of the repeat unit of the polymer. Chain configuration is the organization of the polymer chain, the way it is built up. The existing configuration of a polymer cannot be changed unless the chain is broken in some way, as through depolymerization. When polymers have the same molecular formula but different configuration, the polymers are called isomers (Fried, 2014). There are three types of tacticity, isotactic, syndiotactic and atactic. Atactic tacticity is the unordered type where monomers are coupled in a random fashion regarding the methyl group, that is having a random distribution in space. Isotactic tacticity is fully ordered where all the methyl groups are placed in the same direction from the chain backbone. Syndiotactic is ordered by altering.

In isotactic polypropylene (homo-PP), which is the type that is used in the experiments and analysed in the paper, the monomers are coupled the same way with the methyl group on the same side. To achieve isotactic polypropylene two common methods of synthesize can be used, Ziegler-Natta polymerization or metallocene catalysed polymerization. The isotacticity generates a more crystalline polymer which results in a stiffer polymer. It is rare to reach a 100% ideal tacticity in practice, which is resulting in different grades of crystallinity. These occasional defects that interrupt the isotactic ordered chain is decreasing the crystallinity. (Edward P. Moore, 1996) The extent of the crystalline region is a function of the crystallization speed. The crystallization speed strongly depends on the temperature and the chain length. For Polypropylene, the necessary condition for crystallization is the configuration of the CH_3 – group, the side group. Only for isotactic and syndiotactic PP crystallization is possible. (Spoormaker, 2002)

2.2.3 Crystallinity - Morphology

Polymers are either amorphous or semi-crystalline. Amorphous polymers have a disordered state of chains with a random coil shape and semi-crystalline polymers have partly a crystalline (ordered 3D crystal lattice) partly an amorphous ordering of chains (Fried, 2014). In other words, semi-crystalline polymers are consisting of two or more solid phases, where one is build up from chain segments organized into crystal and one phase is disordered. The amorphous non-crystalline phases build up a matrix wherein the crystalline parts are embedded (Xiong, 2014), see Figure 2. When a polymer melt is cooled down and if the condition is favourable, polymers that are able to crystallize will do so. Polymer chains start to orient themselves to a semi-crystalline structure. The crystal structure depends among other on order of repeat unit, flexibility, monomer type and tacticity.

Semi-crystalline polymers have two temperatures of major practical interest where the properties of the polymer changes; the glass transition temperature (T_g) and the melting point (T_m). At the melting point the crystalline structure melts, hence, amorphous polymers that lack crystalline structure have no melting point. T_g exists for all polymers and at this temperature the mechanical properties of the polymer change. When the polymer exhibits temperatures above T_g , the polymer is in rubbery state. When the polymer exhibits temperatures below T_g , it is in glassy state. In the glassy state the only molecular motions that can occur is movement as short-range motions of chain segments, vibrations and movement of substituent groups. These movements are called secondary relaxations. In the rubbery state the polymer has more freedom to move, there is an increase in the number of possible conformations of the polymer chains. (Fried, 2014)

Crystallization begins with formation of nuclei's at different points in the melt. Nuclei's is different regions where the polymer molecules are more aligned, forming ordered regions. After this step, crystal growth starts (Arrighi, u.d.). From here, polymers start to crystallize in structures that are called lamellas. The lamellas consist of arrays of folded polymer chains. This crystal structure is folded so that the polymer chains are laying perpendicular towards the elongation of the lamellar sheet. The lamella structures form aggregates, building up larger structures where the most common one is called spherulite. In spherulites the lamellas are arranged radially from the centre. Hence, the chains in the crystallites are lying tangentially from the centre of the spherulite (Edward P. Moore, 1996). Between the lamellar structures there are amorphous regions. See Figure 2 for illustration. Smaller molecules crystallize very quickly, but for larger macromolecules as polymers this is a process that takes time (Arrighi, u.d.).

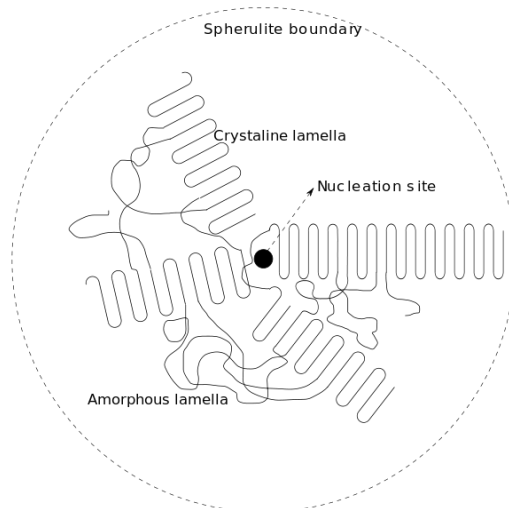


Figure 2. Schematic picture of how the semi-crystalline lamella grow from a nucleation site and the amorphous material is packed between the crystalline lamellas. (Gillis, 2007)

Polymorphism is present in isotactic PP, which means that the polymer exhibits more than one crystalline form. The spherulites that can be formed in isotactic PP are α -, β -, γ - and one liquid crystal form named the smectic phase, all have been observed by X-ray scattering in various research. Which type/types that are present in a PP depends strongly on the thermo-mechanical conditions from melt. (Martin, et al., 2009) The α form, which is the dominant one, has a monoclinic unit cell and is sometimes divided into 2 different types of α_1 and α_2 forming two different space group symmetries. It is suggested that some form of heating or melting is required to promote the transition from α_1 to α_2 symmetry. (Edward P. Moore, 1996) The α form is formed by crystallisation from melt or solution. T_m for the α spherulite is recorded to be 174.2 °C (Nakamura, et al., 2008). The β form a hexagonal thermodynamically less stable unit cell under normal crystallisation conditions. Often the β form can only be formed together with other crystal forms in samples. A transformation of the β form into α form can take place by melt recrystallization at elevated temperature close to T_m of the sample. (Karger-Kocsis, 1995) The β form is obtained from temperature gradient crystallisation, crystallisation under molecular orientation or induced by special nucleating agents. T_m for the β form is 169.4 °C (Nakamura, et al., 2008). The β form improve the elongation before break and the impact strength, but reduce the modulus and tensile strength. (Mi, et al., 2016) The γ form a triclinic lattice in rare situations, observed in low molecular weight isotactic PP. (Karger-Kocsis, 1995) The smectic (sometimes called quenched) phase is identified as a pseudo-hexagonal unit cell structure and have minor occurrence. All the crystal structures are build up by individual chains in a 3_1 helical conformation with three monomer units per helix, illustration of this can be seen in Figure 3. (Martin, et al., 2009) It is a helix with 6.5 Å chain axis repeat distance, and is the only helical conformation involved in isotactic polypropylene (Lotz, et al., 1996) (Nakamura, et al., 2008).

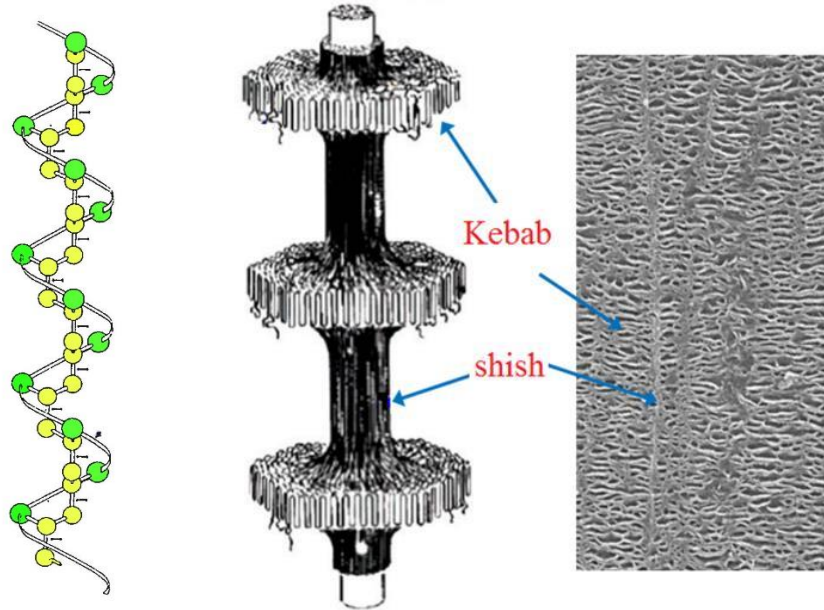


Figure 3. (left) The 3_1 helical conformation with three monomer units per helix lap, in isotactic PP. (Lieberman, 1988)

Figure 4. (right) Illustration of the shish-kebab structure. (Kolnaar, 1997)

Another structure that can be formed by semi-crystalline polymers as polypropylene is shish-kebab structure (seen in Figure 4). The shish kebab structure can occur when the polymer crystallises during strain or elongation. The structure consists of transverse lamellae structure parallel to the central nucleus, growing from a central linear thread. Adjacent lamellae are not in contact, having a gap generally 3-4 nm between. (Monks, et al., 1996) Studies have showed that with a thicker shish-kebab layer, formed as skin layer, the mechanical strength increases. Formation of the layer is hard to control and depends on the conditions when the polymer crystallises. For the formation to happen, the molecules cannot be allowed to relax before crystallisation. They could for example form on the cold moulding surface during injection moulding. With an increased thickness of layer (as a ratio of the total thickness of the injection moulded part) the elongation before break decrease. The shish-kebab structure can simultaneously improve impact strength, tensile strength, modulus, stiffness and thermal stability together with decreased permeability. (Mi, et al., 2016)

2.2.4 Post crystallisation

Post crystallisation is a phenomenon that typically occurs in injection moulded polypropylene and other semi-crystalline polymers. Post crystallisation is a slow addition and reformation of the of the crystalline structure that can take place after the polymer have been cooled and frozen in the mould under strain. It occurs due to rapid cooling when chains inside of the polymers not are relaxed, due to shear forces during processing. Post crystallisation can involve transformation between crystal structures and amorphous material that is close to the crystalline areas, that bind to the crystalline area and enhance the rate of crystallinity. (Fiebig, et al., 1999) Free volume in the polymer and size of chains and temperature affect this phenomenon.

2.2.5 Physical ageing

Another phenomenon that can change the properties in the material after injection moulding of PP is physical ageing. Physical ageing takes place in the amorphous phase of the semi-crystalline polymer. In fully amorphous polymers, physical ageing can only take place below T_g of the polymer, but in semi-crystalline polymers the crystalline areas hinder the free movement of the amorphous part. The amorphous phase acts as links between the crystalline segments, hence, strongly influencing the mechanical properties. The amorphous fractions close to the crystalline segments are hindered in movement, in contrast to the amorphous areas that are further away from these crystalline areas. Hence, the main theory behind physical ageing is that there is a reduction in segmental mobility over time, extending the T_g of the polymer up in temperatures (due to the restricted segments of the polymer). (Struik, 1987) Physical ageing can take place in PP at room temperature.

In a study (Krishnaswamy, et al., 2003) where influence of physical ageing on poly(phenylene sulphide) were examined, it was assumed that the rate of physical ageing is strongly dependent on the semi-crystalline morphology. It was assumed that it was not the weight fraction of crystallinity that was of importance, but the enthalpic relaxation that is dependent on the rigid amorphous phase fraction. Larger fraction of this phase is promoting rate of ageing.

Physical ageing can be examined using X-ray, density measurements or mechanical tests, but not through crystallinity measurements by DSC. Density is increasing in the amorphous phase of the material when physical ageing take place, resulting in an overall denser material (Schultz & Agarwal, 1981) (Fiebig, et al., 1999). Physical ageing is not that widely examined, but in an early report on PP films examined above room temperature ageing was found to give rise to increase in modulus and a decrease in impact strength, together with an increase in density (Schael, 1966).

2.2.5.1 DSC – Differential Scanning Calorimetry

To examine the crystallisation of semi-crystalline polymers a couple of different methods can be used. One of the most widely used method is DSC, Differential Scanning Calorimetry. It consists of two individual heaters containing one platinum holder each. The technology builds upon maintaining the same temperature for both platinum holders. One of the holders contain a small polymer sample mechanically sealed in a small aluminium pan. The other platinum holder contains an empty reference pan. What is measured is the different addition of power to keep the equal temperature in the chambers. The measurement can be done either from cooling to heating or the reverse. (Fried, 2014) The power is recorded as a function of temperature. If running the test while heating, at some temperature above T_g the chains have enough energy to break its crystalline formations and melt. Since melting of crystalline areas is an endothermic process (it takes heat /energy) to break the ordered structure, more energy will be added to keep the same temperature in the chambers. An endothermic peak is observed. The opposite happens when cooling the sample from melted state, crystallization is an exothermic process, heat is released to the surroundings and an exothermic peak is recorded. These are illustrated in Figure 5. (Humbold, u.d.) This information will give certain

peaks where there is a larger difference in need of power, revealing where the crystalline structures are present. This method can show which crystalline phases that are present in the sample. (Karian, 2003) What also is of interest is the total enthalpy it takes to melt the crystal structure. This can reveal the total amount of crystallinity in the sample.

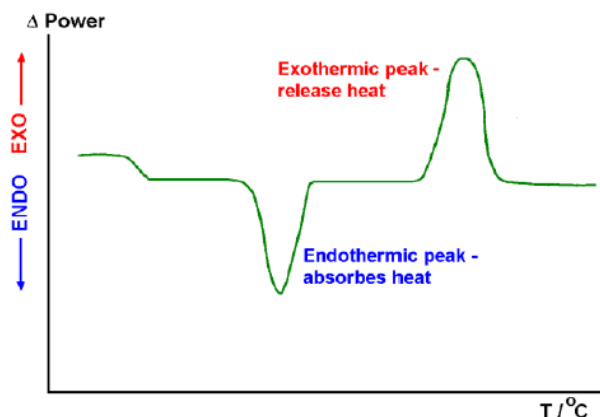


Figure 5. Graph showing an endothermic melt peak that absorbs energy to break crystals, and an exothermic crystallisation peak that release energy when ordering chains into crystal structures (Kodre, et al., 2014).

2.2.5.2 WAXS and SAXS

Diffraction techniques can also be used to determine crystal structures. X-ray diffraction is a method that can provide information about both the crystalline phase and the amorphous. X-rays are high energy photons with short wavelength that interact with the electrons in the polymer material. The electrons in the material interact with the X-ray beam, some electrons will be absorbed, some transmitted unmodified and other will be scattered due to interaction with electrons. By measuring angles and intensities of the incident beam information can be given about the electron density, implying how the atoms are oriented in the polymer. Hence, the crystal structures present. WAXS is wide angle X-ray scattering and SAXS is small angle X-ray scattering. WAXS is normally used for smaller structures, as dimensions in unit cells ($<10 \text{ \AA}$) and SAXS is used above this, to analyse large morphology up to $10 \mu\text{m}$. (Fried, 2014). These type of diffraction techniques will not be used during this work due to lack of time and resource, but would still be good methods to use to study the morphology.

2.2.6 Mechanical response

The morphology, time of deformation, temperature and humidity (history and present) decide the response of a polymer when exhibiting deformation. This is due to the viscoelastic intrinsic properties of polymers, where the polymer is behaving both as a viscous liquid and an elastic solid.

Depending on temperature and stress level, the polymer act differently and undergo for example linear elastic behaviour, yield phenomena or/and plastic deformation. Different stress (force) to polymer material could be applied and measured differently; e.g. shear, strain or compression.

If solids like polymers, when the material is being examined by shear strain (measure the magnitude of deformation), the response is called modulus of rigidity. If the solid is compressed or tensile strained the material response is known as Young's modulus. The modulus is the measure of a materials resistance to deformation, telling how stiff the material is. Modulus reflects the material's capacity to store deformational energy and regain its shape after being deformed. Deformation is instant with no time lag. Resilience is the ability to return to its original shape after it has been stretched or pulled. (Crawford, 1998)

2.2.6.1 Tensile test

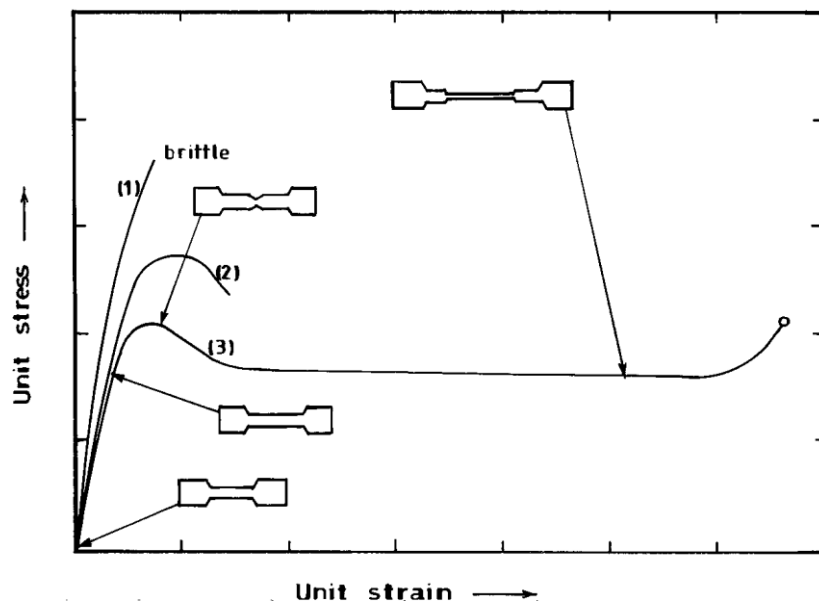


Figure 6. Tensile test performed on dogbone. (1) indicate a brittle polymer that do not exhibit yielding, (2) indicates a polymer that starts to yield and then rupture after lower yield stress, (3) indicates a polymer exhibit strain hardening. Picture from Fried, J.R., *Plast. Eng.*, 38(7), 27. 1982. (Ebewele, 2000)

A tensile test is carried out by using a dogbone shaped piece of plastic and stretching it out by either using a constant force or constant deformation rate. The result is plotted as a graph with the force (N) on the y-axis and elongation (mm) on x-axis, or the stress (Pa) on the y axis and the strain (%) on the x axis, see Figure 6. The stress is proportional to the force and strain is a way to note the elongation. The first area that is observed is the elastic area, noted as the dogbone before necking occurs, where the Young's modulus is possible to extract. (Ebewele, 2000) This modulus is in this work extracted as the 1% secant modulus, and is an approximation of the tangent that should be valid to do, since this range is linear.

During this part of testing when the material still behaves elastic, no slip between crystalline areas occurs (see Figure 7). Where the linear regime stops and a maximum occurs the yielding starts, noted as the necked dogbone in Figure 6. This point is called the yield point, beyond this point the material starts to flow and the deformation is permanent. This type of slip around yield point is called fine slip, see Figure 7. The yield point is also called the upper yield stress. The material might rupture at this point if being very brittle, and if no rupture occurs, the force (stress) will be reduced to a minimum value called the drawing stress or the

lower yield stress. Here coarse slip is observed. Existence of this point can be discussed, since the lowering of stress also depends on that necking occurs, resulting in a smaller cross-section area, hence, less area to bare the same stress. Figure 7 below show a schematic graph from a fracture curve with true stress/true strain, when the true cross section area is used to calculate resulting stress. After this point the polymer will either rupture or experience strain hardening. In strain hardening the polymer chains are assumed to slip past each other, plastically deforming the material. When the polymer chains cannot dissipate the force by stretching chains, uncoiling or slip the polymer will eventually fail, and rupture. This is the point of elongation at break (Ebewele, 2000)

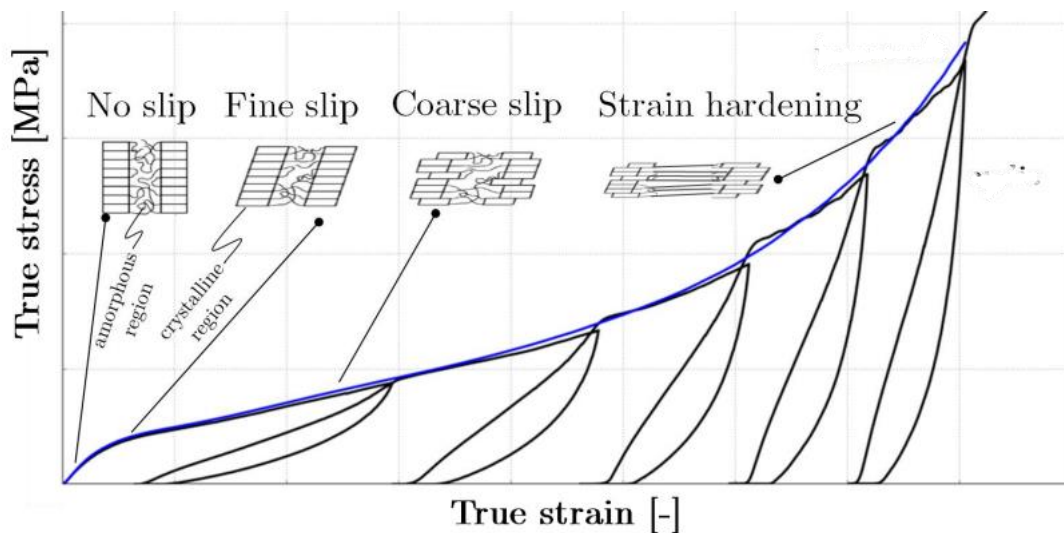


Figure 7. Polymer slip, this illustration is regarding polymer film but it is same behaviour as thicker polymer which is examined in this thesis (plates at 0.6 mm thickness). Picture is modified to only show relevant information for this thesis. (Jönsson & Sandgren, 2013).

2.2.6.2 Tensile Impact

Tensile impact is used to mechanically characterise a polymers resistance to impact at high rate of deformation, where the materials resilience is the parameter most commonly extracted. A dogbone shaped sample is being hit by a pendulum hammer during this test. The sample is mounted with one end of the dogbone in a fixed holder and the other end in a gross-head. The pendulum hammer will hit the polymer at an impact velocity approximately 2.9 m/s, the sample is deformed and ultimately fractured during a time period of a few milliseconds. This will generate a voltage use as a function of time, where the voltage can be converted to a force. This force together with the length of deformation is used to calculate resilience which is a material specific parameter. The computer software will also generate a force – deformation curve where e.g. resilience, total deformation, energy at peak deformation and total energy uptake can be obtained. (Andersson, 2012)

2.2.7 Microscopy techniques

2.2.7.1 SEM

SEM, or Scanning Electron Microscopy, is a microscopy method that allows high resolution, down to 10 nm, if performed correctly. A focused electron beam is scanned across the sample,

where different events take place. Some of the electrons in the beam will backscatter, or cause ejection of secondary electrons originally belonging to the sample. These different events are detected by a detector. By angle and energy of scattered electrons it can be understood from which event the electrons belonged and from where they are scattered. Hence, a picture of electron density from potential gradients reveals position of atoms, hence, structure can be realized. Pictures arising from the secondary electrons are the once utilised in this work, and are called SEI (secondary electron image) or LEI (low secondary electron image) by detector. SEM must be carried out during high vacuum in order to not interact with electrons in the air.

When using SEM to analyse soft materials as polymers, it's a must to consider beam damage. When shooting electrons on a material that is sensitive to breakage of bonds, there is a risk of breakage of the chain or side groups to detach, leaving reactive free radicals. These may crosslink and form new structures. Hence, the material might change during the analysis, resulting in faulty pictures. Damage from radiation can also result in causing crystalline areas to lose crystallinity. Sometimes this can be prevented by staining the polymer with a heavy metal solution that is sinking into the sample, but, when doing this the structure can be affected and the chemistry changed from its original. (Williams, David B., Carter, C. Barry, 2009) Another option is to cover the specimen with a thin metal to enhance the imaging. Sputtering of gold is common, which also makes the surface conductive so that the specimen does not get charged. If the sample would get charged it would disturb the image by causing bright hotspots and streaks in the sample, and increase the noise.

What limits the resolution in SEM is lenses and aberrations in lenses, diffraction effects, voltage of the electron beam, electron source, sample condition (as charging and contamination), mechanical vibrations and instabilities in environment. (Wells, 1974)

2.2.8 Rheology of polymers

Rheology is the science regarding flow and deformation, where viscosity is the measure of resistance to flow. If a polymer flows easily it has low viscosity (as water) and if opposite it has high viscosity (as honey). This property is highly influenced by M_w and MWD, where a polymer with higher M_w and narrow MWD normally have a higher viscosity. Within industry rheology is of great importance since it can determine the polymers processability, where the polymer must flow to be injection moulded or extruded. A polymer is viscoelastic, behaving both as a solid and a fluid. In a melt or dilute solution, a polymer shows both of these properties when exposed to a mechanical force and when analysing polymers these two properties are normally separated into *loss* and *storage modulus*.

The storage modulus is the elastic response and is normally noted G' , acting as a solid. When the force is applied and removed the polymer chains return to its original shape. The loss modulus is the viscous response, and is normally noted as G'' , acting as a fluid. When the polymer acts viscous it loses memory of its original shape of the chains. The response from

the polymer is strongly affected by time of mechanical deformation and the temperature. The viscosity (shear viscosity) is noted η and is defined as (Fried, 2014):

$$\eta = \frac{\sigma}{\dot{\gamma}}$$

Where σ is the shear stress and $\dot{\gamma}$ is the shear rate the polymer exhibits. In experiments, either the shear rate or the shear stress is applied and the other is measured. Shear viscosity is describing the flow behaviour of a polymer flowing around in a uniform channel under stress. When a polymer is under lower shear rate it normally has a higher viscosity, and is independent of shear rate. In a graph this shows as a plateau called the first plateau (in Figure 8 it is called “1st Newtonian plateau”). This higher viscosity arises from entangled polymer chains that hinder the flow. With an increasing shear rate, the viscosity lowers. This behaviour is called shear thinning and comes from that the chains are untangling from each other and aligning in the direction of shear, flow easier after aligning. When the chains are aligned there is a new plateau, the 2nd Newtonian plateau. In polymer melt a second plateau is rare since the shear rate that is needed for the chains to be totally aligned is so high that the chains normally break before reaching these high rates.

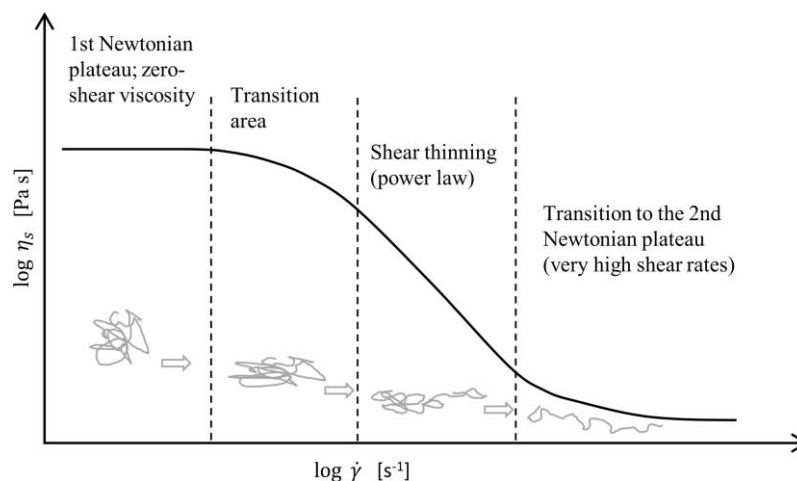


Figure 8. Illustrating how the viscosity change with shear rate in a shear thinning polymer melt. The second plateau is normally only showing for dilute polymer solutions. Under the graph, the polymer chains are illustrated and how it changes structure with shear rate. (Aho, et al., 2018)

When relating M_w and MWD to rheology, there are certain areas of interest. One important parameter is the *zero shear viscosity*, η_0 . This parameter is the viscosity at very low shear rate, described previously when the viscosity is independent of shear rate (the 1st first plateau). To extract η_0 , one is extrapolating the viscosity to when the shear rate is zero. Since this higher viscosity at low shear rate is due to entangled polymer chains, this is a measurement of the length of polymer chains and its interactions, therefor reflecting MW. If the M_w is higher the onset of shearing starts at a progressively lower shear rate. (Fried, 2014)

Another point of interest is the *cross-over point*. It is extracted by the use of oscillatory rheometry and shows the components G' and G'' . G' represents the characteristic elastic modulus and G'' the viscous response. The response of the chains is related to the relaxation

time and Deborah number (there is plenty of information about these parameters in different text books), which can be said to be the time scale it takes for the polymer chains to relax. At very low shear rates the response is primarily viscous, since the chains have time to relax when deformed. At higher shear rates the chains are in a glassy state and the response from the elastic loss modulus will increase. The cross-over point is where the two different modulus responses are equal, $G' = G''$, at a certain angular frequency ω_{co} . (Sunthar, 2010) The cross-over point is illustrated in Figure 9.

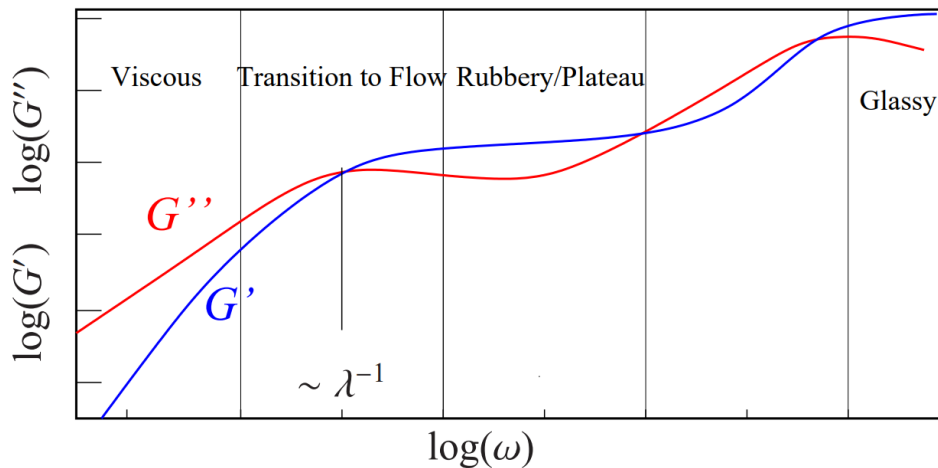


Figure 9. Showing the oscillatory response from a polymer liquid, where G' is the storage modulus and G'' the loss modulus. ω is the angular frequency. λ is the relaxation time. (Sunthar, 2010)

In regards of modulus, there is a *complex modulus*, G^* , that reflects G' and G'' , with the relationship $G^* = G' + iG''$ which is extracted as:

$$G^* = \sqrt{(G')^2 + (G'')^2}$$

This complex modulus can be used differently, but for example, plot versus the loss tangent. The loss tangent is illustrated in Figure 10.

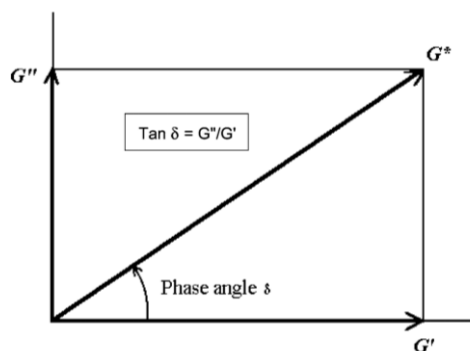


Figure 10. The relationship between loss modulus, storage modulus, complex modulus and the phase angle. (Lee, et al., 2006)

The cross-over point is relatable to the MWD and M_w of the polymer, with a high M_w the cross-over point shifts to lower frequency compared to a low M_w . Hence, a high M_w give a more elastic response. A polymer with a broader MWD has the cross-over point at lower

modulus compared to a polymer with narrow distribution. (Aho, et al., 2018) Another parameter that is relevant when examining the MWD is the relaxation spectrum. With more different length of chains present the polymer will relax at different timeframes. Although, the relaxation time spectra is affected by the present concentrations, the relaxation time of shorter chains is increasing with the concentration of long chains. Longer chains behave as they were shorter in the presence of shorter chains, hence, the spectrum of relaxation time is narrower in a polydisperse polymer than if they would be measured separately in monodisperse polymers. (Lin & Yu, 1996)

When examine these previously mentioned parameters and properties, it is to remember that one must remain in the linear viscoelastic region. With this, it means that the mechanical responds of the polymer during stress or strain must be limited to time only and not the history of stress or strain. The polymer cannot be damaged or degraded during measurements. (Ebewele, 2000)

To examine and compare different polymers and their polydispersity (MWD) some different calculations can be used. The once that is focused on in this thesis are measurements called *PI*, *ER* and *PDR* using data received by frequency sweeps by oscillatory rheometry. *PI*, *ER* and *PDR* are defined as (Shroff & Mavridis, 1995):

$$PI = \frac{10^5 Pa}{G_c} \quad \text{Equation 1}$$

$$ER = C_1 * G' \text{ at } G_{ref}'' \quad \text{Equation 2}$$

$$PDR = \frac{\eta_1^*}{\eta_3^*} * \frac{\sqrt{(\eta_1^* \eta_3^*)}}{\eta_2^*} \quad \text{Equation 3}$$

PI (equation 1) is a measurement of PDI derived from frequency data in the linear viscoelastic region, giving a reported historically as a good correlation between *PI* and M_w/M_n and M_z/M_w for polypropylenes. Since this measure relies on the cross-over modulus, and the cross-over modulus for G' and G'' are to be found at higher frequencies, this is a high frequency method. (Shroff & Mavridis, 1995)

ER (equation 2) is a measure extracted from G' and G'' data, where G_{ref}'' is selected to be a low modulus value, hence corresponding to low frequencies, normally around 500 Pa (which is used in this thesis). C_1 is a constant equal to the slope of the $\log(G')$ vs $\log(G'')$ curve times 10^{-2} Pa^{-1} . *ER* is a measure of polydispersity where influence from the high molecular weight end of the spectra is larger. (Amintowlieh, 2014)

PDR (equation 3) is a measurement that takes a wider range of frequencies into the equation. It uses complex viscosity data connected to complex modulus. η_1^* is picked at G_1^* with a low modulus (corresponding to a low frequency), η_2^* is picked at $G_2^* = \sqrt{G_1^* * G_3^*}$ and η_3^* is picked at G_3^* that is one higher modulus value, corresponding to higher frequencies in the sweep. (Shroff & Mavridis, 1995) For this thesis G_1^* is put to 400 Pa, G_2^* is 4000 Pa and G_3^* to 40000 Pa due to the sweep made and the look of the resulting η^* / G^* graph of the grades.

By comparing these three attributes to SEC data, it is possible to find which of the measurement that best describe the MWD of PP examined. It is possible to compare the different grades to each other, and to couple the measures of MWD to resulting mechanical properties.

2.2.8.1 *Oscillatory Rheometry – Parallel plates*

One of the types of rheometer that can be used for oscillatory testing is the parallel plate. The polymer is pressed together to a dense thick film and placed between the plates and heated up. One of the plates is connected to a motor which is rotating the plate in an oscillatory manner. The response (the delay) from the polymer to the torque is measured by measuring a corresponding deflection angle or resulting rotational speed. This angle is specified in either radians or degrees. By measuring the time this can be related to the angular velocity ω . The spectrum of frequencies the measurements are performed over must match the specific polymer which is related to its relaxation time. If the rotation is slow the polymer has time to relax and get a viscous response, and if the rotation is very fast the polymer acts glassy. Different sweeps are performed at different temperatures, since the temperature also has great influence over the response of the polymer. Higher temperature makes the polymer less viscous, but might also at a certain point damage the chains. To extract the cross-over point and the zero shear viscosity the frequency range together with the temperature the test are performed in must be carefully chosen, otherwise the loss and storage modulus might not cross.

2.2.8.2 *Capillary Rheometer*

The most commonly used measurement of rheological properties is the shear viscosity (η). It describes the flow behaviour when a viscous material is flowing around in a uniform channel under stress, where viscosity is the measure of a material's resistance to flow. (Crawford, 1998).

To measure shear viscosity at high shear rates, the capillary rheometer is an effective instrument. Virgin polymer granules, that are intended to be used in injection moulding or extrusion applications, are the input material. In the capillary rheometer the material being tested undergoes extrusion through a die of defined dimensions, with a temperature controlled barrel. The material is pushed through the capillary die by a piston which is driven at a defined speed, generating the pressure. The pressure is measured by pressure transducers above the capillary dies. The process is repeated over a number of speeds, which covers the shear rate range of interest. The pressure and flow rate through the capillary die are used to determine viscosity. The result is presented in a graph as shear viscosity versus shear rate. If the temperature is low and the strain rate is high, the response is normally more elastic. If the opposite, the response is often viscous.

When using capillary rheometer there is a need of a correction called Bagley to find the true viscosity of a material. The pressure is measured above the die inlet and not inside of the die, therefore the true pressure drop is hidden by an additional pressure drop at the entrance of the die. Turbulence might also be added since the material flow from a wider reservoir into the narrow piston. This can be corrected by assuming that the pressure drop is the same between

measurements keeping constant barrel and capillary diameters but different capillary lengths. This is done by most software's today. (Svensson, 2013)

2.3 Processing/Injection moulding– polymer application

When making products from polymers there are different techniques that can be used. Injection moulding is a commonly used technique to form objects and is most often used in applications as caps. In injection moulding the input is normally pellets and the output is a cooled part that is ejected from the mould. This section will comprehend injection moulding together with compounding, which is performed to combine two polymer grades to one. The section also comprehends information regarding resulting properties after injection moulding.

2.3.1 Injection moulding

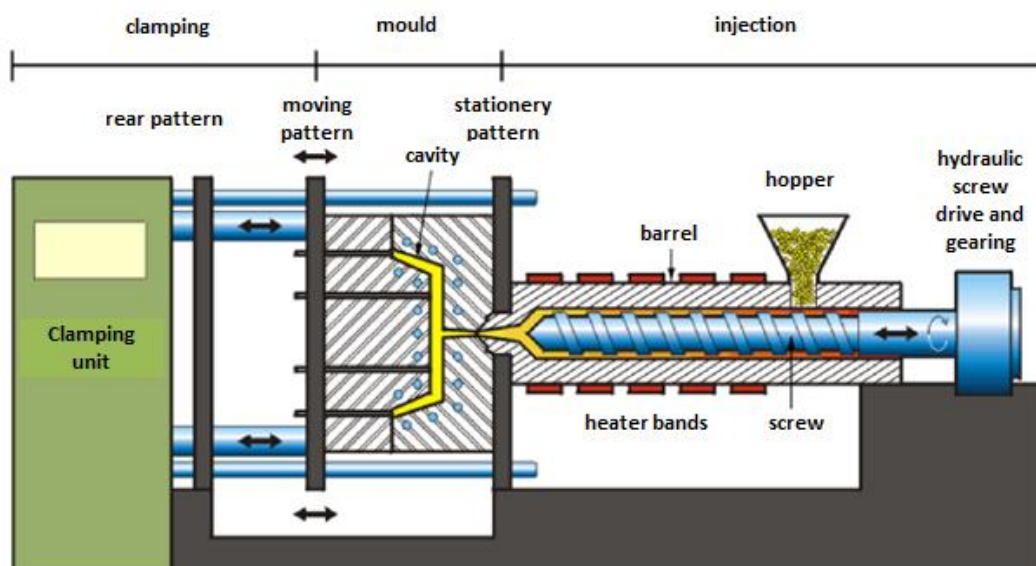


Figure 11. IMM schematics. (Nordgren & Jacobsson, 2012)

Injection moulding is one of the most commonly used techniques to form and creates useful products and is within caps and closures the most important technique. Plastic pellets are entering from a feed hopper into a barrel where the pellets are sheared and melted by friction between the barrel walls and a screw so that it flows, then being injected in the mould (fastened by a clamping unit) through a nozzle and in the mould cooled until it solidifies and then ejected. A schematic picture of the injection moulding machine can be found in Figure 11.

The injection moulding machine (IMM) has three basic units; the injection unit, the clamp unit and the mould. The cycle to produce a part can be divided into 4 steps and are briefly explained below (Ebewele, 2000) (Crawford, 1998):

1. Plasticising/clamping phase: The screw is rotating pulling in new pellets from the hopper, starting to heat the new plastic that is accumulated in front of the screw by moving itself backwards. The output end towards the mould is sealed.
2. Injection phase: When the material is advancing forward towards the mould it gets completely melted by heat and pressure. The valve to the mould opens and the screw is pushing the melt forward through a nozzle into the cavity of the mould.
3. Packing/cooling: There is a build-up of pressure when the plastic is injected, the polymer shrinks when it freezes in the mould, hence, there is a continuous addition of plastic till it is filled.
4. Demould/Ejection: The mould opens and the part is pushed out by an ejector system. The mould is then shut before the next shot is injected.

When the hot polymer melt enters the cold mould, it immediately starts to harden at the walls. Since the temperature is below the melting point the polymer start to solidify, and a so-called skin layer is formed created from the first material that enters the mould. There is an orientation of the polymer chains in this layer due to flow direction. The layer next to the skin layer is called shear zone, where orientation due to shear forces are present. Shear forces together with rapid crystallisation induced by temperature gradient is giving the resulting microstructure. The core layer has a random orientation, where the chains are more relaxed due to slower crystallisation and less shear. The layers are visualised in Figure 12. (Andreasson, et al., 2013).

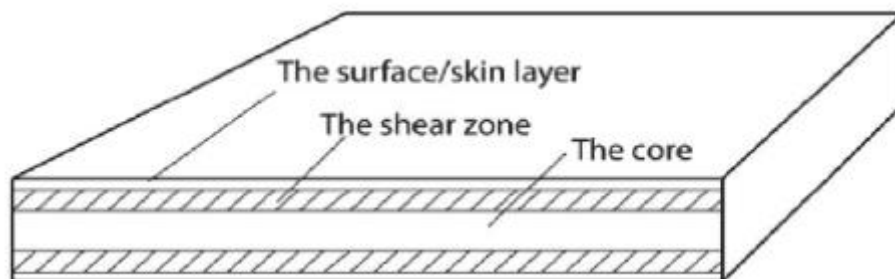


Figure 12 (Lindgren & Hadzic, 2011)

In injection moulding of semi-crystalline polymers such as PP, the spherulite structure will be formed, but most often not in the entire cross section of the material. The spherulite structure is describes more in detail in previous section 2.2.3. *Crystallinity – Morphology*. Depending on which injection speed used, two different types of crystallisation events would take place. Those are called quiescent crystallisation and flow induced crystallisation. Quiescent crystallisation starts due to the shear and elongated flow close to the skin layer, inducing crystallisation even when the temperature is above melting point. The crystallisation mechanism is not fully understood today, where one difficulty is to gain a clear understanding of the nucleating phenomena. Generally, it is accepted that crystallisation is enhanced when a polymer melt is subjected to shear flow. In the core that was previously described, the formation of spherulites occurs. (Han, 2007) The shear zone is assumed to have a morphology

similar to shish-kebabs, providing other mechanical properties to the material. (Mi, et al., 2016). How the actual mechanical properties and microstructure varies in injection moulded polypropylene is very complex. (Gahleitner, et al., 2002)

The process parameters of the injection moulding such as *melt temperature, injection pressure, injection speed, packing pressure* and *packing time* affect the resulting properties of the material created in tensile strength (Singh, et al., 2015). The orientation increase with injection speed (hence, injection pressure) increasing the tensile strength in the machine direction. Although, an increased injection pressure can affect the resulting properties in another way, when causing the mould cavity to fill quicker more relaxation can take place decreasing the orientation. Increase in temperature of the polymer melt cause a decrease in orientation hence decrease in strength. The packing time is if extended to a certain limit increasing the orientation and the temperature of the melt is increasing the orientation if increased hence the strength. If increasing the mould temperature, the orientation decreases. All these properties and how it affects the orientation are illustrated in Figure 13. (Han, 2007)

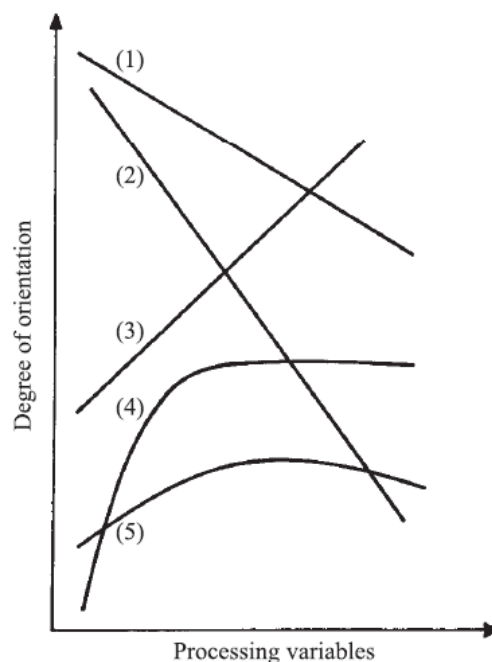


Figure 13. Effect of processing parameters on injection moulded polymer specimen. (1) mould temperature, (2) Cavity thickness, (3) injection pressure, (4) packing time and (5) runner temperature. (Han, 2007)

2.3.2 Compounding - twin screw extruder

When blending polymers in industry one option is to use a twin-screw extruder. The main factors that control the blending are the rheological properties of the different polymers, blend composition, mixing temperature, duration of mixing, design of screws, rotor speed and direction of the twin screws.

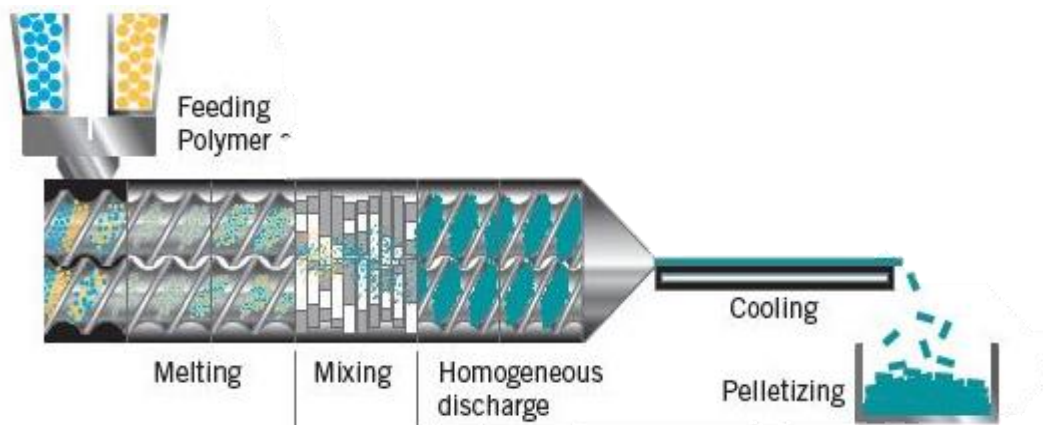


Figure 14. Schematic picture of the twin-screw extruder. (PatricleSciences, u.d.)

In this work, the twin screw extruder was used to create two bimodal polymer samples. The twin screw, instead of single screw, provides a better mixing capacity when compounding. The twin screw can be either co-rotated (both screws rotating in the same direction) or counter-rotated, the one that is used in this work is co-rotated. The twin screw extruder consists kneading elements and mixing chambers, where there normally is 2 - 4 kneading elements and 3 - 5 mixing chambers. The vast majority of the melting takes place in the first kneading element and the molten polymer is then mixed in the mixing chambers. Surrounding the twin screw element there is a heating chamber melting the polymer with different temperature zones. (Han, 2007) There is also a vacuum pump taking away air to minimize air bubbles and other vapours in the polymer. The amount of each polymer to be mixed is measured by sensitive scalars connected to each feeder and a software where the wanted percent (by weight) of each polymer is typed in. A schematic illustration of the twin screw extruder can be seen in Figure 14.

To cool the resulting polymer a water bath was used, see picture 16 (in section 5.3.1). After the cooling the polymer was cut into pellets, which is the resulting product used in injection moulding.

3 Objectives

Objectives of the thesis are to increase the knowledge about how Molecular weight and MWD of isotactic polypropylene affect mechanical and rheological properties, and how it affects the resulting morphology in injection moulding. Part of the objectives are also to examine how the mechanical properties change after injection moulding, during storage, examine when the samples are not changing properties and considered stable.

4 Scope

Examining the influence of Molecular Weight and MWD for isotactic homo-PP, in regards of mechanical properties, rheology, crystallinity and morphology. Also included in the scope of this thesis is to examine how the crystallinity and mechanical properties changes over time in injection moulded plates of polypropylene during storage.

Tensile tests (tensile and tensile impact) are chosen to examine the mechanical properties, and how these change over a specific timeframe. Tensile tests capture certain key-attributes in terms of mechanical properties, as Youngs modulus, yield point of material and elongation at break. Each tensile test will generate a force/displacement graph were these properties can be extracted/calculated. These will be utilised when comparing materials to each other, as well as comparing the same grade to itself, but stored and tested at different timeframes after storage.

Tensile impact tests are performed to study the resilience in the different grades as well as examine if this property changes over time, by being measured at three different occasions over time for each grade.

By using SEM, the aim is to get a better understanding regarding the resulting morphology, since, resulting morphology during injection moulding strongly influence the mechanical properties by creating anisotropic orientation in the polymer.

DSC is chosen as a method to analyse the degree of crystallinity in the different samples. Measurements will be performed at the same occasions as the tensile tests since it is assumed that the degree of crystallinity will change over time. The DCS measurements is assumed to give clues about what happens in the material when stored since post crystallisation is the expected phenomenon to happen and give rise to earlier observed differences in properties during storage.

Rheology measurements by capillary rheometer will be performed to examine how the viscosity changes with different grades, both by comparing bimodal and monomodal grades and within these groups. Rheology measurements by oscillatory rheometry will be used to determine polydispersity by using different kinds of equations describing influence from different parameters and content of chain lengths. These results will then be compared with SEC data received from INEOS, that have contributed with the grades analysed.

5 Experimental Set-Up/Method

5.1 Polypropylene grades

Four grades of homo-PP are received from the polymer supplier INEOS in form of pellets. Two of the grades have approximately the same molecular weight average, a lower, and two of the grades a higher. This correspond to a MI of 25 (lower Mw) and 14 (higher Mw) respectively. The exact M_w and MWD of the polymers are received from the supplier by SEC data, but measurements at Tetra Pak by oscillatory rheometry are also performed to examine how well they correspond. This since it is much more costly and complicated to perform SEC than oscillatory rheometry. The grades are names as following and schematically illustrated in Figure 16.:

Grade 1: Low MW, wide MWD

Grade 2: Low MW, narrow MWD

Grade 3: High MW, narrow MWD

Grade 4: High MW, wide MWD

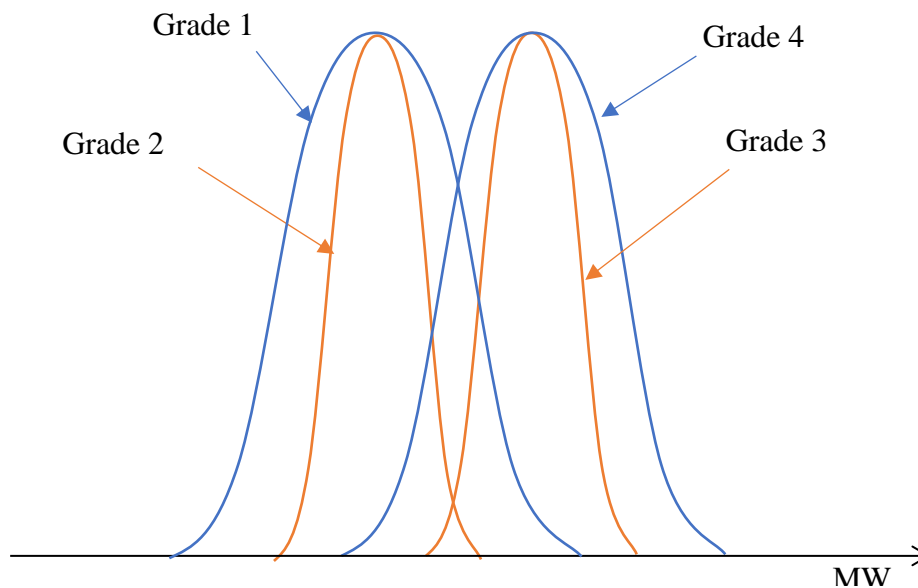


Figure 15. An illustration of how the M_w and MWD differs between the four first grades. This is not a realistic illustration, but illustrate the differences in a schematic manner.

To receive two bimodal polymers, grade 2 are compounded with grade 3 and grade 4 respectively. The compounding takes place in a twin-screw extruder, generating a new bimodal polymer in form of pellets. The grades are mixed 50:50 off each component. To control that no degradation takes place during compounding, onset DSC are performed on all the grades. The new grades are called:

Grade 2 + Grade 3 = 5

Grade 2 + Grade 4 = 6

By the use of capillary rheometry the melt viscosity at higher shear rates are examined to determine the viscosity of the polymer, which is critical in injection moulding. The grades are also examined by tensile testing and tensile impact to tests its mechanical properties, and compared to each other. These properties are known to change over time, being part of the study.

5.2 Test planning

Tensile tests on injection moulded and punched dogbones show certain mechanical properties. By measuring them at different times after injection moulding it can be recorded how the properties change over time. DSC are assumed to reveal plausible changes in degree of crystallinity over time. Tensile tests and DSC measurements are performed at the same occasions to see if changes in mechanical properties are due to changes in crystallinity. The aim is to examine after how long time the crystallisation is finished resulting in a mechanically “stable” polymer. Tests (tensile and DSC) are performed after: ~2.5 hours, one day, three days, 7 days, 2 weeks, 4 weeks and 6 weeks from injection moulding of the grade. If there are strong evidence that the polymer is stable after shorter time, some tests might not be performed, or if no change can be detected.

Strength impact tests are performed after two days, two weeks and four weeks to test if there are any changes in performance. If tensile tests show that there are main changes in the material after this timeframe there would be an addition off more tests.

SEM are used to get a better understanding of the morphology in the injection moulded plates. The aim is to analyse the thickness of the different areas that should form when injection moulding, with skin layer, shear zone and core. This analysis is aimed to be performed after stabilisation of crystallisation have occurred.

5.3 Test set up and procedure

5.3.1 Twin-screw extrusion – Mixing polymer

To compound grade 5 and grade 6 a twin-screw extruder was used (from the manufacturer Leistritz). Grade 5 consisted of equal amount of grade 2 and grade 3 and grade 6 consisted of equal amount of grade 2 and grade 4. The temperature zones that was used for the heating barrels was:

- 1st zone: 180 °C
- 2nd zone: 190 °C
- 3rd to 9th zone: 200 °C

A picture of the hopper and temperature zones can be seen in Figure 17. where the twin screw is inside the barrels with kneading elements. The settings in the program was put to extrude a new polymer with 50:50 weight percent of each component. Cold tap water cooled the polymer in a water bath after the die, picture of this part of the set-up is to be seen in Figure 16. The speed of the extrusion was put to 15 kg/h, which is by previous experiences at Tetra Pak a good speed. This due to the polymer not having too long time in the heating system (and risk to degrade from the heat) and generates a suitable thick extruded rope to cut into pellets with a good size.



Figure 16. Picture of the molten compounded polymer coming out from the extruder, to be cooled in the water bath of cold tap water.

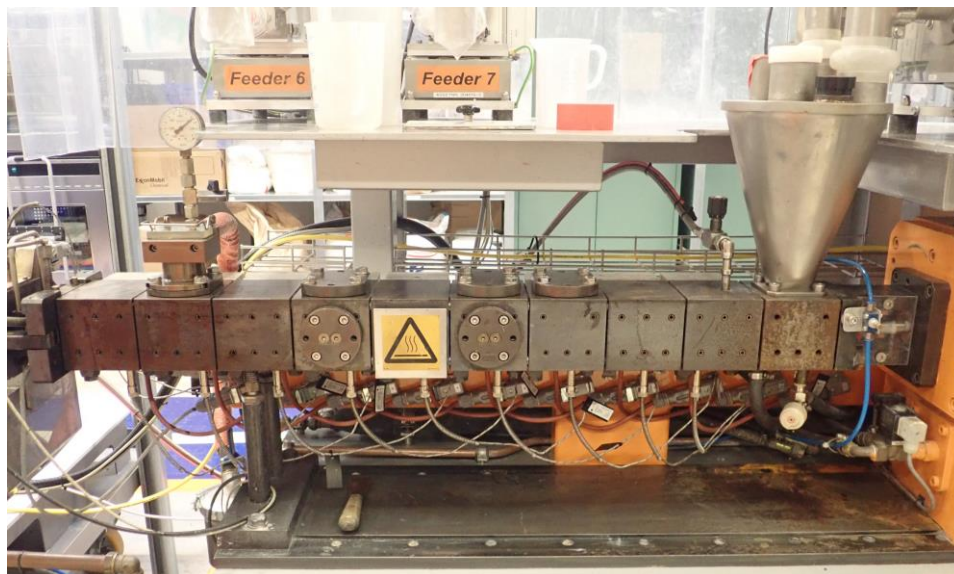


Figure 17. Picture of the hopper and heating elements of the twin screw extruder, where the polymer is entering the extruder and being molten.

5.3.2 Injection moulding

The injection moulding machine used was of model Arburg 470. All grades were injection moulded with fairly the same settings, with 3 holding pressures of 1000, 800 and 600 bars with a holding time of 1 s each. 99% switch over point was used and the injection volume was 11 ccm. Switch over point in ccm was varied between the grades to produce plates of the same thickness for all grades. The mould temperature was 40 °C, the extruder temperature 230 °C and the nozzle temperature 225 °C. The injection speed was put to 25 ccm/s. The settings that were different for the different grades and the resulting injection pressure is to be seen in Table 1. The MWD is affecting the rheology, hence, there is a need to vary the setting a little between the grades. This was done by moving the switch over point, that decides when to switch from filling to packing/holding pressure of the polymer in the mould. The switch over point defines the volume that is left in the extruder when the pressure change from injection to holding pressure. With a more viscous polymer, a lower switch over point is needed.

Grade	MFI (g/10min)	Injection pressure reading (bar)	Injection-volume (ccm)	Switch over point (ccm)	Moulding pressure(bar)
Grade 1	25	1009-1033	11	6	2000
Grade 2	25	1080-1095	11	5	2000
Grade 3	14	1632-1671	11	3.1	2500
Grade 4	14	N/A*	11	3.1	2500
Grade 5	14-25	1481-1513	11	3.2	2000
Grade 6	14-25	1550-1585	11	3.2	2000

Table 1. Injection moulding settings for the different grades. * Value got lost but was similar to the value of grade 3.

The resulting thickness of the polymer plates were in between 0.63-0.60 mm, varying as Figure 18 show. To be able to see the flow lines in the injection moulding of the plates a coloured pellet was added and the result from this is to be seen in Figure 19. Grade 3 and 4 were injection moulded at the same occasion, and grade 5 and 6 were injection moulded at the same occasion. Grade 2 was injection moulded alone. Grade 1 were injection moulded at two different occasions, with the same settings. The reason for not injection moulding more grades at the same time was so that there would be sufficient of time to perform the measurements on the planned test days, as well as a delayed delivery of grade 3 and 4.

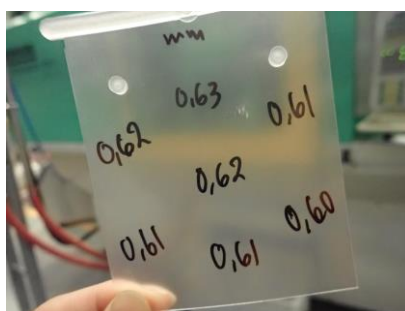


Figure 18. The injection moulded plate and how the thickness vary. Variation is due to the mould being inhomogeneous in thickness, resulting in a possible error source for measurements.



Figure 19. The resulting flowlines when injection moulding the plates, seen by the addition of a pigmented pellet. Orientation of polymer is marked with an arrow. Injection point is outside of picture, on top of the plate (one injection point).

5.3.3 Tensile test

5.3.3.1 Punching dogbones

The dogbones were punched from the injection moulded plates using the punching device seen in Figure 21. The plates were, by the help of markings in an underlying mat, punched in the middle of the plates in different directions. The different directions of punched dogbones analysed was *machine direction (MD)*, *cross direction (CD)* and *diagonal direction (DD)* of the plates. Machine direction is the direction that the polymer moves when filling up the plates, hence, the polymer was sheared in this direction.



Figure 20. Punching device, where all dogbones been punched by hand.

Before punching, the centre of the plates was marked with a line to make it easier to punch consistently. When punching the dogbones in MD the plates was placed with the centre of the plate beneath the centre of the punch, which resulted in a remaining 5 mm of the plate at the bottom edge, see Figure 21. to the left. When punching CD, the plate was centred in the middle of the plate as Figure 21 show (middle). All the dogbones in DD was punched from the top-right corner of the plate to the bottom-left corner, through the centre of the plate (see Figure 21. to the right). To keep track of the origin and direction of the dogbones they were all marked accordingly.

The dogbones and injection moulded plates have all been stored in a climate room in a box being protected from light. The temperature of the room was 23 degrees with 50% relative humidity.

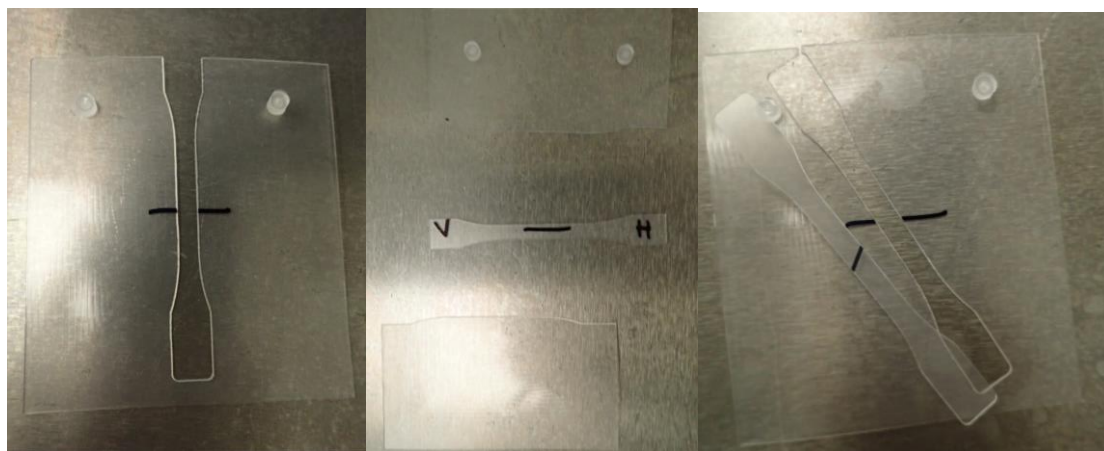


Figure 21. Punching of dogbones in MD, CD and DD on the injection moulded plate, with helplines to easier see the centre of the plate when punching.

5.3.3.2 Tensile testing

To perform the tensile tests the machine *Zwick Z010 Proline with climate chamber* was used together with the software *testXpert II*. The dogbones were punched with help of equipment and method previously described.

When performing the tensile test of the dogbones punched in the machine direction (MD) of the injected moulded plates the upper part of the dogbone (which is the upper part of the plate) were placed upwards in the clams of the tensile machine. When placing the dogbones punched in the cross direction of the plates the right side of the dogbone were places upwards in the tensile machine. When placing the dogbones that were punched in the cross direction of the plates in the clams of the tensile machine, the upper (from the top-right corner of the plate) part of the dogbones were placed upwards in the machine and the bottom corner downwards. A mounted dogbone can be seen in Figure 22.

The tensile tests performed in this study was by static testing, where the machine is stretching the dogbone by the speed of 100 mm/min. Of the clams that the dogbone was mounted in, one was moving and the other was static. The force needed to stretch the sample was recorded. The tensile response was plotted as force (N) versus elongation (mm). From the raw data from

these measurements it was possible to extract Young's modulus, elongation at break and yield point.

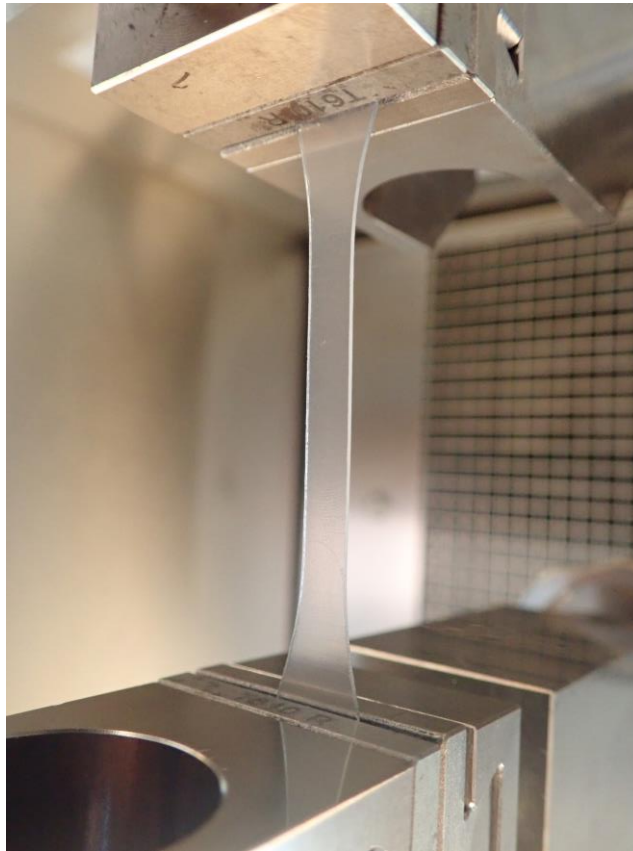


Figure 22. Dogbone mounted in clamps in the tensile test equipment.

5.3.4 Tensile impact

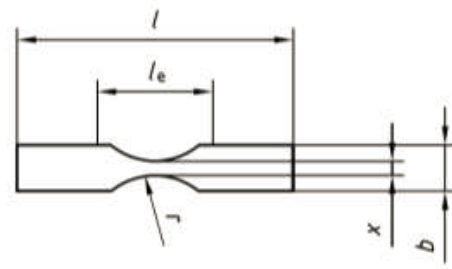
To perform the Tensile impact tests an Instron Ceases 9050 Instrument was used with DAS 64K connected to a PC using the software CWMain 6.01. Dogbones were punched from the injection moulded plates, compared to the dogbones used for tensile measurements these are smaller with the dimensions as specified in the table below, seen in Figure 24. The thickness of the dogbone (at centre) was measured and put into the software, measured with the caliper seen in Figure 23. 10 dogbones were tested in each batch. The instrument is calibrated every second year by the instrument supplier specialist. The hammer is calibrated before each measurement.

The dogbone was mounted by one side in a holder (called cross-head) by a torque wrench, that was set to a predetermined torque of 30 cNm. The sample must be mounted perfectly straight and centred in the holder. The dogbone and cross-head were then mounted in the tensile impact instrument by a fixed sample holder, by help of specimen aligner and centred between two vertical lines to guarantee a straight sample. It



Figure 23. Measuring equipment to determine the thickness of the dogbones used in tensile impact testing.

was then screwed onto place by a torque wrench with the torque of 100 cNm. The sample mounted is shown in Figure 25.



Parameter	Value (mm)
l	60±2
le	25±2
J	15±1
x	3±0.2
b	10±0.2

Figure 24. Dimensions of dogbone, where the parameters are specified in mm in table above. (Andersson, 2012)

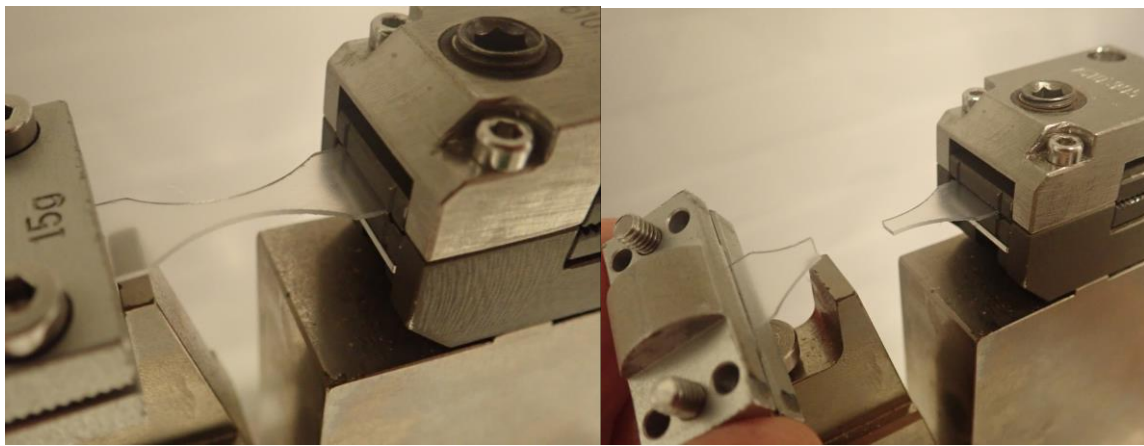


Figure 25. Dogbone before (left) and after (right) performed test, mounted in the test equipment.

The test was performed within the ISO 8256 standards, with the force of the hammer put to 2J (when hitting the sample) giving the velocity ~ 2.9 m/s when hitting the mount (cross-head) of the dogbones on both sides. The weight of the cross-head was 15.0 g, and the sampling frequency 1000 kHz. The number of points sampled was 10000. The test was performed and over within a couple of milliseconds, when deformed and fractured by the hammer.

The raw data obtained was the voltage as a function of time, where the voltage was converted into a force. The force was plotted against time or deformation in the software, where a number of outputs can be obtained. The resilience was calculated as the total energy uptake divided by the initial cross section area of the narrow part of the dogbone.

5.3.5 SEM

The analysis was performed on the different grades by analysing the cross-section at the middle of one dogbone punched in MD direction. To prepare the specimens, the dogbones were notched by a knife and held down into liquid nitrogen to freeze. When holding there for around 20 s the dogbones were broken, to create the surface that was analysed. The surface was then isolated by being cut off from the rest of the dogbone and placed on a specimen-plate with the surface of interest facing upwards. The specimen was placed in a sputter coater

(Balzers, SCD 004) connected to argon gas, sputtered under vacuum (5×10^{-2}) with resulting plasma formation. Settings were 35 s with a current of 35 mA creating a 15 nm layer thick coating of palladium/gold (80/20). Picture of the sputtering during plasma formation can be seen in Figure 26.

After the sputtering the specimen were placed in a holder for three samples, se Figure 28. and Figure 27 for the individual samples. Since the specimen were notched it was of importance to remember what part of the samples that were from the frozen breakage (since this is where there would be a chance to see the different layer structures, the cut would just smudge the polymer). The specimen was hence placed with the part of the surface from the break towards the centre of the round holder. Then the specimen holder was gently placed in the SEM in the vacuum chamber and the analyses performed, and images recorded with the different magnifications of 60/110/230x. The analyse of grade 3 and 4 were carried out 16 days after injection moulding and grade 2 was injection moulded 22 days before analysed, these analyses were performed at the same occasion. The analyse of grade 1 was performed 24 days after injection moulding, and of grade 5 and 6, 31 days after injection moulding, grade 1, 5 & 6 were analysed at the same occasion.

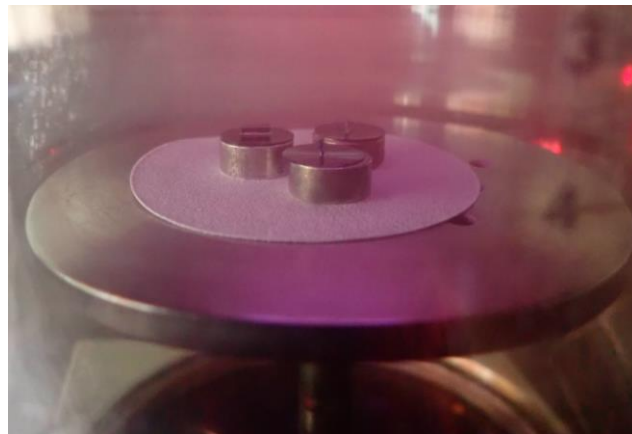


Figure 26. Plasma when sputtering the samples, created by argon gas and palladium/gold.



Figure 27. Specimen holder with polymer on top with the surface of interest facing upwards. The specimen and holder have been sputtered with a 15 nm thick layer of palladium/gold (80/20).



Figure 28. Specimen with specimen holder, where the surface of interest (due to the notch) is placed in towards the centre of the holder.

5.3.6 DSC

5.3.6.1 Enthalpy and heat flow

The DSC was performed on the injected moulded plates at a certain position, see Figure 29 (to the right), to eliminate that the position of the sample would influence the results of the measurements. The position was chosen due to it being the spot where the breakage happened during tensile tests (seemed like a weaker point that would be of interest). A puncher and hammer were used to get the same dimensions of the samples every measurement and two samples were taken from two different plates at every test occasion. The tests were taken at the same days (2.5 hour, 1 day, 3 days, 7 days and 2 weeks) as the tensile testing was performed, to see if there was a correlation between the crystallinity of the plates and the mechanical response. The samples were weighed (with the scale “Mettler Toledo” with a sensitivity of 10^{-5} g) and then placed in a “Tzero Pan: article no: T160606” with a lid “Tzero Lid: article no: T160211”, pressed down by the help of a T-zero press. It was of important that the sample was in contact with the bottom of the pan to guarantee good measurements. The reference sample in the SupplierTa – instrument was an empty pan with lid. The samples were placed in numbered slots in the machine.

The machine and software used for the DSC measurements were DSC Q100 with an upgraded software to Q200 (SupplierTa – instrument), see picture in Figure 29 to the left. The DSC machine is calibrated once a year by TA- instruments. The temperature calibration of the machine is checked every second month with indium to guarantee correct measurements.

The method chosen in the software were called ASTM-D3428_PP and included 2 heating cycles and one cooling. The program used follows:

- Ramp 10 °C/min from 35 °C to 210 °C followed by isothermal holding for 10 min.
- Ramp with -10 °C/min to 0 °C, when reached holding isothermal for 3 min.
- Ramp by 10 °C/min to 220 °C, when reached end of program.

For measurements the weight and program to run was put in the software and the total run-time for one sample was about 1.5 h. From the run the data is interpret by the help of the software TA Universal Analysis and integration in the program by help of a linear baseline. The baseline was after several tries put to be between 100 – 199 °C, since this seemed to give the least of the variations between the measurements that should be identical (the two samples taken at the same time).

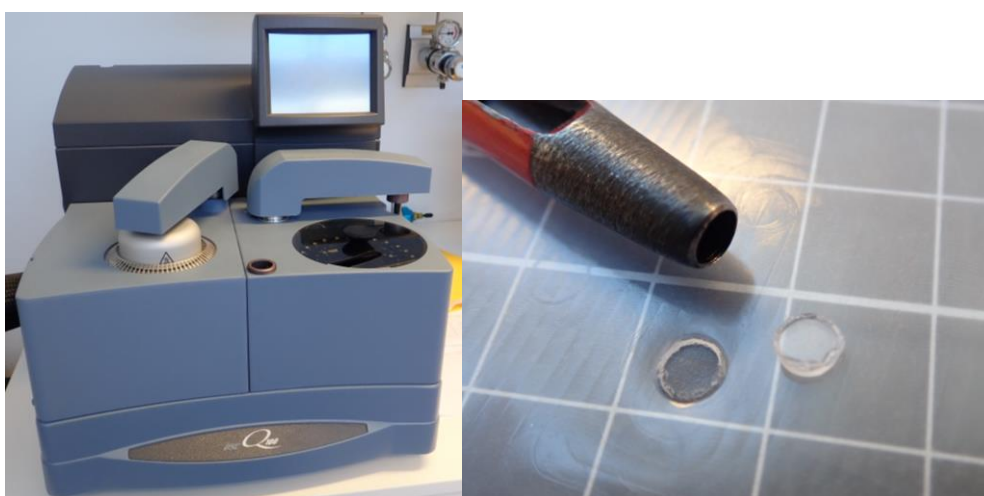


Figure 29. To left: SupplierTa - Instrument Q100 with upgraded software Q200 (DSC). To right: Punching device and plate showing the sample that is put into the pan.

To interpret the results of the DSC enthalpy, baselines between 100 °C and 199 °C were used in the TA universal analysis software. Linear baselines were used, in Figure 30 a typical heat flow graph can be seen with baseline. This specific baseline was used due to experimental trials where this baseline seemed to give the least of fluctuation between the samples that were analysed and taken at the same time. This baseline was used on all analyses. When integrating to examine crystallinity this baseline was used as well and the value 207 J/g for heat fusion. (Wunderlich, 1990) When the software calculates crystallinity, it uses the formula:

$$\%Crystallinity = \frac{\text{area (enthalpy)}}{\text{Heat fusion}} * 100$$

The heat flow graphs received after each measurement were overlaid on top of each other to see if there were any changes in heat flow (hence, enthalpy and crystallinity) over time of storage.

When performing the tests it was observed that there was no clear difference in enthalpy during storage, hence, the 4 weeks and 6 weeks measurement was not carried out. The tests were performed for each grade up to 2 weeks in storage. One measurement occasion is missing from grade 1 at 2.5 hours after injection moulding, this since the reference pan was not in contact during the measurement. Hence, the result is not trustworthy. There was not time to repeat the injection moulding to redo the measurement.

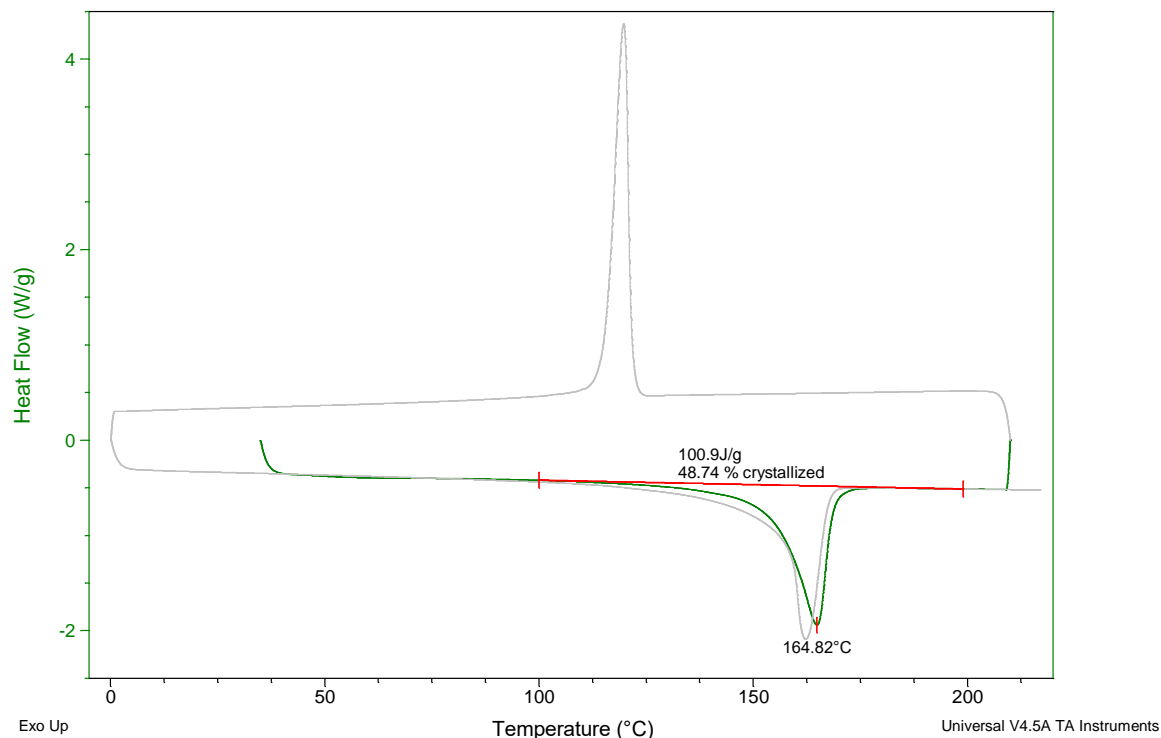


Figure 30. Example of integration made by the help of the software TA universal and raw data obtained. Analysis is performed on the first melting of the polypropylene and the value 207 J/g that is specific for PP is used to calculate crystallinity. The baseline is between 100 °C and 199 °C.

5.3.6.2 DSC Onset

Another DSC test was also performed on all grades one time, on pellets. The purpose of this test was to find out if any degradation takes place during the compounding of the polymers. The polymer pellets were melted during similar conditions as DSC previously described, but this time until melting and degradation of the polymer. Heat flow was recorded as for normal DSC.

5.3.7 Capillary rheometer

Capillary rheometer measurements were performed on pellets, requiring 100 g sample size. The name of the capillary rheometer used were rheography 75. purchased from the supplier Goettfert. The rheometer was calibrated yearly as well as the pressure transducers. The pressure transducer was also controlled 1-2 times a month by performing measurements with reference material. The diameter of the barrels used were 12 mm and the software used were

LabRheo 2.1.4. The shear rates used were 10000. 6000. 2000. 1000. 300 and 100 (1/s) respectively. The tests were performed at 210 °C. When the samples were filled into the rheometer the pellets were manually pushed together to avoid air bubbles. The tests were then performed as specified by standards to the machine, starting when the difference between the temperature zones was less than 0.5 °C.

When the tests are performed the software Win RheoII were used to correct the measurements with Bagley and Rabinowitsch-Weissenberg. Bagley correction was needed as described in the theory section, Rabinovitch-Weissenberg is a correction factor for non-parabolic velocity profile effects due to shear at the wall. The tests for grade 1-4 was performed at one occasion and the test on grade 5 and 6 was performed at another occasion later time.

5.3.8 Oscillatory rheometry

Oscillatory rheometry tests were performed on the rheometer Physica MCR301 purchased from the supplier Anton Paar. The tests were performed on pellets pressed to plates by the machine Laboratory Platen Press, type 200M from supplier Dr. Collin GmbH. The plates were pressed at the temperature 175 °C. The settings were put to 60 s for step one in the press and 90 s for step 2, with 50 bars of pressure in step 2 and a press by 153 N/cm² with a resulting thickness of 1 mm thick plates. Only plates with no resulting air bubbles were used.

The rheometer used was a rheometer building on the parallel plates methodology, having a gap of 0.98 mm between the plates and the diameter of 25 mm. Measurement sweeps were performed at 170 °C, 190 °C, 210 °C and 230 °C. The rheometer was calibrated once per year by Anton Paar and at the beginning of everyday the machine was checked for consistency by doing measurement on a reference sample. η_0 and G' was from this consistency measurement recorded and kept as history. The requirement when controlling the temperature was ± 0.5 °C. The rheometer was running together with the software Rheoplus/32 V3.62. and the rheometer needed both air and nitrogen connection. The nitrogen prevents sample oxidation.

Oscillatory frequency sweeps were then performed according to standards, in the range of 100-0.01 Hz in 20 logarithmic steps. The stress was chosen such, that the resulting strain is lower than 0.4, which is the limit for the viscoelastic region. The sample were put between the plates to melt for 2 minutes, and then trimmed with the oven opened to remove excessive polymer. Each measurement was performed on new plates, with approximately 10 min between each measurement to guarantee stable temperature and force.

These sweeps were then put together by help of the software to 2 master curves for each grade, with 170-210 °C and 190-230 °C respectively.

5.4 Analysis of test methods

5.4.1 Tensile tests

5.4.1.1 Change of direction of punching (CD)

To examine whether any fault in the punching device might influence the result of the tensile tests, 5 dogbone were punched in the cross direction in one way and 5 dogbone punched reversed on the plates. They were put in the machine with the upper part of the plates up in the machine. The average result of the 5 tests each is to be seen in Figure 31. with the data presented in Table 2. The speed that was used was by 50 mm/min, slower than the speed normally used for extra sensitivity. Cross direction was chosen since the elongation at break is shorter, and the standard deviation smaller. The average maximum force at yield was for the normally punched dogbones 99 N and for the reversed punched dogbones 97 N. The standard deviation for the different series are 3.7 N (normal) versus 1.7 N (reverse). The difference in result was very small, not significant, but there might be a tiny impact from the punching of the result. Pictures of the dogbones after tensile testing is to be seen in Figure 32.

Test Serie	Fmax (N)	Stand. dev. (N)	dL at break (mm)	Stand. Dev. (mm)
Normal	99	3.7	7.8	0.57
Reverse	97	1.7	7.9	0.36

Table 2. Showing the result of tensile testing when changing the direction of punching of dogbones in CD. No difference was detected.

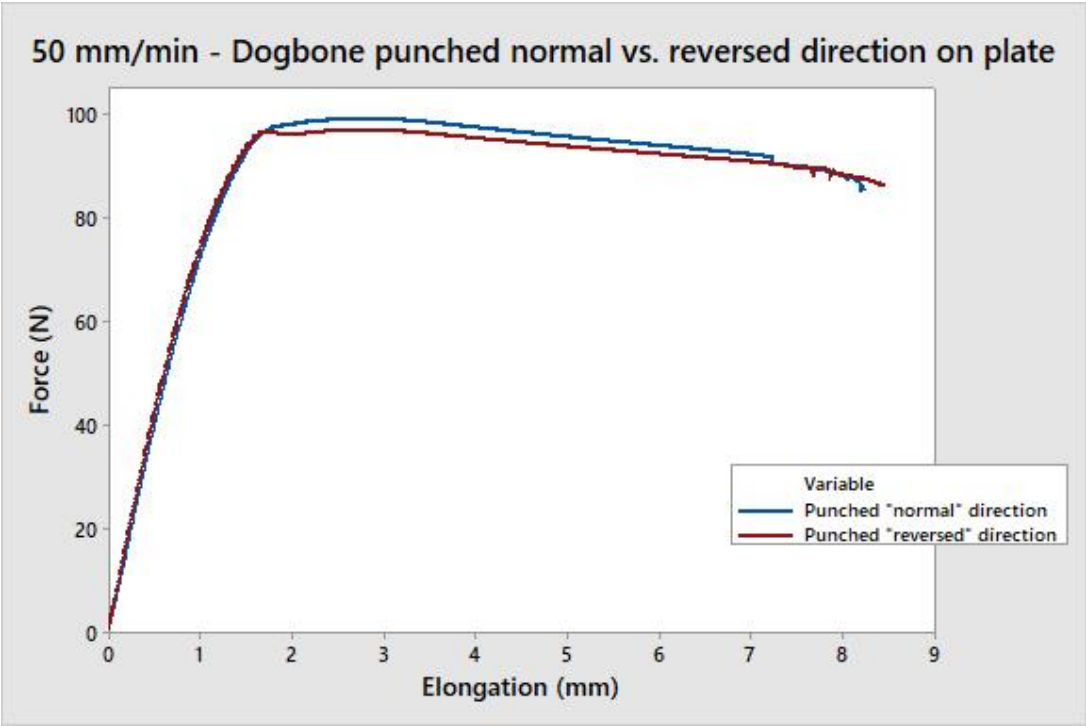


Figure 31. Cross direction punched in normal and reversed way to examine if there is an influence from the punching device on the result.

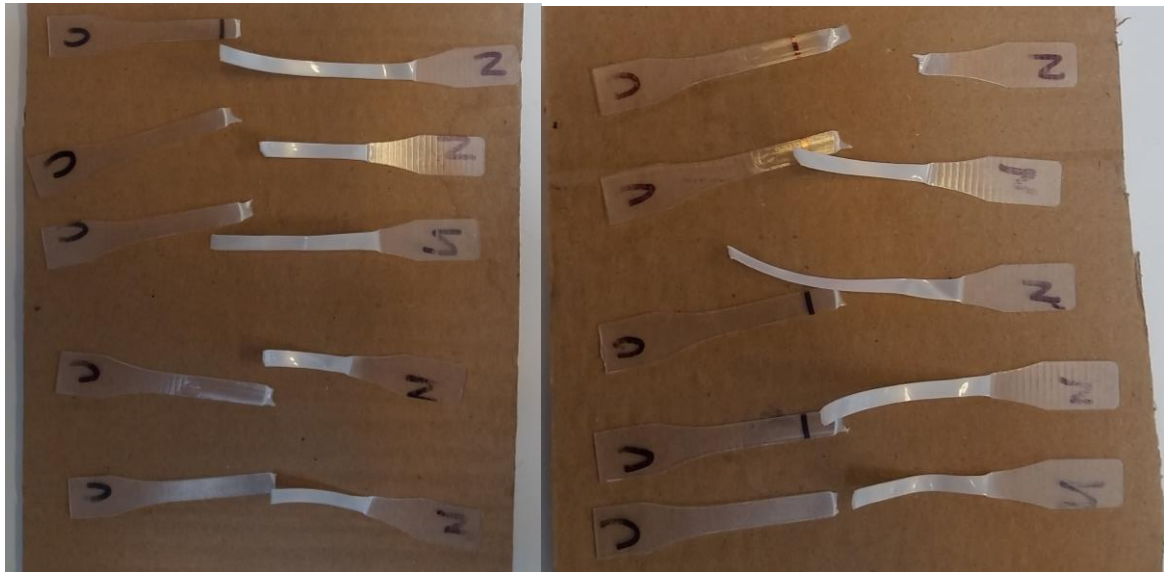


Figure 32. The serie to the left is punched upside down and the serie to the right is punched the normal way. Showing dogbones after tensile testing.

5.4.1.2 Change of speed of tensile test (CD)

To analyse the influence of speed of tensile two different sets of tensile tests were performed with different speed, 50 mm/min and 100 mm/min. The average results are to be seen in Figure 33. with key data presented in Table 3. The maximum average force when yielding received in the case of 50 mm/min is 98 N and when using the speed of 100 mm/min the maximum force when yielding is 105 N. This is well outside the standard deviations of 1.6 N respectively 2.0 N. There is hence a noticeably difference in performance due to what speed that is used. The average elongation at break is for 50 mm/min 7.9 mm with a standard deviation 0.43 mm. The average elongation at break for 100 mm/min is 6.0 mm with a standard deviation 0.73 mm. Hence both the maximum force at yield and the maximum elongation at break is affected by the speed of elongation. The speed used in all measurements will be set to 100 mm/min so that tests can be compared to each other. 100 mm/min will be used for the convenience of faster tests.

Test Serie	F_{max} (N)	Stand. dev. (N)	dL at break (mm)	Stand. Dev. (mm)
50 mm/min (n=9)	98	1.6	7.9	0.43
100 mm/min (n=7)	105	2.0	6.0	0.73

Table 3. Table showing the result when performing the tests in CD, with two different speeds of elongation.

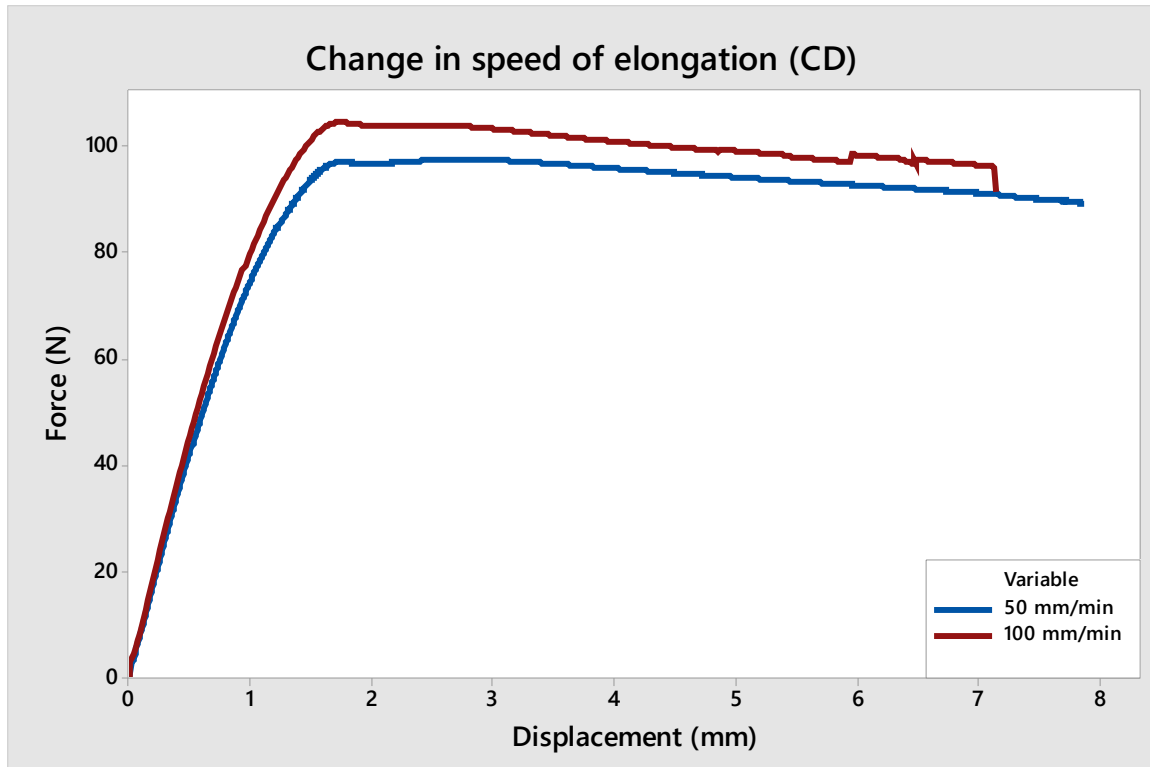


Figure 33. Change of speed of elongation and its influence of average force at yield and elongation. The reason for the non-smooth line when tensile with 50mm/min is that it is an average.

5.4.1.3 Change of direction of dogbone in machine

To analyse if the direction of the dogbone placed in the machine would affect the result 8 dogbones were punched in the machine direction and 4 dogbones were placed with the upper part of the bone up in the machine and 4 was placed with the upper part down. The average result of the both series is to be seen in Figure 34. and some key data in Table 4. The maximum average force received were 130 N respectively 130 N with a standard deviation of 3 N respectively 0.1 N. The average elongation at break received were 32 mm with a standard deviation for the first series of 17 mm and for the second series 43 mm with a standard deviation of 11.7 mm. The elongation at break variations is within the standard deviation and the difference in maximum force at yield is very small (less than 1 N) so it can be stated that the influence of up and down in the machine is close to none. Dogbones after performed test are to be seen in Figure 35.

Test Serie	F_{max} (N)	Stand. dev. (N)	dL at break (mm)	Stand. Dev. (mm)
Normal	130	3.0	32	17.0
Reverse	130	0.1	43	11.7

Table 4. The result from tensile test when the dogbone were placed in two different direction in the machine.

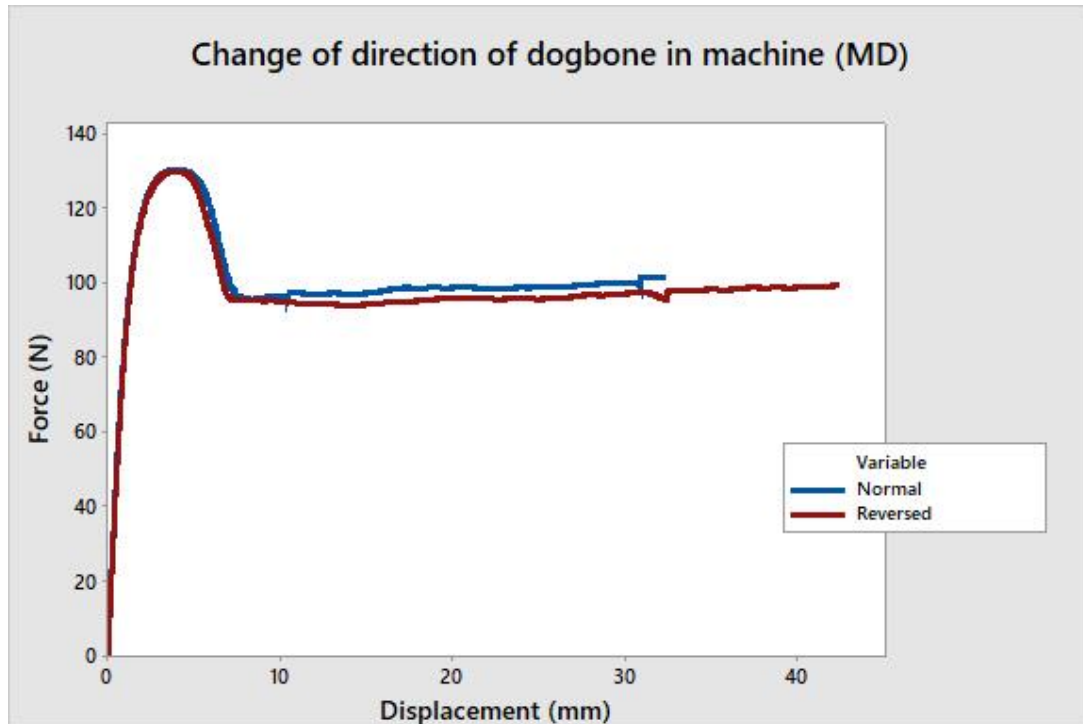


Figure 34. Influence of placement normally and reversed in the machine.

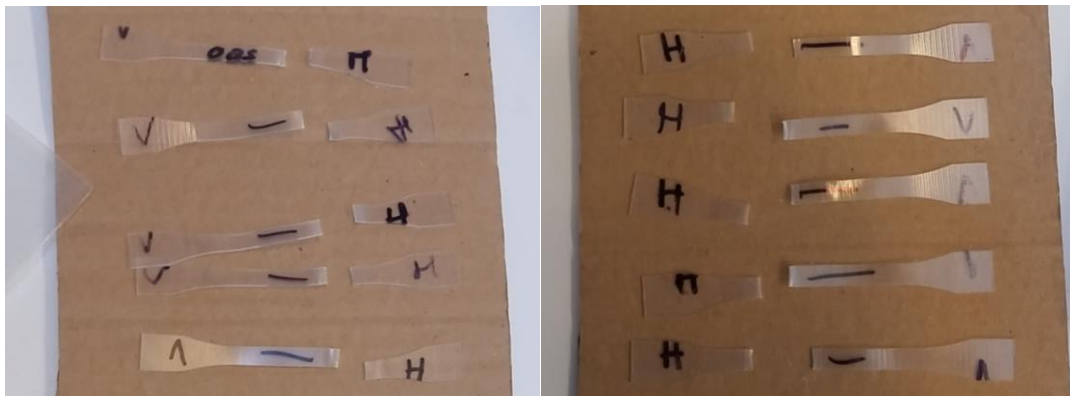


Figure 35. Showing the dogbones after tensile testing, the left picture is the serie called normal and the right is serie reversed. The pieces on the picture to the left has had the end marked V up in the machine and the picture on the right had the end marked H up in the machine. V is the left side of the injection moulded plate and H is the right side of the plate.

5.4.1.4 Change of distance from edge when punching plates (MD)

To examine if there is an impact on test result due to where the centre of the plate is on the dogbone, three different tests were performed with different punching. The background to performing this test was an observation made that the elongation in necking in MD was not random within the thinner area, it was almost always below the middle of the dogbone. To get the centre of the plate in the middle of the dogbone, the dogbone is punched 5 mm from the bottom edge if the plate. The tests that were carried out where 0 mm from the edge, 5 mm from the edge respectively 10 mm from the edge of the plate. 5 tests were performed on each of the series. Dogbone with the distance of 5 mm from edge is to be seen in Figure 36.

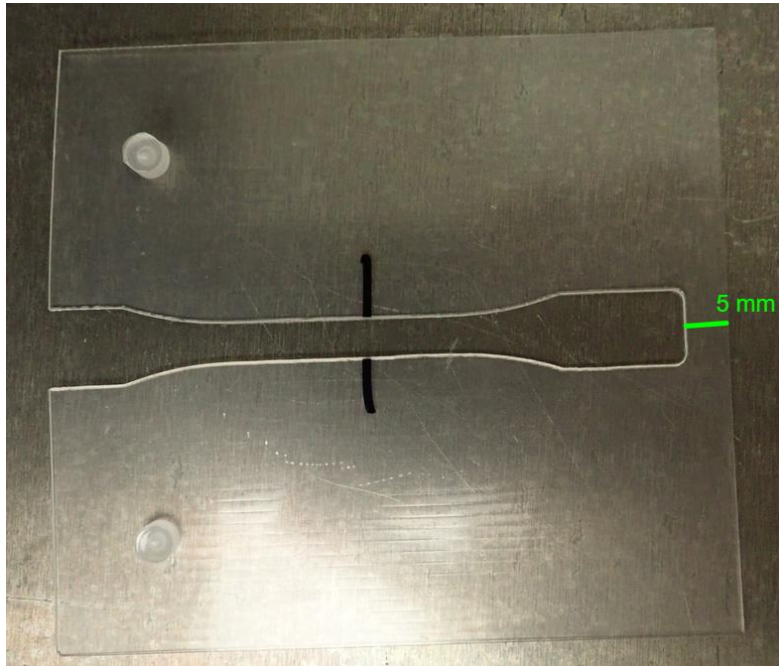


Figure 36. Showing the distance 5 mm from the edge when punching. The tests were performed with punching 10 mm, 5 mm or 0 mm from the bottom edge.

Test serie	F_{max} (N)	Stand. dev. (N)	dL at break (mm)	Stand. Dev. (mm)
0 mm	129	2.2	60	22.7
5 mm	126	2.7	35	15.6
10 mm	136	1.5	26	4.2

Table 5. Tensile tests performed on three different sets of dogbones that were punched with different distance from the edge.

From this result is it possible to observe a change in elongation at break due to how the dogbone is punched, that is illustrated in Figure 38 by plotting, and Table 5 where key values are presented. Comparing 0 mm and 5 mm punching distance there is no clear difference (the confidence interval overlaps at 95%), but when comparing 0 mm and 10 mm there is a difference. Hence, it is of importance to punch all dogbones the same at the plates, since it seems to affect the results of the measurements. 5 mm from the edge with the centre of the plate in centre of the dogbones were chosen to be the punching method to be continued with as used in MD testing. To verify the findings two hypothesis tests were performed that conclude that there is a significant difference among the means of the different punching distances (concluding that 0 mm and 1 cm differ with a 0.05 level of significance in both elongation at break and F_{max}) with the help of *minitab*, these tests can be found in Appendix 11.1.1.

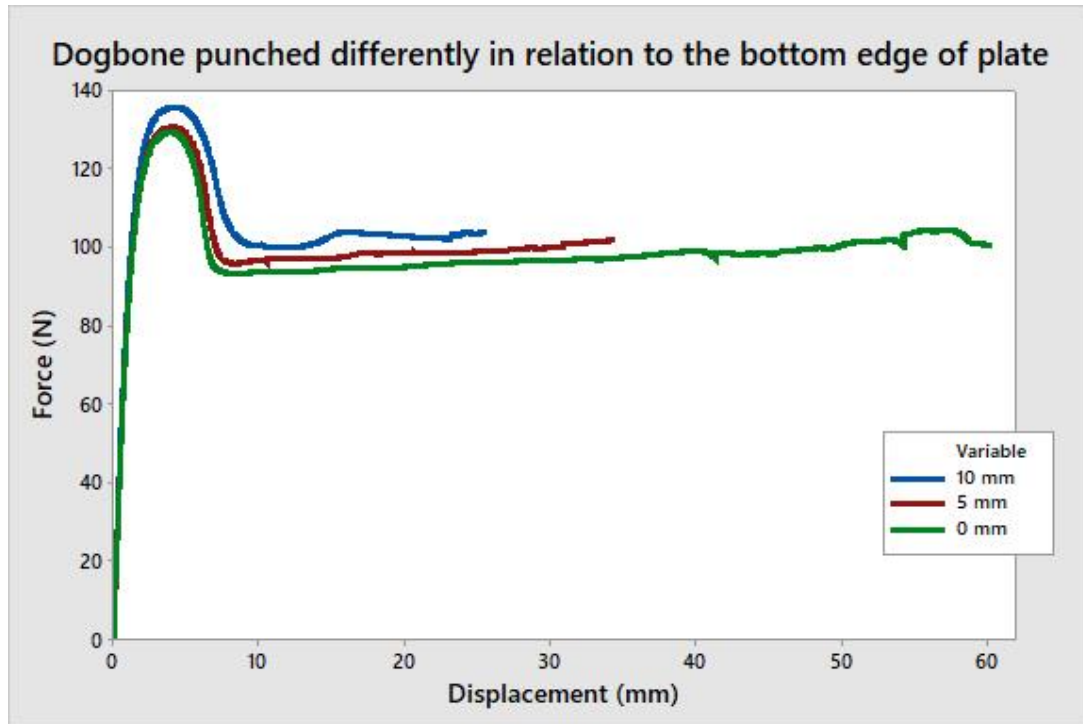


Figure 37. Showing how the tensile test results vary with how the dogbone is punched.



Figure 38. Tensile tested dogbones, punched:(left) 0 mm, (middle) 5 mm, (right) 10 mm from the edge of the plate. The middle of the plate is marked by a line.

5.4.1.5 Observed difference in tension between CD, MD and DD

As shown in Figure 39 there was a big difference in elongation at break and how the sample was elongated between CD, MD and DD. In CD the dogbone breaks without much elongation, in MD the dogbones break after elongation and in DD the break takes place after yield and strain hardening. To receive a proper stress/strain graph the elongation of the dogbone must take place only in the thinner region of the dogbone with define dimensions. This was not the case for MD and DD elongation, where the elongation occasionally in MD occurred outside of this area, and in DD happened consistently throughout the measurements. Instead of stress/strain graphs, force/elongation graphs were used to illustrate the tensile test results. What also can be noticed was that the break does not happen randomly in the middle

on the dogbones, it happens closer to the right side of the CD dogbones and closer to the lower part of the injection moulded plates bottom than the centre. Almost all of the elongation occurred below the centre of the dogbones in MD. When observing tension of the DD dogbones strain hardening occurs over the entire dogbone and fibres were a result after break.

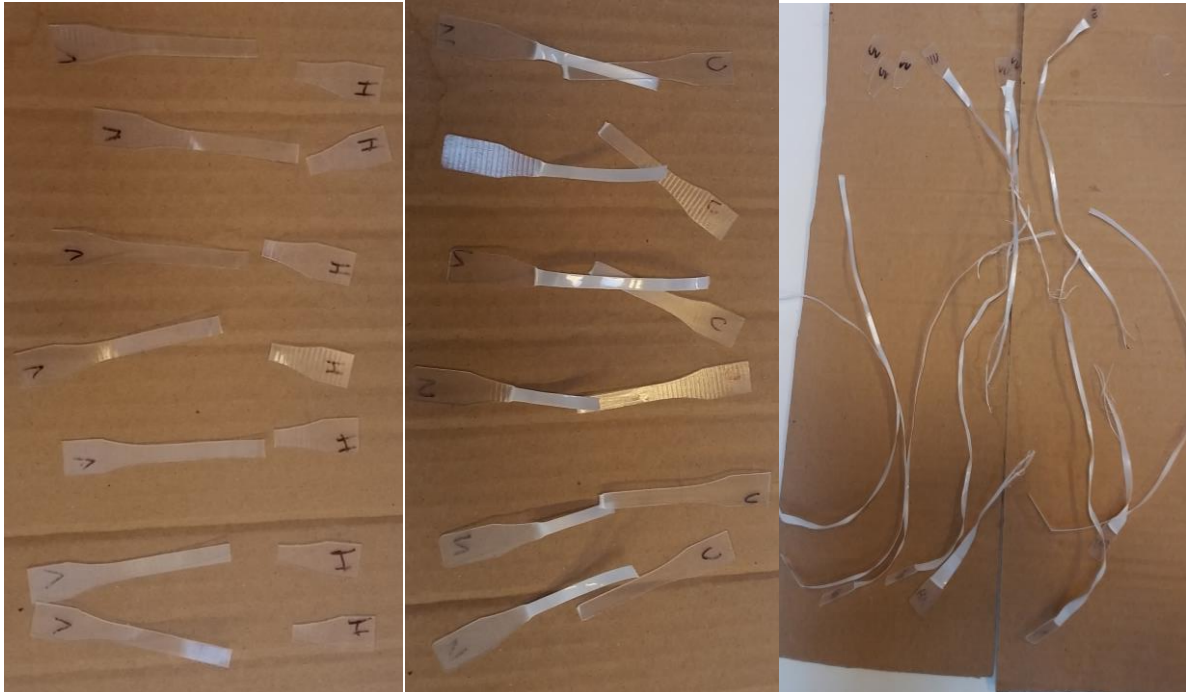


Figure 39. Picture showing dogbones after tensile testing. Left: Cross Direction. Middle: Machine Direction. Right: Diagonal Direction.

5.4.1.6 Conclusion

Summarising the findings;

- It was not of importance to keep track of up and down of the plate when mounted in the machine, this does not affect the results of the measurements noticeably (see section “*Change of direction of dogbone in machine*”).
- It was not of great importance if the dogbone is punched reverse or not (see section “*Change of direction of punching*”).
- When performing the tensile testing it was important to punch the dogbone at the same place in the plate to guarantee as little variation as possible, see section “*Change of distance from edge when punching on plate*”. This variation might be due to several properties on the plate, but the estimated two most prominent factors was most likely a slight thickness variation over the plate together with different orientation of molecule chains due to cooling in the mould and shearing.
 - a. When punching dogbones in CD, the bones were punched with the centre of the plate in the middle
 - b. When punching the dogbones in MD, the centre of the plate was in centre of the bone, where the punch was 5 mm from the edge of the plate.

- c. For DD punching the centre was put in the middle of the dogbone and was tilted so that the top corner of the dogbone was left/up on the plate and the bottom was right/down on the plate.
- When analysing the results from tensile tests it was more correct to use a force/displacement graph than stress/strain since the elongation take place outside of the fixed dimensions of the neck as the specimen was deformed.

5.4.2 DSC

Initially when performing DSC on the first test series an inconsistency in results was observed. Therefore, an analysis was performed to see if the results would vary depending on where on the plate the piece for analyse were taken. The samples were taken as seen in Figure 40. In the table an integration over both generated melt peaks from the first and second cycle is compared to study the deviation but only a graph (Figure 41) of the first melting is displayed beneath (with the 5 tests overlayers). This since the memory of the polymer that was of relevance should not be present during the second heating. Result was that the first test differs from the other. To minimise errors, the tests were performed on the same position on the plate as described in method section.



Figure 40. Showing where the test pieces were samples on the plate.

The corresponding DCS analyses were as follows and the results are assembled in Table 6:

Grade 1. tests (22/2) (Not used, IMM test batch)

<i>Test</i>	<i>First melt integration (J/g)</i>	<i>Peak melt Temperature, First (C°)</i>	<i>Second melt integration (J/g)</i>	<i>Peak melt Temperature, Second (C°)</i>
1	94	165	103	160
2	96	164	105	160
3	95	164	106	159

Grade 1. tests (22/2) (Not used, IMM test batch)

Test	First melt integration (J/g)	Peak melt Temperature, First (C°)	Second melt integration (J/g)	Peak melt Temperature, Second (C°)
4	97	164	106	159
5	96	164	106	160
Std. Dev.	1	0.5	1	0.1

Table 6. Different tests by DSC were made to determine enthalpy and examine if the result varies depending on where the sample is taken.

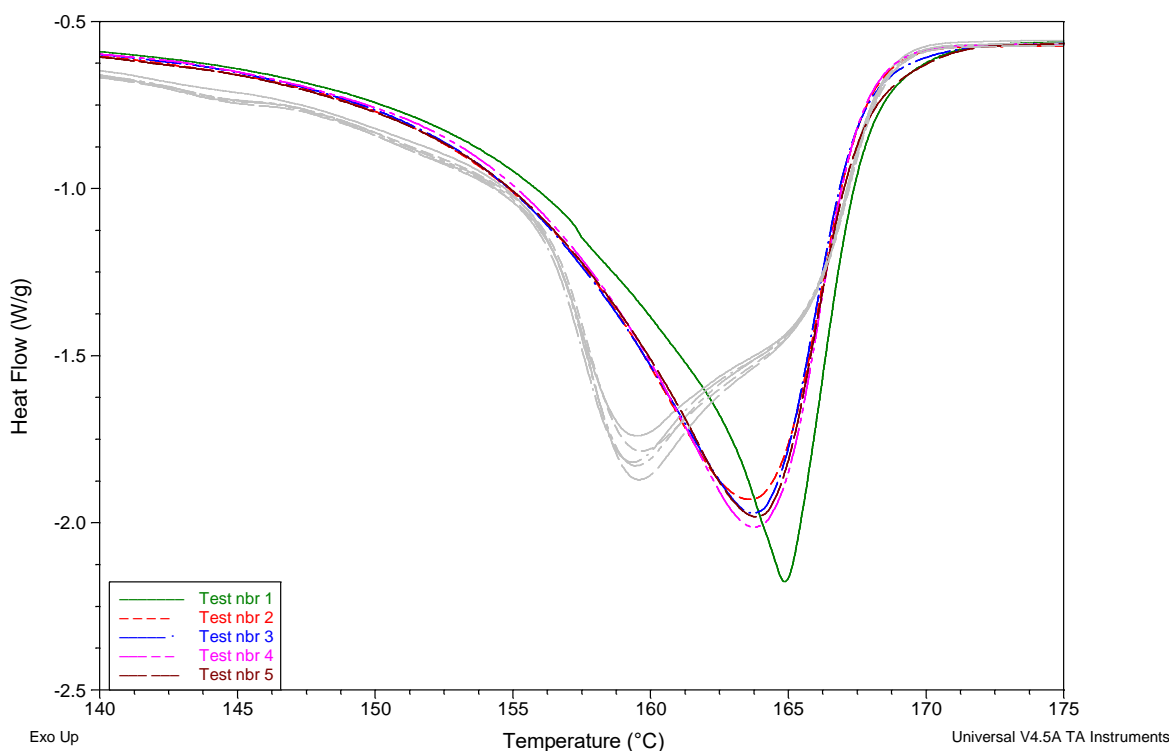


Figure 41. DSC Curves overlaid for the different tests performed. One of the curves (test number 1) differs from the other. This might be due to contact with the pan or due to other errors in the measurement, or due to the material properties.

5.4.2.1 Conclusion

Summarising the findings;

- The melt enthalpy varies between the point of measure in the same plate at the same storage time, by the standard deviation 1 J/g (when 5 tests were performed)
- Peak melt temperature varies over the plate by 0.5 °C in first melt cycle
- Tests will be performed at the same place on the plate to minimise source of errors.

6 Results

6.1 Oscillatory rheometry

To interpret the experimental results in Table 22-27 (in Appendix 11.2) for grade 1 - grade 6 different calculations were used, *equations to be found in theory section*. The aim is to study the rheology to determine the polydispersity of the grades and correlate this to the MWD of the different polymers.

To calculate the different parameters described in the theory part (PI, ER and PDR) equation [1-3] was used. G' is reflected in ER measure. To find the values needed in the equations from Table 22-27 interpolation was used by the linear equation. The received values describing polydispersity of the different grades are presented in Table 7 together with received SEC data from supplier. SEC data received from supplier are presented in a graph (Figure 108) in Appendix 11.7 together with raw data in Table 35. To examine which rheology measure that fit best to the polydispersity form SEC, plotting as seen in Figure 42 was performed.

grade nr:	MFI (g/10min)	From SEC - INEOS					From MA Lab – Tetra Pak			
		M_n (g/mol)	M_w (g/mol)	M_z (g/mol)	M_w/M_n	M_z/M_w	PI	G' at ref (Pa)	ER (Pa)	PDR
1	25	25400	151500	432900	6	2.9	4.69	79.9	0.14	4.14
2	25	34900	154700	355400	4.4	2.3	3.48	48.2	0.09	2.67
3	14	50200	165700	343100	3.3	2.1	2.84	60.6	0.11	2.30
4	14	42600	191000	530200	4.5	2.8	4.10	74.4	0.13	3.51
5(2+3)	N/A*	41600	163500	357600	3.93	2.2	3.52	45.4	0.10	2.57
6(2+4)	N/A*	38000	172900	432600	4.55	2.5	4.17	59.2	0.11	3.15

Table 7. * Not measured but should have a MFI between 14 and 25. Equation 1-3 were used to calculate the values together with data presented in Table 22-27 in Appendix 11.2. SEC results were received from INEOS lab, and raw data to this are presented in Table 35 in Appendix 11.7.

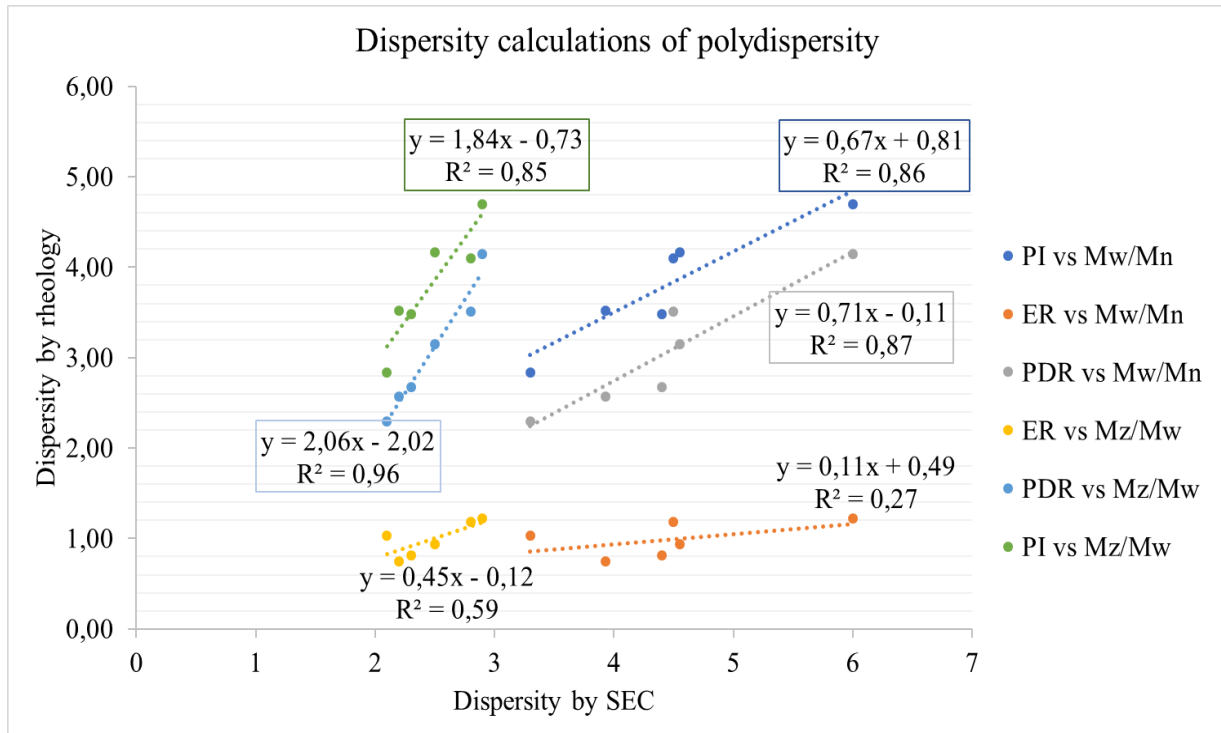


Figure 42. Rheology measures were fit with SEC data to find which rheology measure that is best for homo-PP.

6.2 Tensile tests

From all tensile tests performed, tensile graphs with raw data from Force (N)/Elongation (mm) was put together from raw data. These graphs are not presented for each grade, but example graphs are presented to give an understanding of the shapes of the curves. The example graphs presented are built from averages, from set of measures, at each time after storage with a sample size of 7-10 dogbones. Key values below are presented in another type of graph for all grades (visualised in Figure 43):

- Yield point, reported as stress (MPa) by calculation with cross section of the sample
- Youngs modulus, by reading the stress at 1% strain (GPa)
- Elongation at break, reported as strain (dL/L₀) (%)

The raw data for the graphs can be obtained in Appendix, 11.3. Table 28-30. The graphs presented in the thesis with the key values are including all grades and the measurements performed over time (by averages), with confidence interval by 95% marked with bars. *The axis for time of measurements is not proportional over time.* The reader is recommended to keep a copy of the last page in Appendix (11.8) where the properties of the grades are written out, keeping the different grades in mind.

Regarding the discussion about stability observed in the grades, “stable” indicates that the measurements was at the approximate same average value as later measurements performed in time. The analysis was performed by a 95% confidence interval, where the individual results for each dogbone measurement have been utilized. This is true if nothing else is

specified in the tables over stability. Not stable means that the measured value was different from the measurement made later in time.

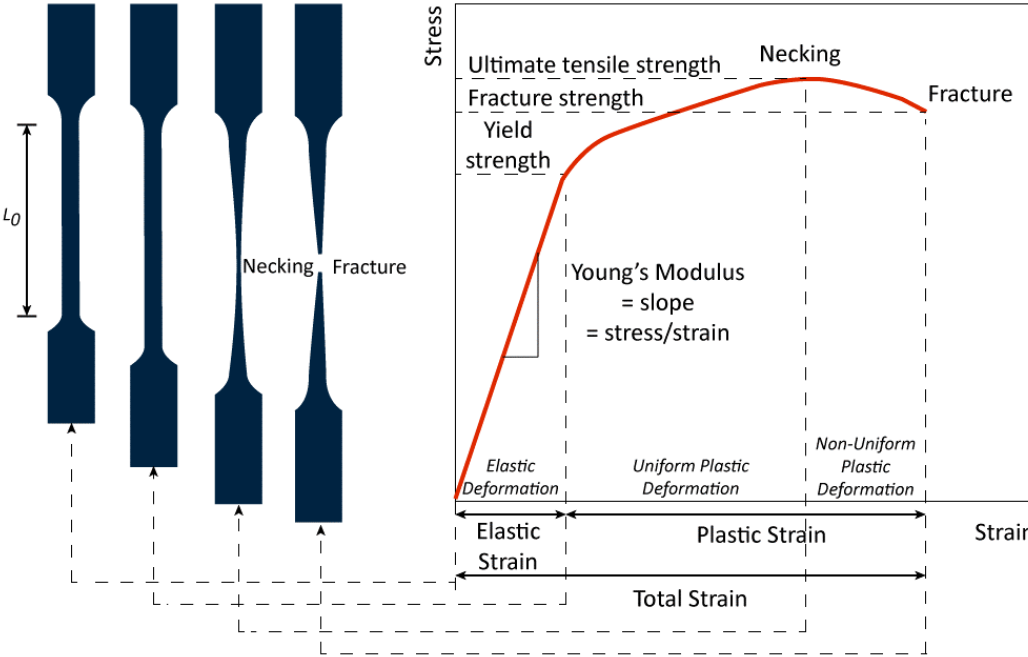


Figure 43 Another illustration of the different properties of relevance. (Yalcin, 2017).

6.2.1 Machine direction (MD)

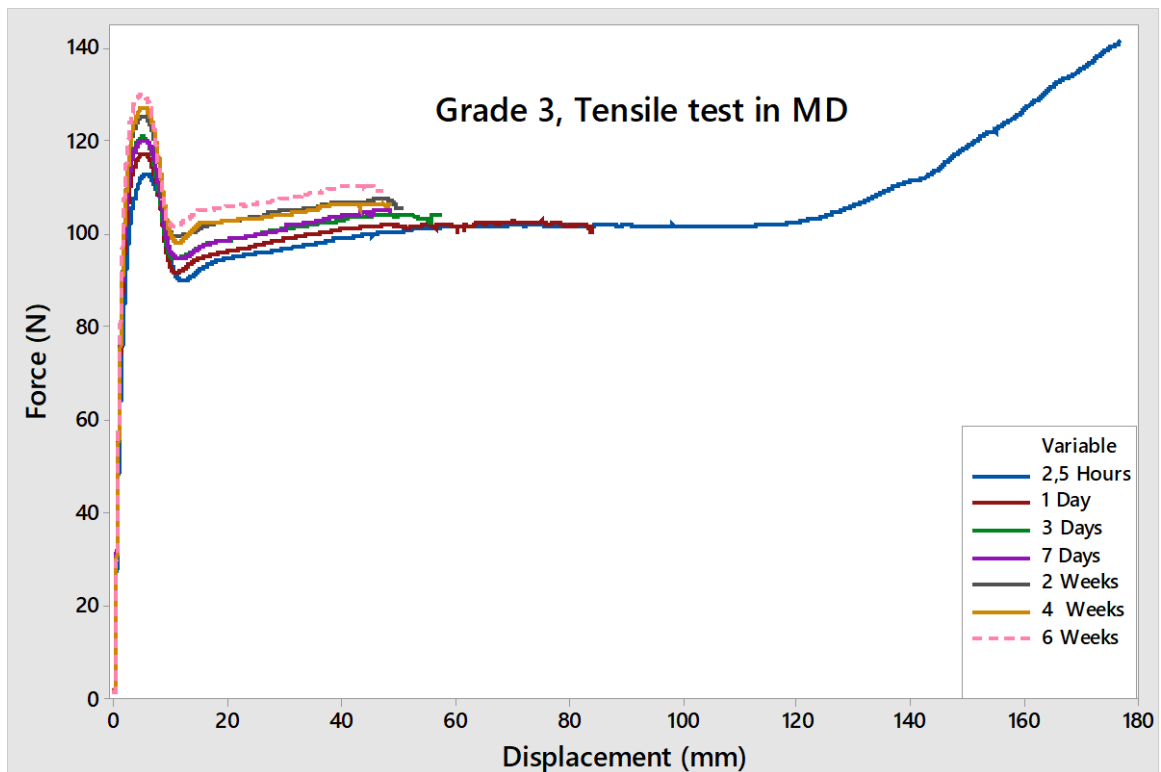


Figure 44. Tensile test performed of grade 3, MD. Samples are stored at 23 °C, 50% humidity. Averages from sets of measures are presented, with a size of samples 7-10.

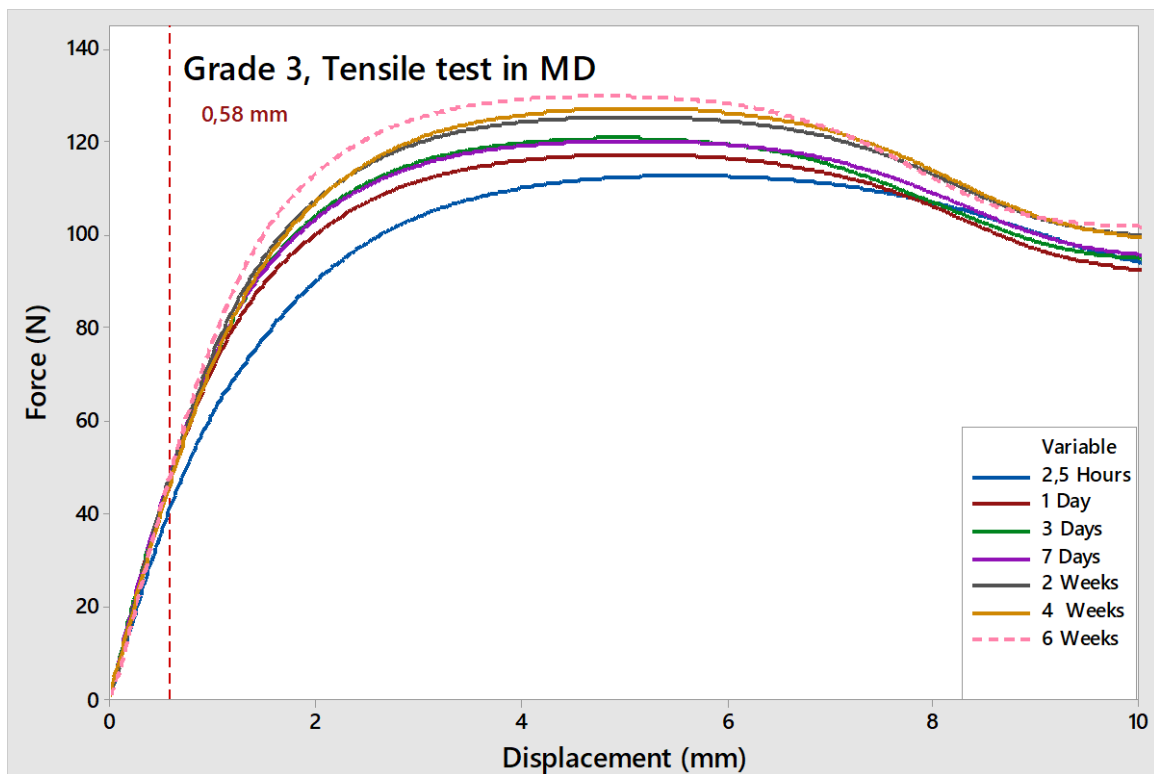


Figure 45. Magnification at the force/displacement curve received from MD, grade 3. 0.58 mm is marked, where Young's modulus is extracted and calculated.

6.2.1.1 Yield point

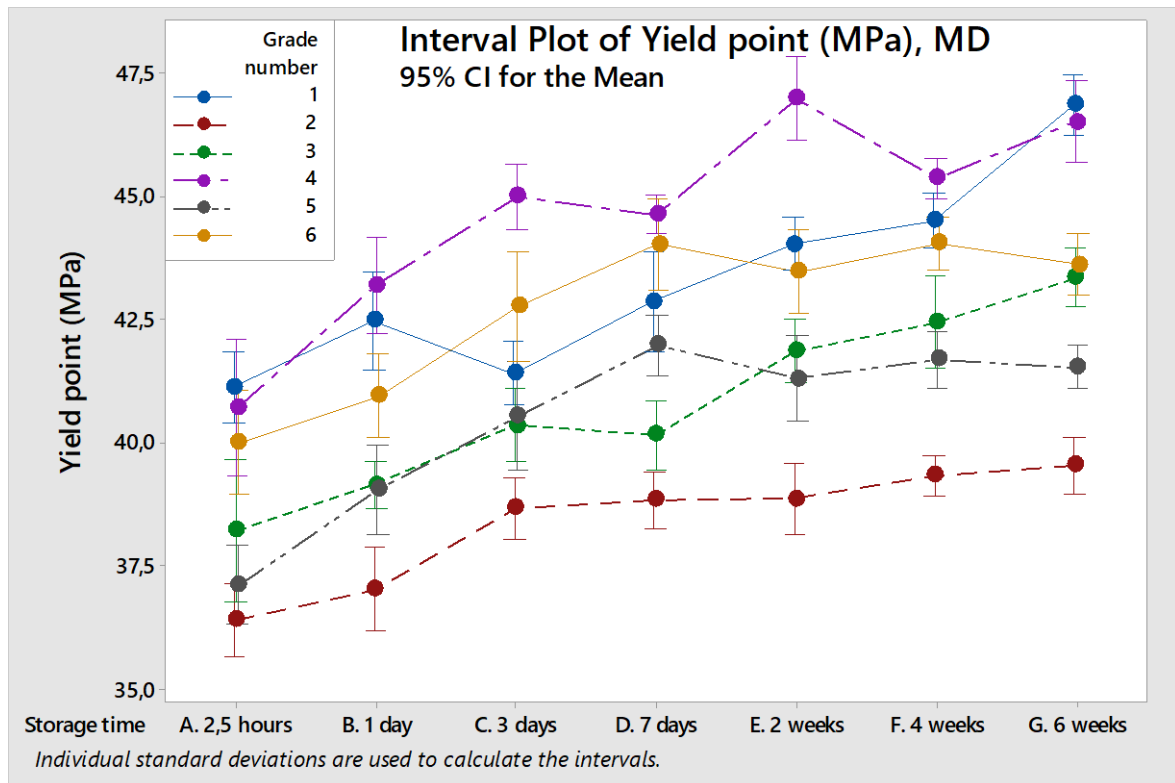


Figure 46. Plot showing how the yield point of the materials vary over time, and between grades. Standard deviation is marked with bars, at a confidence level of 95%. The measures are performed in MD.

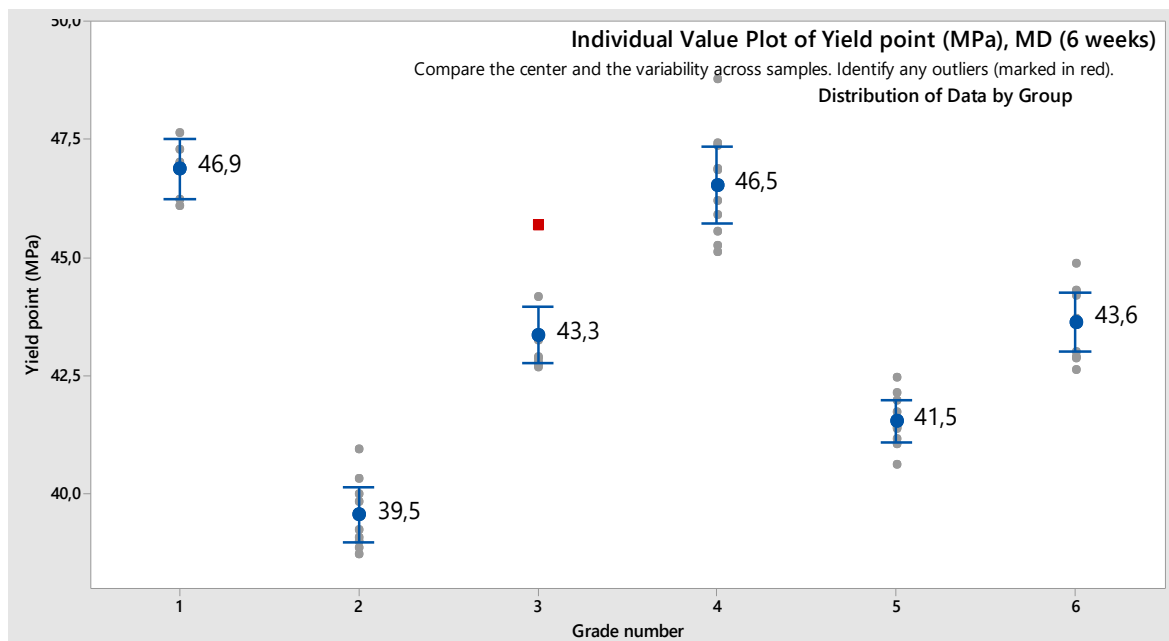


Figure 47. Yield point in MD for the different grades after 6 weeks from injection moulding, when they are all considered stable. The standard deviation with a CI of 95% is marked, as well as statistical outlier in red.

Observations (Figure 46 and 47):

- Grade 2 starts to flow at a lower yield stress than the rest of the materials.
- Grade 4, 1 and 6 have a higher modulus (higher yield stress) than the other grades.
- Grade 3 and 5 have a similar yield point initially, but grade 5 get a higher yield point than grade 3 during storage.

All grades increase their strength before yielding by storage time, where there is a significant difference between the measurement storages times within each grade, marked in Table 8:

	2.5 h	1 d	3 d	7 d	2 w	4 w	6 w
Grade 1	Not stable	Not stable	Not stable	Not stable	Not stable	Not stable	Stable*
Grade 2	Not stable	Not stable	Stable	Stable	Stable	Stable	Stable
Grade 3	Not stable	Not stable	Not stable	Not stable	Not stable	Stable	Stable
Grade 4	Not stable	Not stable	Not stable	Not stable	Stable	Stable	Stable
Grade 5	Not stable	Not stable	Stable	Stable	Stable	Stable	Stable
Grade 6	Not stable	Not stable	Stable	Stable	Stable	Stable	Stable

Table 8.* if measurement after 6 weeks was not performed, the polymer would be stable after 7 days

6.2.1.2 Youngs modulus

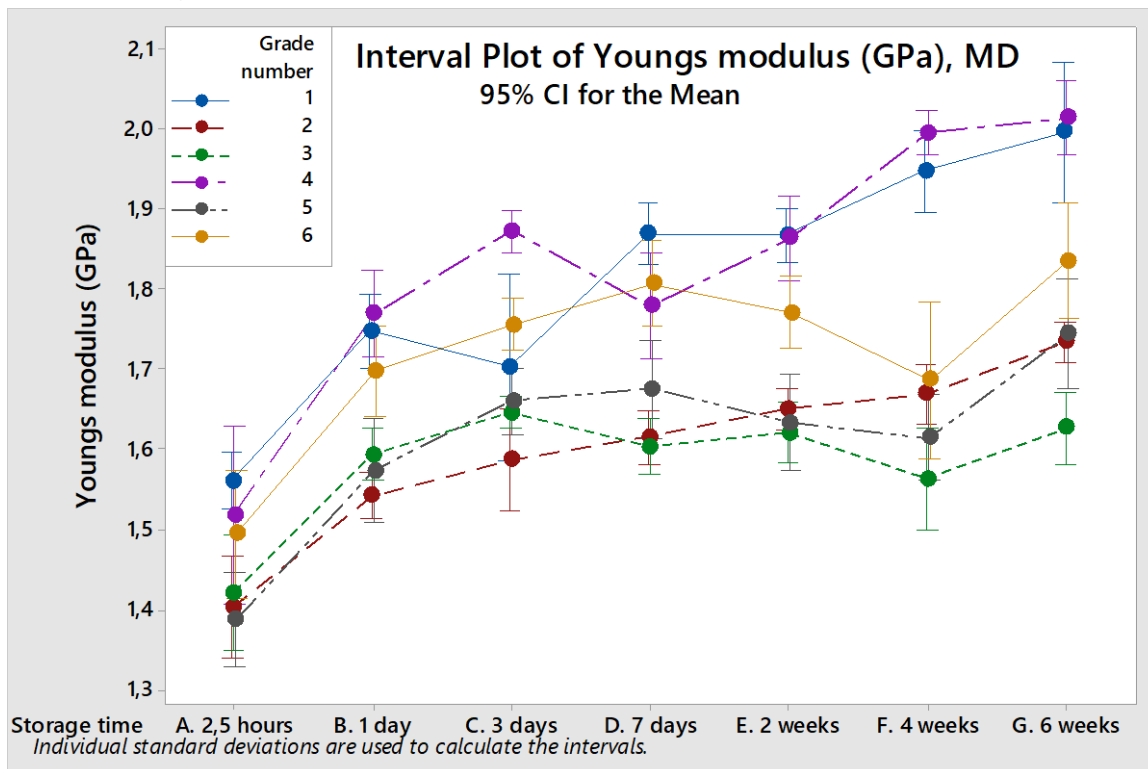


Figure 48. Plot showing how Young's modulus of the materials vary over time, and between grades. Standard deviation is marked with bars, at a confidence level of 95%. The measures are performed in MD.

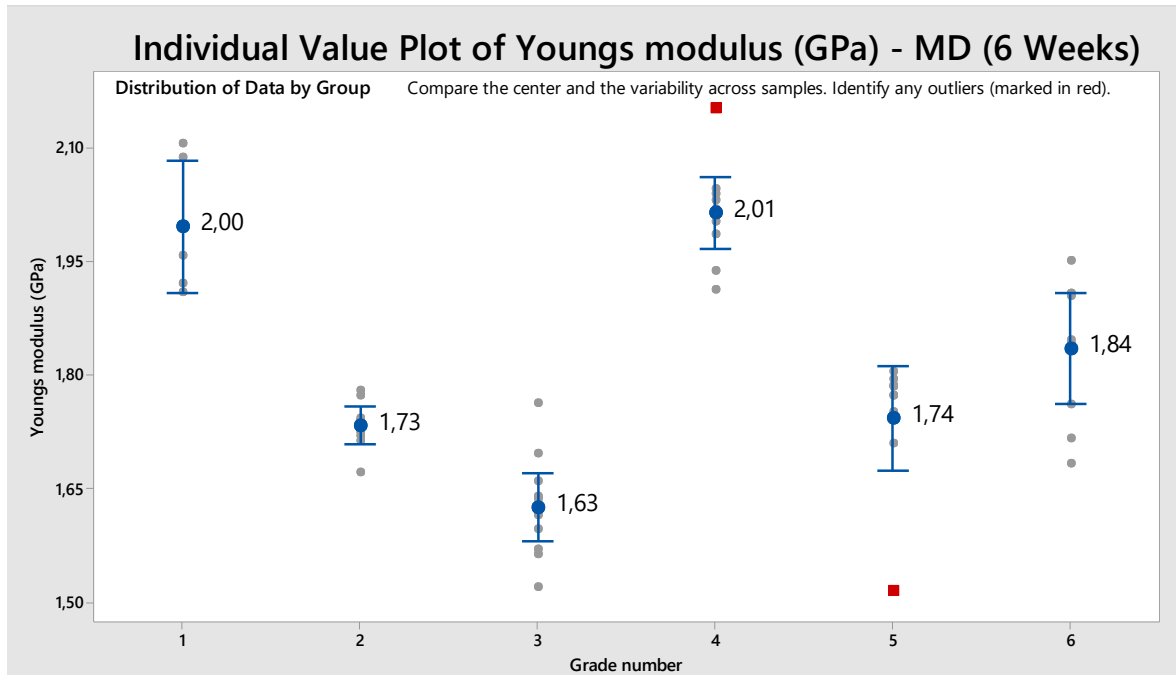


Figure 49. Values of Young's modulus for the different grades after 6 weeks, when they are all considered stable. The standard deviation with a CI of 95% is marked, as well as statistical outliers.

Observations (Figure 48 and 49):

- In all grades, Young's modulus increases over time in proportions to the values of 2.5 hours measurement.
- Grade 1 and 4 have approximately the same average young modulus during all measurements performed over time in storage.
- Grade 1 and 4 have the highest modulus, and grade 3 the lowest.

The grades seem to increase in modulus until they reach a plateau value, which is when the grade is noted below as "stable" in Table 9:

	2.5 h	1 d	3 d	7 d	2 w	4 w	6 w
Grade 1	Not stable	Not stable	Not stable	Not stable*	Not stable*	Stable	Stable
Grade 2	Not stable	Not stable	Not stable	Not stable	Not stable	Not stable*	Stable
Grade 3	Not stable	Stable	Stable	Stable	Stable	Stable	Stable
Grade 4	Not stable	Not stable	Not stable	Not stable	Not stable	Stable	Stable
Grade 5	Not stable	Stable	Stable	Stable	Stable	Stable	?
Grade 6	Not stable	Not stable	Stable	Stable	Stable	Stable	?

Table 9 * This measurement set does overlap with the confidence interval for measurements done later in time with CI 95%. Although, with CI of 90% it does not overlap, hence, the measurements are not considered stable.

6.2.1.3 Elongation at break

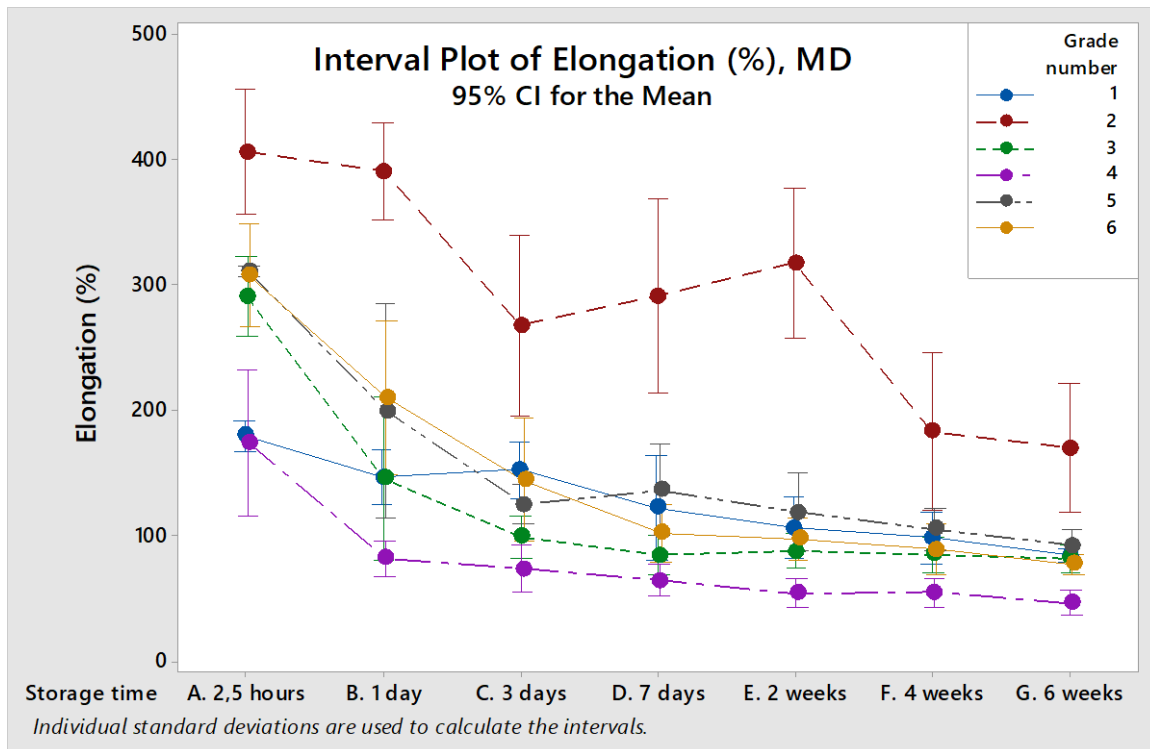


Figure 50. Plot showing how the elongation at break of the materials vary over time, and between grades. Standard deviation is marked with bars, at a confidence level of 95%. The measures are performed in MD.

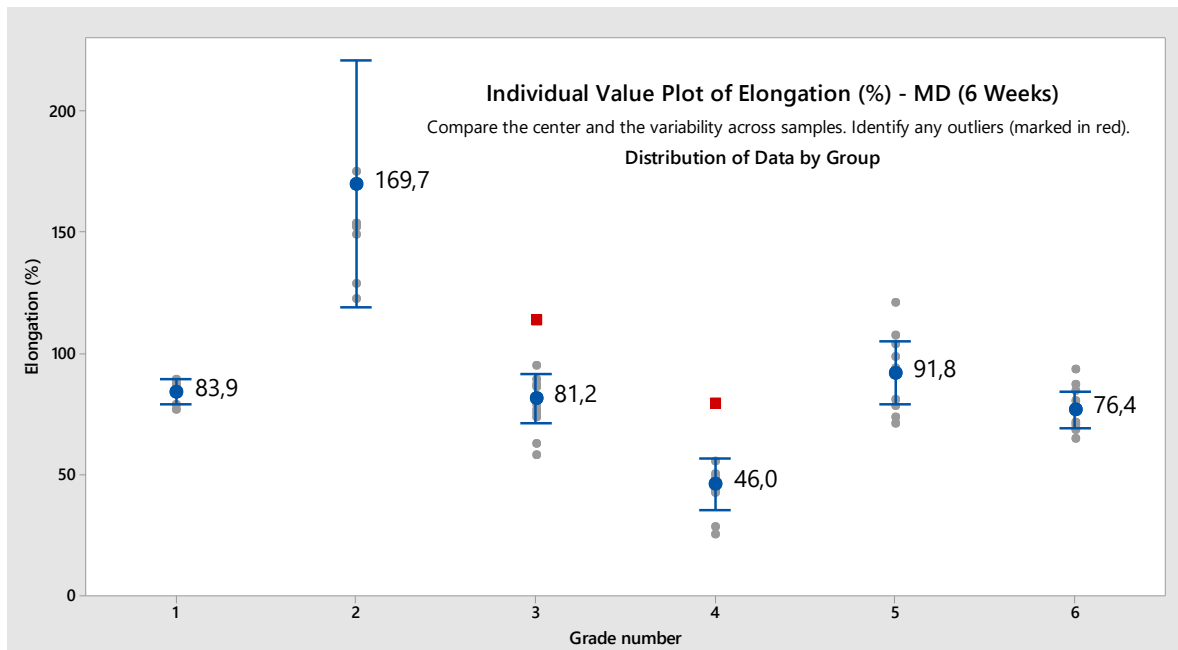


Figure 51. Elongation at break in MD for the different grades after 6 weeks from injection moulding, when they are all considered stable. The standard deviation with a CI of 95% is marked, as well as statistical outlier in red.

Observations (Figure 50 and 51):

- Elongation at break of the samples does vary by the same trend; they break earlier over time.
- The Measurements performed close to injection moulding (2.5 h, 1 day, 3 days) have (in most cases) a larger standard deviation, showing that the grades are not “stable” having a large spread and variety in resulting elongation at break.
- The grades with lowest Mw takes the longest time to get stable.
- There is a big difference on elongation at break observed between grade 2 and the other grades, where grade 2 (with low Mw and narrow MWD) have the longest elongation at break.

The grades decreases in elongation at break over storage until they reach a plateau value, which is when the grade is noted below as “stable” in Table 10:

	2.5 h	1 d	3 d	7 d	2 w	4 w	6 w
Grade 1	Not stable	Not stable	Not stable	Not stable*	Stable**	Stable**	Stable
Grade 2	Not stable	Not stable	Not stable*	Not stable*	Not stable*	Stable	Stable
Grade 3	Not stable	Not stable	Not stable*	Stable	Stable	Stable	Stable
Grade 4	Not stable	Not stable	Not stable	Stable	Stable	Stable	Stable
Grade 5	Not stable	Not stable	Stable	Stable	Stable	Stable	Stable
Grade 6	Not stable	Not stable	Not stable*	Stable	Stable	Stable	Stable

Table 10. * This measurement set does overlap with the confidence interval for measurements done later in time, but is considered not stable due to the large spread of elongation at break within this test batch and the difference in mean value from what is considered stable. ** This measurement has a different mean and wider confidence interval than the last measurement in the serie, but is considered stable since no later measurements can be performed within the timeframe for this work and since the CI is still overlapping.

6.2.2 Cross direction (CD)

6.2.2.1 General shape of measured force/displacement curve, key values

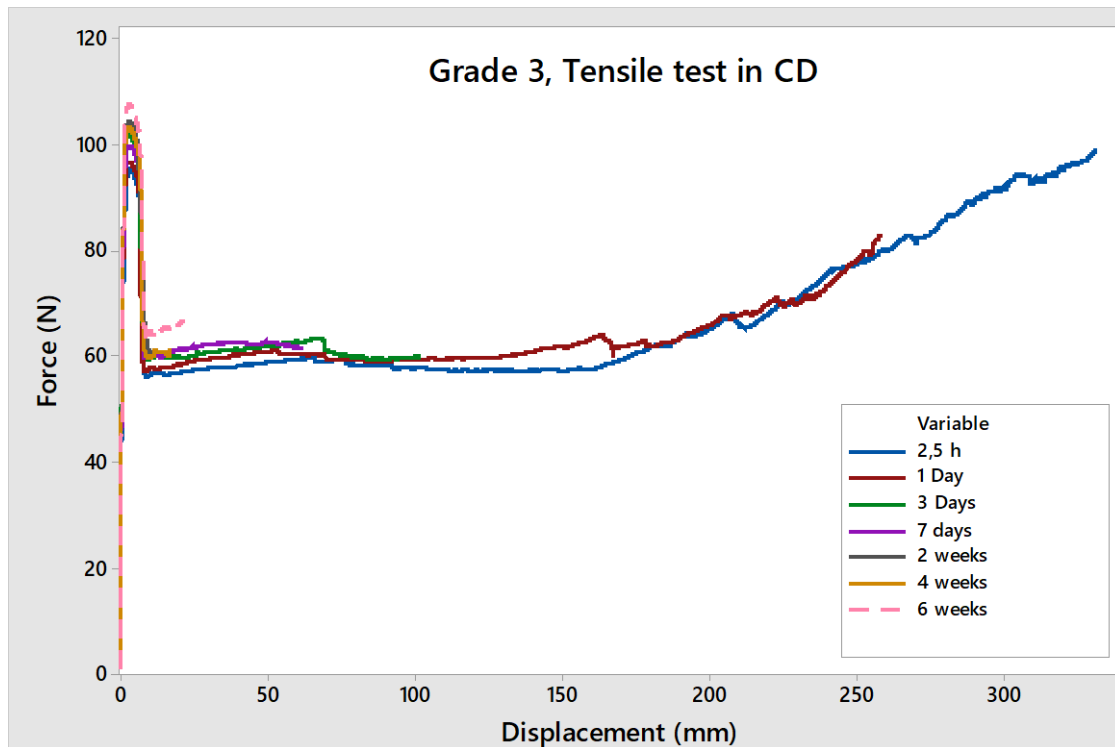


Figure 52. Tensile test performed of grade 3, CD. Samples are stored at 23 °C, 50% humidity. Averages from sets of measures are presented, with a size of samples 7-10.

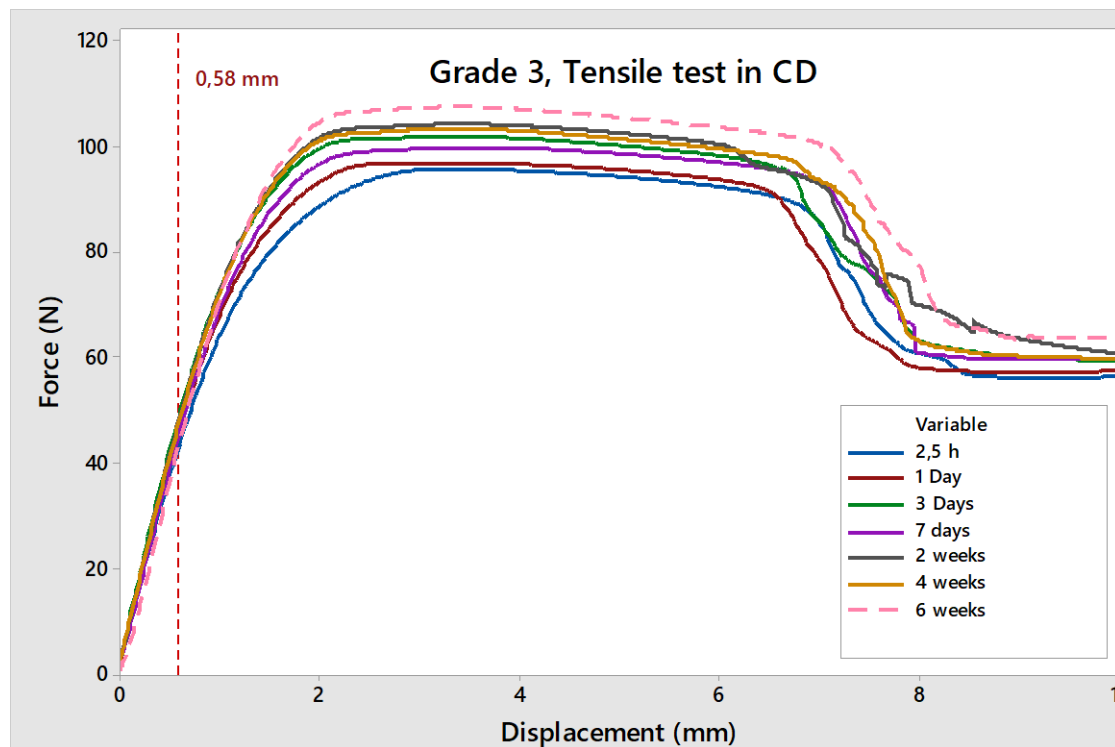


Figure 53. Zoom in at the force/displacement curve received from CD, grade 3. 0,58 mm is marked, where Young's modulus is extracted and calculated.

6.2.2.2 Yield point

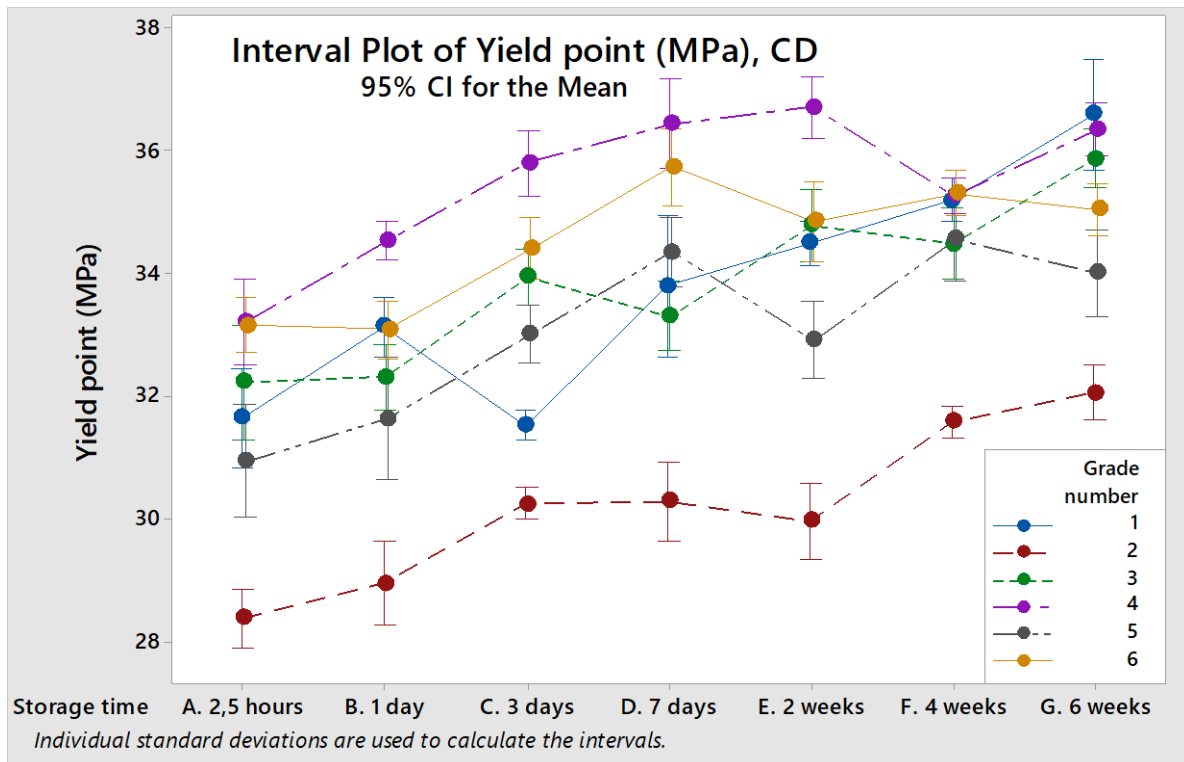


Figure 54. Plot showing how the yield point of the materials vary over time, and between grades. Standard deviation is marked with bars, at a confidence level of 95%. The measures are performed in CD.

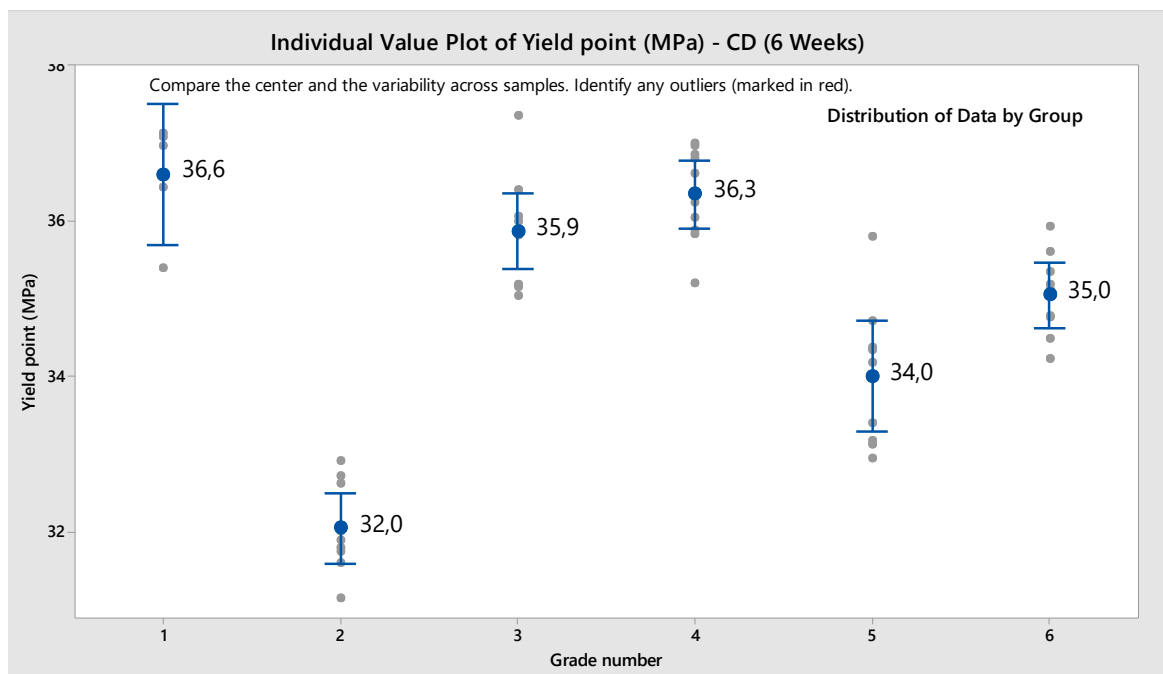


Figure 55. Yield point in CD for the different grades after 6 weeks from injection moulding, when they are all considered stable. The standard deviation with a CI of 95% is marked, and there are no outliers.

Observations (Figure 54 and 55):

- Grade 2 (low Mw and narrow MWD) have the lowest yield point.
- Grade 4 have the highest yield point initially, after 6 weeks of storage grade 1 and 4 have equal yield point (wide MWD).
- The bimodal grades follow the same trends, having a higher yield point than grade 2 and lower than its respective other component.
- Grade 3, after 6 weeks of storage, have a high yield point, indicating that presence of long chains is of importance for this property.

The grades seem to increase in yield point until they reach a plateau value, which is when the grade is noted below as “stable” in Table 11:

	2.5 h	1 d	3 d	7 d	2 w	4 w	6 w
Grade 1	Not stable	Not stable	Not stable	Not stable	Not stable	Not Stable*	Stable
Grade 2	Not stable	Not stable	Not stable	Not stable	Not stable	Stable	Stable
Grade 3	Not stable	Not stable	Not stable	Not stable	Not stable	Not stable*	Stable
Grade 4	Not stable	Not stable	Stable	Stable	Stable	Stable**	Stable
Grade 5	Not stable	Not stable	Not Stable*	Stable***	Stable	Stable	Stable
Grade 6	Not stable	Not stable	Not stable*	Stable***	Stable	Stable	Stable

Table 11. * This measurement set does overlap with the confidence interval for measurements done later in time with CI 95%. Although, with CI of 90% it does not overlap, hence, the measurements are not considered stable.

** This measurement is noticeably low, the yield point is lower than previous measurements (Grade 4:7 days and 2 weeks)

***This measurements are performed on the same day, it seems like both measurements (day 7, grade 5 and 6) are too high and standing out from their series.

6.2.2.3 Youngs modulus

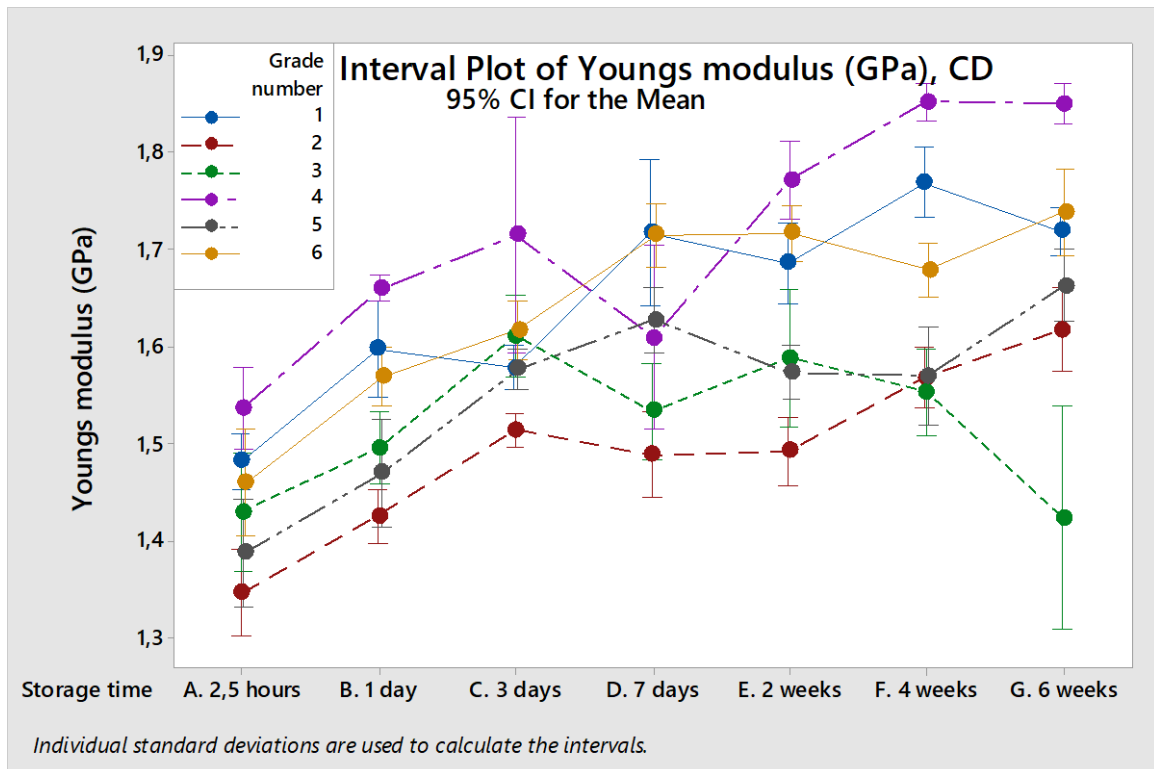


Figure 56. Plot showing how Young's modulus of the materials vary over time, and between grades. Standard deviation is marked with bars, at a confidence level of 95%. The measures are performed in CD.

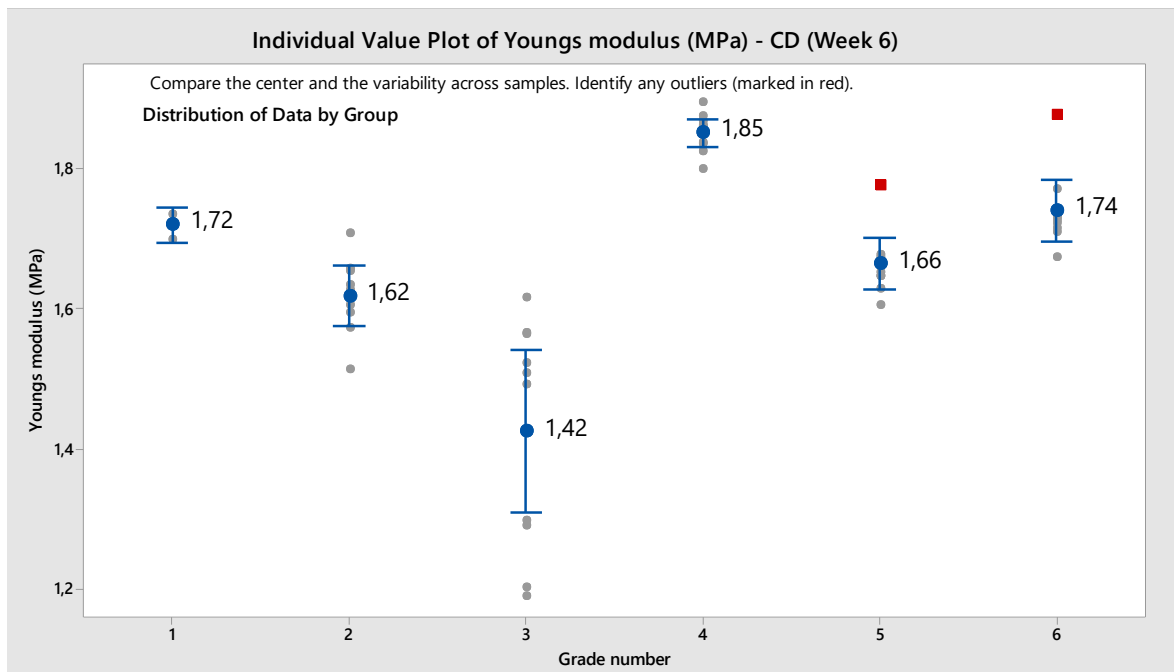


Figure 57. Values of Young's modulus for the different grades after 6 weeks, when they are all considered stable. The standard deviation with a CI of 95% is marked, as well as statistical outliers.

Observations (Figure 56 and 57):

- Regarding grade 3, the last measure is assumed to be wrong, since there is no obvious reason for that drop in modulus to happen.
- The grades with wide MWD have a higher modulus than the grades with low MWD.
- Grade 4 have the highest modulus
- Grade 1 and 6 have very similar modulus during time of storage.

The grades increase in modulus until they reach a plateau value, which is when the grade is noted below as “stable” in Table 12:

	2.5 h	1 d	3 d	7 d	2 w	4 w	6 w
Grade 1	Not stable	Not stable	Not stable	Stable	Stable	Stable	Stable
Grade 2	Not stable	Not stable	Not stable	Not stable	Not stable	Stable	Stable*
Grade 3	Not stable	Stable	Stable	Stable	Stable	Stable	Stable*
Grade 4	Not stable	Not stable	Not stable	Not stable	Not stable	Stable	Stable
Grade 5	Not stable	Not stable	Stable	Stable	Stable	Stable	Stable
Grade 6	Not stable	Not stable	Not stable	Stable	Stable	Stable	Stable

Table 12. *This measurement set have a noticeably high standard deviation and does probably contain measurements that are not valid. Something must have been wrong, as slip in the clamps of the tensile machine.

6.2.2.4 Elongation at break

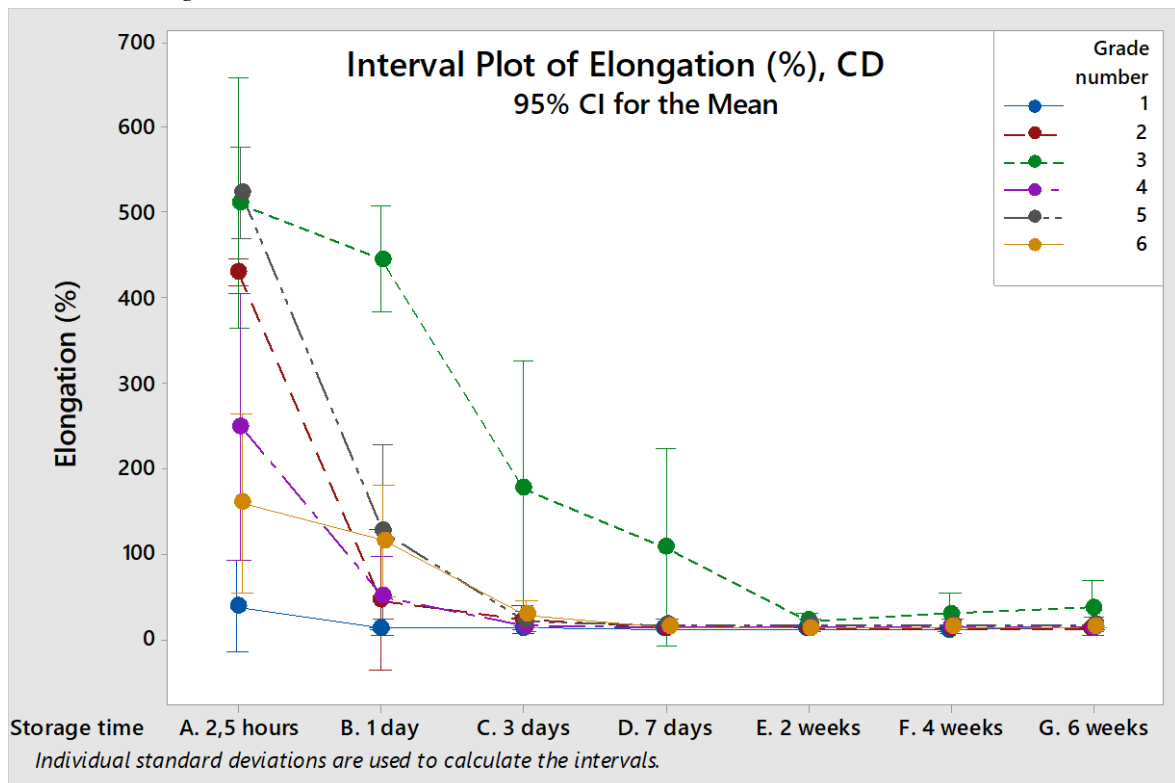


Figure 58. Plot showing how the elongation at break of the materials vary over time, and between grades. Standard deviation is marked with bars, at a confidence level of 95%. The measures are performed in CD.

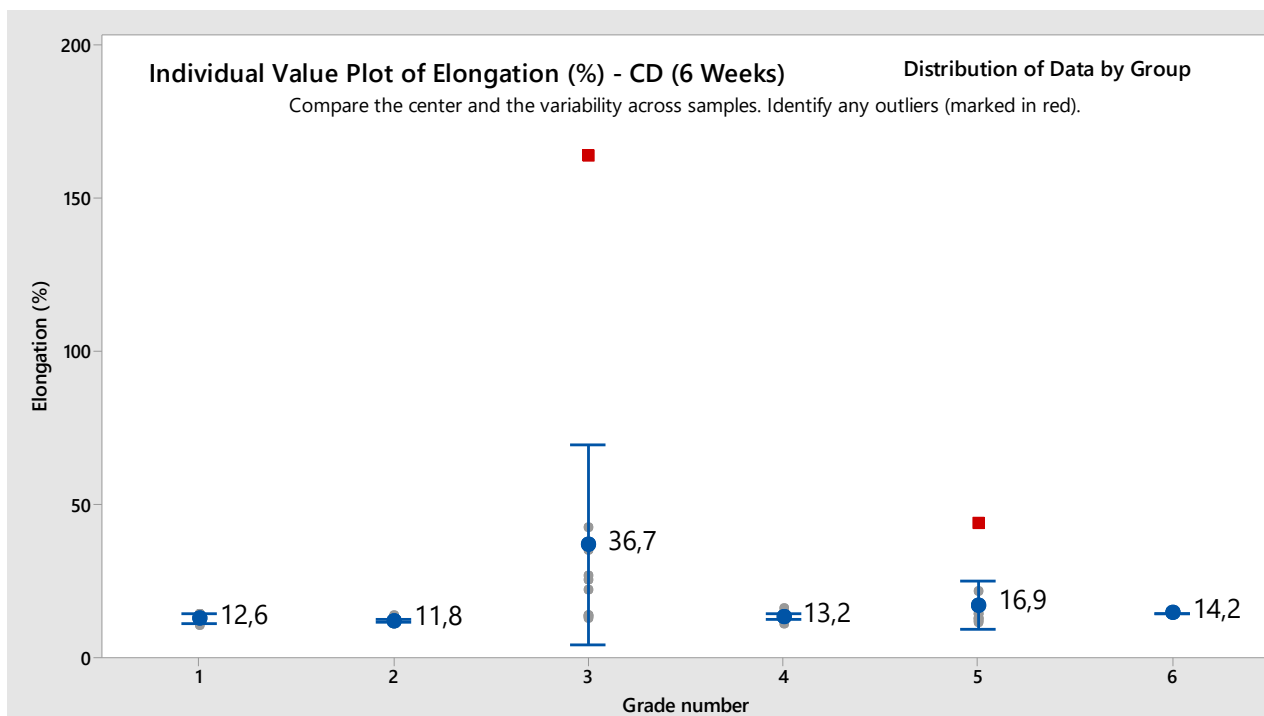


Figure 59. Elongation at break for the different grades after 6 weeks from injection moulding, when they are all considered stable. The standard deviation with a CI of 95% is marked, as well as statistical outliers in red.

Observations (Figure 58 and 59):

- Grade 3 have the longest elongation at break, except for measure after 2.5 hour where the elongation at break is equal the one of grade 5 (that grade 3 is a component of).
- Grade 3 never reaches a stable value with as low standard deviation as the other grades.
- The grades with narrow MWD have much longer elongation at break initially
- Grade 1, 4 and 6 have the lower elongation at break, where grade 6 reach the shorter elongation at break a bit slower than the other grades.

The grades decreases in elongation at break over storage until they reach a plateau value, which is when the grade is noted below as “stable” in Table 13:

	2.5 h	1 d	3 d	7 d	2 w	4 w	6 w
Grade 1	Not stable	Stable	Stable	Stable	Stable	Stable	Stable
Grade 2	Not stable	Not stable*	Not stable*	Stable	Stable	Stable	Stable
Grade 3	Not stable	Not stable	Not stable*	Not stable*	Stable	Stable	Stable
Grade 4	Not stable	Not stable*	Stable	Stable	Stable	Stable	Stable
Grade 5	Not stable	Not stable*	Stable	Stable	Stable	Stable	Stable
Grade 6	Not stable	Not stable	Not stable*	Stable	Stable	Stable	Stable

Table 13. * This measurement set does overlap with the confidence interval for measurements done later in time, but is considered not stable due to the large spread of elongation within this test batch and the difference in mean value from what is considered stable.

6.2.3 Diagonal direction (DD)

6.2.3.1 General shape of measured force/displacement curve

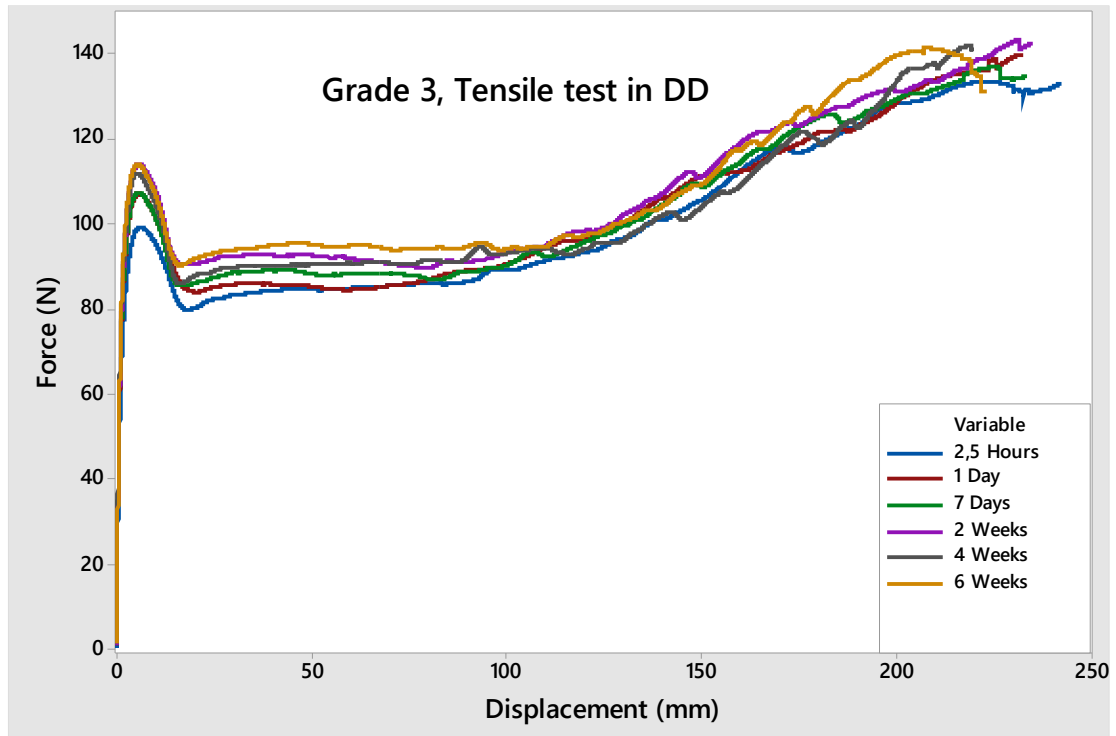


Figure 60. Tensile test performed of grade 3. DD. Samples are stored at 23 °C, 50% humidity. Averages from sets of measures are presented, with a size of samples 5-6.

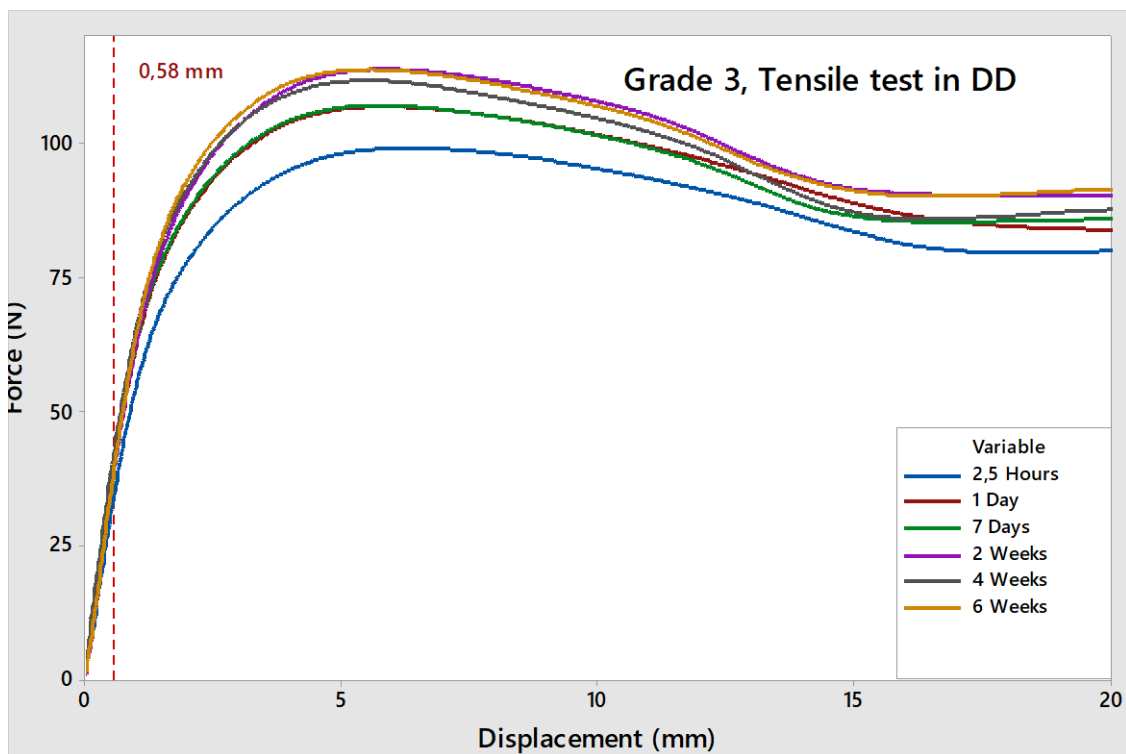


Figure 61. Zoom in at the force/displacement curve received from CD, grade 3. 0.58 mm is marked, where Young's modulus is extracted and calculated. Notice that in compare to MD and CD, this x-axis is of other scale.

6.2.3.2 Yield point

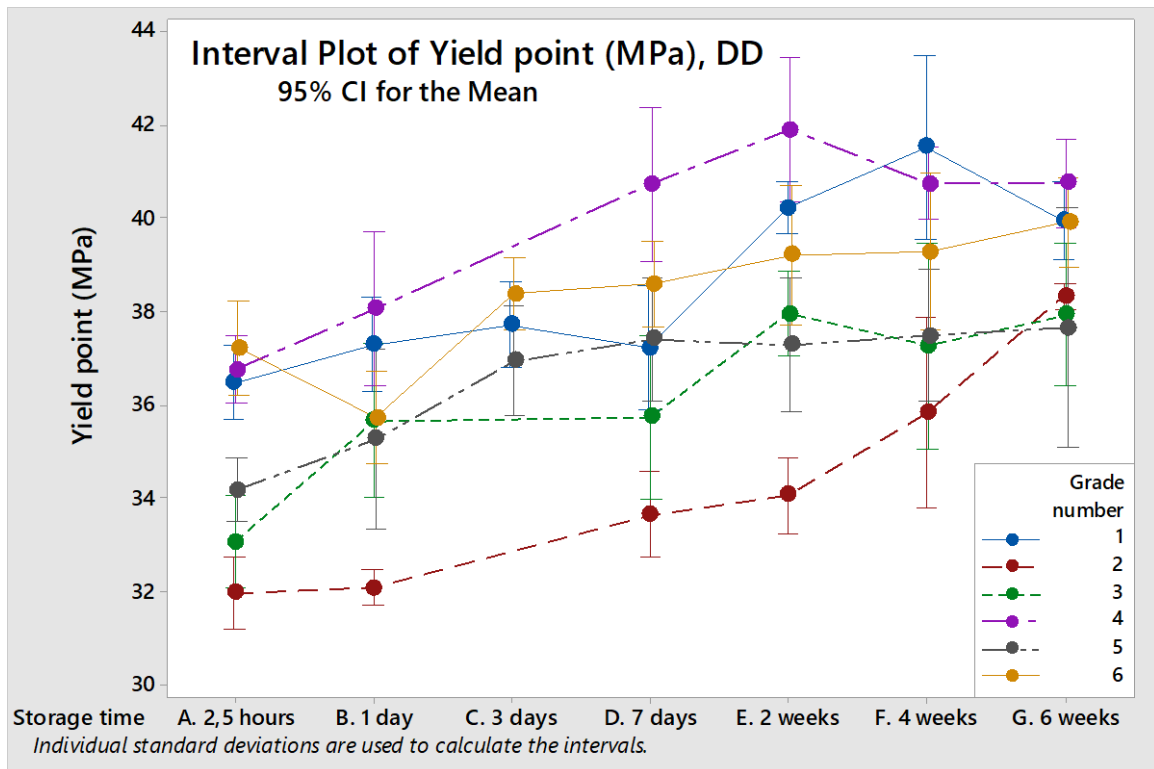


Figure 62. Plot showing how the yield point of the materials vary over time, and between grades. Standard deviation is marked with bars, at a confidence level of 95%. The measures are performed in DD.

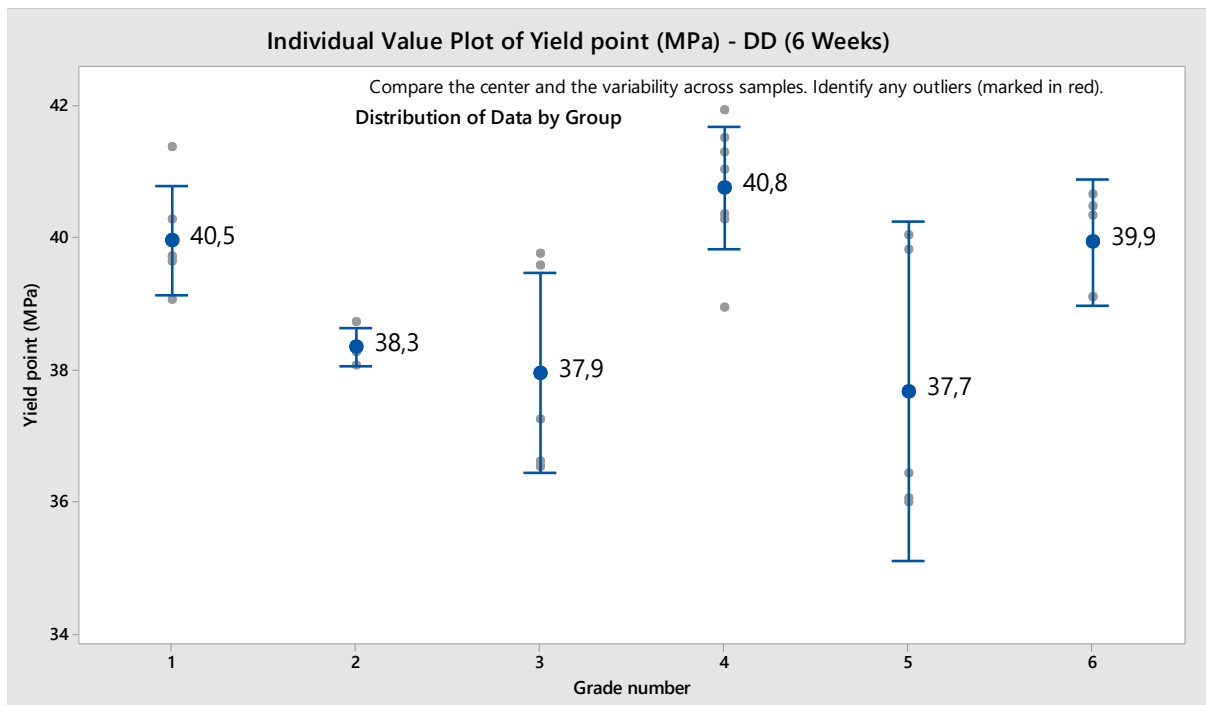


Figure 63. Yield point for the different grades in DD after 6 weeks from injection moulding, when they are all considered stable. The standard deviation with a CI of 95% is marked, there are no outliers.

Observations (Figure 62 and 63):

- The yield point of grade 2 is continuously rising over the time of storage, reaching after 6 weeks same value as grade 5 and 3 (that also have narrow MWD).
- Grades with wide MWD follow each other in performance, where grade 4 have slightly higher yield point.
- It takes shorter time of storage for the grades that are bimodal to reach a stable value.

The grades increase in yield point until they reach a plateau value, which is when the grade is noted below as “stable” in Table 14:

	2.5 h	1 d	3 d	7 d	2 w	4 w	6 w
Grade 1	Not stable	Not stable	Not stable	Not stable	Stable	Stable	Stable
Grade 2	Not stable	Not stable	N/A	Not stable	Not stable	Not Stable*	Stable**
Grade 3	Not stable	Not stable*	N/A	Not stable*	Stable	Stable	Stable
Grade 4	Not stable	Not stable	N/A	Stable	Stable	Stable	Stable
Grade 5	Not stable	Not stable*	Stable	Stable	Stable	Stable	Stable
Grade 6	Not stable	Not stable	Stable	Stable	Stable	Stable	Stable

Table 14. * This measurement set does overlap with the confidence interval for measurement done later in time, but is considered not stable due to the large standard deviation overlapping with both previous measurements and later within this test batch and the difference in mean value from what is considered stable. N/A due to that it was decided that the diagonal measurement was not equally interesting and that time by the machine was limited. **Since there are no later measures it is not possible to say that it is stable, but the grade is assumed to be.

6.2.3.3 Youngs modulus

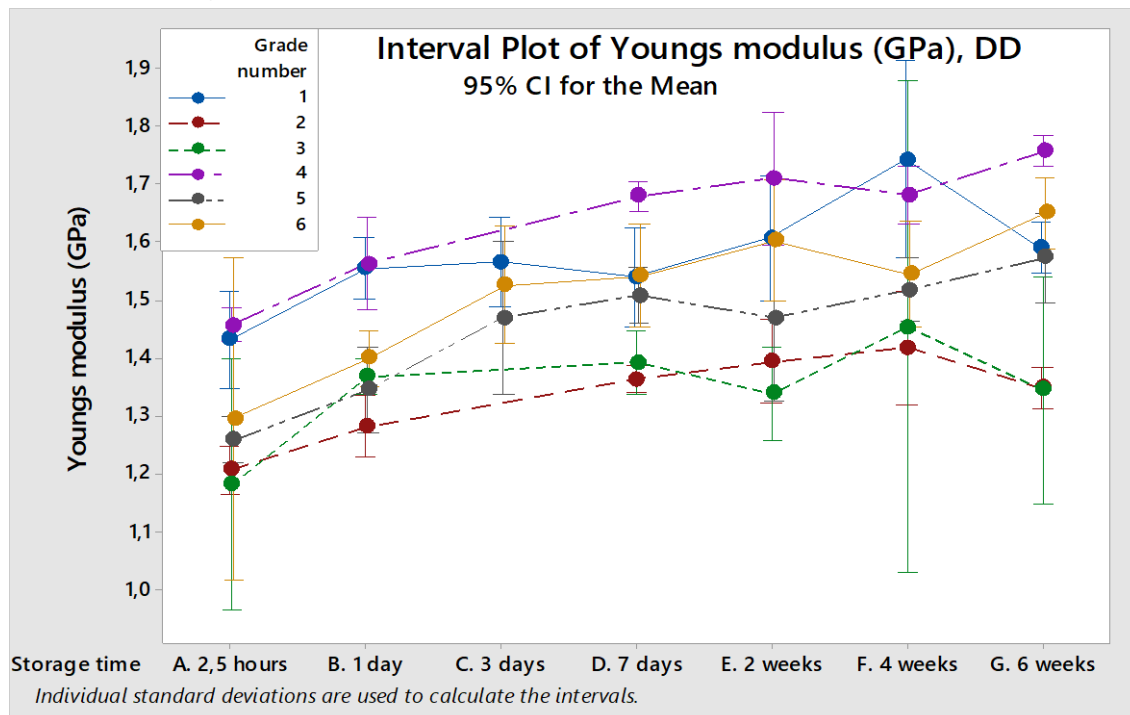


Figure 64. Plot showing how Young's modulus of the materials vary over time, and between grades. Standard deviation is marked with bars, at a confidence level of 95%. The measures are performed in DD.

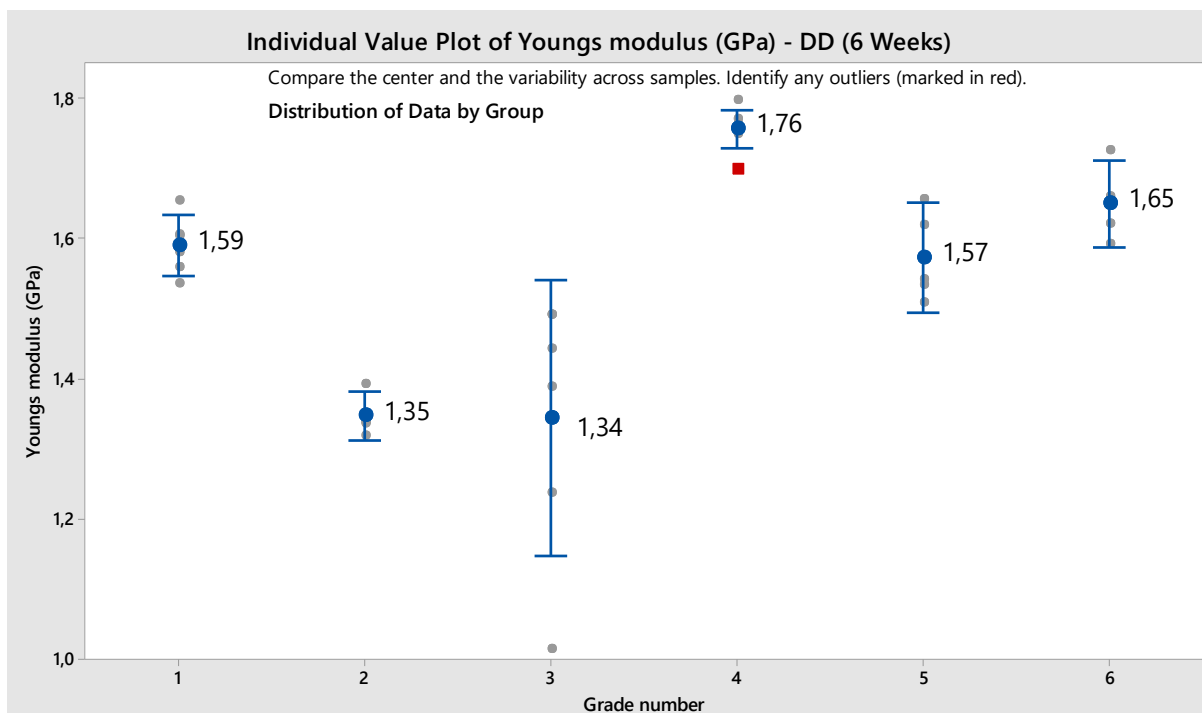


Figure 65. Values of Young's modulus for the different grades after 6 weeks of storage, when they are all considered stable. The standard deviation with a CI of 95% is marked, as well as statistical outlier in red.

Observations (Figure 64 and 65):

- Young's modulus is varying for all grades between 2.5 hours and 1 day
- The grades are all stable after maximum 7 days
- The grades with wide MWD follow each other quite well, where grade 4 has the highest modulus.
- Grade 1 and 3 have very similar modulus.

Regarding changes of properties over time, there is a slight increase between 4 and 6 weeks in Young's modulus for grade 4, 5 and 6, but it is not of statistical significance. The grades are noted as previous, when they do not change over time they are noted as stable in Table 15.

	2.5 h	1 d	3 d	7 d	2 w	4 w	6 w
Grade 1	Not stable	Stable	Stable	Stable	Stable	Stable	Stable
Grade 2	Not stable	Not stable*	N/A	Stable	Stable	Stable	Stable
Grade 3	Not stable	Stable**	N/A	Stable**	Stable**	Stable**	Stable**
Grade 4	Not stable	Not stable	N/A	Stable	Stable	Stable	Stable
Grade 5	Not stable	Not stable	Stable	Stable	Stable	Stable	Stable
Grade 6	Not stable	Not stable	Stable	Stable	Stable	Stable	Stable

Table 15. * This measurement set does overlap with the confidence interval for measurement done later in time, but is considered not stable due to the large standard deviation overlapping with both previous measurements and later within this test batch and the difference in mean value from what is considered stable. N/A due to that it was decided that the diagonal measurement was not equally interesting and that time by the machine was limited. ** All confidence interval is overlapping in this serie, but it is noted that the mean differs from measurement after 2.5 h and the rest, therefore the conclusion is that the polymer is stable after 1 day and not earlier.

6.2.3.4 Elongation at break

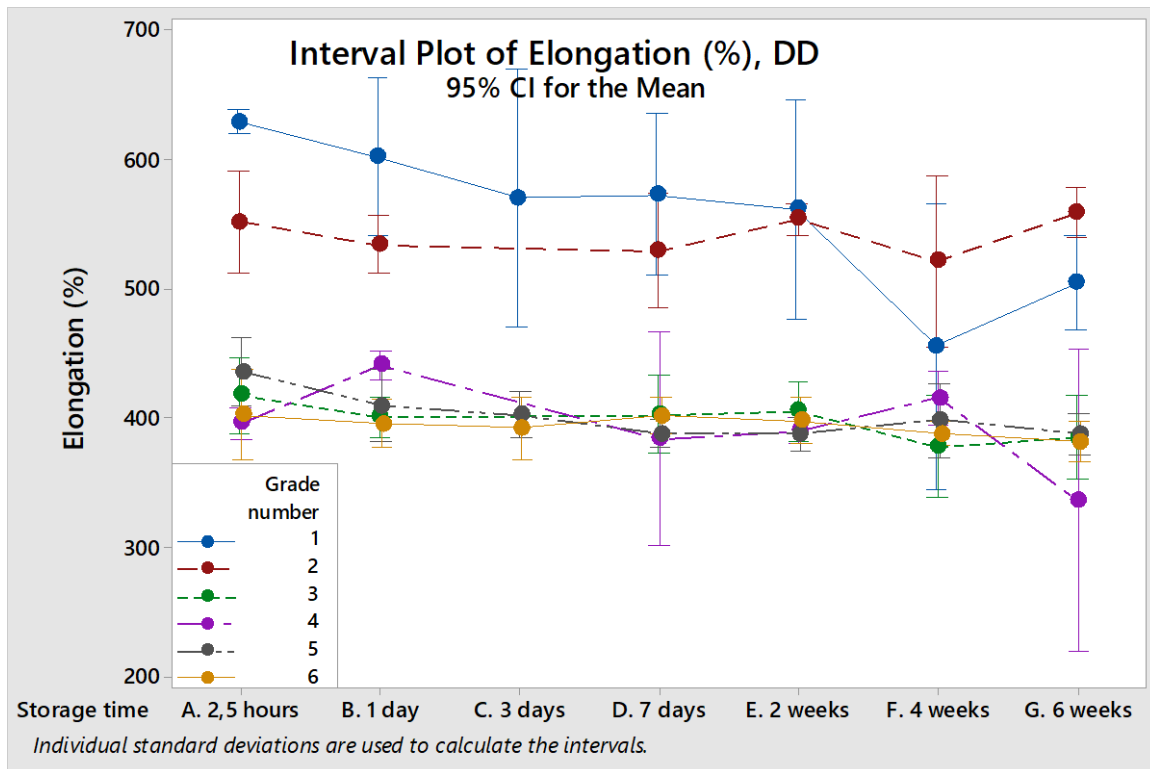


Figure 66. Plot showing how the elongation at break of the materials vary over time, and between grades. Standard deviation is marked with bars, at a confidence level of 95%. The measures are performed in DD.

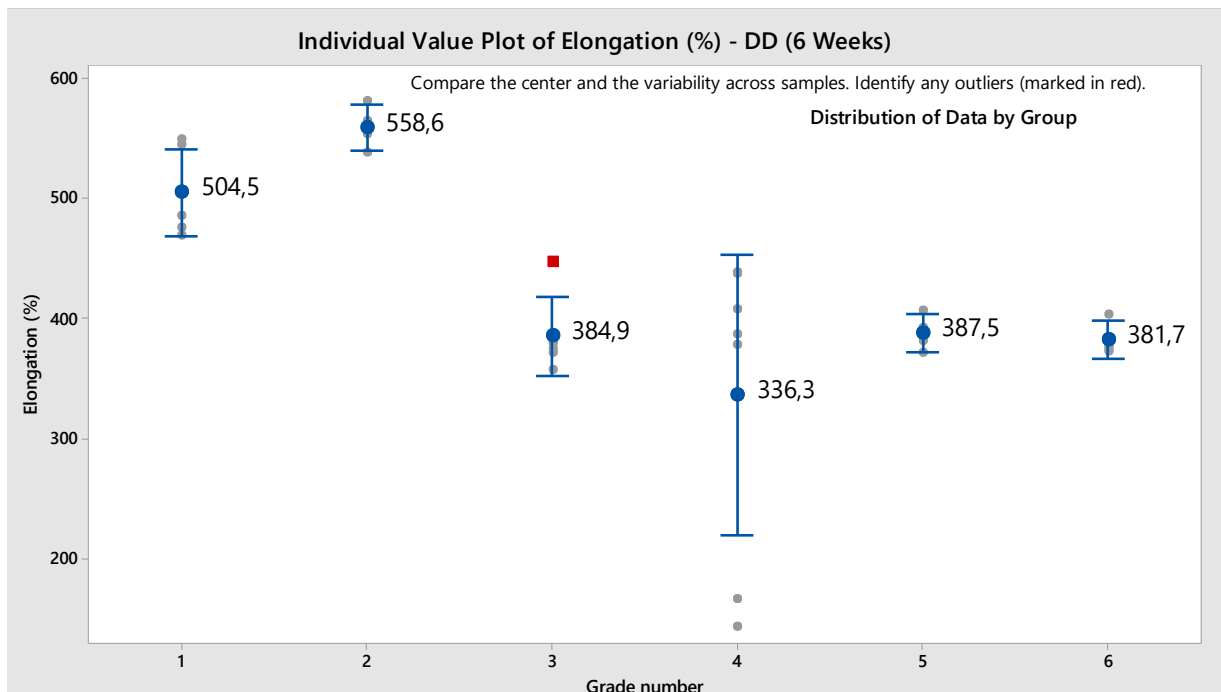


Figure 67. Elongation at break for the different grades after 6 weeks from injection moulding, when they are all considered stable. The standard deviation with a CI of 95% is marked, as well as statistical outlier in red.

Observations (Figure 66 and 67):

- The elongation at break of the grades with low M_w is much longer than the other grades.
- The elongation at break for the most grades do not change much in time.
- There is a big standard deviation for grade 1, 2 and 4.
- The bimodal grades have almost the same behaviour as each other, but also as its component with higher M_w .

Some of the grades do not change in elongation at break over time, and some do. When the grades have a stable elongation at break, the grade is noted below as “stable” in Table 16:

	2.5 h	1 d	3 d	7 d	2 w	4 w	6 w
Grade 1	Not stable	Not stable*	Not stable*	Not stable*	Not Stable*	Stable**	Stable**
Grade 2	Stable	Stable	Stable	Stable	Stable	Stable	Stable
Grade 3	Stable	Stable	Stable	Stable	Stable	Stable	Stable
Grade 4	Stable	Stable	Stable	Stable	Stable	Stable	Stable
Grade 5	Not stable	Not stable	Not stable**	Stable	Stable	Stable	Stable
Grade 6	Not Stable***	Not Stable***	Stable	Stable	Stable	Stable	Stable

Table 16. * This measurement set does overlap with the confidence interval for measurement done later in time, but is considered not stable due to the large standard deviation overlapping with both previous measurements and later within this test batch and the difference in mean value from what is considered stable. ** The mean value is much lower in elongation at break for these measurements, but does not statistically differ with a CI of 95%. *** These measures have a much higher standard deviation than the other in the series, and are hence not considered stable.

6.2.4 Summary of stability

Direction	Property	Grade 1	Grade 2	Grade 3	Grade 4	Grade 5	Grade 6
MD	Yield point	6 weeks	3 days	4 weeks	2 weeks	3 days	3 days
	Youngs Modulus	4 weeks	6 weeks	1 day	4 weeks	1 day	3 days
	Elongation	2 weeks	4 weeks	7 days	7 days	3 days	7 days
CD	Yield point	6 weeks	4 weeks	6 weeks	3 days	7 days	7 days
	Youngs Modulus	7 days	4 weeks	1 day	4 weeks	3 days	7 days
	Elongation	1 day	7 days	2 weeks	3 days	3 days	7 days
DD	Yield point	2 weeks	6 weeks	2 weeks	7 days	3 days	3 days
	Youngs Modulus	1 day	7 days	1 day	7 days	3 days	3 days
	Elongation	4 Weeks	2.5 hours	2.5 hours	2.5 hours	7 days	3 days

Table 17. Summarising when the grades reach a plateau value, not changing its properties.

Observations (Table 17):

- Grade 1 - Stable after 2 weeks in terms of elongation at break, after 4 weeks for Young's modulus and 6 weeks yield point
- Grade 2 - Varies in all properties up to 6 weeks (Young's modulus and yield point) and 4 weeks for elongation at break
- Grade 3 - vary in elongation at break and Young's modulus up to 2 weeks. The yield point is not stable until after 6 weeks
- Grade 4 - increases in Young's modulus in up to 4 weeks, but differences in elongation at break stop after one week. Differences in yield point can be noted up to 2 weeks
- Grade 5 - Stable in yield point after 1 week, and in the other properties after 3 days
- Grade 6 - Stable after 1 week in all measures

6.2.5 Pictures of fractured dogbones

Documentation, by taking pictures, of the broken dogbones were performed after each measurement. The type of tension that takes place when the dogbones are elongated is similar between the grades in MD (Figure 68 and 69), CD (Figure 70 and 71) and DD (Figure 72 and 73) respectively. A selection of a few dogbones after elongation and break are presented to illustrate how the different elongation looks in the different directions, how the plastic deformation and strain hardening differ.



Figure 68. Dogbones after tensile test when elongation and broken in MD by grade 3, when stored in 6 weeks. This elongation is shorter than the one in DD, but longer than the general, stable, break in CD.



Figure 69. Closer look at the elongated, necked, area in MD, by grade 4 stored 6 weeks. There are no flow lines of polymer to be observed, the polymer is homogeneous white.

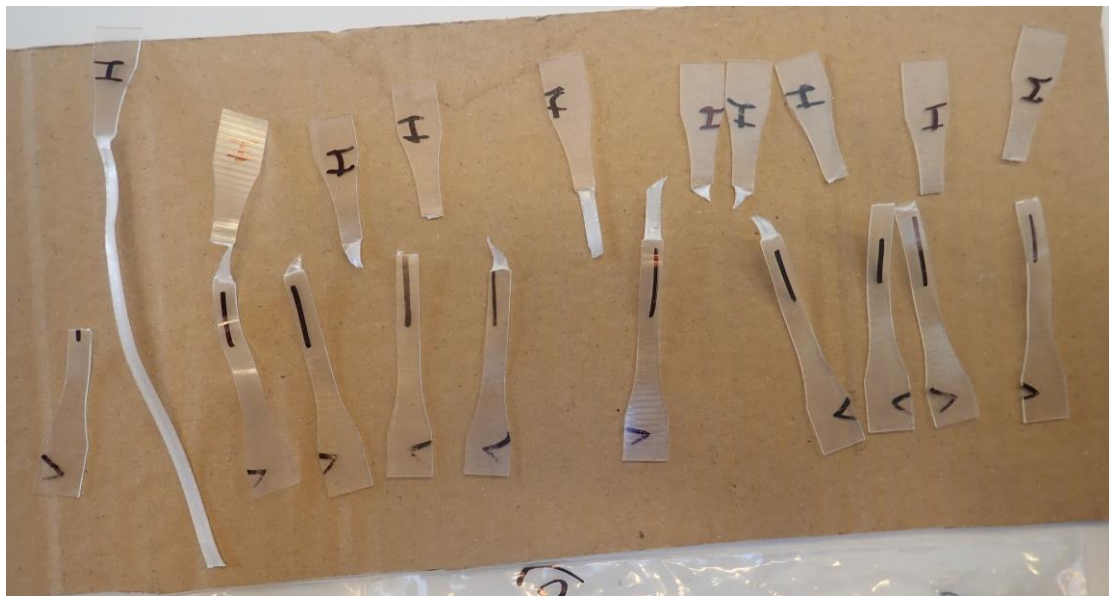


Figure 70. Dogbones after tensile test in CD by grade 3, when stored in 6 weeks. The elongation is shorter than the one in MD and DD (except for one that differs from the rest).



Figure 71. Closer look at the flow pattern in CD, grade 3 after stored 6 weeks. A clear pattern can be seen in the elongated part.



Figure 72. Dogbones after tensile test in DD by grade 3, when stored in 6 weeks. The elongation in DD is longer than the elongation in MD and CD by stable homo-PP.



Figure 73. Closer look at the elongated area close to the point of break, in DD, grade 3 stored 6 weeks. The area is not smooth and it looks like fibre has been formed.

6.3 Tensile Impact

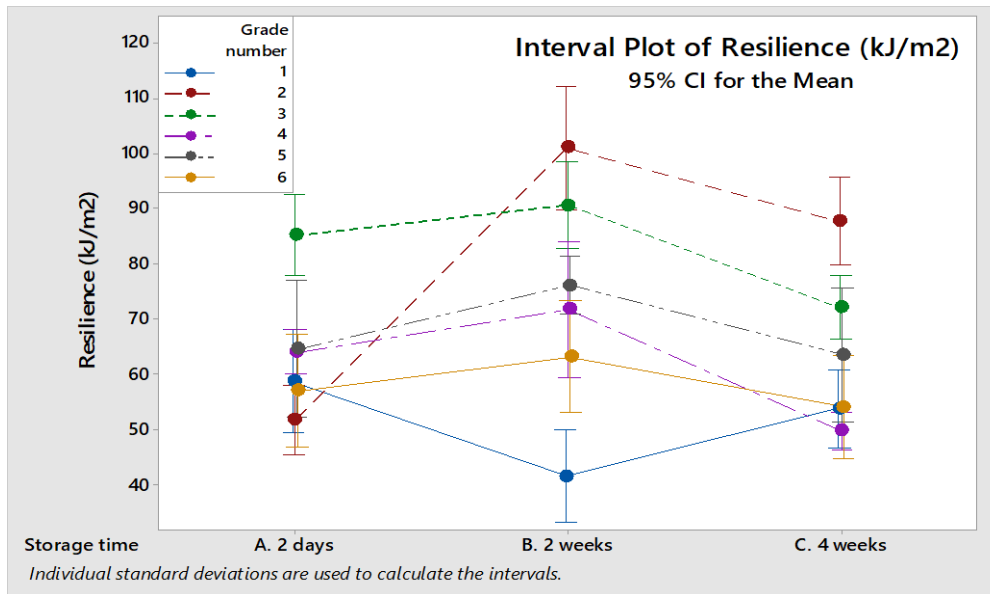


Figure 74. Measures where resilience is attained through calculations by software from energy and cross-section area of samples. Time of measurements are 2 days, 2 weeks and 4 weeks after injection moulding. Not proportional time scale.

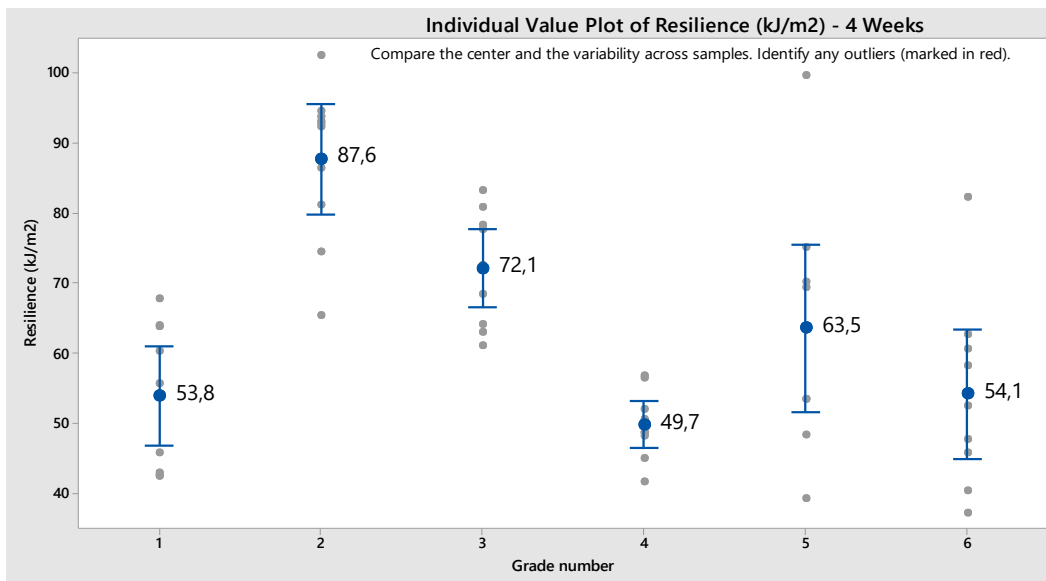


Figure 75. Individual value plot of resilience of the grades after storage of 4 weeks. No outliers are reported. CI of 95%.

Observations (Figure 74 and 75):

- The grades with narrow MWD (grade 2 and grade 3), have a higher observed resilience than the grades with wide MWD (grade 1 and grade 4) after storage.
- Resilience increase (between 2 days and 2 weeks) for the grade with narrow MWD and low Mw (grade 2).
- Significant decrease in resilience after storing can be seen in the two grades with high Mw (grade 3 and grade 4).

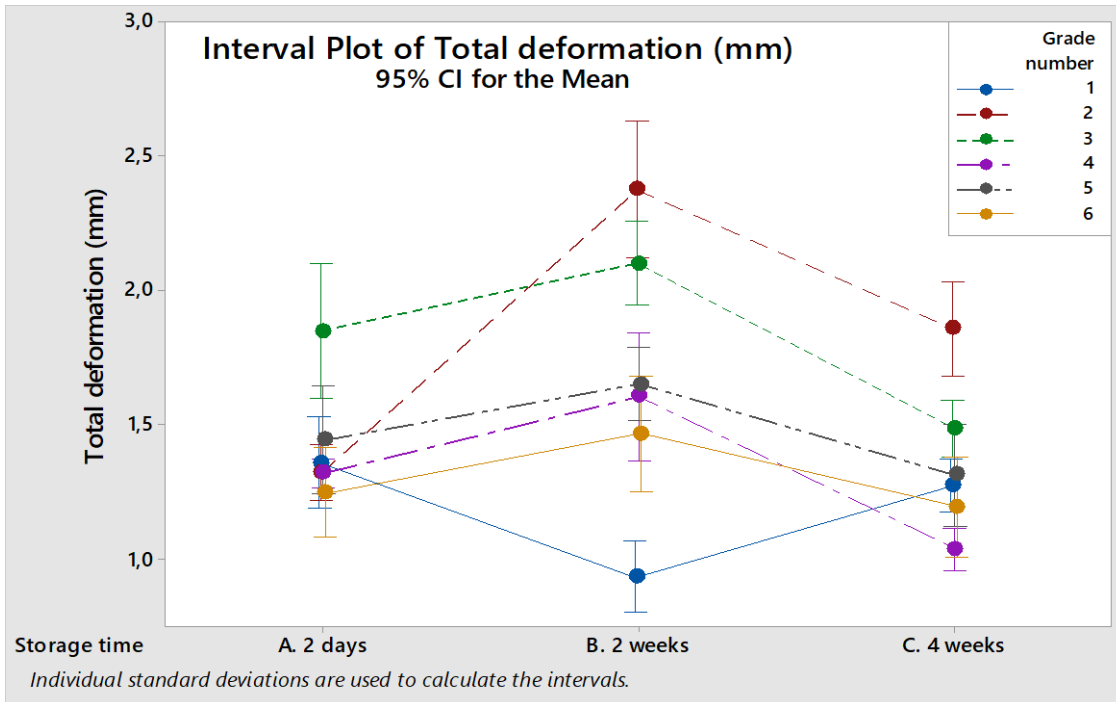


Figure 76. Measures where the total deformation before rupture is reported in mm. Time of measurements are 2 days, 2 weeks and 4 weeks after injection moulding. Notice the not proportional time scale.

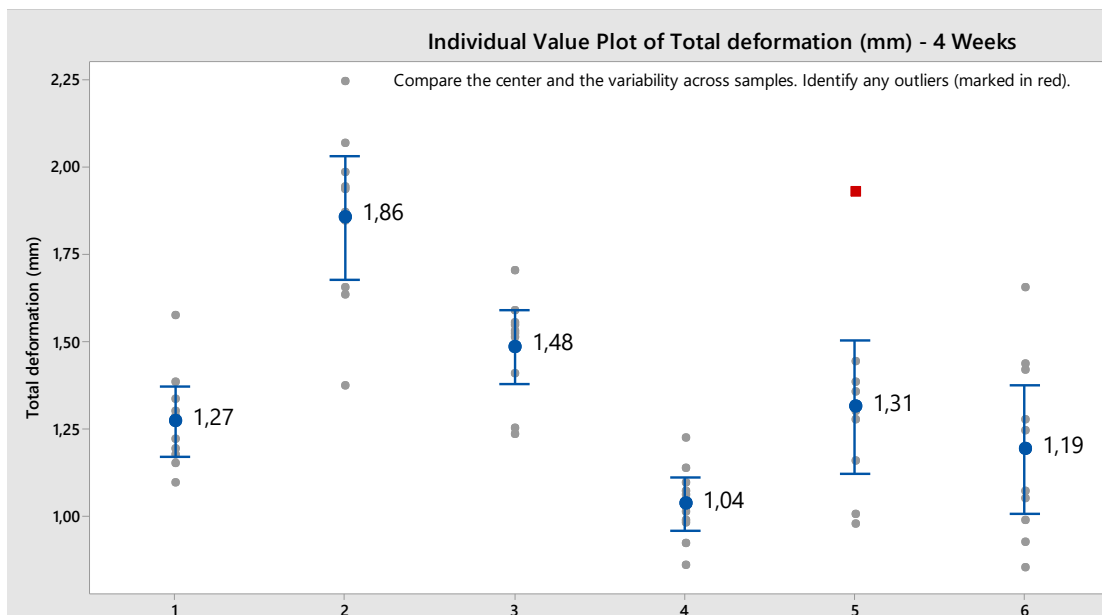


Figure 77. Individual value plot of total deformation (mm) of the grades after storage 4 weeks in tensile impact testing. Outlier is marked in red, and bars marking CI of 95%.

Observations (Figure 76 and 77):

- The total deformation follows the same trends as the resilience.
- Grade with narrow MWD and low Mw (grade 2) have a longer elongation before rupture between 2 days and 2 weeks, and then decreasing in elongation after 2 weeks (but still being significantly higher than its original elongation).

- Significant decrease in deformation between 2 weeks and 4 weeks measure for all grades, except for grade 1 (Wide MWD, low Mw) that have a shorter elongation after 2 weeks compared to 2 days and 4 weeks, and grade 6 bimodal grade with narrow and wide MWD content) which does not change in time.
- Since resilience and total deformation follow the same trends, it could be assumed that the decrease in elongation is the reason for the decrease in elongation, and that grades that get a longer total deformation also have higher resilience.

Values for the graphs are found in Table 31 in Appendix 11.4 where resilience, total deformation and peak force is reported (and standard deviation for those).

6.4 SEM

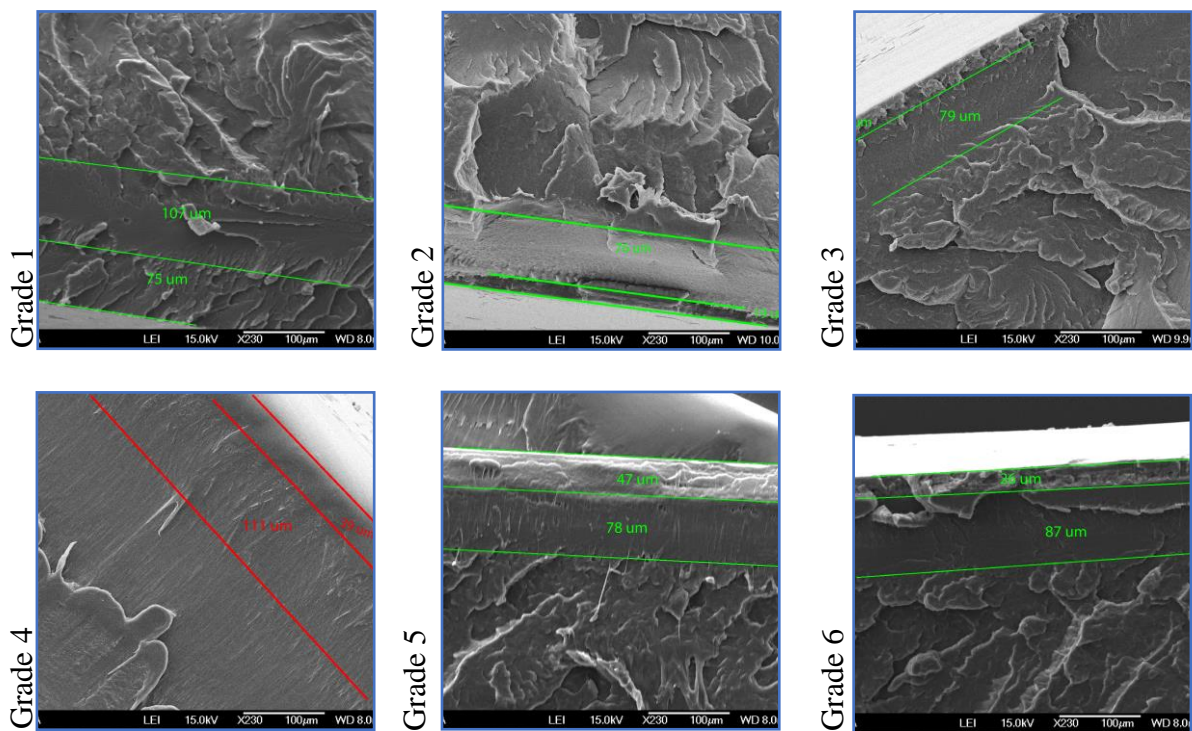


Figure 78. These SEM pictures are taken by magnification 230x by LEI detector, as previously described under methods. The distances are measured in JImage, and edited in Illustrator with measurements and lines.

To attain these magnified areas of interest (images in Figure 78), SEM pictures were taken with less magnification to get a better understanding of the layers observed, where they start and stop. From the overview, it was assumed that there is a core, shear and skin layer present in the dogbones. A few of these pictures are presented in Figure 79 and 80 as example. The magnifications used were 60x, 110x and 230x. All pictures were taken with LEI detector, giving in this case the best resolution. All pictures are taken in low mag. Pictures were taken at both edges of the polymer, but analyses were done at the side that was easiest to interpret. The thickness of the different structures was put together in Table 18.

Grade	skin layer (μm)	Shear zone (μm)	Oriented zones added (μm)
1	75	107	182
2	19	76	95
3	26	79	105
4	39	111	150
5	47	78	125
6	26	87	113

Table 18. Measurements of thickness of shear zone and skin layer, performed in Jimage on the SEM pictures received.

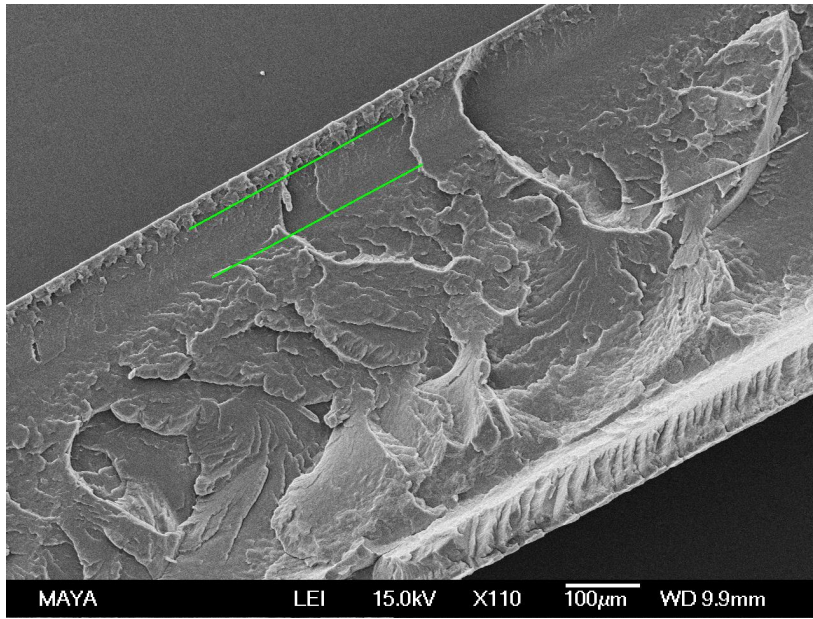


Figure 79. Grade 3, overview.

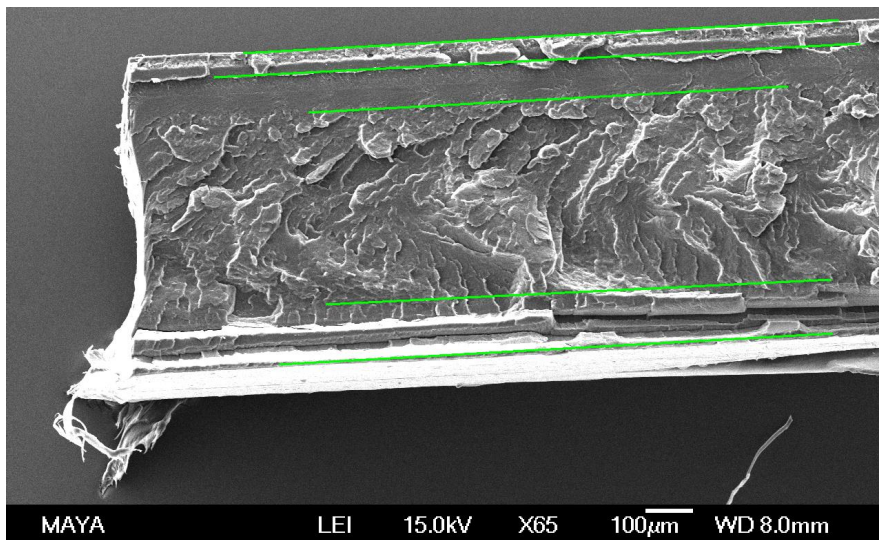


Figure 80. Grade 6, overview.

6.5 DSC

6.5.1 Enthalpy and heat flow diagrams

The heat flow curves made of each grade from 2.5 hours after injection moulding up to 2 weeks can be found in Appendix 11.4. For grade 1 the heat flow curve for 2.5 hour measurement is missing due to fault in the measuring equipment (reference pan not in contact), and for grade 5 and 6 measurement after 2 weeks are missing due to the same problem. The baseline to receive the enthalpy as described in previous chapter were used for all grades (100 °C-199 °C) and the peak melting temperature received from this integration. Since two measurements were performed on each test are the average values for enthalpy and melt temperature reported in Appendix, 11.5. A similar table is reported for the second melting of the grades.

When analysing these results, it can be stated that no difference in melt entropy happens during storage, except for grade 2. In this case the enthalpy goes from average 92 J/g to 97-98J/g, which is a noticeable increase not seen in any other grades. Since 2.5 hour measurement for grade 1 is missing, it cannot be said if something similar to grade 2 happens.

When looking at the heat flow curves for the grades, for grade 1, 3 and 4 there are no fit to an increase of crystallinity with increased time of storage. The chronological order is not reflected in the curves, onset of melting is random. For grade 2 there is a noticeable difference between measurement after 2.5 hours and the other measurements. The peak for 2.5 hours is narrower. A slight trend on a later onset of melting is seen in grade 5 and 6. Further discussion of this is to be red under discussion 7.5.

Similarly, the crystallinity of the grades was calculated as described by the software (in method section), but no difference could be observed over time and the crystallinity varies with the enthalpy of the polymers. A crystallinity between 46-51% was observed in the grades.

6.5.2 Onset

<i>Property</i>	<i>Grade 1</i>	<i>Grade 2</i>	<i>Grade 3</i>	<i>Grade 4</i>	<i>Grade 5</i>	<i>Grade 6</i>
<i>Average °C</i>	189	189	187	186	184	187
<i>Std. dev</i>	1.0	2.1	2.5	2.9	1.4	1.4
<i>n =</i>	2	2	4	4	2	4

Table 19. Onset of degradation of the grades, showing no significant difference between the grades.

It cannot be stated statistically by these measurements that a degradation of the polymer takes place, that would create an earlier onset of the melting of the polymer, based on the information put together in table 19.

6.6 Capillary rheometry

To show the result from capillary rheometry measures, the grades were plotted as to be seen in Figure 81. Raw data is accessible in Appendix 11.6. Table 34.

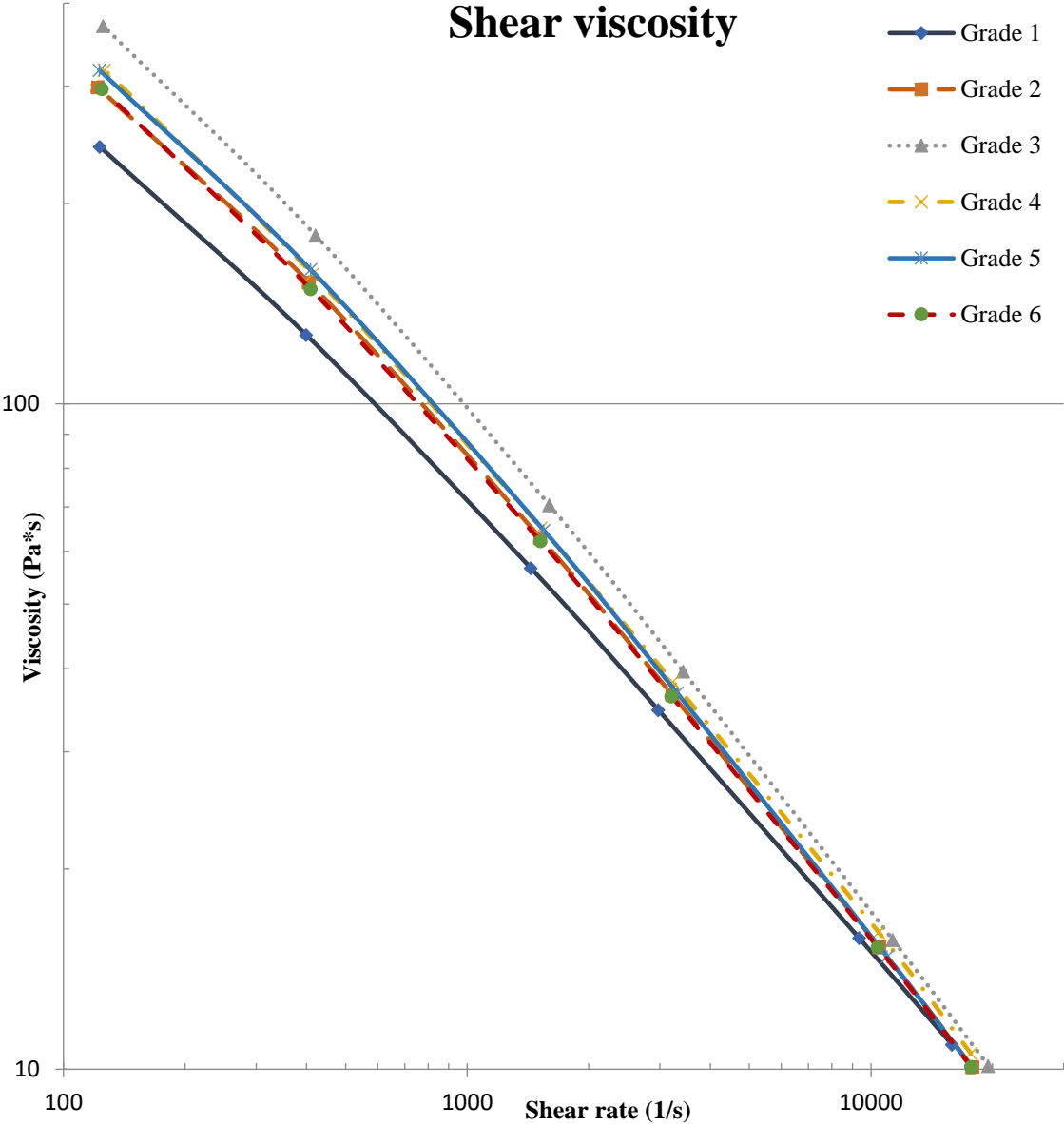


Figure 81. Corrected shear viscosity diagram of the different grades. Corrected with Bagley and Rabinovitch-Weissenberg. Data for plot are to be found in Appendix 11.6. Table 34.

Ranking at low shear rates (from low to high viscosity):

- 1) Grade 1 (243 Pa*s) (wide MWD, low M_w)
- 2) Grade 6 (297 Pa*s) + Grade 2 (299 Pa*s) (Bimodal, grade 2+4) (narrow MWD, low M_w)
- 3) Grade 4 + Grade 5 (317 Pa*s) (wide MWD, high M_w) (Bimodal, grade 2+3)
- 4) Grade 3 (370 Pa*s) (narrow MWD, high M_w)

When comparing the grades having fairly the same MW, it can be stated that the grades having the wider MWD was less viscous, hence, flowing easier. Grade 3 was more viscous than grade 4, grade 2 was more viscous than grade 1, and grade 5 was more viscous than grade 6. Comparing the grades within the wide/narrow groups of polymers the grades with shorter chains (higher MI) flows easier. The grades with lower M_w and wide MWD flow the easiest at low shear rates.

At higher shear rates the grades were very similar to each other which is normal since orientation in the shear direction of the longer chains ease the flow, hence, lower the viscosity.

7 Discussion

7.1 Oscillatory rheometry

The purpose of measuring frequency sweeps with oscillatory rheometry was to examine how homo-PP best is categorised by PDI, when compared to what was assumed to be the “real” distribution measured by SEC. Instead of performing more complicated SEC measures, it was of interest for Tetra Pak to find out how it was possible to examine the MWD of the grades with rheology. Depending on type and quality of polymer, different equations with information from different frequency regions might show best fit. PDR, ER and PI was examined by being plotted towards both M_w/M_n and M_z/M_w , where M_w/M_n is the most frequently used measure of PDI, and M_z/M_w is a PDI measure where the amount of long heavier chains is affecting the result more.

The best fit was received by the rheology PDI measure PDR, second PI and worst ER. The SEC polydispersity measure that was fitting best to the rheology measures was M_z/M_w . M_z/M_w is a measure that better reflects the content of longer chains, which do affect rheology measures.

Between the different rheology PDI measures, PDR takes information from both the beginning, middle and end of the frequency range into account when determining the PDI, PI is using information in the higher frequency range and ER information in the lower frequency range of the sweeps. Hence, it seems like it was of importance to use information in the higher frequency range when analysing PDI by rheology of homo-PP, this since the ER measure gave a quite bad fit to the SEC data.

Conclusions are then that rheology measures best fit the M_z/M_w for homo-PP (MI 14-25), using PDR.

7.2 Tensile tests

7.2.1 General discussion

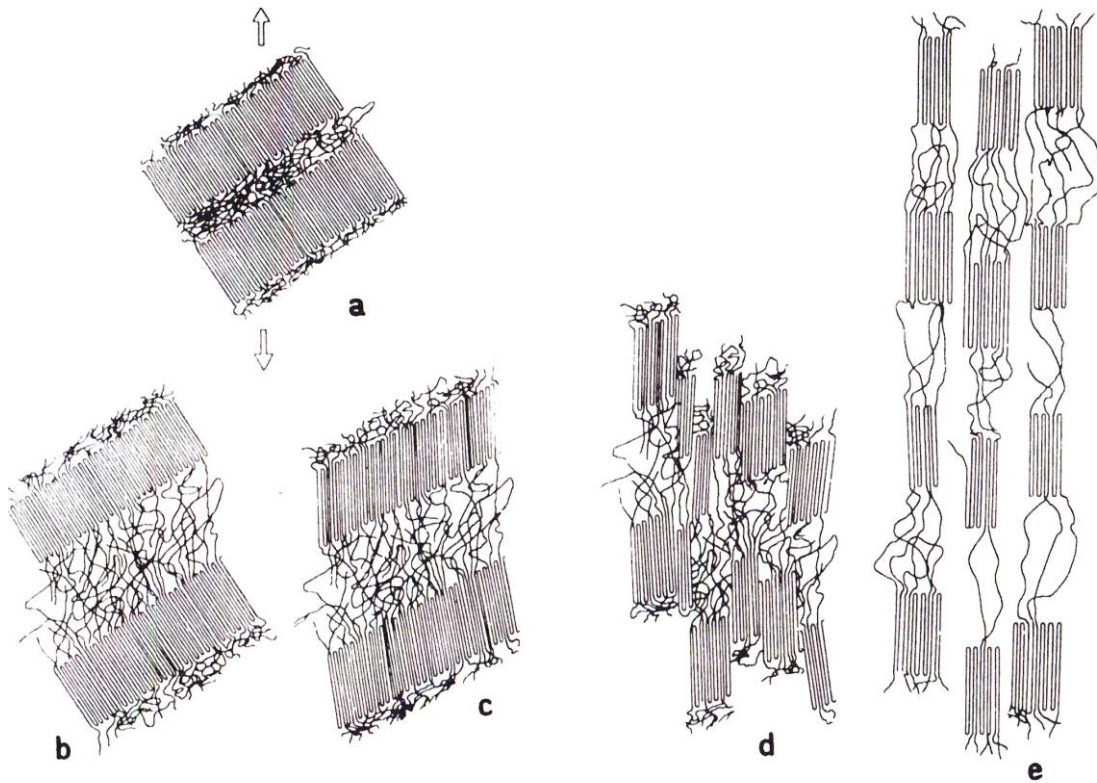


Figure 82. Semi-crystalline polymer during tension. (Schultz, 1974)

Tensile tests were performed on injection moulded plates, where processing (shear and flow) affect the resulting properties in the different directions. The polymer chains get oriented in direction of shear, which is the machine direction on the plates due to where the injection point was placed. The modulus was higher in the direction of shear, since part of the chains are oriented in this direction and provide strength in the material. In cross direction the chains were oriented parallel to as they were in MD, increasing the brittleness and ease of crack propagation in the material (since the orientation was in the other direction). Hence, different types of modulus and yield point were observed in MD, CD and DD.

The elongation at break has been observed to be the longest in DD, second in MD and shortest in CD (when polymer was stable). During elongation the elongated part (necking) turns white, showing that strain hardening takes place, or other type of re-crystallisation. The reason behind the white colour, is that different phases in the polymer (crystalline and amorphous) have different refractive index, hence, refracting the light differently. During the elongation, the crystalline part in the polymer increase. This is possible because the amorphous phase, previously entangled and un-stretched, is stretching out, allowing crystallisation. Different type of elongation was observed in the different directions as can be seen in Figure 69-74 in result 6.2.5.

In MD the elongation was supported and restricted by the orientation, creating the highest modulus and yield point among the directions. The chains, as they were already oriented in the direction of tension, will be extended even more, stretching the amorphous phase and allowing strain hardening. This was observed during tension in DD as well, with a stronger formation of fibre and longer elongation at break, see comparison between Figure 74 and 70. It is assumed that the tension in DD was very similar to the tension illustrated in Figure 83. where the amorphous area is stretched out between the crystalline areas. Fibres were observed in areas around the final break, picture of this is to be seen in Figure 74. A hypothesis regarding why the elongation at break in DD is the longest is that larger yield zones get activated due to the angle towards the orientation. The chains are not as restricting, but still oriented in a way that hinder crack propagation.

The tension in CD differs quite a lot from MD and DD, where a different pattern was observed in the elongated area (see Figure 72). A possible explanation could be that the chains that are aligned and crystallised in the direction across the sample (see arrows on Figure 84), gets separated and that the amorphous phase between the crystalline segments is elongating and crystallisation takes place during the elongation. The crystalline areas that are perpendicular to the elongation, ease the crack propagation, reducing the elongation at break. During tensile test it was noted that the breakage almost always happened on the right side on the dogbone, as seen in Figure 71. noted H for the right side. This is probably due to two things, inhomogeneous thickness in the plate (where the right side is slightly thinner) and flow pattern in the mould.

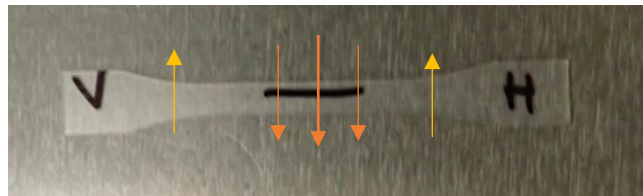


Figure 83. Picture of the dogbone in CD, with orientation due to flow direction in mould marked.

Since there will be different degree of orientation in the different layers (skin, shear zone and core) of the injection moulded plate, they provide different properties of strength and elongation to the plate. It is assumed that the core, which should contain spherulites, give a more isotropic behaviour to the material, and the orientation in shear zone and skin layer provide a stronger anisotropic behaviour. What structure formation and which type of spherulites there are in the plates needs further examination, by for example SAXS or WAXS. A suggestion could be shish-kebab structure in shear zone and a core with spherulites, as suggested by an examination of injection moulded isotactic-PP using X-ray, SEM and polarised light microscopy (Mi, et al., 2016). The researchers proof that the rate of orientation in injection moulded PP decrease with distance into the sample, from the skin to the core.

To further examine how Young's modulus, yield point and elongation at break differ between grades and the observed changes in time, the rest of this section will be divided into a section where the grades are compared to each other, and the other discussing the property change over time.

7.2.2 Young's modulus, yield point and elongation at break

Most of the analysis that follows was based on performance during week 6, since all grades then were considered “stable”. In general, in all directions, grades with wide MWD (grade 1 and 4) have the highest modulus and yield point, followed by grade 6. Next in order are grades with narrow MWD but higher M_w (grade 5 and 3). In general, the grade with narrow MWD and low M_w (grade 2) have the lowest yield point and modulus. In elongation at break, grade 2 and 3 (narrow MWD) have the longest elongation (shifting between directions), followed by grade 1, 5 and 6. Grade 4 with wide MWD and high M_w have the shortest elongation.

The analyses that follows for Young's modulus and yield point were based on plots and observations. The plots consist of the examined property after 6 weeks, when all the grades are considered stable, versus a measure of polydispersity or average molecular weight. The measures of polydispersity are either from SEC data or rheology measures. Linear fitting has been used to determine how well the property (y-value) fit towards each MWD or M_w (x-value). The received R^2 value are assumed to tell how well the model can predict the effect from MWD and M_w . Regarding the mechanical properties used as y-values, averages have not been used, but the real measure from each dogbone. The plots can be found in Appendix 11.3.4-11.3.5. The overall best fit between the mechanical properties and PDI measure was in MD. This is assumed to be since the degree of orientation was affected strongly from MWD, where an increased MWD give a higher orientation, hence, stronger properties in that direction.

7.2.2.1 Youngs modulus

<i>PDI measure or Average molecule weight</i>	<i>Youngs modulus</i>		
	<i>MD</i>	<i>CD</i>	<i>DD</i>
<i>PI</i>	0.65	0.53	0.49
<i>ER</i>	0.32	0.06	0.23
<i>PDR</i>	0.72	0.48	0.33
M_w/M_n	0.5	0.34	0.1
M_z/M_w	0.78	0.54	0.42
M_n	0.23	0.16	0
M_w	0.18	0.26	0.45
M_z	0.67	0.56	0.69

Table 20. R^2 values from linear plotting of Young's modulus (after 6 weeks of storage) vs. different measures of PDI or average molecular weights. Plots are to be found in Appendix 11.3.4. Figure 86-91. Better fit (higher R^2 vaule) means that the measure can be used to predict the resulting yield point of the grade.

MD

From observations it has been realised that MWD affect Young's modulus, where a wider MWD gives a higher modulus. To validate this, plotting as previously described towards different measures have been performed. The result was that the best measure to predict the resulting Young's modulus is the PDI measurement M_z/M_w , from SEC data (presented in Table 20). R^2 value received from this measure is 0.78, which is a good value of prediction. PDR was also a good fit towards Young's modulus in MD ($R^2 = 0.72$).

It can be understood that both the polydispersity and content of long chains (reflected in M_z) are important factors in the resulting modulus, where wider MWD and longer chains increase the modulus.

The M_n , M_w and M_z was plotted towards Young's modulus and the result validates previous finding, the plot showed that M_z was the measure of the polymer that strongest affect Young's modulus (with a resulting R^2 value of 0.67, found in Appendix 11.3.4. Figure 86 and 87).

CD

When performing the same analyse for Young's modulus in CD direction, the best fit was the M_z/M_w measurement ($R^2 = 0.54$, table 20), same as in MD. The second best describing measure (could be regarded as equally good) is the fit towards PI ($R^2 = 0.53$). PI is a measure of polydispersity from the cross-section between G' and G'' , at higher frequencies (by oscillatory rheometry).

It should be noted that the overall fit to polydispersity is worse in CD compared to MD. When plotting Young's modulus towards average molecular weight, the best fit is towards M_z ($R^2=0.56$), implying that the content of long chains is of importance. This is probably true, since Young's modulus is a measure of elasticity/stiffness, where long chains could decrease the elasticity and increase the stiffness due to more restricted chains in the semi-crystalline structure. **Hence, the long chain content increases the yield point of the material.**

DD

The best received R^2 value when repeating the same plotting as previous, was with M_z value from SEC on the grades ($R^2=0.69$. presented in Table 20). **Youngs modulus seems to be the most dependent on the longest chains present in the polymers, which in this case is the grades with wider MWD.**

7.2.2.2 Yield point

<i>PDI measure or Average molecule weight</i>	<i>Yield point</i>		
	<i>MD</i>	<i>CD</i>	<i>DD</i>
<i>PI</i>	0.3	0.22	0.35
<i>ER</i>	0.78	0.63	0.3
<i>PDR</i>	0.51	0.2	0.37
M_w/M_n	0.18	0.02	0.21
M_z/M_w	0.53	0.21	0.45
M_n	0.01	0.04	0.07
M_w	0.26	0.24	0.16
M_z	0.54	0.27	0.49

Table 21. R^2 values from linear plotting of yield point (after 6 weeks of storage) vs. different measures of PDI or average molecular weights. Higher R^2 value is a better fit, where the plots and equation for each linear fit can be found in the Figures 92-97 in Appendix 11.3.5. Better fit means that the measure can be used to predict the resulting yield point of the grade.

MD

Plotting as previously described was performed, resulting in best fit towards ER ($R^2=0.78$, table 21) and M_z ($R^2=0.54$). One again, it seems like the weight fraction of higher weight

molecules influence the resulting property the most, together with MWD. ER is a measure of PDI based on oscillatory rheometer measurements, at low frequencies. At low frequencies the influence from the high molecular weight end of the spectra is larger than low weight molecular end. ER was the measure that fit the worst to the SEC data, but seems to describe the effect from MWD on yield point well. **The yield point is increasing with higher ER, hence, higher molecular weight end of the polymer and broader MWD.**

CD

Regarding what influence the resulting yield point in CD, plotting yield point towards measures of PDI and average molecular weight, only ER gave a fit ($R^2=0.63$, Table 21). Previous discussion as in MD seems to be valid for CD. In CD the lowest measured yield point is by the grade with narrow MWD and low M_w (grade 2). A possible explanation to this could be that there are no longer chains present that can tie the crystalline parts together when separated in CD (which is perpendicular towards the orientation). Hence, **longer chains present** (higher weight fraction of long chains) **will increase the yield point.**

DD

The yield point in DD have a value somewhere in between MD and CD, where the grades with wide MWD have a higher yield point than the grades with narrow. When plotted towards polydispersity and average molecular weight no good fit was received, where no R^2 value was higher than 0.5. The best received was the fit towards M_z ($R^2 = 0.49$), once again showing on an influence from the higher weight fraction of long chains on the resulting yield point, **where an increased M_z result in a higher yield point.**

7.2.2.3 *Elongation at break*

MD

Plots like previously discussed have been performed with elongation at break, but finding a good match between a certain measure of polydispersity by linear equation was unsuccessful (hence, these plots are not in appendix). Findings in a report (Mi, et al., 2016) is that the ratio between shear layer and core thickness is strongly influencing the elongation at break in MD. The researchers provided a model for the effect from ratio of shear/core thickness on elongation at break, where an increased thickness gave a decrease in elongation. This model has been tried to fit the result from tensile tests performed versus the thickness of layer measured by analyse in SEM. Unfortunately, the model does not fit, but it would be rather strange if it did. In their research they examined only one type of homo-PP, by adjusting the injection moulding settings to receive different layers of thickness in the shear zone. In this research, where the resulting thickness of the layers arise from different polymers with different chain length and polydispersity, the model would have to be highly adjusted to fit.

Still, the shear zone and skin later are assumed to influence the elongation at break of the sample, where the **grades with thicker zones have a shorter elongation at break in MD.** Hence, the thickness of oriented layer is assumed to affect the elongation, but not only itself. The polydispersity and average molecular weights are assumed to influence the elongation, but not in a linear way. There are large standard deviations in elongation at break between the

samples which makes it harder to fit the result with a good model. From just analysing at the difference in elongation between the grades, the grades with narrow MWD are more elongated at break than the grades with wide MWD (in MD). **The grade most elongated have a low M_w and narrow MWD, hence, this is assumed to promote the elongation before break** (which also is the grade with thinnest oriented zone).

CD

It is observed that the grades with wide MWD have a shorter elongation at break than grades with narrow when the grades are stable. In these grades, the break was almost instant when performing tensile test, and very little necking (if necking at all) occurs. This could be due to that the grades with wider MWD have a stronger orientation in the shear zone, and that there was less amorphous segments with possibility to move and crystallise in the direction of tension. In the grades with narrow MWD, the orientation is less, which would imply that they have more isotropic behaviour. This might be why the elongation at break is slightly longer in CD for these grades. Since grade 2 is having the same elongation at break as the grades with wide MWD (in CD), it is suggesting that length of chains is of important. This could be because the same chain could take place in different crystal formations. Conclusion would be, that **the elongation at break is promoted by long chains present, but narrow MWD.**

DD

The elongation at break in DD is the longest by the grades having the lower M_w , Grade 1 and 2. The shortest elongation at break is measured by grade 4 (after 6 weeks). Grade 3, 5 and 6 have fairly the same elongation at break when stable. From this, it is assumed **that a low M_w is increasing elongation before break.**

7.2.2.4 *Performance measured from compounded grades*

The two compounded grades 5 (grade 2 + 3) and grade 6 (2 + 4) do most of the time perform somewhere in between the grades they are compounded from, but not in all attributes. Grade 6 have higher modulus and yield point than grade 5, or equal. Grade 6 have shorter elongation at break than grade 5. Their performance in each property compared to its components in compounding the grades are summarised as follow:

Yield point:

- Grade 6 have a yield point more similar to grade 4 than grade 2, indicating that the MWD is of high relevance for this property.
- Grade 5 have a yield point measured to be in between the grades 2 and 3 in MD and CD, but closer to the yield point of grade 3 in DD (lower than both grade 2 and 3)

Youngs modulus:

- Grade 6 have a modulus below both its components in MD, closer to the one of low M_w in CD (but still between), and a modulus between the grades in DD.

- Grade 5 have a Young's modulus that is closer to the high MW content in MD, and higher than both its components in CD and DD. This might be due to the increased M_z grade 5 have compared to its components.

Elongation at break:

- Grade 6 have an elongation at break between its components in MD and DD, but closer to the grade of high M_w (influencing a shorter elongation). In CD, grade 6 have a shorter elongation at break than both its components (might be due to the lower M_z than its components).
- Grade 5 have an elongation at break between its components in all directions, where the elongation is closer to the grade of high M_w (grade 3). Hence, it's elongation is shorter than in between the components it is compounded from.

To summarise the finding, it is assumed that the differences observed in how they relate to the grades they are compounded from, are much due to the resulting MWD, M_w and M_z . Grade 6 have a narrower MWD than grade 1 and 4 (if using PDI measure M_z/M_w , ER and PDR). Hence it will have a lower yield point and young's modulus in general, which also is observed. Grade 5 gets a wider MWD than grade 3 with a higher M_z , making young's modulus higher than grade 3, and same or higher than grade 2. The yield point of grade 5 is between the grades, where the influence from MWD still makes a difference between narrow and wide, but within the class of narrow grades not seems to influence the resulting yield point. Here, the M_w is of higher influence, where the compounded grade gets a M_w between the components, resulting in a yield point between the grades.

7.2.3 Change of properties during storage

Difference in performance during storage are assumed to due to two different phenomena's, physical ageing and post-crystallisation. Physical ageing is taking place in the amorphous phase and is increasing its density. The amorphous areas are rearranging themselves (getting more dense) due to relaxation, building in tensions between the crystalline areas that are locked in position. Post-crystallisation is assumed to either increase the crystalline phase over time, or change the structure of the crystals. If the crystalline area is getting larger, there is a need for mobility of shorter chains (so that they can move into position to post-crystallise). Hence, **grades with higher content of short chains are expected to post-crystallise more. Physical ageing is reported to lead to a stiffer material, where Young's modulus and yield point are increasing over time of storage, and elongation at break decreasing.** Physical ageing is assumed to be enhanced by the rigidity of the amorphous phase, together with the semi-crystalline morphology details, which unfortunately have not been examined in this thesis.

Observations are that grade 1, 2, 3 and 4 change mechanical properties over a longer time frame than the bimodal grades (5 and 6). Within grade 1- 4, it is grade 1 and 2 that change the most during storage. This might be due to the shorter chains present in the grades, that are assumed to have a higher mobility.

In general, it can be observed that during storage, the modulus and yield point increase, and the elongation at break decrease. The polymers get stiffer over time.

The bimodal grades differ much less in mechanical properties during storage, they are both completely stable after 7 days. What this is due to is not known or fully understood by the author, but speculations can be done. Either it is due to the bimodal nature of the grades, or due to the different settings during injection moulding or due to difference in pellet size. The other four grades are processed by Tetra Pak supplier and have a different (larger) pellet size. When compounding the pellets at Tetra Pak the shape is not round, it is cylindrical and a bit smaller. This could influence the injection moulding and mixing in the extruder. Other explanation could be that the created bimodal-nature of the grades would influence the phases (crystalline and amorphous) so that there are more restrictions of movement, and less possibility of physical ageing or post-crystallisation.

7.2.4 General conclusions

What is observed is that there are many similarities between grade 4 and grade 1, in terms of yield point and Young's modulus. In machine and diagonal direction (MD/DD) the results are almost identical, during the different measurements made during storage. In elongation at break, it is observed that that grade 4 is a bit stiffer than grade 1, that has a slight longer elongation. This is due to the lower M_w , where smaller chains have more freedom to move and recrystallise during elongation.

The elongation at break is long for samples with lower Young's modulus (when comparing elongation and Young's modulus within the same direction of tensile testing). Young's modulus is a measure of stiffness, about the polymers resistance to plastic deformation and its elasticity. When having a long elongation, the polymer is deforming. The grades having a stiffer nature (grade 1, 4 and 6) also have a shorter elongation at break when stable. Grade 1 is in the grey zone, where short chains present enhance the elongation at break a bit compared to grade 3. Grade 2 and 3 show a low Young's modulus and a long elongation at break in all directions (except grade 2 in CD elongation, where long chains present is important for elongation).

It should be noted that the SEC data of M_n and M_w seem to have very low influence over the mechanical response over all. Influence from M_z is superior.

Summary:

Youngs modulus

- Highest Young's modulus is measured in MD, second CD and lowest in DD
- Youngs modulus is influenced by polydispersity and M_z , where more content of longer chains and wider PDI are increasing the modulus

- The grade with the narrowest MWD (grade 3) also have the lowest measured Young's modulus in all directions.
- Youngs modulus is highest after storage in the grades with wide MWD

Yield point

- Highest yield point is measured in MD, second in DD and lastly in CD, where the one in DD is almost between the one in MD and CD in strength.
- Yield point seems to be influenced by a wide MWD with a high molecular weight end, a content of long chains
- Yield point is decreased by a majority of short chains in resin combined with narrow MWD.

Elongation at break

- Longest elongation at break (when stable) occur in DD, second MD, shortest CD. Thinner skin and shear zone seems to extend the elongation before break.
- Elongation at break is promoted by a decreased orientation of chains in the direction of tensile testing. Short chains in resin allows more freedom to elongate, hence, promoting the elongation. In the case of tensile testing perpendicular to the orientation, longer chains present will enhance the tie at a macromolecular scale, allowing a bit more elongation. Narrow MWD decrease the orientation, hence, increasing the elongation before break.

During storage

- Overall, the modulus and yield point increase, and the elongation at break decrease with time from injection moulding.
- The elongation at break in DD is decreasing in grade 1, 5 and 6, the other grades do not change in elongation at break over time.
→The elongation at break in CD and MD seems to be the most affected during storage.
- Less changes in properties over time are by the bimodal grades (stable after 7 days)
- The grades with lower Mw seems to change the most over time, assumed to be due to higher inner mobility of the chains

7.2.5 Discussion regarding validity

The validity of the measurements must also be discussed. Since all dogbones were punched by hand with no exact fixed position, there is a slight variation in measurements due to inhomogeneous in plates. Since the thickness vary over the plates, and also the orientation due to flow lines, variations in how the dogbones are punched can be of great importance. During the punching, this have been kept in mind to get as similar bones as possible, but will still result in an error. Another source of possible error is the punching, where some grades are stiffer than other. Depending on how long time after injection moulding the dogbones are punched, crack formation from the knife might take place. All dogbones are punched within

three days of injection moulding, but on these three day the stiffness of the material is increasing. Due to lack in time has it not been possible for all grades to punch the same day as injection moulding.

Other sources of errors are the placing in the tensile machine, where the dogbones are mounted manually. They might be tilted, which can influence the measured properties. If tilted, they might get an enhanced elongation since slip in more dimensions might be allowed (compare elongation in MD/DD/CD where elongation at break in DD is the greatest).

Possible calibration of machine might as well affect the result. No major calibration was performed during the measurement series, but measurements performed by other at Tetra Pak might use the machine differently. What also have been noticed during the tests is that the machine takes differently long time to start the measurements, and sometimes when the machine is waiting a long time to perform the measurement the yield point gets noticeably higher than the other measurements. These measurements have then been removed.

Regarding precision of days measurements were aimed to be performed at, all tests performed between storage time of 2.5 hour to 3 days was performed as they should. Due to public holiday the 7 days measurement was performed after 8 days for grade 5 and 6. Small variations in time of performance for measurements after 4 and 6 weeks in storage have been the case for some of the grades due to occupied tensile test machine and public holidays, but it is assumed not to affect the results.

For grade 1, injection moulding has been performed twice due to that the plates finished. The same settings are used for the injection moulding, but there might still be slight variations. One batch is used for measurements when stored: 2.5 h, 1 day, 3 days, 7 days and 2 weeks, and one other batch is used for 4 weeks and 6 weeks measurements.

To increase the validity of the tensile testing a couple of samples have been tested simultaneously (between 7 and 10 samples for MD and CD) at each time of storage. For the diagonal testing have only 5 samples normally been tested to save time. There should hence be an increased validity in MD and CD versus DD.

To increase the validity samples have been stored at 23 degrees and 50% relative humidity, but they have occasionally been moved to the test equipment and the punching room where the temperature is not controlled.

All this different source of errors must be kept in mind when analysing the results and its validity.

7.3 Tensile impact

The tensile impact test performed have a large standard deviation (from Tetra Pak lab, normally it's reported a standard deviation for resilience below 10 is acceptable) and the result received was not expected. The increase in modulus observed in the tensile tests do not seem to be reflected in the tensile impact testing. What can be observed is that the total deformation follows the measured resilience very well. The explanation for this could be that

since more of the material is expanded when having larger deformation, a larger amount of the material can help absorb the energy from the hammer before fracture through crack propagation.

What is also observed is that the grades with narrow MWD have a higher resilience than the grades with wide MWD. This influence could affect the grades in a couple of different ways. Wider MWD of polymers generate higher rate of crystallinity (see theory section), but this difference is quite small when comparing the grades (although there is a noticeable difference in crystallinity between grade 2 and 3 compared to grade 1 and 4, see discussion DCS). Higher rate of crystallinity creates a stiffer material; hence, this might influence the result.

Another possible explanation to why the grades with wide molecular distribution have lower resilience after storage than the narrower grades, is that they get more brittle during physical ageing. This brittleness will reduce the total force the specimen can absorb before breakage, and crack propagation in the material will happen earlier. When comparing wide and narrow distribution, the grades with narrow MWD have a longer total deformation length than the grades having a wide MWD.

It might also be an effect of morphology due to difference in viscosity during shear, resulting in different types of flow pattern and microstructures. Unfortunately, there have not been enough time to examine the different grades in light microscopy revealing its microstructure, size of spherulites and similarities, to correlate this to the mechanical response.

7.4 SEM

When analysing the thickness of the skin layer and shear zone combined, a finding is that the materials that have a higher modulus and yield point (grade 1 and 4) also have a thicker oriented zone than the other materials.

The core in the structure is the part which is assumed to give a more isotropic module to the materials. When analysing the tensile tests, it can be stated that the grades with the most anisotropic behaviour are grade 1 and 4 (in Young's modulus and yield point)

When analysing the materials by SEM, the specimens have been frozen before broken by help of a notch. The different mechanical properties in the material (read; the different zones) should be visual. This give validity to the result of the analyses. Also, polymer is very sensitive for SEM and other microscopy analyses including electron guns, but before analysing the specimen have been covered with a very thin coating, which also increase the validity of the findings.

What is decreasing the validity of this finding, is that only one test of each grade has been performed. The validity of this finding would be highly increased if the analysis was repeated with the same findings. Although, since this difference in modulus is measured between the materials in tensile testing, it is very likely that these grades do have a thicker oriented zone. Since more longer chains are present in these grades, it should generate higher rate of orientation and hence, a thicker skin layer and shear zone.

7.5 DSC

It was anticipated to record a change in enthalpy and the resulting heat flow diagrams from DSC, where a lower enthalpy was expected after injection moulding and a higher after storage due to post crystallisation phenomena. This behaviour was recorded for grade 2, where the 2.5-hour measurement showed a noticeably lower enthalpy than the rest after storage. In the heat flow diagram, the entire peak is narrower than the other curves, which could be a sign of post-crystallisation. In later measurements the melting starts earlier, which could be a result of that amorphous areas close to the crystalline segments transform into crystalline structures between 2.5 hour measurement and 1 day measurement. The 2.5 hour measurement peak is narrower on both sides, indicating that crystal structures seems to grow (structures that takes higher temperature to melt). To draw any further conclusions of this, it would be needed to repeat these measurements, to examine if the result would be the same.

In regards of grades 1, 3, 4, 5 and 6 there are no obvious trends to discuss in the form of enthalpy changes during storage, the measurements performed in time do not correlate to any specific enthalpy change. Although, if looking carefully at the heat flow curves for grade 5 and 6, there is a slight difference on the onset of melting for the 2.5 hour measure. This might arise from the contribution of grade 2 in the mixture that grade 5 and 6 are compounded from, enhancing that the difference recorded for grade 2 is not an error in set-up, instead a post crystallisation phenomenon.

Since there might be a post-crystallisation event taking place the first 24 hours, when comparing the melt enthalpy (first melting) of the grades, an average of measurements performed 1 day, 3 days and 7 days after injection moulding have been utilised. When discussing rate of crystallisation, enthalpy will be utilized and compared, since rate of crystallisation is directly proportional to enthalpy when comparing homo-PP to another. When comparing the grades, the finding is that grade 2 and 3 have significantly (CI 95%) lower enthalpy than grade 1 and 4, and grade 3 alone differ from grade 6 (having lower enthalpy). This is the expected case, since a narrow MWD should result in lower crystallinity.

When studying and comparing the second melting of the grades, it was assumed that they would overlap perfectly since this should erase the memory of the injection moulding (hence the orientation and crystal structures resulting from shear, as well as post crystallisation) but it was not the case. Why it is not, is out of this scope but would be interesting to examine further.

The shape of the heat flow curves for grade 1 and 2 in its second melting differs a lot from the other grades. Grade 1 and 2 have shorter chains (lower M_w) and these earlier melting peaks might be signs of that other spherulite structures are present, or other low crystalline regimes that are present. For grade 1 there are peaks in the second melting at the temperatures 145 °C, 152 °C and 160 °C. For grade 2 there is one melting peak at 145 °C, one at 152 °C and a larger one with maximum at 156 °C but a smaller peak at 164 °C. These peaks are very similar in temperature and differences are to be ignored. Hence, peaks at approximately 145 °C, 152 °C and 160 °C occur. They differ largely from the first melting of the polymer, which

is at approximately 164 °C for all grades. Another important thing to consider is that the first structure of the polymer is due to shear during injection moulding, which force the polymer chains into orientation. During the DSC, after the first melting, the polymer is slowly cooled (without shear) and the polymer have much longer time to re-crystallise. This will result in that some of the earlier amorphous areas crystallise, increasing the degree of present crystalline areas. Hence, areas that earlier were amorphous are now low crystalline shifting the melt peak to the left.

Although, from the DSC the major finding is that it is not possible to couple any change in crystallinity to the changes observed in modulus and stiffness over time (where mechanical differences are recorded over a much longer time of storage). Post crystallisation might take place during longer time than 24 hours, but DSC is not a sensitive enough technology to use to record this.

7.6 Capillary Rheometer

When choosing material for processing for injection moulding thinner parts as caps and closures, the ease of flow in the mould is very important. In injection moulding of caps and closures, shear rates vary between 100 and 100 000 1/s. If the polymer flows easy, injection can be performed at lower temperatures, hence, the cycle time can be reduced resulting in higher output. What could have been expected from the measurements are the received result, that the polymers with the wide MWD are less viscous at low shear rates due to the presence of shorter chains, lubricating the flow and making it possible for the longer chains to flow easy. Grade 1 flows the easiest due to lower M_w (shorter chains as average) and the presence of very short chains, grade 2 and 6 due to the low M_w of grade 2 and regarding grade 6, the wider dispersity but not as long chains as average as grade 4 has. Next grade 4 and 5 have equal viscosity, for grade 4 due to presence of very short molecules (wide MWD) and grade 5 due to the part of the grade arising from grade 2, with lower average M_w . Grade 3 is the most viscous polymer, with low amount of short chains and high M_w .

The grades having a wider MW would be better for processing, due to lubricating from smaller chains, lowering the viscosity.

8 Conclusions and major findings

8.1 Rheology

- From capillary rheometry it has been detected that low M_w and wide MWD decrease the viscosity, making the polymer possible to injection mould with shorter cycle time.
- The best fit for rheological measures on MWD for homo-PP with MI between 14-25 are by the measure PDI.

8.2 MWD and Mw influence on mechanical properties

- Tensile impact measures resulted in the observation that grades with narrow MWD have a higher resilience than the grades with wide MWD.
- Tensile tests resulted in the observation that the grades with a wide MWD make the material stiffer (higher modulus and yield point) and shorter in elongation at break. Higher M_z increase modulus and yield point and decrease elongation at break in MD, but increase the elongation at break in CD. In CD, elongation at break is promoted by narrow MWD and longer chains.
- High concentrations of shorter chains seems to allow more post-crystallisation.
- Post crystallisation and physical ageing take place, resulting in a stiffer material during storage with increased Young's modulus and yield point and shorter elongation at break.
- The bimodal grades are observed to change less in properties over time of storage.
- The bimodal grades seem to be more influenced by resulting MWD than the specific components they are designed from.

8.3 Crystallinity and microstructure

- DSC has shown not being an exact enough method to use when studying changes in the crystallinity of these grades, findings would hence be, that another method of analyse is needed.
- Findings are that the thickness of skin layer and shear zone seems to increase with width of MWD, increasing the amount of orientation in the injection moulded samples.

9 Proposals for future work

To further examine the post-crystallisation and ageing phenomenon, a new measurement after 6 months is recommended, to follow up if there are further increase in modulus and yield point, and decrease in elongation at break. It would be of interest to examine the ageing that is assumed to occur in polypropylene over time of storage, by for example density measures and X-ray. When this thesis started, the ageing phenomena was not considered, hence, not examined. DSC is either to insensitive to detect post-crystallisation, or there is no post crystallisation taking place after 24h from injection moulding. Either way, it would be of interest to examine this, by for example flash DCS or by microscopy technology. It would be of interest to redo the measure of injection moulded PP of grade 2, to confirm what was observed in change of enthalpy. Grade 1 would also be interesting to examine after 2.5 hours and compared with other measures, since this measure was not performed due to previous mentioned reasons.

In this work, only homo-PP have been examined, with different M_w and MWD. It would be interesting to see if this increase in modulus and yield point, and decrease in elongation at break, would happen over storage in co-PP (or syndiotactic PP) and to what extent. If physical ageing is the main reason for these mechanical changes in behaviour, how would this affect a more amorphous semi-crystalline polymer?

To examine the microstructure further and size of different zones (skin, shear and core) use of light microscopy (polarized) would be of interest. SEM gave a brief guidance on the different layers, but would have to be repeated to give any stronger scientific guidance.

Many tests have been performed and lots of data generated, but there has been a lack of time to interpret all results. The reasons for this are among other that the different grades were received quite late, and that the measurements took longer time than expected to perform. This due to that variation in performance over storage time lasted longer than expected. There might be more information regarding behaviour of these grades to collect from the tests performed.

In tensile testing large variations in MD, CD and DD were observed in elongation at break. The reason for this is assumed to be due to resulting microstructure from injection moulding and difference in possibility of slip, but exactly what happens and why in the different directions is not understood. A better understanding is assumed to be reached if tensile tests were filmed and the slip taking place observed by X-ray microscopy.

Tensile testing methodology could be improved to reduce noise in measures. Since the position of where the dogbone is punched on the plate influence the result of the measurements, it is suggested that some kind of frame is used in the future to reduce this source of error. Flowlines and orientation varies over the plate, giving different rate of orientation depending on which direction the test is performed. Just a slight variation to the more diagonal tilt would for example enhance the elongation at break.

10 References

- Aho, J., Boetker, J., Baldursdottir, S. & Rantanen, J., 2018. Rheology as a tool for evaluation of melt processability of innovative dosage forms. *International Journal Of Pharmaceutics*, Volume 494. pp. 623-642.
- Amintowlieh, Y., 2014. *Rheological Modification of Polypropylene by Incorporation of Long Chain Branches Using UV Radiation*, Waterloo: University of Waterloo.
- Andersson, A., 2012. *Tensile Impact - Laboratory method*, Lund: Tetra Pak internal.
- Andreasson, E., Persson, L., Jacobsson, H. & Nordgren, J., 2013. *Integrating Moldflow and Abaqus in the Package Simulation Workflow*, s.l.: SIMULIA Community Conference.
- Arrighi, D. V., n.d. *Crystallization from the Melt*. [Online]
Available at:
<http://www.che.hw.ac.uk/teaching/B11MS1/Material/Week%206/Week6CrystallizationFRomTheMelt.htm>
- Crawford, R. J., 1998. *Plastics Engineering*. Third ed. s.l.:Elsevier.
- Ebewele, R. O., 2000. *Polymer Science and Technology*. Benin, Florida: CRC Press LLC.
- Edward P. Moore, J., 1996. *Polypropylene handbook*. Munich, Vienna, New York: Carl Hanser Verlag.
- Fiebig, J., Gahleitner, M., Paulik, C. & Wolfschwenger, J., 1999. Ageing of polypropylene: processes and consequences. *Polymer Testing*, Volume 18. p. 257–266.
- Fried, J. R., 2014. *Polymer science and technology*. Upper Saddle River NJ: Prentice Hall.
- Gahleitner, M. et al., 2002. Post-crystallization and physical ageing of polypropylene: materials and processing effects. *JOURNAL OF MACROMOLECULAR SCIENCE*, B41(4-6), p. 833–849.
- Gillis, J., 2007. *File:Spherulite.svg*. [Online]
Available at: <https://en.wikipedia.org/wiki/File:Spherulite.svg>
[Accessed 11 05 2018].
- Han, C. D., 2007. *Rheology and Processing of Polymeric Materials*. 2 ed. New York: Department of Polymer Engineering.
- Jönsson, J. & Sandgren, M., 2013. “*Deformation and Damage Mechanisms in thin ductile polymer films - Experimental tests in combination with numerical simulations - Master Thesis*”, Lund : Division of Solid Mechanics.
- Karger-Kocsis, J., 1995. *Polypropylene Structure, blends and composites: Volume 1 Structure and Morphology*. s.l.:Chapman and Hall.
- Karian, H. G., 2003. *Handbook of Polypropylene and Polypropylene Composites, Revised and Expanded*. 2 ed. s.l.:Taylor & Francis.

- Kodre, K. et al., 2014. Differential Scanning Calorimetry: A Review. *Research & Reviews: Journal of Pharmaceutical Analysis*, 3(3), p. 17.
- Kolnaar, K. A., 1997. *Processing of polymers*. 18 ed. New York: Meijer HEH.
- Krishnaswamy, R. K., Geibel, J. F. & Lewis, B. J., 2003. Influence of Semicrystalline Morphology on the Physical Aging Characteristics of Poly(phenylene sulfide). *Macromolecules*, Volume 36. pp. 2907-2914.
- Lee, J.-H., Um, C.-M. & Lee, I.-b., 2006. Rheological properties of resin composites according to variations in monomer and filler composition. *Dental Materials*, 22(6), pp. 515-526.
- Lieberman, R. B. B., 1988. *Encyclopedia of Polymer Science and Engineering (1988)*. s.l.:s.n.
- Lindgren, G. & Hadzic, L., 2011. *Simulations in MOLDEX3D SOLID - Injection molding and injection compression molding*, Malmö: Malmö University, Faculty of Media Technology and Product Development.
- Lin, H. L. & Yu, T. L., 1996. Polymer Molecular Weight, Zero Shear Viscosity, Steady State Compliance and Binary Blending Law. *Journal of Polymer Research*, 3(1), pp. 49-57.
- Lotz, B., Wittmann, J. & Lovinger, A., 1996. Structure and morphology of poly(propylenes): a molecular analysis. *Polymer*, pp. Volume 37. Issue 22. Pages 4979-4992.
- Martin, J., Bourson*, P., Dahoun, A. & Hiver, J. M., 2009. The β -Spherulite Morphology of Isotactic Polypropylene Investigated by Raman Spectroscopy. *SAGE journals*, pp. 1377-1381.
- Mi, D. et al., 2016. Quantification of the Effect of Shish-Kebab Structure on the. *Macromolecules*, Volume 49. pp. 4571-4578.
- Mink, R. et al., 1996. *Process for controlling the MWD of a broad/bimodal resin produced in a single reactor*. US, Patent No. 5525678 A.
- Monks, A. W., White, H. M. & Bassett, D. C., 1996. On shish-kebab morphologies in crystalline polymers. *Polymer*, 37(26), pp. 5933-5936.
- Nakamura, K. et al., 2008. Temperature Dependence of Crystal Growth Rate for alpha and beta forms of isotactic polypropylene. *Polymer Journal*, pp. 915-922. Vol. 40. No. 9.
- Nordgren, J. & Jacobsson, H. I., 2012. *Integration of Moldflow and Abaqus in the Workflow*, Lund University: Division of Solid Mechanics.
- PatricleSciences, n.d. *Hot melt extrusion*. [Online]
Available at: <http://www.particlesciences.com/news/technical-briefs/2011/hot-melt-extrusion.html>
[Accessed 14 5 2018].
- Polymerdatabase, 2015. *Molecular weight and and molecular weight distribution*. [Online]
Available at: <http://polymerdatabase.com/polymer%20physics/Molecular%20Weight.html>

- Rea, M., 2017. *Analysis of Polypropylene by HT-GPC, Polymer Solutions*. [Online] Available at: <https://www.polymersolutions.com/blog/analysis-of-polypropylene-by-ht-gpc/> [Accessed 12 2 2018].
- Schael, G. W., 1966. A study of the morphology and physical properties of polypropylene films. *Applied Polymer Science*, Volume 10. pp. 901-915.
- Schultz, J., 1974. *Polymer Material Science*, New Jersey: Prentice-Hall Englewood Cliffs.
- Schultz, M. K. & Agarwal, J. M., 1981. The physical aging of isotactic polypropylene. *Polymer engineering & science*, 21(12), pp. 776-781.
- Shroff, R. & Mavridis, H., 1995. *New measures of polydispersity from rheological data on polymer melts*, Northlake drive: Quantum Chemical co, Allen research center.
- Singh, G., Pradhan, M. K. & Verma, A., 2015. Effect of Injection Moulding Process Parameter on Tensile Strength Using Taguchi Method. *World Academy of Science, Engineering and Technology, International Journal of Industrial and Manufacturing Engineering*, 9(10).
- Spoormaker, J. L., 2002. *Ten essential pictures for understanding the mechanical behaviour of plastics*, Delft: Delft University of Technology.
- Struik, L. C. E., 1987. *The mechanical and physical ageing of semicrystalline polymers: 1*. Delft: Plastics and Rubber Research Institute TNO.
- Sunthar, P., 2010. Polymer rheology. In: *Rheology of complex fluids*. Bombay, Mumbai: Department of Chemical Engineering, Indian Institute of Technology (IIT), pp. 171-191.
- Svensson, K., 2013. *Capillary Rheometer - Laboratory Method*, Lund: Tetra Pak.
- Universität, H., n.d. *Investigation of Polymers with Differential Scanning*. [Online] Available at: <https://polymerscience.physik.hu-berlin.de/docs/manuals/DSC.pdf>
- Wells, O. C., 1974. *Scanning electron microscopy*. s.l.:McGraw-Hill.
- Williams, David B., Carter, C. Barry, 2009. *Transmission Electron Microscopy - A textbook for Material Science*. 2 ed. s.l.:Springer US.
- Wunderlich, B., 1990. Thermal Analysis. *Academic Press*, pp. 417-431.
- Xiong, B., 2014. *Contribution to the study of elastic and plastic deformation mechanisms of polyethylene and polypropylene as a function of microstructure and temperature*, Lyon: INSA de Lyon.
- Yalcin, D., 2017. *Effect of Specimen Geometry on Tensile Testing Results*. [Online] Available at: <https://www.admet.com/effect-specimen-geometry-tensile-testing-results/> [Accessed 22 01 2018].

11 Appendix

11.1 Test analysis

11.1.1 Punching of dogbones

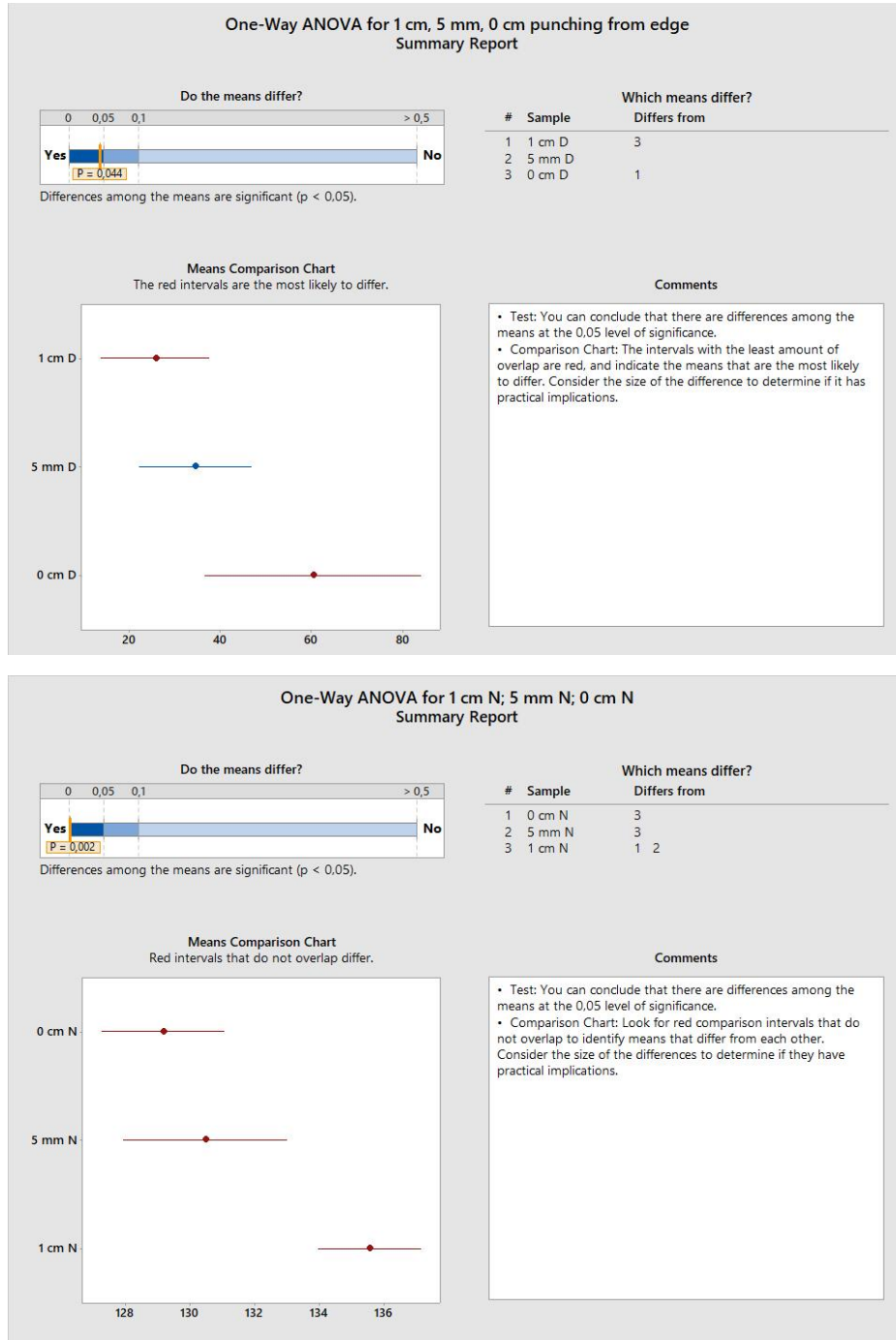


Figure 84. ANOVA test performed in minitab, to examine if there are any statistical differences between the different ways of punching.

11.2 Oscillatory rheometer

Grade 1 – master data from 190-230 °C frequency sweeps, shifted to 210 °C

<i>Frequency</i>	<i>Phase Angle</i>	<i>Complex Modulus</i>	<i>Storage Modulus</i>	<i>Loss Modulus</i>	<i>Complex Viscosity</i>
[Hz]	[°]	[Pa]	[Pa]	[Pa]	[Pa·s]
0.01	88.0	37.5	1.3	37.5	890
0.01	87.5	55.0	2.4	55.0	883
0.01	86.9	63.7	3.5	63.6	878
0.02	86.5	86.5	5.2	86.4	864
0.02	86.4	92.4	5.8	92.2	863
0.02	86.1	108	7.4	107	864
0.03	85.2	145	12.3	145	845
0.03	85.2	155	13.0	155	844
0.03	84.8	181	16.4	180	845
0.05	83.9	243	25.8	242	823
0.05	83.5	260	29.4	258	821
0.06	83.1	302	36.3	300	820
0.08	82.1	403	55.5	399	793
0.09	81.5	430	63.7	425	790
0.10	81.0	497	77.7	491	785
0.14	79.8	660	117	650	755
0.15	79.1	701	133	688	750
0.17	78.6	805	159	789	740
0.24	77.2	1060	236	1040	708
0.26	76.5	1120	261	1090	698
0.30	75.8	1290	315	1250	687
0.41	74.3	1680	454	1620	651
0.44	73.6	1770	500	1700	640
0.51	72.7	2020	599	1930	627
0.71	71.1	2610	844	2470	588
0.76	70.4	2740	918	2580	575
0.88	69.4	3110	1090	2910	561
1.22	67.7	3980	1510	3680	521
1.30	66.9	4150	1620	3810	507
1.51	65.9	4680	1910	4270	492
2.09	64.2	5930	2580	5330	452
2.24	63.3	6150	2760	5490	437
2.60	62.3	6890	3210	6100	422
3.59	60.5	8630	4250	7510	383
3.84	59.6	8900	4500	7680	369
4.47	58.3	9840	5160	8380	350
6.17	56.8	12300	6720	10300	316
6.61	55.8	12500	7040	10300	301
7.69	54.2	13700	8030	11200	285

<i>Frequency</i>	<i>Phase Angle</i>	<i>Complex Modulus</i>	<i>Storage Modulus</i>	<i>Loss Modulus</i>	<i>Complex Viscosity</i>
10.60	52.9	16900	10200	13500	254
11.40	51.7	17200	10600	13500	241
13.20	50.1	18700	12000	14400	226
18.20	49.0	22800	15000	17200	199
19.50	47.7	23000	15500	17000	188
22.70	46.1	25100	17400	18100	176
31.40	45.3	30100	21100	21400	153
33.60	43.6	30400	22000	21000	144
39.10	42.4	33200	24500	22400	135
53.90	41.8	38700	28900	25800	114
57.70	40.0	39500	30300	25400	109
67.10	39.9	42900	32900	27500	102
92.70	38.9	48900	38100	30700	84.0
99.20	37.0	50300	40200	30300	80.8
159.00	38.9	59700	46500	37500	59.6

Table 22. Grade 1 master data, 190-230 °C frequency sweeps, shifted to 210 °C

Grade 2 – master data from 190-230 °C frequency sweeps, shifted to 210 °C

<i>Frequency</i>	<i>Phase Angle</i>	<i>Complex Modulus</i>	<i>Storage Modulus</i>	<i>Loss Modulus</i>	<i>Complex Viscosity</i>
[Hz]	[°]	[Pa]	[Pa]	[Pa]	[Pa·s]
0.01	89.6	30.7	0.24	30.7	774
0.01	89.2	48.1	0.64	48.1	768
0.01	89.2	52.5	0.76	52.5	769
0.02	88.5	81.6	2.09	81.5	758
0.02	88.5	90.0	2.37	89.9	767
0.02	88.6	88.2	2.14	88.1	749
0.03	87.8	139	5.28	139	752
0.03	87.6	144	5.92	143	751
0.03	87.6	154	6.46	153	761
0.05	86.8	232	13.0	232	749
0.05	86.6	237	14.1	236	745
0.06	86.5	262	16.1	262	756
0.08	85.6	375	28.9	374	745
0.09	85.0	402	35.1	400	735
0.09	85.0	443	38.5	441	743
0.13	83.9	601	64.2	598	735
0.15	82.9	673	83.1	668	716
0.16	83.0	738	90.6	733	720
0.21	81.8	951	136	941	716
0.26	80.6	1110	182	1090	686
0.28	80.5	1220	201	1200	690
0.34	79.3	1480	273	1450	684
0.44	77.6	1800	385	1760	648
0.48	77.5	1970	425	1920	650
0.56	76.7	2260	520	2200	645
0.76	74.3	2860	773	2760	600
0.83	74.1	3130	857	3010	601
0.91	73.6	3410	962	3270	600
1.31	70.6	4460	1480	4210	543
1.42	70.3	4860	1640	4570	543
1.47	70.3	5040	1700	4750	546
2.25	66.6	6780	2690	6220	480
2.39	66.7	7330	2900	6730	489
2.45	66.3	7360	2960	6730	478
3.86	62.4	10000	4650	8900	414
3.87	63.0	10400	4740	9290	429
4.21	62.0	10900	5090	9580	410
6.29	59.2	14600	7460	12500	369
6.64	58.1	14500	7630	12300	347
7.24	57.6	15600	8340	13200	343

<i>Frequency</i>	<i>Phase Angle</i>	<i>Complex Modulus</i>	<i>Storage Modulus</i>	<i>Loss Modulus</i>	<i>Complex Viscosity</i>
10.20	55.5	19900	11300	16400	309
11.40	53.8	20300	12000	16300	283
12.40	53.3	21800	13000	17500	279
16.60	51.5	26300	16400	20600	252
19.60	49.6	27600	17900	21000	224
21.40	48.9	29800	19600	22500	222
26.90	47.6	34300	23100	25300	203
33.70	45.4	36700	25800	26100	173
36.80	45.2	40100	28200	28400	173
43.70	44.1	43700	31400	30400	159
58.00	42.1	47800	35500	32000	131
71.00	40.4	55000	41900	35700	123
115.00	37.5	68000	54000	41400	94

Table 23. Grade 2 master data, 190-230°C frequency sweeps, shifted to 210°C

Grade 3 – master data from 190-230 °C frequency sweeps, shifted to 210 °C

<i>Frequency</i>	<i>Phase Angle</i>	<i>Complex Modulus</i>	<i>Storage Modulus</i>	<i>Loss Modulus</i>	<i>Complex Viscosity</i>
[Hz]	[°]	[Pa]	[Pa]	[Pa]	[Pa·s]
0.01	89.4	62.1	0.66	62.1	991
0.02	89.1	93.2	1.53	93.2	978
0.02	89.0	100	1.78	100	983
0.02	88.7	107	2.45	107	997
0.02	88.5	151	3.99	150	973
0.03	88.3	162	4.77	162	977
0.03	88.2	174	5.49	174	995
0.04	87.5	243	10.8	243	966
0.04	87.4	261	11.9	261	972
0.05	87.4	281	12.8	281	991
0.06	86.5	391	23.7	390	958
0.07	86.3	421	27.1	420	964
0.07	86.2	453	30.3	452	984
0.11	85.1	626	54.0	624	945
0.11	84.9	674	60.2	671	952
0.12	84.7	722	66.4	719	965
0.17	83.0	994	120	987	924
0.18	83.0	1060	130	1060	926
0.19	82.7	1140	145	1130	939
0.28	80.8	1560	249	1540	891
0.30	80.5	1660	275	1640	892
0.31	80.2	1780	302	1760	904
0.45	78.1	2400	497	2350	847
0.48	77.7	2570	546	2510	848
0.51	77.4	2740	599	2680	857
0.73	74.8	3650	955	3520	793
0.78	74.5	3890	1040	3750	791
0.83	74.1	4150	1140	4000	799
1.19	71.3	5440	1740	5150	727
1.27	70.9	5800	1890	5480	725
1.34	70.5	6170	2060	5810	730
1.93	67.5	7940	3040	7340	654
2.07	67.1	8440	3290	7770	650
2.18	66.6	8960	3560	8220	654
3.14	63.4	11300	5070	10100	575
3.35	63.0	12000	5460	10700	571
3.54	62.5	12700	5870	11300	572
5.10	59.3	15900	8100	13600	495
5.45	59.1	16800	8640	14400	491
5.75	58.4	17600	9250	15000	488

<i>Frequency</i>	<i>Phase Angle</i>	<i>Complex Modulus</i>	<i>Storage Modulus</i>	<i>Loss Modulus</i>	<i>Complex Viscosity</i>
8.27	55.2	21600	12300	17700	415
8.84	54.7	22600	13100	18500	408
9.34	54.2	23900	14000	19400	407
13.4	50.9	28500	18000	22100	338
14.4	50.5	30000	19100	23100	332
15.2	50.1	31600	20300	24300	332
21.8	46.8	37000	25300	26900	270
23.3	46.6	38800	26700	28200	265
24.6	46.2	41100	28400	29600	265
35.4	42.8	47000	34500	31900	211
37.9	42.7	49300	36200	33400	207
40.0	43.0	52300	38300	35700	208
57.5	39.0	58600	45600	36900	162
61.5	39.5	61400	47400	39100	159
93.4	35.5	72100	58700	41900	123
152	32.8	87600	73600	47400	91.9

Table 24. Grade 3 master data, 190-230 °C frequency sweeps, shifted to 210 °C

Grade 4 – master data from 190-230 °C frequency sweeps, shifted to 210 °C

<i>Frequency</i>	<i>Phase Angle</i>	<i>Complex Modulus</i>	<i>Storage Modulus</i>	<i>Loss Modulus</i>	<i>Complex Viscosity</i>
[Hz]	[°]	[Pa]	[Pa]	[Pa]	[Pa·s]
0.0062	88.2	52.3	1.63	52.2	1340
0.010	87.4	83.3	3.71	83.2	1330
0.010	87.2	84.1	4.12	84	1330
0.016	86.7	129	7.53	129	1320
0.016	86.3	133	8.64	133	1310
0.016	86.3	135	8.79	134	1310
0.025	85.2	205	17.2	204	1290
0.026	85.0	212	18.4	211	1280
0.027	85.1	215	18.4	214	1290
0.041	83.8	325	35.2	323	1260
0.043	83.6	336	37.3	334	1260
0.043	83.5	341	38.5	339	1260
0.067	81.8	511	72.5	506	1220
0.069	81.8	529	75.4	523	1210
0.070	81.6	537	78.5	531	1220
0.11	79.8	794	141	782	1170
0.11	79.6	823	148	809	1160
0.11	79.4	832	153	818	1160
0.18	77.6	1220	263	1190	1110
0.18	77.2	1260	278	1230	1100
0.19	77.1	1270	284	1240	1100
0.29	75.0	1850	480	1790	1030
0.30	74.7	1900	503	1840	1020
0.30	74.4	1930	518	1850	1020
0.46	72.1	2760	848	2620	947
0.48	71.8	2840	887	2690	938
0.49	71.5	2860	908	2710	933
0.75	69.1	4040	1450	3780	856
0.78	68.7	4150	1510	3870	845
0.79	68.3	4190	1550	3890	841
1.22	65.8	5830	2390	5320	759
1.27	65.4	5980	2490	5440	750
1.29	65.0	6020	2540	5450	744
1.98	62.4	8250	3820	7320	662
2.06	62.0	8460	3960	7470	653
2.09	61.6	8480	4030	7460	646
3.22	58.9	11500	5920	9830	567
3.35	58.6	11800	6130	10000	559
3.39	58.1	11700	6190	9950	550
5.23	55.4	15600	8880	12900	476

<i>Frequency</i>	<i>Phase Angle</i>	<i>Complex Modulus</i>	<i>Storage Modulus</i>	<i>Loss Modulus</i>	<i>Complex Viscosity</i>
5.44	55.1	15900	9120	13100	467
5.51	54.6	15900	9210	12900	459
8.49	52.0	20900	12900	16500	392
8.83	51.5	21200	13200	16600	382
8.95	51.0	21100	13300	16400	375
13.8	48.4	27200	18100	20300	314
14.3	48.0	27800	18600	20600	308
14.5	47.6	27500	18500	20300	301
22.4	44.9	34800	24700	24600	248
23.3	44.6	35600	25400	25000	244
23.6	44.3	35300	25200	24700	238
36.4	41.6	43800	32800	29100	192
37.8	41.0	45100	34000	29600	190
38.3	41.8	44500	33100	29600	185
59.0	38.5	54400	42600	33900	147
61.4	37.8	56300	44500	34500	146
95.9	36.0	66400	53700	39000	110

Table 25. Grade 4 master data, 190-230 °C frequency sweeps, shifted to 210 °C

Grade 5 – master data from 190-230 °C frequency sweeps, shifted to 210 °C

<i>Frequency</i>	<i>Phase Angle</i>	<i>Complex Modulus</i>	<i>Storage Modulus</i>	<i>Loss Modulus</i>	<i>Complex Viscosity</i>
[Hz]	[°]	[Pa]	[Pa] G'	[Pa] G''	[Pa·s]
0.01	89.4	50.8	0.55	50.8	814
0.01	89.0	52.3	0.95	52.3	800
0.02	89.1	77.7	1.19	77.7	805
0.02	88.9	86.8	1.65	86.7	809
0.02	88.7	89.8	1.96	89.8	800
0.03	88.2	133	4.17	132	799
0.03	87.9	148	5.34	148	805
0.03	88.0	154	5.27	154	797
0.05	87.0	226	11.6	225	791
0.05	87.0	253	13.3	253	799
0.05	86.8	263	14.5	263	793
0.08	85.9	383	27.7	382	782
0.09	85.7	431	32.6	430	791
0.09	85.2	446	37.1	444	781
0.13	84.1	647	66.5	643	767
0.15	83.9	724	76.5	720	773
0.16	83.2	744	88.4	739	759
0.23	81.8	1070	153	1060	742
0.26	81.5	1200	176	1190	745
0.27	80.6	1230	201	1210	729
0.40	79.0	1750	334	1720	704
0.44	78.7	1960	383	1920	707
0.46	77.5	1990	430	1950	687
0.68	75.7	2810	694	2730	657
0.76	75.4	3130	792	3030	659
0.79	74.0	3170	874	3050	636
1.17	72.0	4410	1370	4200	600
1.30	71.6	4910	1550	4660	601
1.36	70.1	4920	1680	4620	574
2.01	67.9	6770	2550	6270	535
2.24	67.5	7510	2880	6930	534
2.34	65.8	7440	3040	6790	505
3.46	63.6	10100	4490	9040	464
3.85	63.1	11200	5050	9960	462
4.03	61.4	10900	5230	9610	432
5.95	59.2	14700	7540	12600	393
6.61	58.6	16100	8400	13800	388
6.93	56.9	15600	8530	13100	359
10.2	54.7	20600	11900	16800	321
11.4	54.1	22700	13300	18400	317

<i>Frequency</i>	<i>Phase Angle</i>	<i>Complex Modulus</i>	<i>Storage Modulus</i>	<i>Loss Modulus</i>	<i>Complex Viscosity</i>
11.9	52.4	21600	13200	17200	289
17.6	50.2	28200	18100	21700	256
19.5	49.8	30900	19900	23600	252
20.5	47.9	29300	19600	21700	228
30.2	45.9	37600	26200	27000	198
33.6	45.4	41000	28800	29200	194
35.2	44.2	38700	27700	27000	175
52.0	41.7	48500	36200	32300	149
57.8	41.8	53000	39500	35300	146
89.4	37.8	61600	48700	37800	110

Table 26. Grade 5 master data, 190-230 °C frequency sweeps, shifted to 210 °C

Grade 6 – master data from 190-230 °C frequency sweeps, shifted to 210 °C

<i>Frequency</i>	<i>Phase Angle</i>	<i>Complex Modulus</i>	<i>Storage Modulus</i>	<i>Loss Modulus</i>	<i>Complex Viscosity</i>
[Hz]	[°]	[Pa]	[Pa]	[Pa]	[Pa·s]
0.006	89.2	35.7	0.47	35.7	907
0.010	88.5	57.0	1.53	57.0	914
0.011	88.4	60.9	1.72	60.9	901
0.017	87.6	97.1	4.14	97.0	906
0.017	88.1	96.9	3.22	96.9	898
0.019	87.4	104	4.62	104	893
0.029	86.8	165	9.19	165	896
0.030	86.8	165	9.16	164	888
0.032	86.5	177	10.6	177	885
0.050	85.5	279	21.9	278	882
0.051	85.3	278	22.8	277	873
0.055	85.1	300	25.4	299	873
0.087	83.7	469	51.7	466	862
0.087	83.7	468	51.1	465	853
0.094	83.3	501	58.8	498	849
0.15	81.5	777	115	768	830
0.15	81.6	777	113	768	824
0.16	81.0	826	129	816	814
0.26	78.9	1260	244	1240	785
0.26	79.1	1270	240	1250	784
0.28	78.3	1340	273	1310	769
0.44	75.8	2020	495	1960	731
0.44	76.1	2030	488	1980	730
0.48	75.1	2140	549	2070	714
0.76	72.4	3170	958	3030	668
0.76	72.8	3200	946	3060	669
0.82	71.7	3350	1050	3180	650
1.30	68.8	4880	1770	4550	597
1.31	69.2	4930	1750	4610	599
1.41	67.9	5130	1930	4750	579
2.24	64.8	7320	3110	6630	521
2.25	65.3	7420	3100	6740	524
2.42	63.9	7660	3360	6880	502
3.84	60.7	10700	5240	9340	443
3.87	61.2	10900	5240	9530	447
4.17	59.8	11100	5600	9620	425
6.61	56.5	15200	8410	12700	367
6.66	57.0	15600	8490	13100	373
7.17	55.5	15800	8930	13000	350
11.4	52.2	21100	13000	16700	296

<i>Frequency</i>	<i>Phase Angle</i>	<i>Complex Modulus</i>	<i>Storage Modulus</i>	<i>Loss Modulus</i>	<i>Complex Viscosity</i>
11.4	52.8	21600	13000	17200	300
12.3	51.2	21700	13600	16900	281
19.5	48.1	28500	19100	21300	233
19.7	48.6	29200	19300	21900	236
21.2	46.8	29300	20100	21400	221
33.6	43.8	37800	27300	26200	179
33.8	44.5	38600	27500	27100	182
36.4	42.8	39000	28600	26500	170
57.7	39.9	49300	37800	31600	136
58.1	40.7	49800	37800	32400	136
62.6	40.1	50600	38700	32600	129
99.2	37.0	62800	50100	37800	101
99.9	37.5	62900	49900	38300	100

Table 27. Grade 6 master data, 190-230 °C frequency sweeps, shifted to 210 °C

11.3 Tensile tests

11.3.1 MD – all grades

<i>Grade</i>	<i>Parameter</i>	<i>2.5 hours</i>	<i>1 day</i>	<i>3 days</i>	<i>7 days</i>	<i>2 weeks</i>	<i>4 weeks</i>	<i>6 weeks</i>
1	Nbr of measurments	10	10	9	7	9	8	6
1	Tensile strength at yield (MPa)	41.1	42.5	41.4	42.9	44.0	44.5	46.9
1	<i>Tensile Standard deviation (MPa)</i>	<i>1.0</i>	<i>1.39</i>	<i>0.84</i>	<i>1.1</i>	<i>0.69</i>	<i>0.61</i>	<i>0.60</i>
1	Elongation at break (%)	180	146	152	122	106	97.9	83.9
1	<i>Standard deviation (%)</i>	<i>17.9</i>	<i>31.1</i>	<i>28.9</i>	<i>45.5</i>	<i>32.9</i>	<i>25.5</i>	<i>5.0</i>
1	Youngs modulus (GPa)	1.56	1.75	1.70	1.87	1.87	1.95	2.00
1	<i>Youngs Standard deviation (GPa)</i>	<i>0.05</i>	<i>0.06</i>	<i>0.15</i>	<i>0.04</i>	<i>0.04</i>	<i>0.06</i>	<i>0.08</i>
2	Nbr of measurments	5	6	10	10	9	9	9
2	Tensile strength at yield (MPa)	36.1	37.0	38.7	38.8	38.9	39.3	39.5
2	<i>Tensile Standard deviation (MPa)</i>	<i>0.24</i>	<i>0.81</i>	<i>0.85</i>	<i>0.82</i>	<i>0.96</i>	<i>0.50</i>	<i>0.76</i>
2	Elongation at break (%)	426	391	267	291	317	183	170
2	<i>Standard deviation (%)</i>	<i>5.2</i>	<i>37.6</i>	<i>101</i>	<i>109</i>	<i>77.4</i>	<i>81.2</i>	<i>66.4</i>
2	Youngs modulus (GPa)	1.40	1.54	1.59	1.61	1.67	1.67	1.73
2	<i>Youngs Standard deviation (GPa)</i>	<i>0.07</i>	<i>0.03</i>	<i>0.09</i>	<i>0.05</i>	<i>0.03</i>	<i>0.05</i>	<i>0.03</i>
3	Nbr of measurments	10	10	10	9	9	8	11
3	Tensile strength at yield (MPa)	37.7	39.1	40.4	40.2	41.9	42.4	43.3
3	<i>Tensile Standard deviation (MPa)</i>	<i>1.12</i>	<i>0.65</i>	<i>1.02</i>	<i>0.90</i>	<i>0.86</i>	<i>1.11</i>	<i>0.88</i>
3	Elongation at break (%)	304	145	98.7	83.9	87.1	84.2	81.2
3	<i>Standard deviation (%)</i>	<i>13.4</i>	<i>90.6</i>	<i>23.5</i>	<i>20.2</i>	<i>17.7</i>	<i>16.6</i>	<i>15.4</i>
3	Youngs modulus (GPa)	1.40	1.59	1.65	1.60	1.62	1.56	1.63
3	<i>Youngs Standard deviation (GPa)</i>	<i>0.06</i>	<i>0.04</i>	<i>0.03</i>	<i>0.05</i>	<i>0.04</i>	<i>0.08</i>	<i>0.07</i>
4	Nbr of measurments	10	10	10	10	10	9	10
4	Tensile strength at yield (MPa)	41.5	43.2	45.0	44.6	47.0	45.4	46.5
4	<i>Tensile Standard deviation (MPa)</i>	<i>0.92</i>	<i>1.4</i>	<i>0.94</i>	<i>0.53</i>	<i>1.2</i>	<i>0.55</i>	<i>1.1</i>
4	Elongation at break (%)	159	81.6	73.1	63.8	53.8	54.2	46.0
4	<i>Standard deviation (%)</i>	<i>65.9</i>	<i>19.9</i>	<i>26.5</i>	<i>17.7</i>	<i>15.7</i>	<i>15.4</i>	<i>14.9</i>
4	Youngs modulus (GPa)	1.56	1.77	1.87	1.78	1.86	2.00	2.01
4	<i>Youngs Standard deviation (GPa)</i>	<i>0.10</i>	<i>0.07</i>	<i>0.04</i>	<i>0.09</i>	<i>0.07</i>	<i>0.04</i>	<i>0.07</i>
5	Nbr of measurments	8	9	10	10	8	9	9
5	Tensile strength at yield (MPa)	36.9	39.0	40.5	42.0	41.3	41.7	41.5
5	<i>Tensile Standard deviation (MPa)</i>	<i>0.98</i>	<i>1.2</i>	<i>1.5</i>	<i>0.85</i>	<i>1.03</i>	<i>0.75</i>	<i>0.58</i>
5	Elongation at break (%)	311	199	124	136	118	105	91.8

<i>Grade</i>	<i>Parameter</i>	<i>2.5 hours</i>	<i>1 day</i>	<i>3 days</i>	<i>7 days</i>	<i>2 weeks</i>	<i>4 weeks</i>	<i>6 weeks</i>
5	<i>Standard deviation (%)</i>	4.1	112	21.1	51.1	37.1	22.9	17.2
5	Youngs modulus (GPa)	1.36	1.57	1.66	1.67	1.63	1.61	1.74
5	<i>Youngs Standard deviation (GPa)</i>	0.10	0.08	0.06	0.09	0.07	0.07	0.09
6	<i>Nbr of measurments</i>	9	10	10	10	9	9	9
6	Tensile strength at yield (MPa)	40.0	40.7	42.3	44.0	43.2	44.0	43.6
6	<i>Tensile Standard deviation (MPa)</i>	1.3	0.77	0.80	1.3	0.64	0.70	0.81
6	Elongation at break (%)	308	210	144	102	97.1	88.4	76.4
6	<i>Standard deviation (%)</i>	6.7	85.0	41.3	32.6	22.1	26.8	10.0
6	Youngs modulus (GPa)	1.49	1.70	1.75	1.81	1.77	1.69	1.84
6	<i>Youngs Standard deviation (GPa)</i>	0.10	0.08	0.04	0.07	0.06	0.13	0.09

Table 28. Averages present of measurements performed in MD of the injection moulded plates.

11.3.2 CD – all grades

<i>Grade</i>	<i>Attribute</i>	<i>2.5 hours</i>	<i>1 day</i>	<i>3 days</i>	<i>7 days</i>	<i>2 weeks</i>	<i>4 weeks</i>	<i>6 weeks</i>
1	<i>Nbr of measurments</i>	11	9	8	5	9	8	5
1	Tensile strength at yield (MPa)	31.6	33.1	31.5	33.8	34.5	35.2	36.6
1	<i>standard deviation (MPa)</i>	1.20	0.63	0.29	0.92	0.46	0.44	0.73
1	Elongation at break (%)	38.2	12.6	12.8	11.4	11.8	10.6	12.6
1	<i>standard deviation (%)</i>	79.8	1.08	1.11	0.85	0.95	1.17	1.40
1	Youngs modulus (GPa)	1.48	1.60	1.58	1.72	1.69	1.77	1.72
1	<i>standard deviation (GPa)</i>	0.04	0.06	0.03	0.06	0.05	0.04	0.02
2	<i>Nbr of measurments</i>	6	6	10	10	10	9	9
2	Tensile strength at yield (MPa)	28.4	28.9	30.2	30.3	30.1	31.6	32.0
2	<i>standard deviation (MPa)</i>	0.42	0.60	0.33	0.87	0.91	0.32	0.59
2	Elongation at break (%)	430	45.6	22.8	12.6	12.6	12.1	11.8
2	<i>standard deviation (%)</i>	14.1	71.6	22.6	0.80	2.33	1.35	0.82
2	Youngs modulus (GPa)	1.35	1.43	1.51	1.49	1.49	1.57	1.62
2	<i>standard deviation (GPa)</i>	0.04	0.02	0.02	0.06	0.04	0.04	0.06
3	<i>Nbr of measurments</i>	8	10	10	9	9	9	10
3	Tensile strength at yield (MPa)	31.9	32.3	33.9	33.3	34.8	34.5	35.9
3	<i>standard deviation (MPa)</i>	0.90	0.74	0.63	0.74	0.75	0.75	0.68
3	Elongation at break (%)	572	445	176	107	21.4	29.6	36.7
3	<i>standard deviation (%)</i>	46.7	86.5	211	151	10.2	31.5	45.8
3	Youngs modulus (GPa)	1.41	1.50	1.61	1.53	1.59	1.55	1.42
3	<i>standard deviation (GPa)</i>	0.04	0.05	0.06	0.06	0.09	0.06	0.16
4	<i>Nbr of measurments</i>	10	10	9	10	10	9	10
4	Tensile strength at yield (MPa)	33.5	34.5	35.8	36.4	36.7	35.3	36.3
4	<i>standard deviation (MPa)</i>	0.79	0.45	0.69	1.02	0.69	0.37	0.60

<i>Grade</i>	<i>Attribute</i>	<i>2.5 hours</i>	<i>1 day</i>	<i>3 days</i>	<i>7 days</i>	<i>2 weeks</i>	<i>4 weeks</i>	<i>6 weeks</i>
4	Elongation at break (%)	208	50.3	14.9	14.2	13.7	14.2	13.2
4	<i>standard deviation (%)</i>	220	63.8	1.29	1.55	2.16	1.35	1.45
4	Youngs modulus (GPa)	1.56	1.66	1.72	1.61	1.77	1.85	1.85
4	<i>standard deviation (GPa)</i>	0.04	0.02	0.16	0.13	0.06	0.03	0.03
5	Nbr of measurments	8	10	10	10	8	9	9
5	Tensile strength at yield (MPa)	31.0	31.6	33.0	34.4	32.9	34.6	34.0
5	<i>standard deviation (MPa)</i>	0.93	1.40	0.67	0.79	0.75	0.92	0.93
5	Elongation at break (%)	510	126	21.0	16.5	16.4	16.5	16.9
5	<i>standard deviation (%)</i>	64.8	143	15.5	7.55	8.58	7.13	10.4
5	Youngs modulus (GPa)	1.39	1.47	1.58	1.63	1.57	1.57	1.66
5	<i>standard deviation (GPa)</i>	0.06	0.08	0.03	0.05	0.03	0.07	0.05
6	Nbr of measurments	10	10	10	9	9	9	9
6	Tensile strength at yield (MPa)	33.2	33.1	34.4	35.7	34.8	35.3	35.0
6	<i>standard deviation (MPa)</i>	0.63	0.66	0.70	0.82	0.83	0.48	0.54
6	Elongation at break (%)	160	116	28.8	14.4	13.5	14.7	14.2
6	<i>standard deviation (%)</i>	146	91.9	22.9	1.10	1.01	1.97	0.27
6	Youngs modulus (GPa)	1.46	1.57	1.62	1.72	1.72	1.68	1.74
6	<i>standard deviation (GPa)</i>	0.08	0.04	0.04	0.04	0.03	0.04	0.06

Table 29. Averages present of measurements performed in CD of the injection moulded plates.

11.3.3 DD – all grades

<i>Grade:</i>	<i>Attribute</i>	<i>2.5 hours</i>	<i>1 day</i>	<i>3 days</i>	<i>7 days</i>	<i>2 weeks</i>	<i>4 weeks</i>	<i>6 weeks</i>
1	Nbr of measurments	6	5	5	5	5	5	6
1	Tensile strength at yield (MPa)	36.1	37.3	37.7	37.2	40.2	41.5	40.0
1	<i>standard deviation (MPa)</i>	1.0	0.8	0.7	1.1	0.5	1.6	0.8
1	Elongation at break (%)	629	602	570	573	562	456	504
1	<i>standard deviation (%)</i>	8.47	49.7	80.6	50.7	68.2	89.1	34.7
1	Youngs modulus (GPa)	1.4	1.6	1.6	1.5	1.6	1.7	1.6
1	<i>standard deviation (GPa)</i>	0.09	0.04	0.06	0.07	0.09	0.14	0.04
1	Nbr of measurments	5	5	N/A	5	5	5	5
2	Tensile strength at yield (MPa)	32.0	32.1	N/A	33.7	34.1	35.8	38.3
2	<i>standard deviation (MPa)</i>	0.6	0.3	N/A	0.7	0.7	1.6	0.2
2	Elongation at break (%)	552	534	N/A	529	554	521	559
2	<i>standard deviation (%)</i>	31.7	18.0	N/A	35.3	10.1	54.0	15.7
2	Youngs modulus (GPa)	1.2	1.3	N/A	1.4	1.4	1.4	1.3
2	<i>standard deviation (GPa)</i>	0.03	0.04	N/A	0.02	0.06	0.08	0.03
3	Nbr of measurments	5	5	N/A	5	5	3	6
3	Tensile strength at yield (MPa)	33.1	35.7	N/A	35.7	38.0	37.3	37.9
3	<i>standard deviation (MPa)</i>	0.8	1.3	N/A	1.4	0.7	0.9	1.4
3	Elongation at break (%)	418	401	N/A	403	405	378	385

<i>Grade:</i>	<i>Attribute</i>	<i>2.5 hours</i>	<i>1 day</i>	<i>3 days</i>	<i>7 days</i>	<i>2 weeks</i>	<i>4 weeks</i>	<i>6 weeks</i>
3	<i>standard deviation (%)</i>	24.1	12.8	N/A	24.5	18.9	15.7	31.4
3	Youngs modulus (GPa)	1.2	1.4	N/A	1.4	1.3	1.5	1.3
3	<i>standard deviation (GPa)</i>	0.17	0.02	N/A	0.04	0.07	0.17	0.19
4	Nbr of measurments	5	5	N/A	5	5	5	7
4	Tensile strength at yield (MPa)	36.7	38.1	N/A	40.2	42.2	40.7	40.8
4	<i>standard deviation (MPa)</i>	0.6	1.3	N/A	1.1	1.0	0.6	1.0
4	Elongation at break (%)	396	441	N/A	376	397	416	336
4	<i>standard deviation (%)</i>	10.1	8.66	N/A	84.8	16.9	16.7	126
4	Youngs modulus (GPa)	1.5	1.6	N/A	1.7	1.7	1.7	1.8
4	<i>standard deviation (GPa)</i>	0.02	0.06	N/A	0.02	0.06	0.04	0.03
5	Nbr of measurments	5	5	5	5	5	5	5
5	Tensile strength at yield (MPa)	34.2	35.3	36.9	37.4	37.3	37.5	37.7
5	<i>standard deviation (MPa)</i>	0.6	1.5	0.9	1.3	1.2	1.2	2.1
5	Elongation at break (%)	436	410	403	388	387	398	387
5	<i>standard deviation (%)</i>	21.2	22.0	14.3	10.5	10.8	23.0	13.0
5	Youngs modulus (GPa)	1.3	1.3	1.5	1.5	1.5	1.5	1.6
5	<i>standard deviation (GPa)</i>	0.03	0.06	0.11	0.05	0.11	0.04	0.06
6	Nbr of measurments	5	5	5	5	5	5	5
6	Tensile strength at yield (MPa)	37.2	35.7	38.4	38.6	39.2	39.3	39.9
6	<i>standard deviation (MPa)</i>	0.8	0.8	0.6	0.7	1.2	1.3	0.8
6	Elongation at break (%)	403	396	392	402	398	388	382
6	<i>standard deviation (%)</i>	28.3	14.8	19.2	11.3	14.2	7.18	12.8
6	Youngs modulus (GPa)	1.3	1.4	1.5	1.5	1.6	1.5	1.6
6	<i>standard deviation (GPa)</i>	0.22	0.04	0.08	0.07	0.08	0.07	0.05

Table 30. Averages present of measurements performed in DD of the injection moulded plates.

11.3.4 Youngs modulus

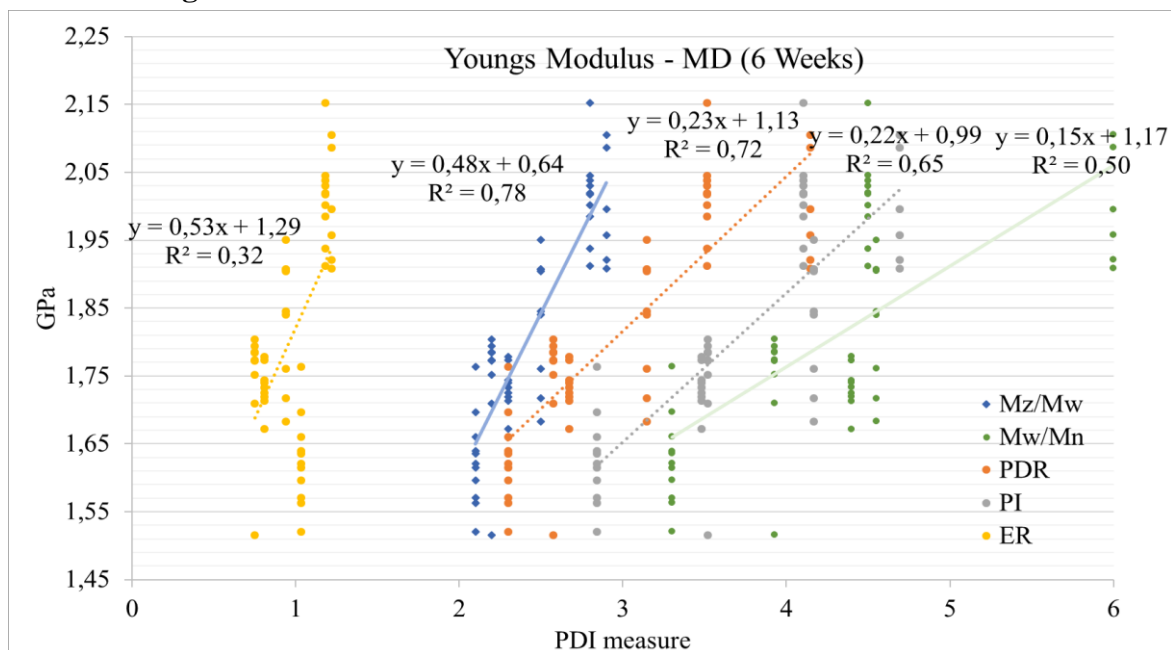


Figure 85. Showing the Young's modulus after 6 weeks in MD, plotted towards different measures of polydispersity by linear equation.

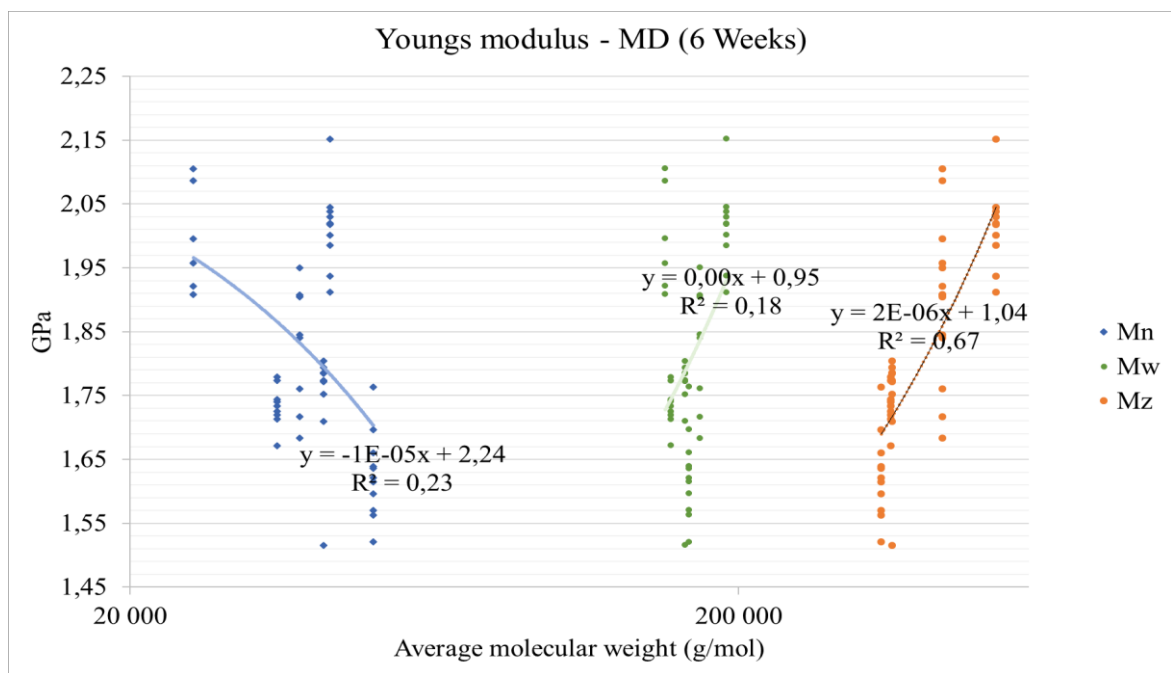


Figure 86. Showing the Young's modulus after 6 weeks in MD, plotted towards different measures of average molecular weight by linear equation. The x-axis is logarithmical.

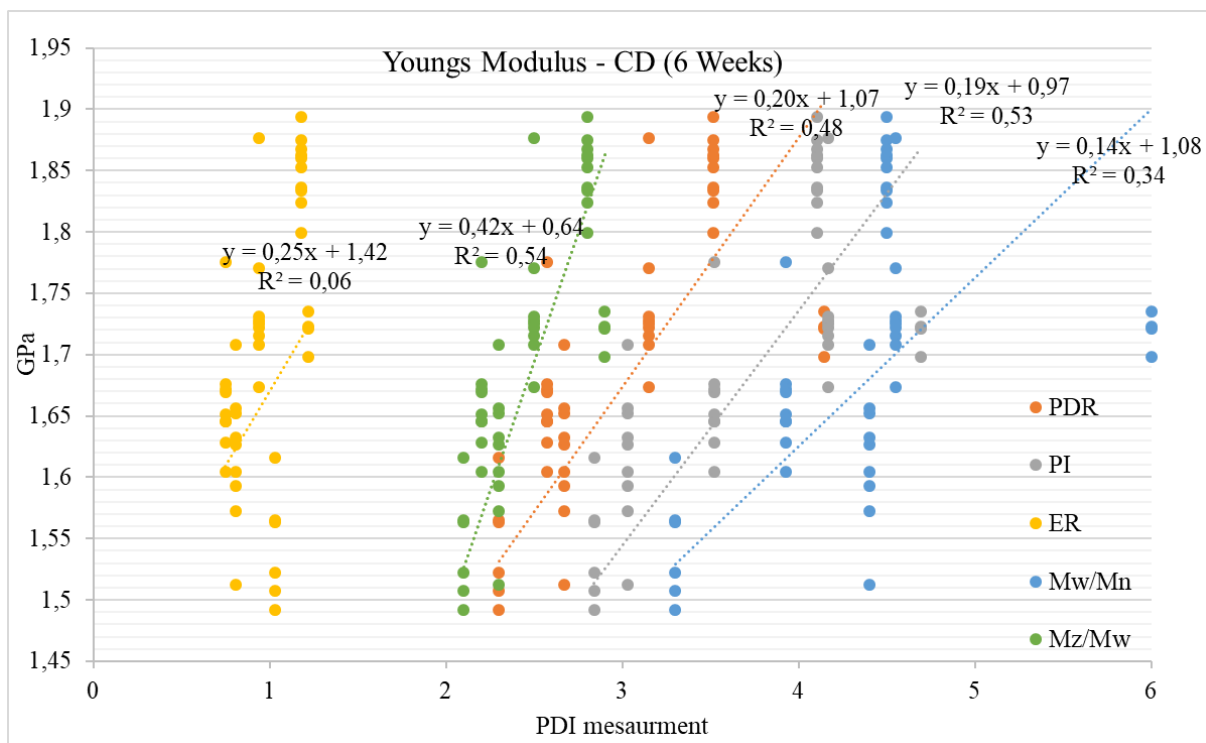


Figure 87. Showing the Young's modulus after 6 weeks in CD, plotted towards different measures of polydispersity by linear equation.

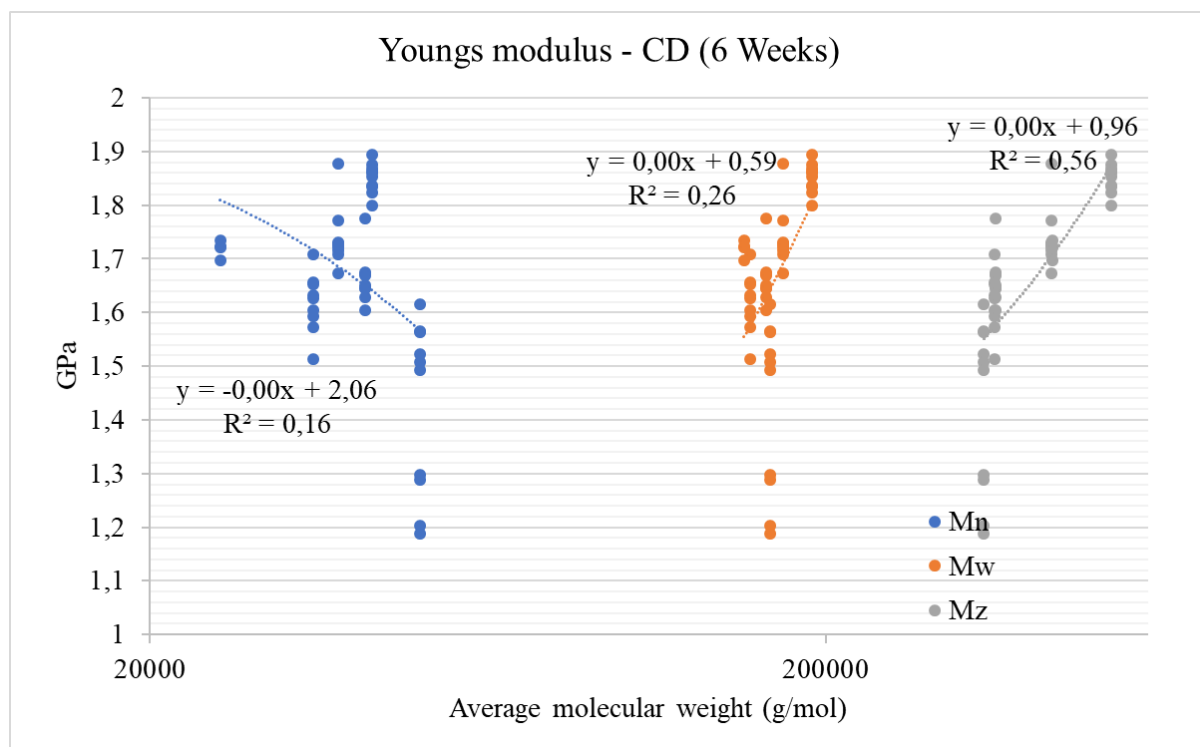


Figure 88. Showing the Young's modulus after 6 weeks in CD, plotted towards different measures of average molecular weight by linear equation. The x-axis is logarithmical.

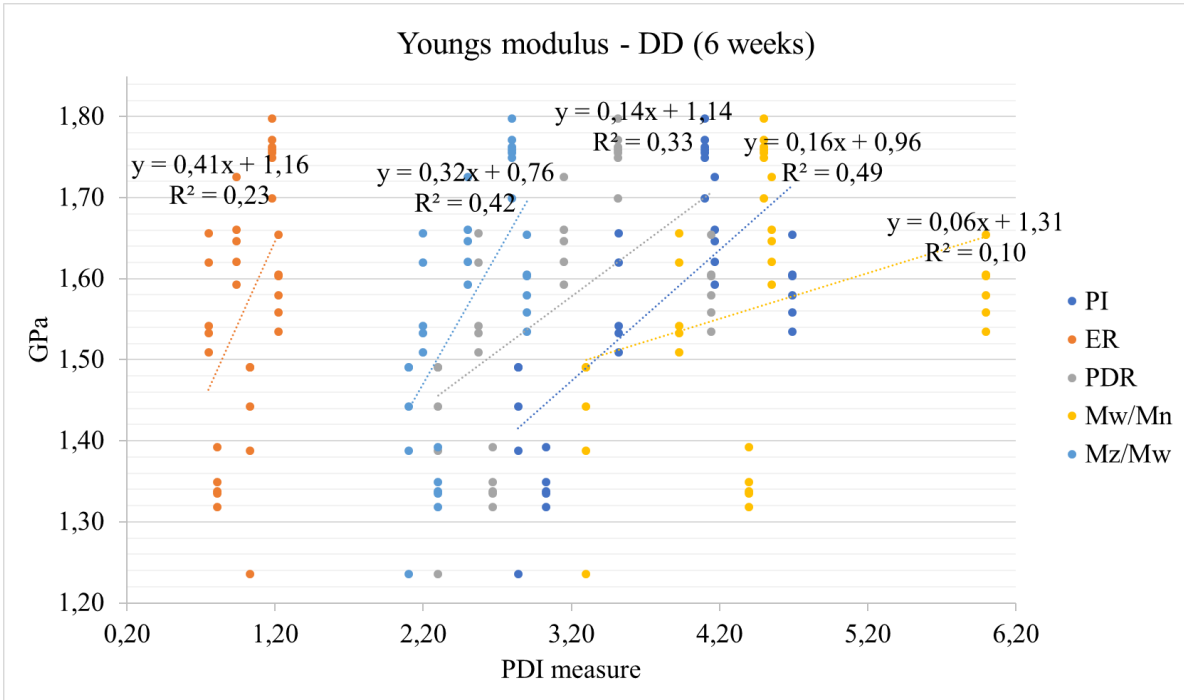


Figure 89. Showing the Young's modulus after 6 weeks in DD, plotted towards different measures of polydispersity by linear equation. The x-axis is logarithmical.

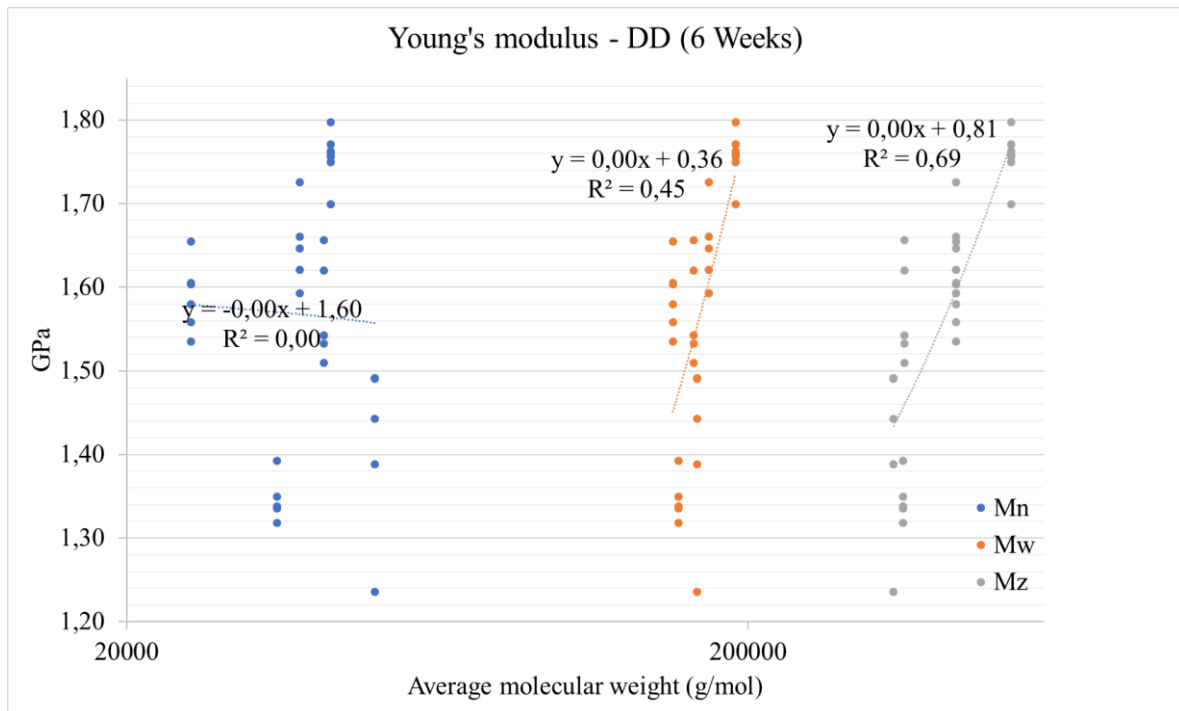


Figure 90. Showing the Young's modulus after 6 weeks in DD, plotted towards different measures of average molecular weight by linear equation. The x-axis is logarithmical.

11.3.5 Yield point

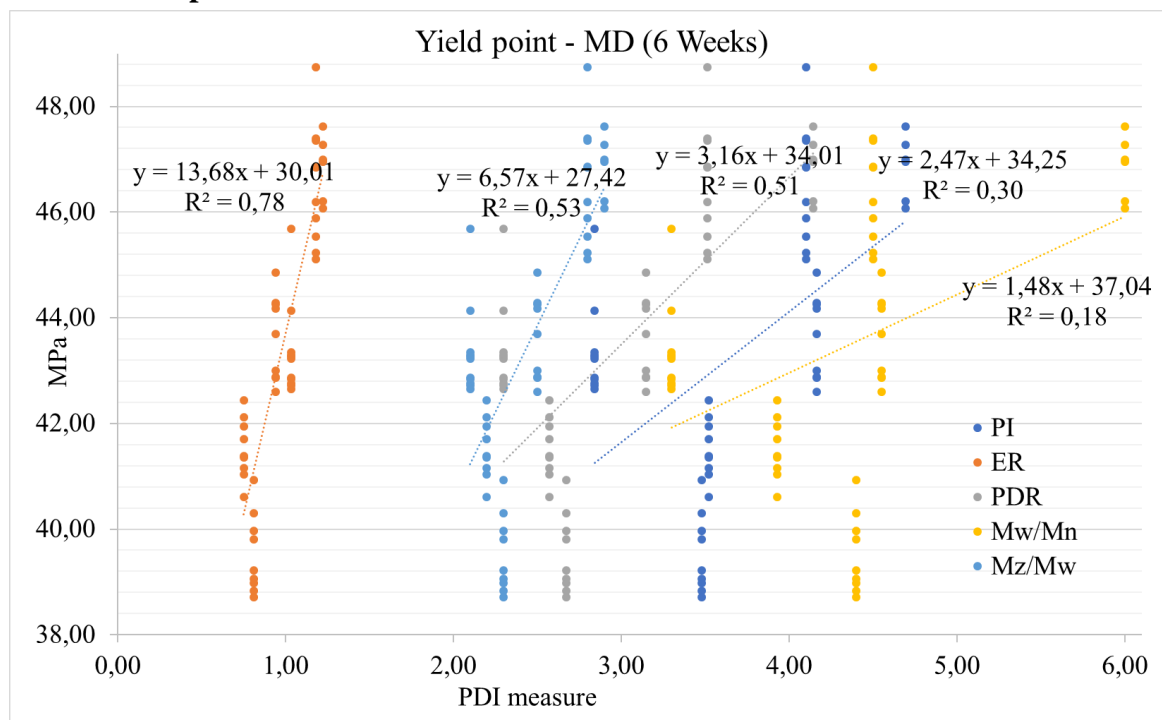


Figure 91. Showing the yield point after 6 weeks in storage in MD, plotted towards different measures of polydispersity by linear equation.

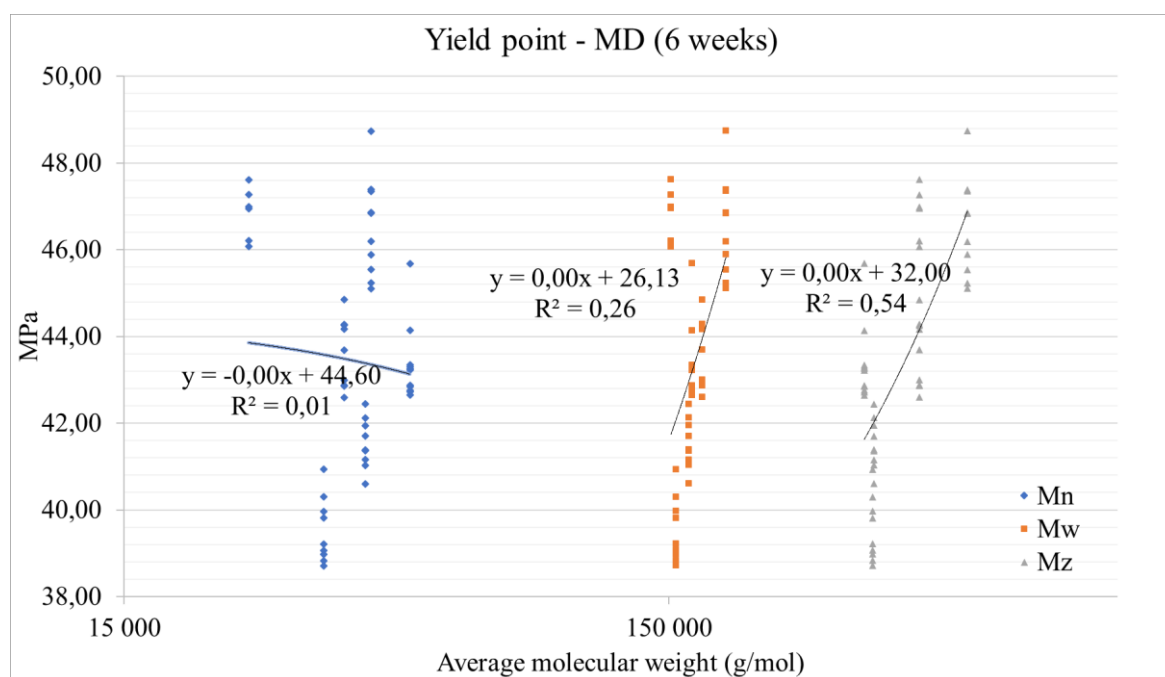


Figure 92. Showing the yield point after 6 weeks of storage in MD, plotted towards different measures of polydispersity by linear equation. The x-axis is logarithmical.

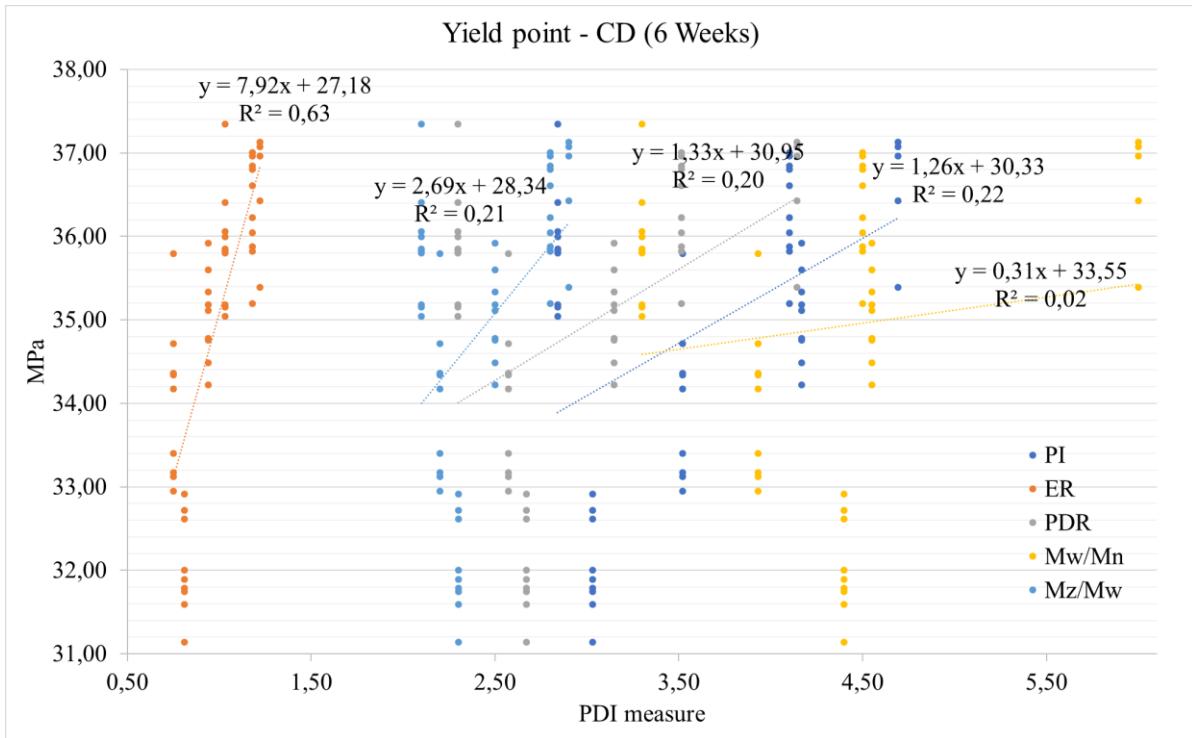


Figure 93. Showing the yield point after 6 weeks in storage in CD, plotted towards different measures of polydispersity by linear equation.

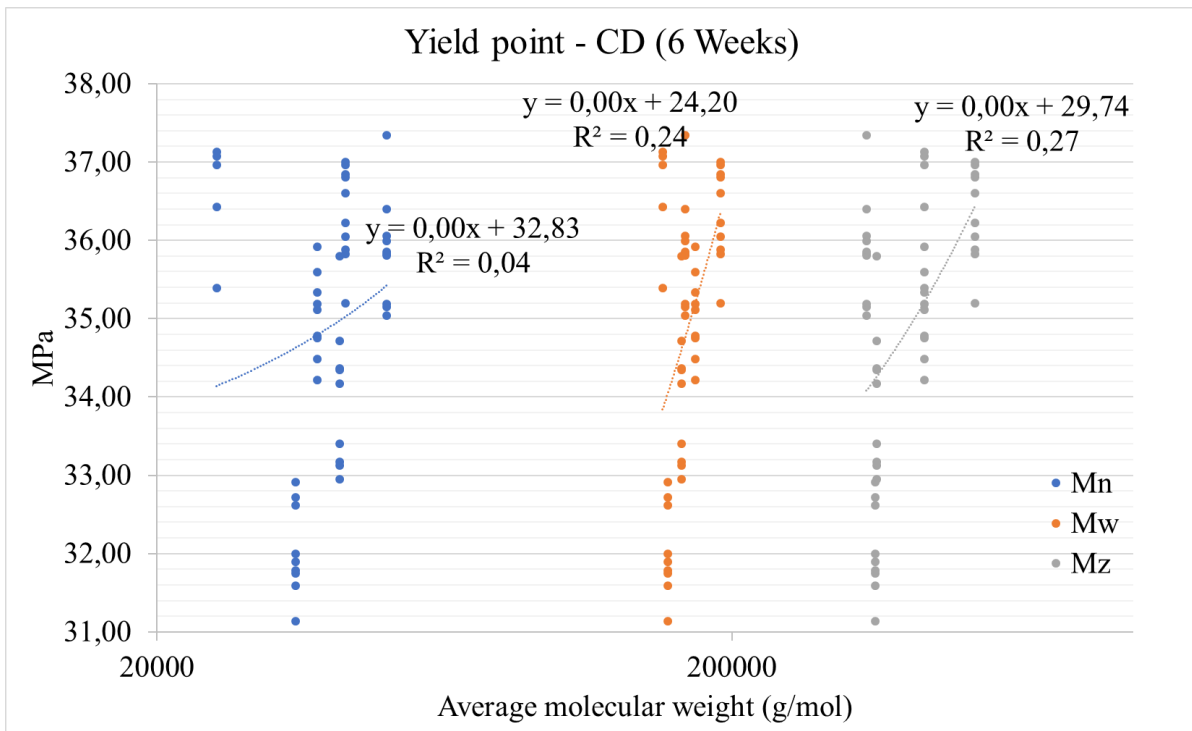


Figure 94. Showing the yield point after 6 weeks of storage in MD, plotted towards different measures of polydispersity by linear equation. The x-axis is logarithmical.

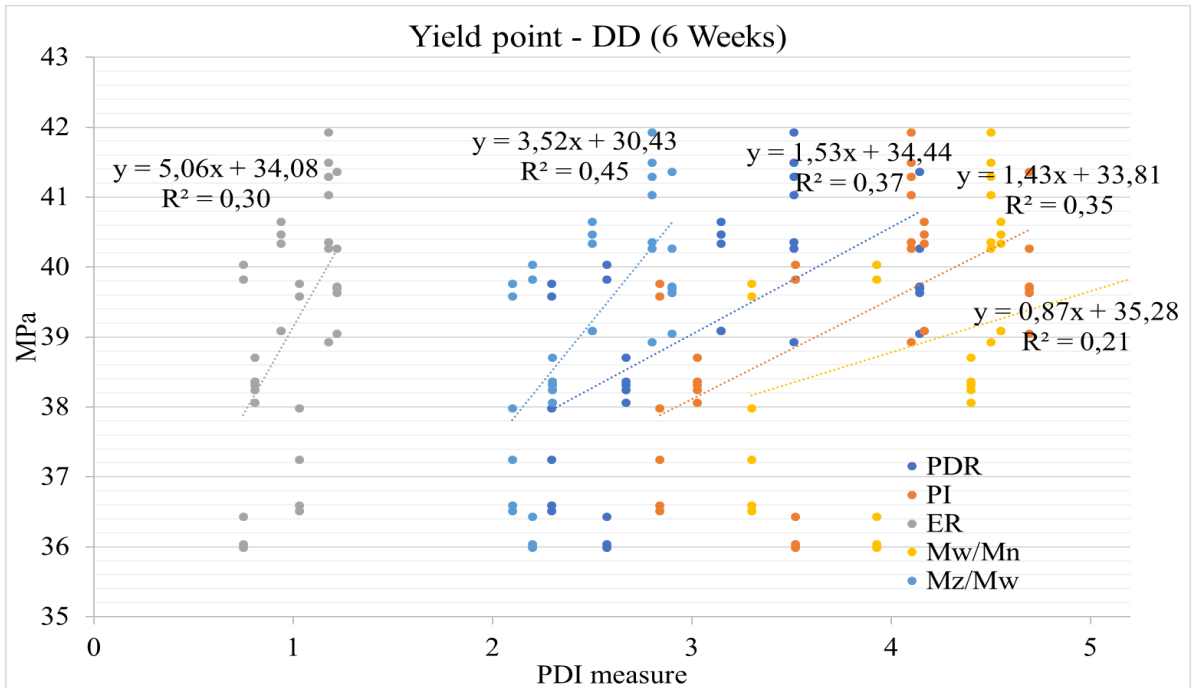


Figure 95. Showing the yield point after 6 weeks in storage in DD, plotted towards different measures of polydispersity by linear equation.

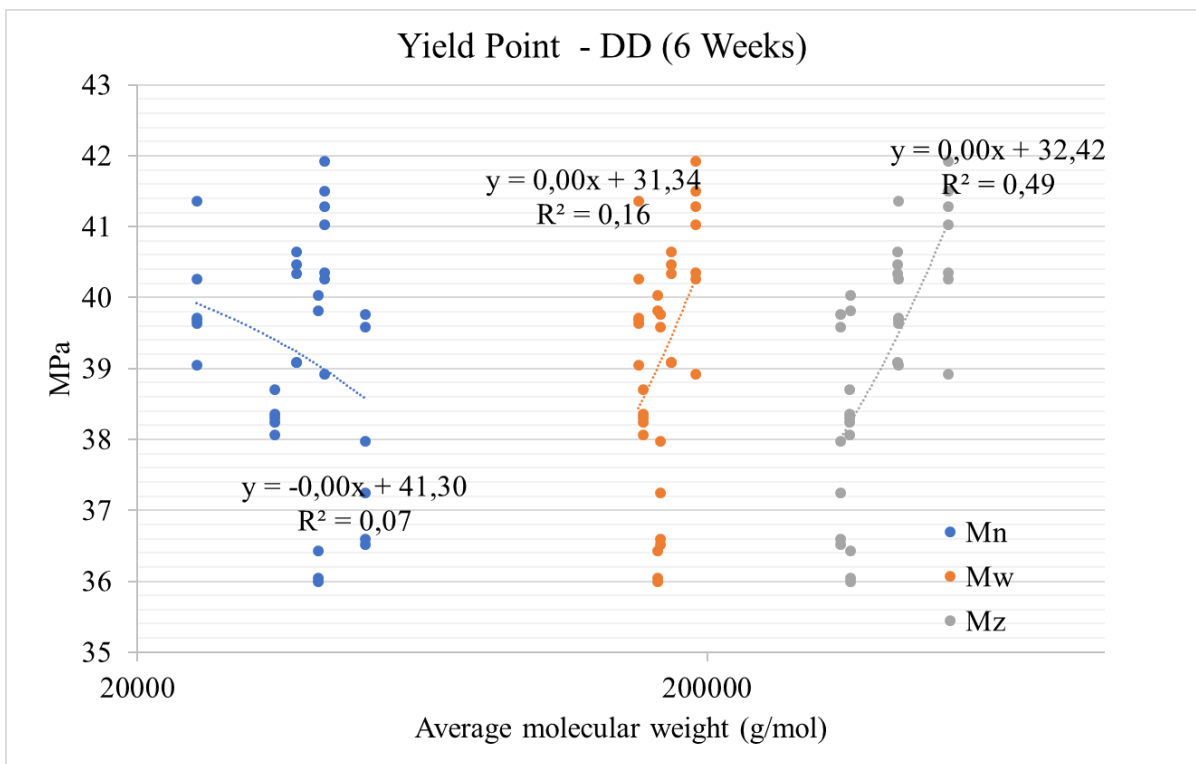


Figure 96. Showing the yield point after 6 weeks in storage in DD, plotted towards different measures of average molecular weight by linear equation. The x-axis is logarithmical.

11.4 Tensile Impact

<i>Grade nbr</i>	<i>Storage</i>	<i>Resilience (kJ/m²)</i>	<i>Std. dev Resilience</i>	<i>Total Defor- mation (mm)</i>	<i>Std. dev Total Def.</i>	<i>Peak Force (N)</i>	<i>Std. dev Peak Force</i>
1	2 days	58	13.0	1.4	0.24	123	3.5
1	2 weeks	42	11.7	0.9	0.18	124	5.7
1	4 weeks	54	9.9	1.3	0.14	121	2.9
2	2 days	52	8.8	1.3	0.15	121	3.8
2	2 weeks	101	13.4	2.4	0.31	117	3.6
2	4 weeks	88	11.0	1.9	0.25	117	2.2
3	2 days	85	10.5	1.9	0.35	122	3.0
3	2 weeks	91	10.9	2.1	0.22	122	3.0
3	4 weeks	72	7.9	1.5	0.08	130	2.5
4	2 days	64	5.2	1.3	0.07	135	9.2
4	2 weeks	72	17.1	1.6	0.33	126	4.0
4	4 weeks	50	4.6	1.1	0.09	132	2.6
5	2 days	65	17.2	1.4	0.26	126	2.6
5	2 weeks	76	7.5	1.7	0.18	121	1.9
5	4 weeks	64	16.8	1.3	0.27	125	3.2
6	2 days	57	14.2	1.2	0.23	128	3.7
6	2 weeks	63	14.2	1.5	0.30	124	4.3
6	4 weeks	54	13.0	1.2	0.26	130	5.2

Table 31. Resilience, total deformation and peak force measured by tensile impact on dogbones in MD. 10 dogbones were tested at each time.

11.5 DSC

11.5.1 Enthalpy and peak melt temperature – first melting

Grade	Storage time:	2.5 hours		1 day		3 days		7 days		2 weeks	
		ave.	std. dev.	ave.	std. dev.	ave.	std. dev.	ave.	std. dev.	ave.	std. dev.
1	Enthalpy (J/g)	N/A	N/A	99.7	1.33	101.5	0.64	99.9	0.11	101.1	0.21
	Peak melt temperature C°	N/A	N/A	164.3	0.0	164.7	0.05	164.4	0.25	164.2	0.18
2	Enthalpy (J/g)	91.8	0.12	97.7	0.21	97.1	0.57	97.6	0.17	98.4	0.08
	Peak melt temperature C°	164.2	0.13	164.3	0.28	164.1	0.14	164.2	0.17	164.4	0.01
3	Enthalpy (J/g)	95.1	0.69	97.2	0.36	97.4	0.07	95.1	0.31	94.6	4.14
	Peak melt temperature C°	164.2	0.13	164.1	0.01	163.9	0.00	165.4	1.50	164.3	0.16
4	Enthalpy (J/g)	101.3	0.14	102.2	0.42	102.1	1.84	101.2	0.42	100.7	5.20
	Peak melt temperature C°	164.7	0.04	163.4	1.81	164.6	0.06	164.8	0.03	164.9	0.17
5	Enthalpy (J/g)	96.2	0.19	99.7	4.10	96.7	0.54	99.0	2.33	N/A	N/A
	Peak melt temperature C°	164.2	0.05	164.2	0.04	164.1	0.01	164.2	0.05	N/A	N/A
6	Enthalpy (J/g)	96.6	2.37	99.4	0.22	97.5	0.77	100.5	0.42	N/A	N/A
	Peak melt temperature C°	164.7	0.22	164.4	0.09	164.4	0.51	164.4	0.06	N/A	N/A

Table 32. DCS measures where enthalpy and peak melt temperature have been extracted by the help of a baseline between 100-199 C°, in the software TA Universals. This table show the first melting of the injected moulded polymer plate. N/A due to fault in measurement.

11.5.2 Enthalpy and peak melt temperature – second melting

Grade	Storage time:	2.5 hours		1 day		3 days		7 days		2 weeks	
		ave.	std. dev.	ave.	std. dev.	ave.	std. dev.	ave.	std. dev.	ave.	std. dev.
1	Enthalpy (J/g)	N/A	N/A	104.9	1.63	106.9	0.57	105.7	1.13	106.9	0.35
	Peak melt temperature C°	N/A	N/A	160.0	0.1	160.2	0.06	160.0	0.18	160.1	0.08
2	Enthalpy (J/g)	98.3	0.62	N/A	N/A	104.5	1.06	105.0	0.00	105.1	0.07
	Peak melt temperature C°	159.8	0.24	160.1	0.05	160.1	0.05	160.1	0.16	160.2	0.23
3	Enthalpy (J/g)	N/A*	N/A*	106.1	0.21	106.5	0.28	102.6	0.49	104.1	3.82
	Peak melt temperature C°	N/A*	N/A*	161.4	0.04	161.3	0.07	162.2	0.52	161.6	0.35
4	Enthalpy (J/g)	N/A*	N/A*	111.4	0.28	112.6	N/A	110.7	0.07	106.6	1.34
	Peak melt temperature C°	N/A*	N/A*	162.1	0.01	161.9	N/A	162.2	0.04	162.4	0.01
5	Enthalpy (J/g)	105.2	0.07	106.6	0.57	106.7	0.49	107.1	0.07	N/A	N/A
	Peak melt temperature C°	161.4	0.05	161.3	0.08	161.3	0.02	161.4	0.01	N/A	N/A
6	Enthalpy (J/g)	105.6	2.62	110.3	0.85	108.5	1.27	110.6	0.35	N/A	N/A
	Peak melt temperature C°	162.1	0.20	161.8	0.02	161.9	0.69	161.7	0.01	N/A	N/A

Table 33. DCS measures where enthalpy and peak melt temperature have been extracted by the help of a baseline between 100-199 C°, in the software TA Universals. This table show the first melting of the injected moulded polymer plate. N/A due to fault in measurements and problem with the server. N/A*, these measurements were performed with only melting of first peak, no second cycle.

11.5.3 Grade 1

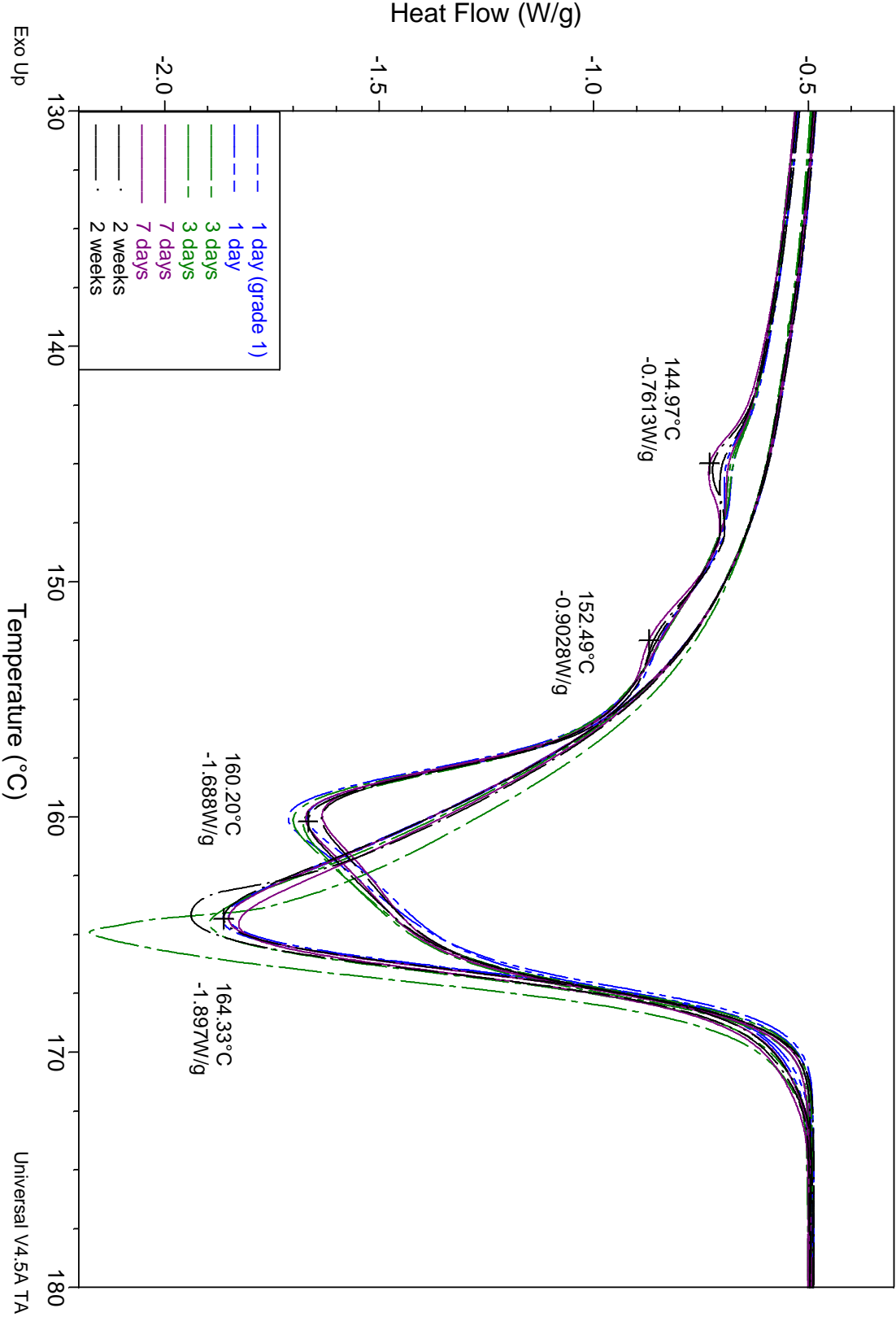


Figure 97. Grade 1 melt peak, where the right peak is the first melt peak and the peak to the left is the second melting after the sample been cooled and re-crystallised once. Measures from day 1, 3, 7 and 2 weeks are overlaid.

11.5.4 Grade 2

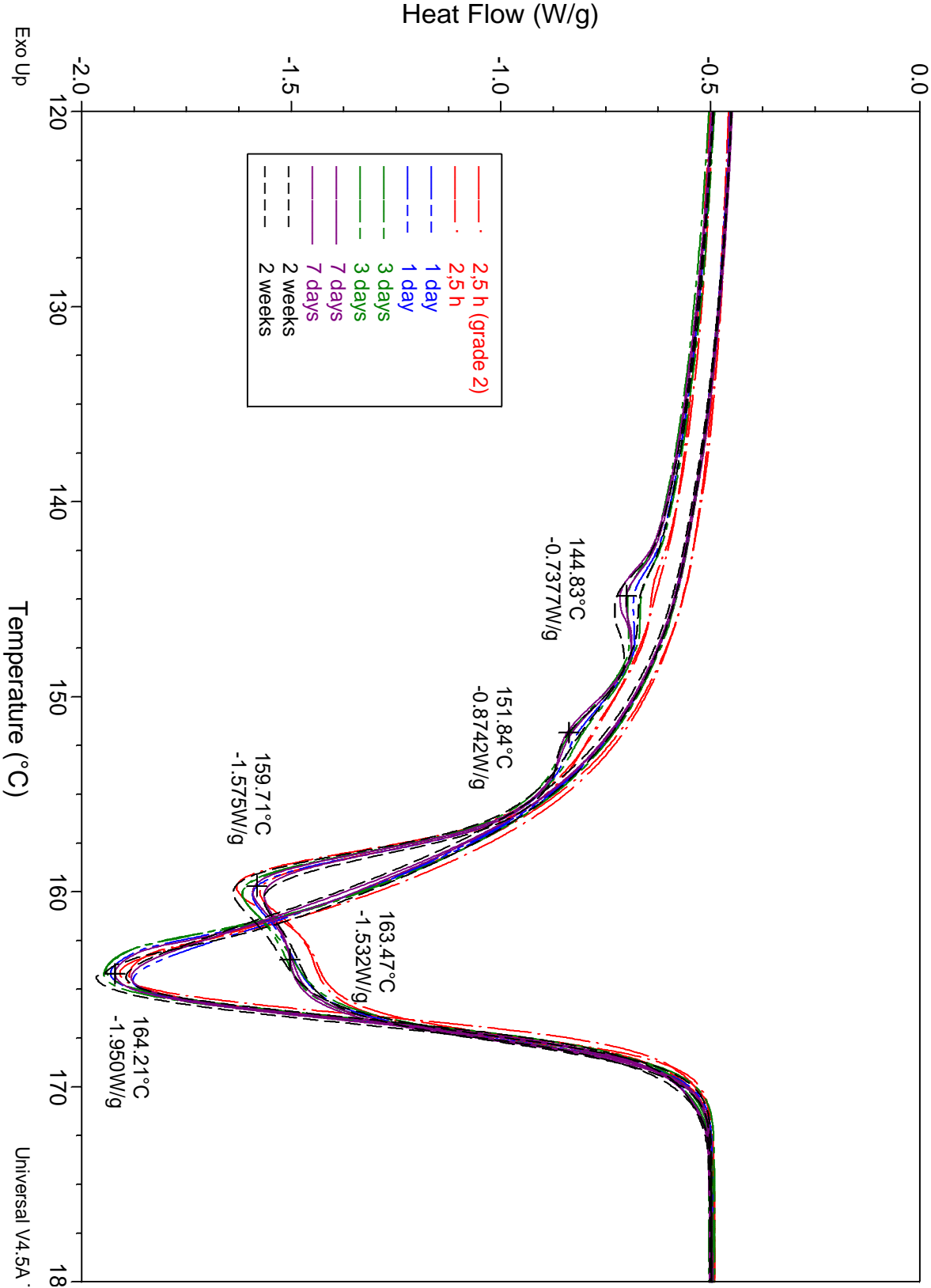


Figure 98. Grade 2 melt peak, where the right peak is the first melt peak and the peak to the left is the second melting after the sample been cooled and re-crystallised once. Measures from 2.5 hour, 1, 3, 7 days and 2 weeks are overlaid.

11.5.5 Grade 3

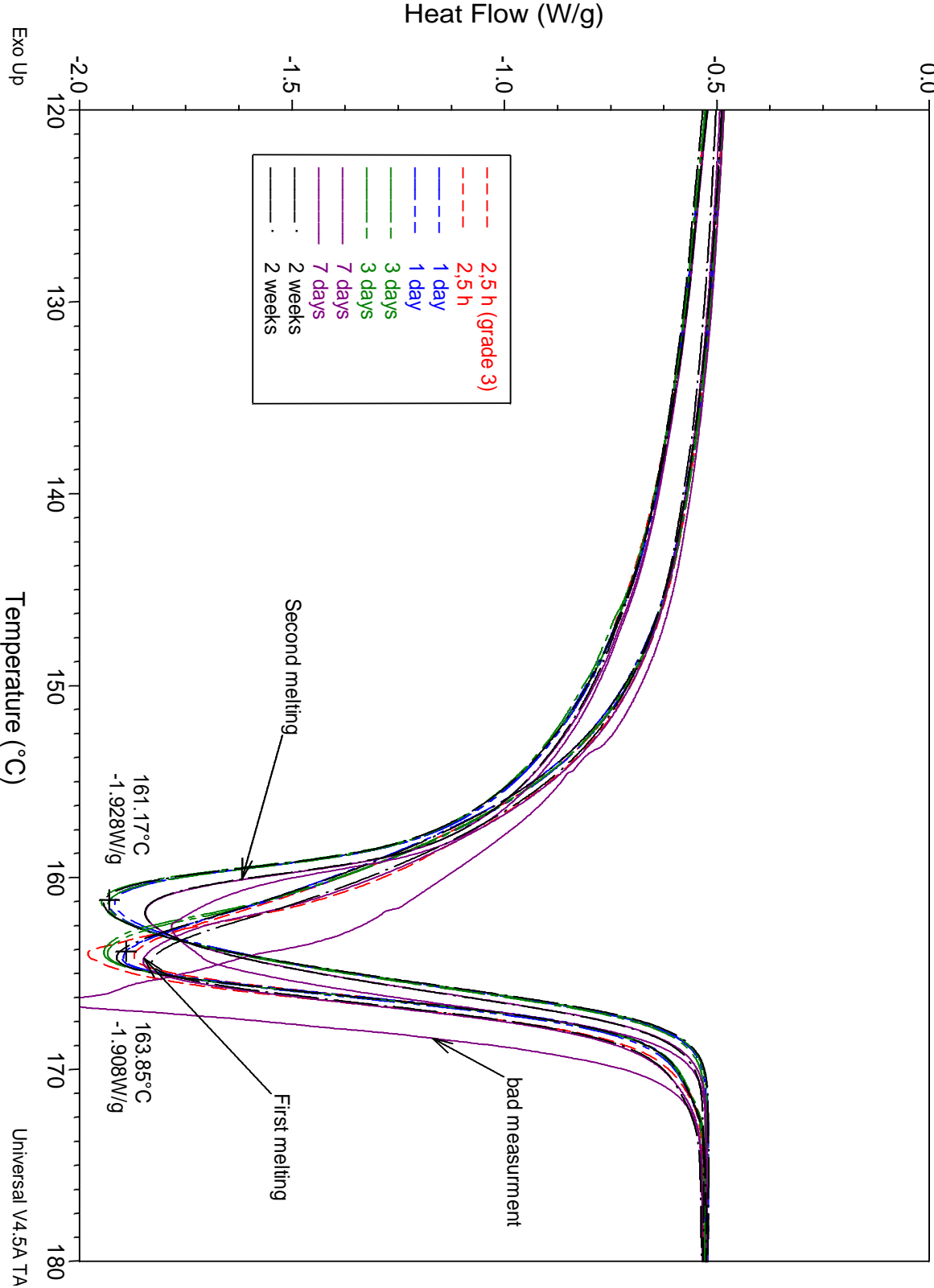


Figure 99. Grade 3 melt peak, where the right peak is the first melt peak and the peak to the left is the second melting after the sample been cooled and re-crystallised once. Measures from 2.5 hour, 1, 3, 7 days and 2 weeks are overlayered.

11.5.6 Grade 4

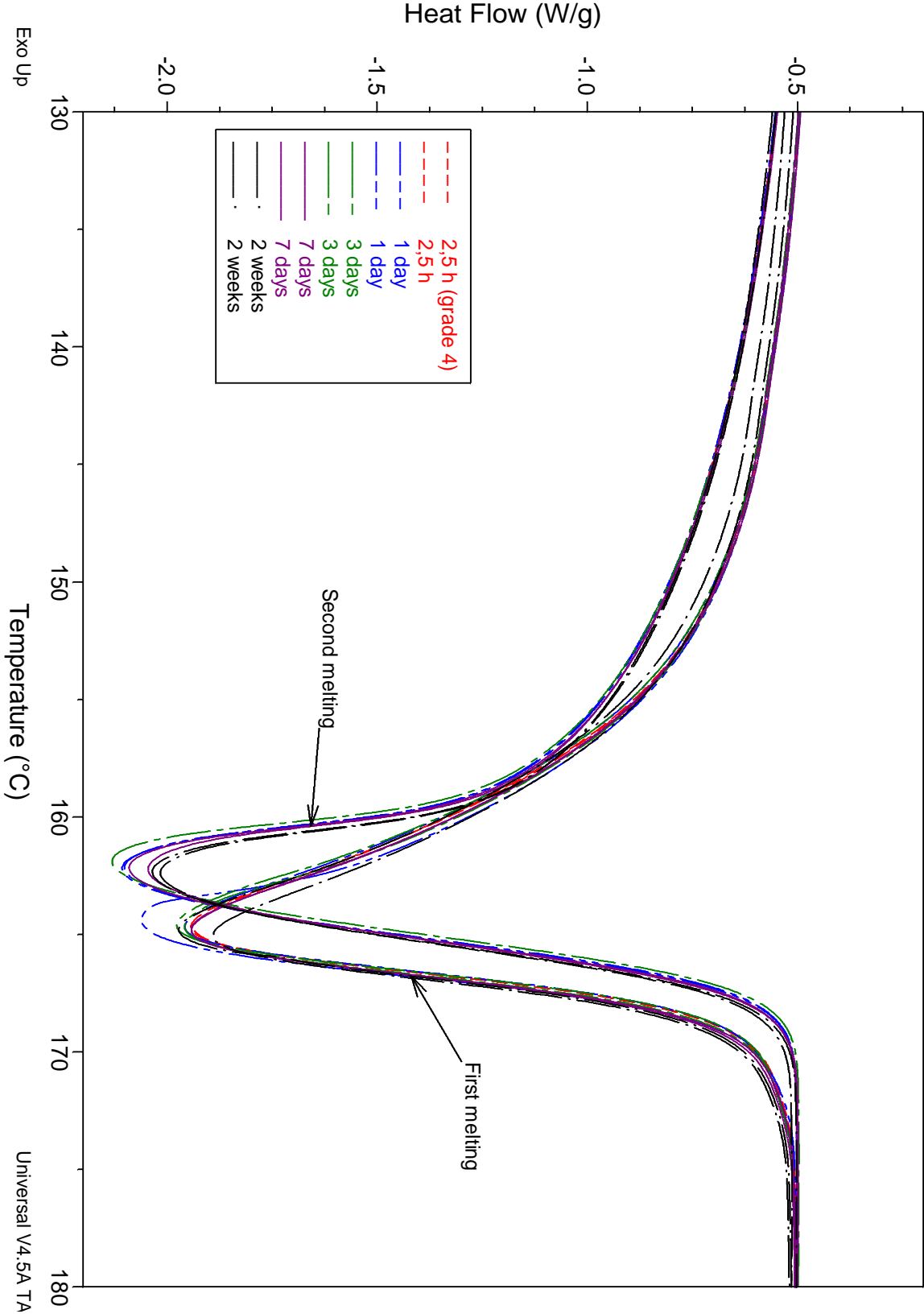


Figure 100. Grade 4 melt peak, where the right peak is the first melt peak and the peak to the left is the second melting after the sample been cooled and re-crystallised once. Measures from 2.5 hour, 1, 3, 7 days and 2 weeks are overlaid.

11.5.7 Grade 5

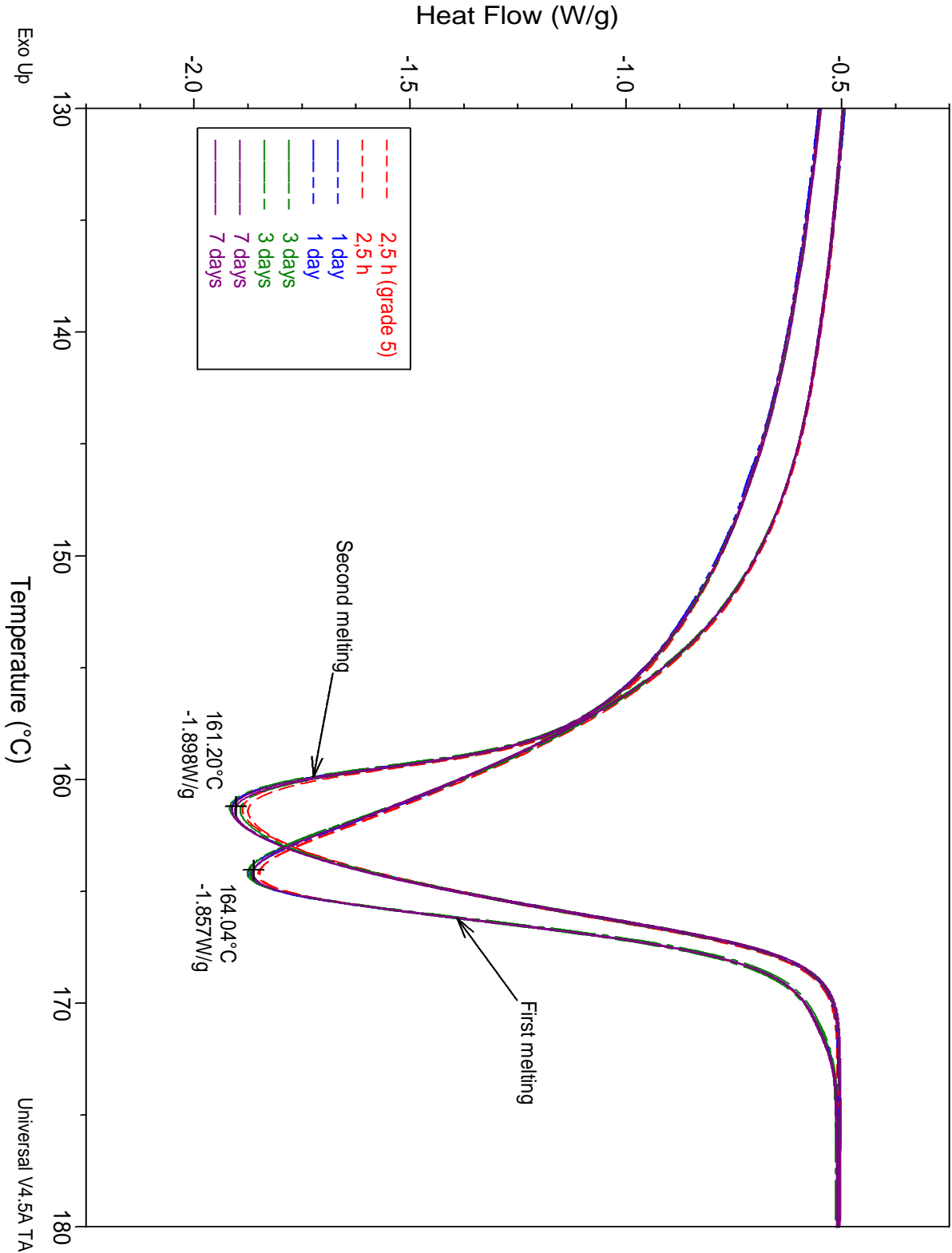


Figure 101. Grade 5 melt peak, where the right peak is the first melt peak and the peak to the left is the second melting after the sample been cooled and re-crystallised once. Measures from 2.5 hour, 1, 3, 7 days and 2 weeks are overlayered.

11.5.8 Grade 6

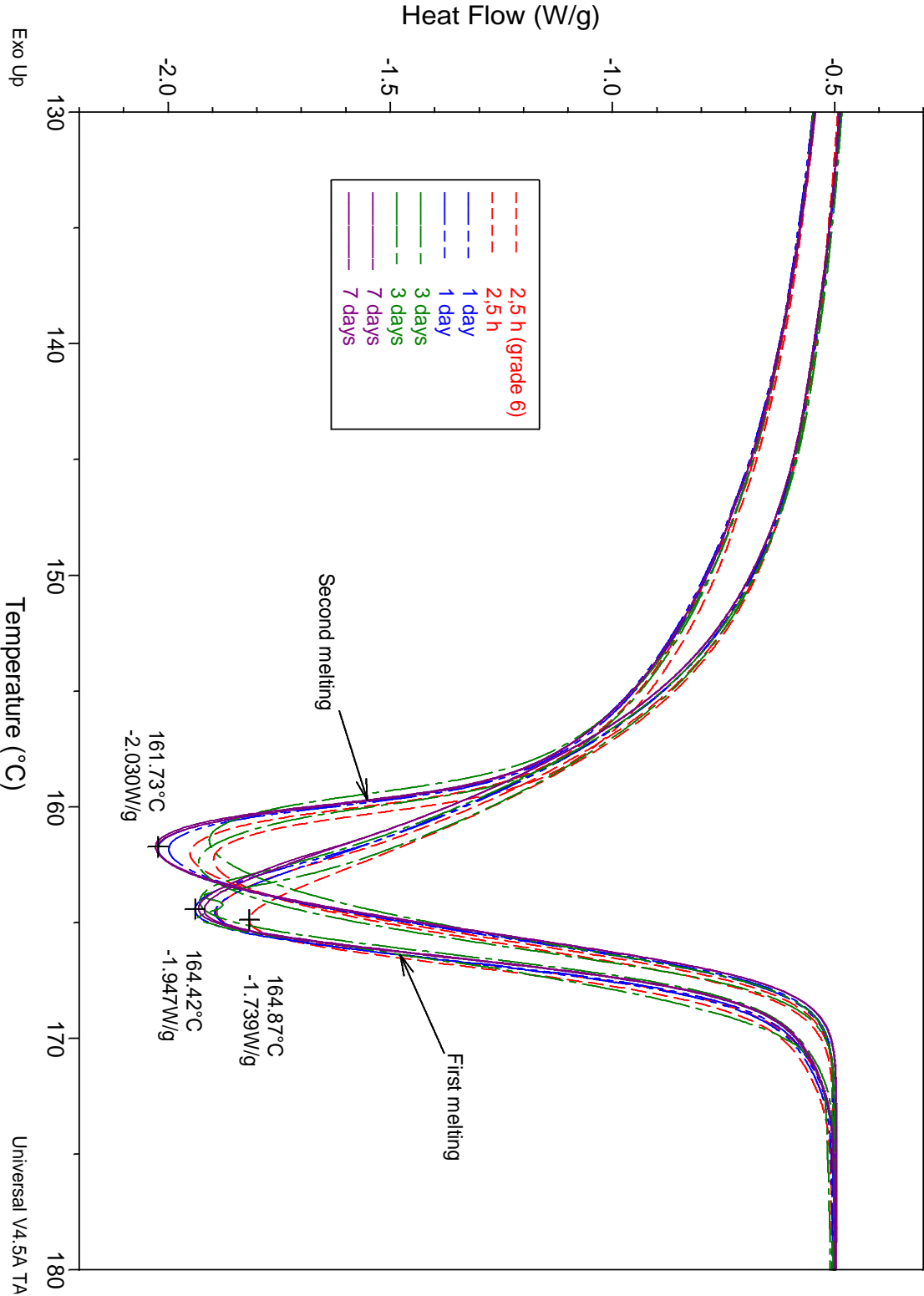
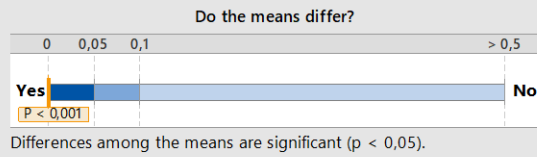


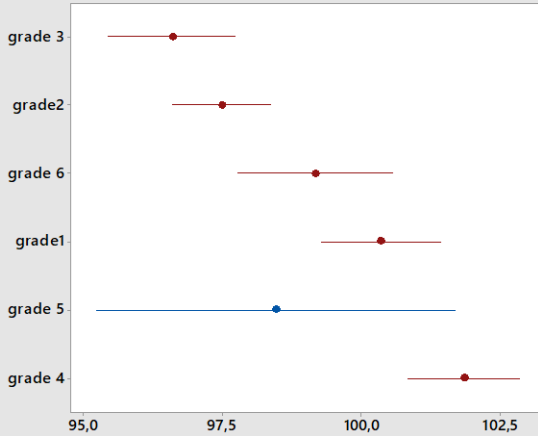
Figure 102. Grade 6 melt peak, where the right peak is the first melt peak and the peak to the left is the second melting after the sample been cooled and re-crystallised once. Measures from 2.5 hour, 1, 3, 7 days and 2 weeks are overlayers.

One-Way ANOVA for melt enthalpy (J/g), after storage 1 day, 3 days and 7 days Summary Report



		Which means differ?		
#	Sample	Differs from		
1	grade 3	3	4	6
2	grade2	4	6	
3	grade 6	1	6	
4	grade1	1	2	
5	grade 5			
6	grade 4	1	2	3

Means Comparison Chart
Red intervals that do not overlap differ.

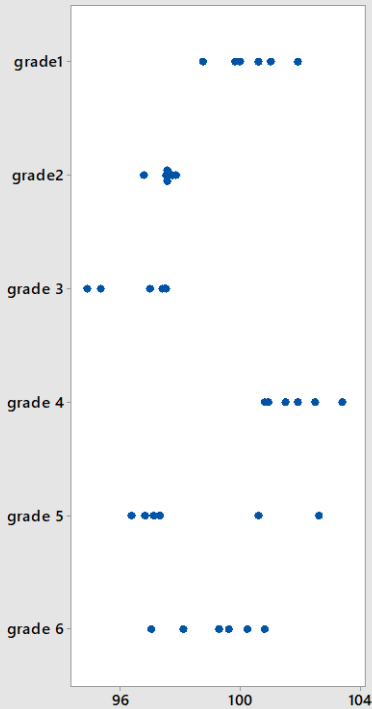


Comments

- Test: You can conclude that there are differences among the means at the 0,05 level of significance.
- Comparison Chart: Look for red comparison intervals that do not overlap to identify means that differ from each other. Consider the size of the differences to determine if they have practical implications.

One-Way ANOVA for melt enthalpy (J/g), after storage 1, 3 and 7 days

Distribution of Data
Compare the location and spread.



Data in Worksheet Order
Investigate any outliers (marked in red).

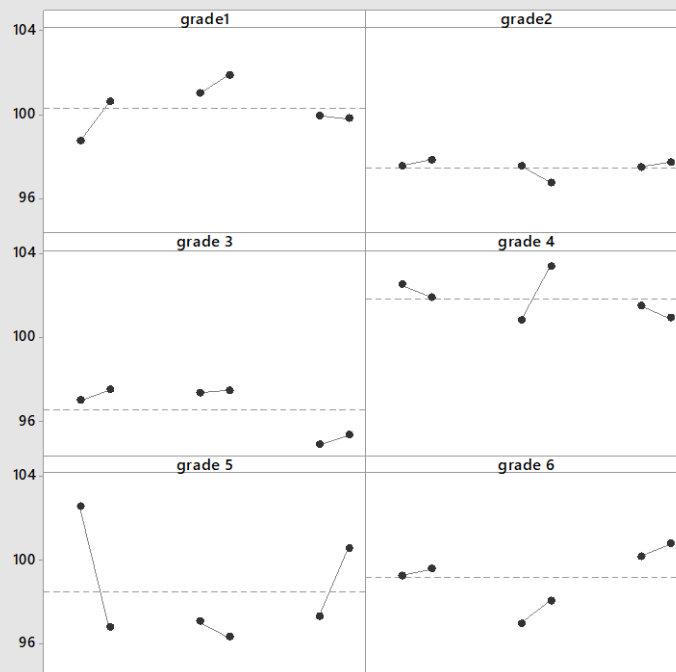


Figure 103. ANOVA report generated by minitab to statistically determine if there are a difference in enthalpy between the grades. By the CI of 95% there is a higher melt enthalpy in grade 1 and 4 vs grade 2 and 3. Hence, a higher rate of crystallinity.

11.6 Capillary rheometry

Values are corrected with Bagley and Rabinowitsch-Weissenberg

Material	Corrected Shear rate [1/s]	Shear stress [Pa]	Viscosity [Pa*s]
<i>Grade 1</i>	15874	172875	11
	9352	147209	16
	2976	103106	35
	1438	81429	57
	399	50697	127
	123	29944	243
<i>Grade 2</i>	17836	179696	10
	10489	159997	15
	3219	117555	37
	1517	95410	63
	405	61748	152
	122	36340	299
<i>Grade 3</i>	19525	197568	10
	11324	177205	16
	3426	135777	40
	1599	112578	70
	421	75443	179
	125	46398	370
<i>Grade 4</i>	17671	186686	11
	10452	167833	16
	3229	123475	38
	1525	99252	65
	414	64853	157
	126	40111	317
<i>Grade 5</i>	18868	181042	10
	10960	161861	15
	3311	121709	37
	1548	99918	65
	409	65144	159
	123	38948	317
<i>Grade 6</i>	17701	178533	10
	10393	158534	15
	3205	116497	36
	1519	94447	62
	410	60935	149
	125	37028	297

Table 34. Shear viscosity measured by capillary rheometer by grade 1-6.

11.7 SEC result plot and raw data

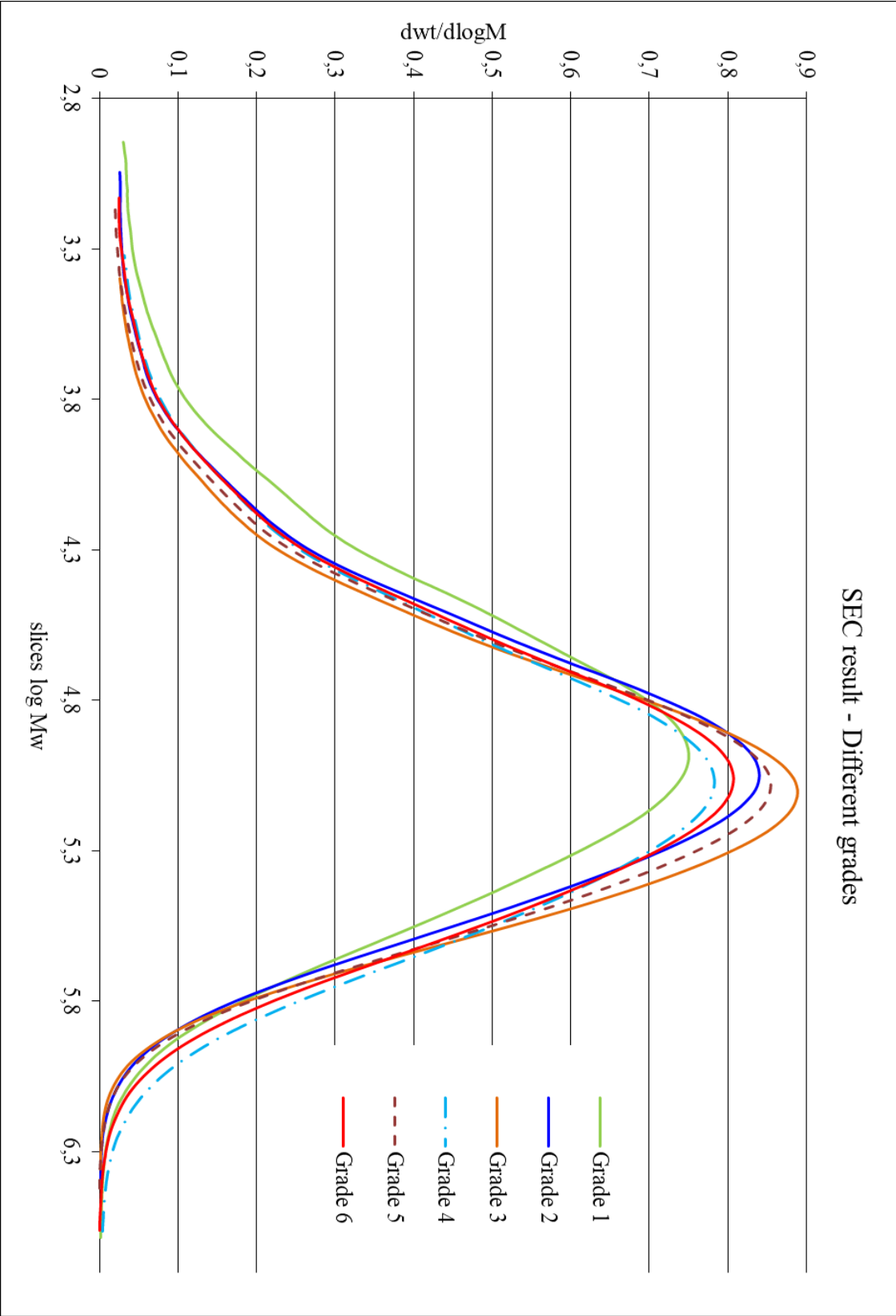


Figure 104. SEC data received from external source.

Grade 1		Grade 2		Grade 3		Grade 4		Grade 5		Grade 6	
LogM	MMD	LogM	MMD	LogM	MMD	LogM	MMD	LogM	MMD	LogM	MMD
6.5848	0.0013	6.4134	0.0015	6.3583	0.0019	6.5640	0.0042	6.4216	0.0004	6.5613	0.0002
6.5709	0.0014	6.3998	0.0016	6.3448	0.0020	6.5502	0.0044	6.4080	0.0005	6.5474	0.0003
6.5570	0.0016	6.3862	0.0017	6.3314	0.0021	6.5363	0.0048	6.3944	0.0005	6.5335	0.0005
6.5431	0.0018	6.3727	0.0018	6.3179	0.0021	6.5225	0.0052	6.3808	0.0006	6.5197	0.0008
6.5292	0.0019	6.3591	0.0019	6.3045	0.0023	6.5087	0.0054	6.3673	0.0008	6.5059	0.0010
6.5154	0.0021	6.3456	0.0021	6.2911	0.0025	6.4949	0.0057	6.3537	0.0011	6.4921	0.0013
6.5016	0.0022	6.3321	0.0023	6.2777	0.0028	6.4812	0.0061	6.3402	0.0013	6.4784	0.0017
6.4878	0.0024	6.3187	0.0024	6.2643	0.0031	6.4675	0.0065	6.3268	0.0016	6.4647	0.0019
6.4741	0.0025	6.3053	0.0026	6.2510	0.0035	6.4538	0.0068	6.3133	0.0020	6.4510	0.0022
6.4603	0.0028	6.2918	0.0029	6.2376	0.0039	6.4401	0.0073	6.2999	0.0026	6.4373	0.0024
6.4466	0.0030	6.2785	0.0033	6.2244	0.0043	6.4264	0.0080	6.2864	0.0031	6.4236	0.0027
6.4330	0.0032	6.2651	0.0037	6.2111	0.0048	6.4128	0.0085	6.2731	0.0035	6.4100	0.0030
6.4193	0.0034	6.2518	0.0041	6.1978	0.0054	6.3992	0.0091	6.2597	0.0041	6.3964	0.0033
6.4057	0.0037	6.2384	0.0048	6.1846	0.0061	6.3856	0.0100	6.2463	0.0048	6.3828	0.0038
6.3921	0.0041	6.2251	0.0057	6.1714	0.0070	6.3721	0.0107	6.2330	0.0055	6.3693	0.0043
6.3785	0.0044	6.2119	0.0067	6.1582	0.0080	6.3585	0.0117	6.2197	0.0060	6.3558	0.0048
6.3650	0.0049	6.1986	0.0078	6.1451	0.0092	6.3450	0.0127	6.2065	0.0068	6.3422	0.0057
6.3514	0.0054	6.1854	0.0088	6.1319	0.0106	6.3316	0.0140	6.1932	0.0079	6.3288	0.0064
6.3379	0.0059	6.1722	0.0103	6.1188	0.0124	6.3181	0.0151	6.1800	0.0091	6.3153	0.0074
6.3244	0.0064	6.1590	0.0116	6.1057	0.0143	6.3047	0.0164	6.1668	0.0104	6.3019	0.0080
6.3110	0.0069	6.1458	0.0132	6.0926	0.0165	6.2913	0.0178	6.1536	0.0120	6.2885	0.0090
6.2975	0.0076	6.1327	0.0150	6.0796	0.0190	6.2779	0.0194	6.1404	0.0137	6.2751	0.0101
6.2841	0.0082	6.1196	0.0170	6.0666	0.0219	6.2645	0.0212	6.1273	0.0157	6.2617	0.0112
6.2707	0.0093	6.1065	0.0194	6.0536	0.0250	6.2512	0.0231	6.1142	0.0178	6.2484	0.0124
6.2574	0.0103	6.0934	0.0216	6.0406	0.0283	6.2379	0.0256	6.1011	0.0202	6.2351	0.0138
6.2440	0.0115	6.0804	0.0244	6.0276	0.0322	6.2246	0.0278	6.0880	0.0228	6.2218	0.0156
6.2307	0.0127	6.0674	0.0273	6.0147	0.0363	6.2113	0.0304	6.0750	0.0257	6.2085	0.0174
6.2174	0.0140	6.0543	0.0303	6.0017	0.0412	6.1980	0.0332	6.0619	0.0290	6.1952	0.0195
6.2041	0.0152	6.0414	0.0338	5.9888	0.0465	6.1848	0.0360	6.0489	0.0326	6.1820	0.0217
6.1909	0.0166	6.0284	0.0376	5.9760	0.0522	6.1716	0.0390	6.0359	0.0366	6.1688	0.0241
6.1777	0.0184	6.0155	0.0417	5.9631	0.0586	6.1584	0.0421	6.0230	0.0411	6.1556	0.0265
6.1645	0.0201	6.0025	0.0462	5.9503	0.0655	6.1453	0.0457	6.0100	0.0458	6.1425	0.0291
6.1513	0.0224	5.9896	0.0511	5.9374	0.0728	6.1321	0.0495	5.9971	0.0511	6.1293	0.0319
6.1381	0.0246	5.9767	0.0565	5.9246	0.0805	6.1190	0.0534	5.9842	0.0567	6.1162	0.0350
6.1250	0.0273	5.9639	0.0621	5.9119	0.0888	6.1059	0.0578	5.9713	0.0630	6.1031	0.0384
6.1119	0.0304	5.9511	0.0682	5.8991	0.0977	6.0928	0.0625	5.9585	0.0696	6.0900	0.0423
6.0988	0.0331	5.9382	0.0747	5.8864	0.1071	6.0798	0.0673	5.9456	0.0766	6.0770	0.0464
6.0857	0.0364	5.9254	0.0817	5.8736	0.1170	6.0668	0.0725	5.9328	0.0842	6.0640	0.0509
6.0726	0.0398	5.9127	0.0893	5.8609	0.1277	6.0538	0.0778	5.9200	0.0922	6.0509	0.0556
6.0596	0.0435	5.8999	0.0968	5.8483	0.1390	6.0408	0.0836	5.9072	0.1008	6.0380	0.0607
6.0466	0.0473	5.8872	0.1051	5.8356	0.1512	6.0278	0.0898	5.8945	0.1097	6.0250	0.0661
6.0336	0.0515	5.8744	0.1139	5.8230	0.1637	6.0149	0.0962	5.8817	0.1192	6.0121	0.0718

Grade 1		Grade 2		Grade 3		Grade 4		Grade 5		Grade 6	
LogM	MMD	LogM	MMD	LogM	MMD	LogM	MMD	LogM	MMD	LogM	MMD
6.0206	0.0560	5.8617	0.1231	5.8104	0.1768	6.0019	0.1030	5.8690	0.1293	5.9991	0.0778
6.0077	0.0608	5.8491	0.1326	5.7978	0.1907	5.9890	0.1101	5.8563	0.1399	5.9862	0.0842
5.9948	0.0657	5.8364	0.1424	5.7852	0.2050	5.9762	0.1177	5.8436	0.1510	5.9733	0.0910
5.9819	0.0707	5.8238	0.1529	5.7726	0.2196	5.9633	0.1255	5.8310	0.1624	5.9605	0.0981
5.9690	0.0767	5.8112	0.1638	5.7601	0.2346	5.9505	0.1335	5.8183	0.1744	5.9476	0.1056
5.9561	0.0826	5.7986	0.1750	5.7475	0.2501	5.9376	0.1419	5.8057	0.1870	5.9348	0.1136
5.9433	0.0888	5.7860	0.1870	5.7350	0.2659	5.9248	0.1506	5.7931	0.1999	5.9220	0.1222
5.9305	0.0954	5.7734	0.1991	5.7226	0.2821	5.9121	0.1600	5.7805	0.2133	5.9092	0.1307
5.9177	0.1023	5.7609	0.2117	5.7101	0.2987	5.8993	0.1693	5.7679	0.2270	5.8965	0.1399
5.9049	0.1101	5.7483	0.2245	5.6976	0.3156	5.8866	0.1792	5.7554	0.2410	5.8837	0.1494
5.8921	0.1177	5.7358	0.2375	5.6852	0.3328	5.8739	0.1894	5.7429	0.2554	5.8710	0.1593
5.8794	0.1255	5.7234	0.2509	5.6728	0.3503	5.8612	0.1997	5.7304	0.2702	5.8583	0.1694
5.8667	0.1338	5.7109	0.2643	5.6604	0.3680	5.8485	0.2107	5.7179	0.2851	5.8457	0.1799
5.8540	0.1423	5.6984	0.2780	5.6480	0.3855	5.8358	0.2214	5.7054	0.3003	5.8330	0.1908
5.8413	0.1513	5.6860	0.2921	5.6357	0.4032	5.8232	0.2324	5.6930	0.3159	5.8204	0.2019
5.8286	0.1601	5.6736	0.3064	5.6233	0.4208	5.8106	0.2438	5.6805	0.3316	5.8077	0.2134
5.8160	0.1692	5.6612	0.3209	5.6110	0.4386	5.7980	0.2555	5.6681	0.3476	5.7951	0.2251
5.8034	0.1787	5.6488	0.3354	5.5987	0.4559	5.7854	0.2673	5.6557	0.3635	5.7826	0.2372
5.7908	0.1883	5.6365	0.3500	5.5864	0.4732	5.7728	0.2792	5.6433	0.3794	5.7700	0.2495
5.7782	0.1981	5.6241	0.3647	5.5741	0.4906	5.7603	0.2916	5.6310	0.3954	5.7574	0.2619
5.7656	0.2085	5.6118	0.3794	5.5619	0.5078	5.7478	0.3038	5.6186	0.4113	5.7449	0.2748
5.7531	0.2190	5.5995	0.3938	5.5496	0.5247	5.7352	0.3162	5.6063	0.4272	5.7324	0.2879
5.7405	0.2296	5.5872	0.4083	5.5374	0.5413	5.7228	0.3286	5.5940	0.4429	5.7199	0.3012
5.7280	0.2404	5.5749	0.4228	5.5252	0.5580	5.7103	0.3412	5.5817	0.4585	5.7075	0.3145
5.7155	0.2513	5.5627	0.4373	5.5130	0.5742	5.6978	0.3540	5.5694	0.4740	5.6950	0.3279
5.7031	0.2623	5.5504	0.4520	5.5009	0.5902	5.6854	0.3668	5.5572	0.4894	5.6826	0.3414
5.6906	0.2730	5.5382	0.4663	5.4887	0.6059	5.6730	0.3797	5.5449	0.5044	5.6702	0.3550
5.6782	0.2840	5.5260	0.4807	5.4766	0.6214	5.6606	0.3922	5.5327	0.5195	5.6578	0.3685
5.6658	0.2956	5.5138	0.4949	5.4644	0.6364	5.6482	0.4049	5.5205	0.5345	5.6454	0.3818
5.6534	0.3067	5.5017	0.5088	5.4523	0.6512	5.6359	0.4172	5.5083	0.5491	5.6330	0.3953
5.6410	0.3182	5.4895	0.5230	5.4403	0.6656	5.6235	0.4295	5.4962	0.5637	5.6207	0.4088
5.6286	0.3297	5.4774	0.5364	5.4282	0.6799	5.6112	0.4416	5.4840	0.5779	5.6084	0.4223
5.6163	0.3412	5.4653	0.5499	5.4161	0.6933	5.5989	0.4538	5.4719	0.5920	5.5960	0.4355
5.6040	0.3526	5.4531	0.5632	5.4041	0.7067	5.5866	0.4659	5.4597	0.6058	5.5838	0.4485
5.5916	0.3635	5.4411	0.5766	5.3921	0.7197	5.5743	0.4777	5.4476	0.6192	5.5715	0.4617
5.5794	0.3751	5.4290	0.5898	5.3801	0.7322	5.5621	0.4894	5.4355	0.6324	5.5592	0.4747
5.5671	0.3865	5.4169	0.6027	5.3681	0.7443	5.5498	0.5010	5.4235	0.6453	5.5470	0.4875
5.5548	0.3978	5.4049	0.6155	5.3561	0.7560	5.5376	0.5122	5.4114	0.6579	5.5348	0.5003
5.5426	0.4089	5.3929	0.6280	5.3441	0.7675	5.5254	0.5233	5.3994	0.6701	5.5226	0.5127
5.5304	0.4198	5.3809	0.6403	5.3322	0.7783	5.5132	0.5344	5.3873	0.6821	5.5104	0.5249
5.5182	0.4308	5.3689	0.6524	5.3202	0.7888	5.5011	0.5456	5.3753	0.6938	5.4982	0.5370
5.5060	0.4417	5.3569	0.6645	5.3083	0.7989	5.4889	0.5566	5.3633	0.7052	5.4861	0.5491

Grade 1		Grade 2		Grade 3		Grade 4		Grade 5		Grade 6	
LogM	MMD	LogM	MMD	LogM	MMD	LogM	MMD	LogM	MMD	LogM	MMD
5.4938	0.4523	5.3449	0.6760	5.2964	0.8086	5.4768	0.5672	5.3514	0.7163	5.4739	0.5607
5.4816	0.4629	5.3330	0.6874	5.2845	0.8179	5.4647	0.5778	5.3394	0.7271	5.4618	0.5722
5.4695	0.4737	5.3211	0.6987	5.2727	0.8267	5.4526	0.5882	5.3274	0.7377	5.4497	0.5837
5.4574	0.4843	5.3091	0.7094	5.2608	0.8351	5.4405	0.5983	5.3155	0.7481	5.4376	0.5951
5.4453	0.4948	5.2972	0.7201	5.2490	0.8427	5.4284	0.6080	5.3036	0.7579	5.4255	0.6061
5.4332	0.5049	5.2853	0.7301	5.2371	0.8500	5.4163	0.6178	5.2917	0.7675	5.4135	0.6171
5.4211	0.5147	5.2735	0.7399	5.2253	0.8565	5.4043	0.6274	5.2798	0.7766	5.4014	0.6279
5.4090	0.5247	5.2616	0.7494	5.2135	0.8625	5.3923	0.6369	5.2679	0.7853	5.3894	0.6385
5.3970	0.5346	5.2498	0.7586	5.2017	0.8678	5.3803	0.6461	5.2561	0.7936	5.3774	0.6490
5.3850	0.5446	5.2379	0.7675	5.1899	0.8725	5.3683	0.6549	5.2442	0.8012	5.3654	0.6593
5.3730	0.5543	5.2261	0.7759	5.1782	0.8769	5.3563	0.6637	5.2324	0.8087	5.3534	0.6692
5.3610	0.5638	5.2143	0.7840	5.1664	0.8804	5.3443	0.6722	5.2206	0.8155	5.3415	0.6788
5.3490	0.5737	5.2025	0.7916	5.1547	0.8834	5.3324	0.6804	5.2088	0.8219	5.3295	0.6882
5.3370	0.5832	5.1908	0.7985	5.1430	0.8857	5.3205	0.6885	5.1970	0.8279	5.3176	0.6975
5.3251	0.5926	5.1790	0.8048	5.1313	0.8872	5.3085	0.6963	5.1852	0.8332	5.3057	0.7065
5.3131	0.6017	5.1673	0.8109	5.1196	0.8885	5.2966	0.7039	5.1734	0.8380	5.2938	0.7152
5.3012	0.6108	5.1555	0.8164	5.1079	0.8890	5.2847	0.7113	5.1617	0.8422	5.2819	0.7237
5.2893	0.6199	5.1438	0.8212	5.0962	0.8888	5.2729	0.7184	5.1499	0.8458	5.2700	0.7319
5.2774	0.6285	5.1321	0.8257	5.0846	0.8878	5.2610	0.7253	5.1382	0.8488	5.2581	0.7399
5.2655	0.6371	5.1204	0.8297	5.0729	0.8864	5.2492	0.7319	5.1265	0.8512	5.2463	0.7472
5.2537	0.6456	5.1087	0.8333	5.0613	0.8843	5.2373	0.7381	5.1148	0.8531	5.2345	0.7546
5.2418	0.6540	5.0971	0.8361	5.0497	0.8813	5.2255	0.7442	5.1031	0.8546	5.2226	0.7612
5.2300	0.6617	5.0854	0.8382	5.0381	0.8778	5.2137	0.7499	5.0915	0.8553	5.2108	0.7677
5.2182	0.6697	5.0738	0.8396	5.0265	0.8738	5.2019	0.7550	5.0798	0.8556	5.1990	0.7737
5.2064	0.6773	5.0621	0.8405	5.0149	0.8691	5.1902	0.7600	5.0682	0.8555	5.1873	0.7791
5.1946	0.6842	5.0505	0.8410	5.0034	0.8638	5.1784	0.7644	5.0565	0.8545	5.1755	0.7844
5.1828	0.6912	5.0389	0.8406	4.9918	0.8578	5.1667	0.7686	5.0449	0.8530	5.1638	0.7888
5.1710	0.6974	5.0273	0.8398	4.9803	0.8516	5.1549	0.7721	5.0333	0.8508	5.1520	0.7930
5.1593	0.7036	5.0157	0.8383	4.9687	0.8446	5.1432	0.7752	5.0217	0.8479	5.1403	0.7965
5.1475	0.7091	5.0042	0.8368	4.9572	0.8372	5.1315	0.7780	5.0101	0.8445	5.1286	0.7995
5.1358	0.7143	4.9926	0.8342	4.9457	0.8291	5.1198	0.7800	4.9986	0.8403	5.1169	0.8023
5.1241	0.7196	4.9811	0.8312	4.9342	0.8207	5.1081	0.7818	4.9870	0.8358	5.1052	0.8044
5.1124	0.7239	4.9696	0.8278	4.9227	0.8121	5.0965	0.7828	4.9754	0.8308	5.0935	0.8060
5.1007	0.7282	4.9580	0.8234	4.9112	0.8028	5.0848	0.7837	4.9639	0.8252	5.0819	0.8070
5.0891	0.7323	4.9465	0.8189	4.8998	0.7933	5.0732	0.7841	4.9524	0.8193	5.0703	0.8078
5.0774	0.7360	4.9350	0.8136	4.8883	0.7834	5.0615	0.7838	4.9409	0.8129	5.0586	0.8081
5.0658	0.7393	4.9235	0.8081	4.8769	0.7733	5.0499	0.7832	4.9294	0.8060	5.0470	0.8076
5.0541	0.7423	4.9121	0.8023	4.8655	0.7628	5.0383	0.7822	4.9179	0.7986	5.0354	0.8066
5.0425	0.7449	4.9006	0.7958	4.8540	0.7518	5.0267	0.7807	4.9064	0.7907	5.0238	0.8053
5.0309	0.7469	4.8892	0.7889	4.8426	0.7403	5.0151	0.7788	4.8949	0.7824	5.0122	0.8035
5.0193	0.7485	4.8777	0.7816	4.8312	0.7287	5.0036	0.7764	4.8835	0.7738	5.0007	0.8012
5.0077	0.7496	4.8663	0.7739	4.8198	0.7167	4.9920	0.7734	4.8720	0.7646	4.9891	0.7981

Grade 1		Grade 2		Grade 3		Grade 4		Grade 5		Grade 6	
LogM	MMD	LogM	MMD	LogM	MMD	LogM	MMD	LogM	MMD	LogM	MMD
4.9961	0.7504	4.8549	0.7657	4.8085	0.7046	4.9805	0.7700	4.8606	0.7553	4.9776	0.7948
4.9846	0.7505	4.8435	0.7570	4.7971	0.6923	4.9689	0.7663	4.8492	0.7456	4.9660	0.7910
4.9730	0.7503	4.8321	0.7478	4.7857	0.6798	4.9574	0.7622	4.8378	0.7357	4.9545	0.7867
4.9615	0.7498	4.8207	0.7385	4.7744	0.6673	4.9459	0.7573	4.8264	0.7254	4.9430	0.7816
4.9500	0.7486	4.8093	0.7286	4.7631	0.6545	4.9344	0.7521	4.8150	0.7148	4.9315	0.7763
4.9385	0.7473	4.7979	0.7187	4.7517	0.6418	4.9229	0.7467	4.8036	0.7040	4.9200	0.7706
4.9270	0.7453	4.7866	0.7085	4.7404	0.6289	4.9115	0.7410	4.7922	0.6929	4.9085	0.7644
4.9155	0.7430	4.7752	0.6980	4.7291	0.6162	4.9000	0.7343	4.7809	0.6816	4.8971	0.7577
4.9040	0.7402	4.7639	0.6875	4.7178	0.6036	4.8885	0.7277	4.7695	0.6700	4.8856	0.7506
4.8925	0.7373	4.7526	0.6768	4.7065	0.5910	4.8771	0.7208	4.7582	0.6583	4.8742	0.7432
4.8811	0.7340	4.7412	0.6654	4.6952	0.5785	4.8657	0.7137	4.7468	0.6465	4.8627	0.7354
4.8696	0.7299	4.7299	0.6543	4.6840	0.5660	4.8543	0.7062	4.7355	0.6344	4.8513	0.7272
4.8582	0.7257	4.7186	0.6427	4.6727	0.5536	4.8428	0.6980	4.7242	0.6226	4.8399	0.7191
4.8468	0.7211	4.7073	0.6313	4.6614	0.5412	4.8314	0.6902	4.7129	0.6106	4.8285	0.7104
4.8353	0.7160	4.6961	0.6194	4.6502	0.5291	4.8201	0.6814	4.7016	0.5987	4.8171	0.7014
4.8239	0.7102	4.6848	0.6076	4.6389	0.5170	4.8087	0.6725	4.6903	0.5870	4.8057	0.6923
4.8125	0.7044	4.6735	0.5968	4.6277	0.5053	4.7973	0.6630	4.6790	0.5751	4.7944	0.6830
4.8012	0.6984	4.6623	0.5854	4.6165	0.4938	4.7860	0.6536	4.6678	0.5635	4.7830	0.6733
4.7898	0.6921	4.6510	0.5744	4.6053	0.4824	4.7746	0.6438	4.6565	0.5517	4.7716	0.6632
4.7784	0.6854	4.6398	0.5634	4.5941	0.4714	4.7633	0.6339	4.6453	0.5403	4.7603	0.6528
4.7671	0.6786	4.6286	0.5525	4.5829	0.4605	4.7519	0.6240	4.6340	0.5291	4.7490	0.6424
4.7557	0.6716	4.6173	0.5421	4.5717	0.4498	4.7406	0.6140	4.6228	0.5179	4.7377	0.6319
4.7444	0.6641	4.6061	0.5311	4.5605	0.4397	4.7293	0.6039	4.6116	0.5071	4.7263	0.6208
4.7331	0.6567	4.5949	0.5208	4.5493	0.4292	4.7180	0.5939	4.6004	0.4963	4.7150	0.6100
4.7218	0.6482	4.5837	0.5104	4.5382	0.4192	4.7067	0.5837	4.5892	0.4859	4.7038	0.5992
4.7104	0.6403	4.5725	0.5001	4.5270	0.4092	4.6954	0.5734	4.5780	0.4756	4.6925	0.5887
4.6992	0.6320	4.5614	0.4904	4.5159	0.3992	4.6842	0.5632	4.5668	0.4653	4.6812	0.5780
4.6879	0.6235	4.5502	0.4802	4.5047	0.3897	4.6729	0.5529	4.5556	0.4550	4.6699	0.5674
4.6766	0.6153	4.5390	0.4704	4.4936	0.3798	4.6617	0.5428	4.5444	0.4450	4.6587	0.5570
4.6653	0.6069	4.5279	0.4604	4.4825	0.3700	4.6504	0.5325	4.5332	0.4352	4.6474	0.5464
4.6541	0.5987	4.5167	0.4503	4.4714	0.3603	4.6392	0.5226	4.5221	0.4253	4.6362	0.5360
4.6428	0.5904	4.5056	0.4403	4.4602	0.3506	4.6279	0.5131	4.5109	0.4153	4.6250	0.5256
4.6316	0.5825	4.4945	0.4301	4.4491	0.3411	4.6167	0.5033	4.4998	0.4057	4.6137	0.5157
4.6203	0.5744	4.4833	0.4199	4.4380	0.3316	4.6055	0.4938	4.4886	0.3960	4.6025	0.5057
4.6091	0.5664	4.4722	0.4097	4.4269	0.3221	4.5943	0.4844	4.4775	0.3861	4.5913	0.4957
4.5979	0.5581	4.4611	0.3996	4.4158	0.3127	4.5831	0.4753	4.4664	0.3763	4.5801	0.4861
4.5867	0.5500	4.4500	0.3897	4.4048	0.3036	4.5719	0.4664	4.4553	0.3666	4.5689	0.4766
4.5755	0.5421	4.4389	0.3795	4.3937	0.2946	4.5607	0.4573	4.4441	0.3569	4.5577	0.4670
4.5643	0.5337	4.4278	0.3695	4.3826	0.2858	4.5496	0.4484	4.4330	0.3472	4.5466	0.4574
4.5531	0.5259	4.4167	0.3596	4.3716	0.2771	4.5384	0.4393	4.4219	0.3377	4.5354	0.4478
4.5419	0.5178	4.4056	0.3497	4.3605	0.2688	4.5272	0.4302	4.4108	0.3282	4.5242	0.4383
4.5307	0.5097	4.3946	0.3400	4.3494	0.2609	4.5161	0.4212	4.3998	0.3190	4.5131	0.4291

Grade 1		Grade 2		Grade 3		Grade 4		Grade 5		Grade 6	
LogM	MMD	LogM	MMD	LogM	MMD	LogM	MMD	LogM	MMD	LogM	MMD
4.5196	0.5015	4.3835	0.3303	4.3384	0.2530	4.5050	0.4121	4.3887	0.3097	4.5019	0.4198
4.5084	0.4929	4.3724	0.3210	4.3274	0.2455	4.4938	0.4030	4.3776	0.3007	4.4908	0.4105
4.4973	0.4847	4.3614	0.3121	4.3163	0.2382	4.4827	0.3940	4.3665	0.2919	4.4797	0.4010
4.4861	0.4760	4.3503	0.3035	4.3053	0.2313	4.4716	0.3850	4.3555	0.2835	4.4686	0.3917
4.4750	0.4673	4.3393	0.2950	4.2943	0.2246	4.4605	0.3762	4.3444	0.2754	4.4574	0.3824
4.4639	0.4584	4.3282	0.2870	4.2833	0.2180	4.4494	0.3672	4.3334	0.2672	4.4463	0.3726
4.4527	0.4495	4.3172	0.2792	4.2722	0.2120	4.4383	0.3582	4.3223	0.2595	4.4352	0.3632
4.4416	0.4404	4.3062	0.2718	4.2612	0.2063	4.4272	0.3494	4.3113	0.2523	4.4241	0.3538
4.4305	0.4309	4.2951	0.2644	4.2502	0.2008	4.4161	0.3403	4.3002	0.2453	4.4130	0.3445
4.4194	0.4218	4.2841	0.2577	4.2392	0.1956	4.4050	0.3313	4.2892	0.2384	4.4019	0.3353
4.4083	0.4121	4.2731	0.2514	4.2282	0.1904	4.3939	0.3226	4.2782	0.2320	4.3909	0.3262
4.3972	0.4025	4.2621	0.2452	4.2172	0.1857	4.3828	0.3140	4.2672	0.2257	4.3798	0.3177
4.3862	0.3935	4.2511	0.2393	4.2063	0.1811	4.3718	0.3055	4.2562	0.2199	4.3687	0.3091
4.3751	0.3847	4.2401	0.2339	4.1953	0.1763	4.3607	0.2972	4.2451	0.2142	4.3577	0.3007
4.3640	0.3761	4.2291	0.2282	4.1843	0.1719	4.3497	0.2894	4.2341	0.2088	4.3466	0.2926
4.3529	0.3674	4.2181	0.2227	4.1733	0.1673	4.3386	0.2818	4.2231	0.2038	4.3356	0.2845
4.3419	0.3593	4.2071	0.2174	4.1624	0.1633	4.3276	0.2743	4.2121	0.1987	4.3245	0.2770
4.3308	0.3510	4.1962	0.2124	4.1514	0.1590	4.3166	0.2672	4.2012	0.1942	4.3135	0.2696
4.3198	0.3428	4.1852	0.2078	4.1404	0.1549	4.3055	0.2604	4.1902	0.1896	4.3025	0.2625
4.3087	0.3350	4.1742	0.2029	4.1295	0.1510	4.2945	0.2540	4.1792	0.1852	4.2914	0.2559
4.2977	0.3275	4.1632	0.1984	4.1185	0.1470	4.2835	0.2475	4.1682	0.1808	4.2804	0.2493
4.2867	0.3205	4.1523	0.1938	4.1076	0.1432	4.2725	0.2416	4.1572	0.1766	4.2694	0.2433
4.2756	0.3133	4.1413	0.1892	4.0966	0.1394	4.2615	0.2359	4.1463	0.1722	4.2584	0.2375
4.2646	0.3070	4.1304	0.1850	4.0857	0.1358	4.2505	0.2302	4.1353	0.1680	4.2474	0.2318
4.2536	0.3007	4.1194	0.1800	4.0747	0.1323	4.2395	0.2249	4.1243	0.1638	4.2364	0.2264
4.2426	0.2943	4.1084	0.1758	4.0638	0.1285	4.2285	0.2196	4.1134	0.1597	4.2254	0.2211
4.2316	0.2885	4.0975	0.1713	4.0529	0.1248	4.2175	0.2148	4.1024	0.1556	4.2144	0.2161
4.2206	0.2831	4.0866	0.1669	4.0419	0.1210	4.2065	0.2102	4.0915	0.1515	4.2034	0.2111
4.2096	0.2779	4.0756	0.1629	4.0310	0.1171	4.1955	0.2057	4.0805	0.1474	4.1924	0.2063
4.1986	0.2726	4.0647	0.1584	4.0201	0.1134	4.1845	0.2015	4.0696	0.1434	4.1814	0.2015
4.1876	0.2676	4.0537	0.1543	4.0091	0.1098	4.1736	0.1970	4.0586	0.1394	4.1704	0.1970
4.1766	0.2631	4.0428	0.1499	3.9982	0.1064	4.1626	0.1931	4.0477	0.1356	4.1595	0.1927
4.1656	0.2580	4.0319	0.1458	3.9873	0.1031	4.1516	0.1889	4.0367	0.1316	4.1485	0.1884
4.1547	0.2531	4.0209	0.1417	3.9764	0.1000	4.1407	0.1847	4.0258	0.1278	4.1375	0.1841
4.1437	0.2482	4.0100	0.1373	3.9654	0.0969	4.1297	0.1807	4.0149	0.1241	4.1266	0.1797
4.1327	0.2436	3.9991	0.1330	3.9545	0.0935	4.1187	0.1765	4.0039	0.1203	4.1156	0.1758
4.1217	0.2390	3.9882	0.1291	3.9436	0.0902	4.1078	0.1727	3.9930	0.1164	4.1047	0.1718
4.1108	0.2341	3.9773	0.1251	3.9327	0.0872	4.0968	0.1685	3.9821	0.1128	4.0937	0.1674
4.0998	0.2294	3.9663	0.1212	3.9218	0.0844	4.0859	0.1645	3.9711	0.1092	4.0828	0.1631
4.0889	0.2245	3.9554	0.1175	3.9109	0.0817	4.0750	0.1604	3.9602	0.1055	4.0718	0.1590
4.0779	0.2195	3.9445	0.1141	3.9000	0.0789	4.0640	0.1564	3.9493	0.1021	4.0609	0.1548
4.0670	0.2146	3.9336	0.1106	3.8891	0.0766	4.0531	0.1525	3.9384	0.0988	4.0499	0.1507

Grade 1		Grade 2		Grade 3		Grade 4		Grade 5		Grade 6	
LogM	MMD	LogM	MMD	LogM	MMD	LogM	MMD	LogM	MMD	LogM	MMD
4.0560	0.2093	3.9227	0.1070	3.8782	0.0742	4.0421	0.1483	3.9274	0.0956	4.0390	0.1467
4.0451	0.2040	3.9118	0.1038	3.8673	0.0719	4.0312	0.1444	3.9165	0.0923	4.0281	0.1427
4.0341	0.1991	3.9009	0.1004	3.8564	0.0697	4.0203	0.1404	3.9056	0.0892	4.0171	0.1388
4.0232	0.1940	3.8900	0.0967	3.8455	0.0675	4.0094	0.1365	3.8947	0.0864	4.0062	0.1348
4.0122	0.1892	3.8791	0.0935	3.8346	0.0652	3.9984	0.1326	3.8838	0.0834	3.9953	0.1310
4.0013	0.1843	3.8682	0.0905	3.8236	0.0631	3.9875	0.1289	3.8729	0.0807	3.9843	0.1272
3.9904	0.1798	3.8573	0.0878	3.8127	0.0612	3.9766	0.1255	3.8620	0.0783	3.9734	0.1233
3.9794	0.1755	3.8464	0.0847	3.8018	0.0594	3.9657	0.1220	3.8510	0.0757	3.9625	0.1196
3.9685	0.1707	3.8355	0.0822	3.7909	0.0575	3.9548	0.1186	3.8401	0.0734	3.9516	0.1160
3.9576	0.1660	3.8246	0.0797	3.7800	0.0559	3.9439	0.1150	3.8292	0.0711	3.9407	0.1127
3.9467	0.1614	3.8137	0.0773	3.7691	0.0543	3.9329	0.1118	3.8183	0.0690	3.9297	0.1091
3.9357	0.1566	3.8028	0.0746	3.7582	0.0528	3.9220	0.1085	3.8074	0.0670	3.9188	0.1058
3.9248	0.1520	3.7919	0.0723	3.7473	0.0513	3.9111	0.1050	3.7965	0.0649	3.9079	0.1027
3.9139	0.1475	3.7810	0.0704	3.7364	0.0500	3.9002	0.1018	3.7856	0.0629	3.8970	0.0996
3.9030	0.1434	3.7701	0.0683	3.7255	0.0485	3.8893	0.0989	3.7747	0.0610	3.8861	0.0963
3.8920	0.1391	3.7592	0.0665	3.7146	0.0472	3.8784	0.0960	3.7638	0.0594	3.8752	0.0932
3.8811	0.1351	3.7483	0.0647	3.7037	0.0462	3.8675	0.0933	3.7529	0.0575	3.8643	0.0903
3.8702	0.1315	3.7374	0.0631	3.6928	0.0451	3.8566	0.0906	3.7420	0.0559	3.8534	0.0875
3.8593	0.1277	3.7265	0.0616	3.6819	0.0441	3.8457	0.0880	3.7311	0.0546	3.8425	0.0847
3.8484	0.1241	3.7156	0.0601	3.6710	0.0430	3.8348	0.0856	3.7201	0.0531	3.8316	0.0821
3.8375	0.1206	3.7047	0.0588	3.6601	0.0421	3.8239	0.0832	3.7092	0.0518	3.8207	0.0797
3.8266	0.1174	3.6938	0.0576	3.6492	0.0413	3.8130	0.0809	3.6983	0.0505	3.8097	0.0772
3.8156	0.1142	3.6829	0.0567	3.6383	0.0403	3.8021	0.0787	3.6874	0.0494	3.7988	0.0750
3.8047	0.1111	3.6719	0.0556	3.6274	0.0393	3.7912	0.0764	3.6765	0.0482	3.7879	0.0728
3.7938	0.1080	3.6610	0.0546	3.6165	0.0385	3.7803	0.0747	3.6656	0.0469	3.7770	0.0709
3.7829	0.1054	3.6501	0.0534	3.6056	0.0377	3.7694	0.0727	3.6547	0.0459	3.7661	0.0688
3.7720	0.1028	3.6392	0.0522	3.5946	0.0367	3.7585	0.0709	3.6438	0.0448	3.7552	0.0672
3.7611	0.1002	3.6283	0.0509	3.5837	0.0359	3.7476	0.0688	3.6328	0.0436	3.7443	0.0655
3.7502	0.0978	3.6174	0.0497	3.5728	0.0350	3.7367	0.0675	3.6219	0.0426	3.7334	0.0641
3.7393	0.0953	3.6065	0.0486	3.5619	0.0344	3.7258	0.0660	3.6110	0.0417	3.7225	0.0625
3.7283	0.0932	3.5956	0.0475	3.5510	0.0337	3.7149	0.0643	3.6001	0.0407	3.7116	0.0610
3.7174	0.0911	3.5847	0.0464	3.5400	0.0331	3.7040	0.0628	3.5891	0.0398	3.7007	0.0598
3.7065	0.0892	3.5737	0.0456	3.5291	0.0325	3.6931	0.0615	3.5782	0.0389	3.6898	0.0583
3.6956	0.0874	3.5628	0.0445	3.5182	0.0317	3.6822	0.0603	3.5673	0.0380	3.6789	0.0570
3.6847	0.0859	3.5519	0.0434	3.5072	0.0312	3.6713	0.0588	3.5564	0.0371	3.6680	0.0558
3.6738	0.0841	3.5410	0.0425	3.4963	0.0307	3.6604	0.0575	3.5454	0.0363	3.6571	0.0545
3.6629	0.0823	3.5301	0.0413	3.4854	0.0300	3.6494	0.0563	3.5345	0.0354	3.6461	0.0533
3.6519	0.0807	3.5191	0.0404	3.4744	0.0294	3.6385	0.0553	3.5236	0.0345	3.6352	0.0522
3.6410	0.0791	3.5082	0.0394	3.4635	0.0291	3.6276	0.0540	3.5126	0.0335	3.6243	0.0511
3.6301	0.0777	3.4973	0.0386	3.4525	0.0288	3.6167	0.0530	3.5017	0.0327	3.6134	0.0500
3.6192	0.0758	3.4863	0.0378	3.4416	0.0283	3.6058	0.0519	3.4907	0.0319	3.6025	0.0490
3.6082	0.0744	3.4754	0.0371	3.4306	0.0278	3.5949	0.0509	3.4798	0.0311	3.5916	0.0479

Grade 1		Grade 2		Grade 3		Grade 4		Grade 5		Grade 6	
LogM	MMD	LogM	MMD	LogM	MMD	LogM	MMD	LogM	MMD	LogM	MMD
3.5973	0.0729	3.4644	0.0364	3.4197	0.0275	3.5840	0.0499	3.4688	0.0306	3.5806	0.0471
3.5864	0.0714	3.4535	0.0358	3.4087	0.0270	3.5730	0.0489	3.4579	0.0298	3.5697	0.0461
3.5755	0.0699	3.4425	0.0350	3.3977	0.0265	3.5621	0.0480	3.4469	0.0292	3.5588	0.0451
3.5645	0.0679	3.4316	0.0343			3.5512	0.0470	3.4360	0.0287	3.5479	0.0442
3.5536	0.0665	3.4206	0.0336			3.5403	0.0459	3.4250	0.0280	3.5369	0.0432
3.5427	0.0650	3.4097	0.0327			3.5294	0.0449	3.4140	0.0273	3.5260	0.0423
3.5317	0.0636	3.3987	0.0320			3.5184	0.0438	3.4031	0.0267	3.5151	0.0412
3.5208	0.0623	3.3877	0.0313			3.5075	0.0427	3.3921	0.0262	3.5041	0.0402
3.5098	0.0607	3.3768	0.0309			3.4966	0.0417	3.3811	0.0258	3.4932	0.0391
3.4989	0.0596	3.3658	0.0306			3.4856	0.0407	3.3701	0.0253	3.4822	0.0381
3.4879	0.0584	3.3548	0.0301			3.4747	0.0398	3.3591	0.0252	3.4713	0.0373
3.4770	0.0572	3.3438	0.0298			3.4637	0.0391	3.3481	0.0248	3.4603	0.0364
3.4660	0.0561	3.3328	0.0294			3.4528	0.0385	3.3371	0.0243	3.4494	0.0355
3.4551	0.0549	3.3218	0.0291			3.4418	0.0378	3.3261	0.0240	3.4384	0.0349
3.4441	0.0540	3.3109	0.0288			3.4309	0.0372	3.3151	0.0236	3.4275	0.0342
3.4331	0.0529	3.2998	0.0285			3.4199	0.0366	3.3041	0.0233	3.4165	0.0336
3.4222	0.0517	3.2888	0.0283			3.4090	0.0361	3.2931	0.0229	3.4055	0.0331
3.4112	0.0505	3.2778	0.0280			3.3980	0.0356	3.2821	0.0226	3.3946	0.0326
3.4002	0.0494	3.2668	0.0278			3.3870	0.0352	3.2711	0.0223	3.3836	0.0321
3.3892	0.0482	3.2558	0.0276			3.3760	0.0348	3.2601	0.0219	3.3726	0.0316
3.3783	0.0471	3.2448	0.0274			3.3651	0.0343	3.2490	0.0216	3.3616	0.0311
3.3673	0.0463	3.2337	0.0272			3.3541	0.0338	3.2380	0.0213	3.3506	0.0305
3.3563	0.0454	3.2227	0.0270			3.3431	0.0332	3.2269	0.0211	3.3396	0.0300
3.3453	0.0446	3.2117	0.0268			3.3321	0.0325	3.2159	0.0209	3.3287	0.0294
3.3343	0.0438	3.2006	0.0268			3.3211	0.0320	3.2048	0.0207	3.3176	0.0289
3.3233	0.0431	3.1895	0.0267					3.1938	0.0206	3.3066	0.0283
3.3123	0.0424	3.1785	0.0265					3.1827	0.0206	3.2956	0.0277
3.3013	0.0417	3.1674	0.0264					3.1716	0.0204	3.2846	0.0272
3.2902	0.0413	3.1563	0.0264					3.1605	0.0202	3.2736	0.0267
3.2792	0.0409	3.1453	0.0265					3.1495	0.0200	3.2626	0.0263
3.2682	0.0405	3.1342	0.0264					3.1384	0.0198	3.2515	0.0259
3.2571	0.0401	3.1231	0.0265							3.2405	0.0256
3.2461	0.0397	3.1120	0.0267							3.2295	0.0254
3.2351	0.0392	3.1009	0.0267							3.2184	0.0253
3.2240	0.0386	3.0898	0.0267							3.2074	0.0251
3.2130	0.0380	3.0787	0.0265							3.1963	0.0250
3.2019	0.0374	3.0675	0.0264							3.1853	0.0250
3.1908	0.0370	3.0564	0.0262							3.1742	0.0250
3.1798	0.0364	3.0453	0.0260							3.1631	0.0250
3.1687	0.0360									3.1520	0.0249
3.1576	0.0358									3.1409	0.0249
3.1465	0.0356									3.1299	0.0250

Grade 1		Grade 2		Grade 3		Grade 4		Grade 5		Grade 6	
LogM	MMD	LogM	MMD	LogM	MMD	LogM	MMD	LogM	MMD	LogM	MMD
3.1354	0.0355										
3.1243	0.0353										
3.1132	0.0354										
3.1021	0.0353										
3.0910	0.0349										
3.0798	0.0345										
3.0687	0.0344										
3.0575	0.0342										
3.0464	0.0340										
3.0352	0.0337										
3.0241	0.0336										
3.0129	0.0335										
3.0017	0.0332										
2.9905	0.0326										
2.9793	0.0320										
2.9681	0.0314										
2.9569	0.0309										
2.9457	0.0302										

Table 35. Raw data received from INEOS from SEC measurement of the different grades.

11.8 Categorising of grades

Grade 1: Wide MWD, low M_w (MI 25)

Grade 4: Wide MWD, high M_w (MI 14)

Grade 2: Narrow MWD, low M_w (MI 25)

Grade 5: Grade (2 + 3) compound

Grade 3: Narrow MWD, high M_w (MI 14)

Grade 6: Grade (2 + 4) compound

Where the raw data obtained from SEC and oscillatory rheometry obtained are:

grade nr:	MFI (g/10min)	From SEC - INEOS					From MA Lab – Tetra Pak			
		M_n (g/mol)	M_w (g/mol)	M_z (g/mol)	M_w / M_n	M_z/M_w	PI	G' at ref (Pa)	ER (Pa)	PDR
1	25	25400	151500	432900	6	2.9	4.69	79.9	0.14	4.14
2	25	34900	154700	355400	4.4	2.3	3.48	48.2	0.09	2.67
3	14	50200	165700	343100	3.3	2.1	2.84	60.6	0.11	2.30
4	14	42600	191000	530200	4.5	2.8	4.10	74.4	0.13	3.51
5	N/A*	41600	163500	357600	3.93	2.2	3.52	45.4	0.10	2.57
6	N/A*	38000	172900	432600	4.55	2.5	4.17	59.2	0.11	3.15

Table 36. SEC and rheology measures to determine polydispersity, performed and calculated for the different grades.

Where the shear viscosity ranking at low shear rates between the grades are (measure by capillary rheometry) from high to low:

1. Grade 3
2. Grade 4 and 5
3. Grade 6 and 2
4. Grade 1